Correlation of ligand density with cell behavior on bioactive hydrogel layers

Dissertation zur Erlangung des naturwissenschaftlichen Doktorgrades der Julius-Maximilians-Universität Würzburg

vorgelegt von

Master of Science Biotechnologin

Meike Vanessa Beer

aus Bonn

Würzburg 2011

Eingereicht bei der Fakultät für Chemie und Pharmazie am

_____

Gutachter der schriftlichen Arbeit

1. Gutachter: _____

2. Gutachter: _____

Prüfer des öffentlichen Promotionskolloquiums

1. Prüfer: _____

2. Prüfer: _____

3. Prüfer: _____

Datum des öffentlichen Promotionskolloquiums

_____

Doktorurkunde ausgehändigt am

_____

Cover illustration

Primary human dermal fibroblasts on functionalized hydrogel surfaces. Adherent cells were illustrated by life cell microscopy or fluorescent staining and microscopy.

***„Damit das Mögliche entsteht, muss immer wieder das Unmögliche versucht werden*.“** - Hermann Hesse -

Table of contents

List of abbreviations

^{3}H, ^{14}C, ^{125}I, ^{131}I	radioactive isotopes of the elemtns hydrogen, carbon, and iodine
^{125}I-YRGDS	peptide: ^{125}I-tyrosine-arginine-glycine-aspartic acid-serine
°	degree
°C	degree celsius
%	percent
Ø	diameter
µCi	microcurie
µg	microgramm
µL	microliter
µm	micrometer
Å	Ångström
AFM	atomic force microscopy
Ar^{+}, He^{+}, Ne^{+}, Xe^{+}	primary ions of the elements argon, helium, neon, and xenon
AS	3-aminopropyl-trimethoxysilan
Au	gold
Bi	bismuth
BSA	bovine serum albumin
C	amino acid cysteine
CH_3CN	acetonitrile
CAM	cell adhesion molecule
CMAC	cell-matrix adhesion complex
CO_2	carbon dioxide
cpm	counts per minute
cm	centimeter
cm^2	square centimeter
d	day
D	amino acid aspartic acid
Da	Dalton
DAPI	4',6-diamidino-2-phenylindol
DMEM	medium for HDFs
DMSO	dimethylsulphoxide
DNA	desoxyribonucleic acid
DSMZ	German collection of microorganisms and cell cultures

EBI	European Bioinformatics Institute
ECM	extracellular matrix
EDTA	ethylenediaminetetraacetic acid
e.g.	*exempli gratia*
ELISA	enzyme linked immunosorbent assay
ELLA	enzyme linked lectin assay
EO	ethylene oxide
et al.	*et altera*
eV	electron volt
F	fluorine
FDA	American food and drug administration
FN	fibronectin
g	gramm
G	amino acid glycin
GAG	glycosaminoglycan
GlcNAc	N-acetylglucosamine
GPa	gigapascal
GRGDS	peptide glycine-arginine-glycine-aspartic acid-serine
GRGES	peptide glycine-arginine-glycine-glutamic acid-serine
GRGDSK-biotin	peptide glycine-arginine-glycine-aspartic acid-serine-lysine-biotin
GSII	lectin II from *Griffonia simplicifolia*
h	hour
H_2O_2	hydrogen peroxide
H_2SO_4	sulfuric acid
HA	hyaluronic acid
HCl	hydrogen chloride
HDF	primary human dermal fibroblast
HEPES	4-(2-hydroxyethyl)-1-piperazineethanesulforic acid
His_6	hexa-histidine-tag
His_6CGL2	His_6 tagged fungal galectin from *Coprinus cinereus* produced in *Escherichica. coli*
hν	energy
IgG	immunoglobulin G
KGRGDSP-3,5-diiodo-T	peptide lysin-glycine-arginine-glycine-aspartic acid-serine-prolin-3,5-diiodo-threonin

I	iodine
IPDI	isophorone diisocyanate
K	amino acid lysin
kDa	kilodalton
keV	kiloelektronvolt
kHz	kilohertz
kPa	kilopascal
kV	kilovolt
L	liter
L929	mouse connective tissue fibroblast cell line
LacNAc	N-acetyllactosamine
m	meter
M	molar
mA	milliampere
mbar	millibar
MCP	micro contact printing
mg	milligramm
min	minute
mL	milliliter
mm	millimeter
mM	millimolar
mol	unit of the amount of substance n
mmol	millimol
MSC	human mesenchymal stem cell
n	amount of substance
N	Newton
$Na^{125}I$	sodium iodine
Na_2CO_3	sodium carbonate
NAD(P)H	nicotinamide adenine dinucleotide phosphate
$NaHCO_3$	sodium hydrogencarbonat
NaOH	sodium hydroxid
NCO	isocyanate group
NCO-sP(EO-*stat*-PO)	six arm star shaped prepolymer with isocyanate endgroups
ng	nanogramm
NH_2	amino group

nm	nanometer
nM	nanomolar
O_2	oxigen
O_3	ozone
OD	optical density
OH	hydroxyl group
OPD	o-phenylenediamine
P	amino acid prolin
PBS	phosphat buffered saline
PEG	poly(ethylene glycol)
PEO	poly(ethylene oxid)
PG-SH	thiol functionalized poly(glycidol)
pH	negative decadic logarithm of H^+ ion concentration
PHEMA	poly(hydroxyethyl methacrylate)
PLGA	poly(D,L-lactide-*co*-glycolide)
PO	propylene oxide
POD	peroxidase
polyLacNAc	poly-N-acetyllactosamine
PS	polystyrene
PVA	poly(vinly alcohol)
QCM	quartz crystal microbalance
R	amino acid arginine
RGD	peptide arginine-glycine-aspartic acid
RP-HPLC	high-performance liquid chromatography
rpm	rounds per minute
RPMI	medium for L929 cells
RU	reference units
S	amino acid serin
SA	streptavidin
SA-POD	streptavidin-peroxidase
SAM	self-assembled monolayer
SAW	surface acoustic wave
sccm	standard cubic centimeters per minute
SDS	sodium dodecyl sulfate
sec	second

Si	silicon
aminosilan	N-[3-(trimethoxysilyl)propyl]ethylendiamin
SiO_2	siliziumdioxid
SPR	surface plasmon resonance
t	time
T	temperature; amino acid threonin
TCPS	tissue culture polystyrene
TFA	trifluoracetic acid
THF	tetrahydrofuran
TOF-SIMS	time-of-flight secondary ion mass spectrometry
UV	ultraviolet light
vol-%	volume percent
W	watt
WST-1	formazan salt
wt-%	weight percent
XPS	X-ray photoelectron spectroscopy
Y	amino acid tyrosine
YRGDS	peptide tyrosine-arginine-glycine-aspartic acid-serine

CHAPTER 1

Scope and structure of the thesis

Since ancient times, materials have been used to replace damaged or lost tissue in order to restore functionality. One of the earliest examples are wood toes in ancient Egypt [1]. Such materials that get in contact with tissue or biological fluids are called biomaterials [2]. Until recently, most materials were not specifically designed for a given medical application, but rather taken from other fields and used for the medical task at hand [2]. These biomaterials served mainly as passive materials, structurally replacing damaged tissue or organs. Since the beginning of the 20th century, ceramics, metals, and synthetic polymers have started to replace natural products [1, 3]. Today, a wide range of synthetic polymers specifically designed for medical applications are commercially available and these materials have to meet high quality standards and expectations concerning their functionality and properties.

Nowadays, a mere replacement of body parts does no longer suffice. Even though a lot of research aims at the optimization of biomaterials, drawbacks like insufficient biocompatibility and consequential problems have still to be overcome. Mesh implants for hernia repair are the most common implants in surgery with millions of implantations worldwide each year [4, 5]. They were shown to cause problems after implantation due to postoperative infections and to have recurrence rates of up to 34 % [4, 6]. Proper control over the interaction of the material surface with proteins and cells is thus crucial for the successful function of the biomaterial in contact with body fluids and tissue. First of all, non-specific protein adsorption, which is the first step in a cascade of inflammatory responses leading to foreign body reactions, must be prevented, e.g. by developing inert surfaces [7]. Furthermore, specifically interacting molecules such as cell adhesion mediating peptides or whole extracellular matrix (ECM) proteins have to be bound to such inert surfaces in a way that preserves their biological function, so as to create materials that are not only tolerated, but recognized by and interacting with the body and eventually degrade by time. Nowadays, research aims at the regeneration of tissue by help of functional biomaterials, going beyond replacing the injured part with synthetic materials [8]. In other words, biomaterials should not only be incorporated in the host without causing any harm, but should interact with surrounding cells in a specific way that triggers them to secrete their natural ECM, thus incorporating or replacing the biomaterial over time.

Beside of morphology and mechanical properties, biomaterial surface modification is still a major challenge. One class of materials that has gained particular importance in the field of biomaterials and tissue engineering in the last years are swollen and crosslinked hydrophilic polymers (hydrogels) as they mimic *in vivo* tissue with their high water content and can be tailored to show mechanical properties similar to those of many tissue [3]. Hydrogels are thus intrinsically cytocompatible and can be bioactivated by chemical modification of the polymer network. Such hydrogels can also be applied as thin and ultrathin coatings for biomaterials. One example for such a hydrogel coating has been developed and established in our group. This system prevents non-specific interactions and can be functionalized with cell adhesion molecules (CAM) [9]. With this system at hands, the major question driving this thesis is '**How much?**'. When such hydrogels are functionalized with CAMs, these are usually distributed randomly within the system. However, only the signals on the very top may interact with cells and tissue. Therefore, the first aim was to quantify the **maximal** amount of ligands in and on the hydrogel layers. Moreover, for hard surfaces it has been shown, that there is a minimal ligand density that is needed for cell adhesion [10]. Hence, a second aim was to determine the **optimal** concentration of ligands regarding cell adhesion and proliferation on top of the functionalized hydrogels that can interact with cells and to evaluate whether these values correlate with hard surfaces.

In the first part of this work (***I Classical quantification***) ligand concentrations in functionalized hydrogel coatings were quantified using radiolabeling (**Chapter 3**), X-ray photoelectron spectroscopy (XPS), and time-of-flight secondary ion mass spectrometry (TOF-SIMS) (**Chapter 4**). With these methods, ligand concentrations in bulk as well as the surface near regions of the hydrogel coatings were determined (Figure 1).

However, it was a very important aspect of my research to apply surface sensitive quantification methods that allow the quantification of the amount of ligands present at the surface of the hydrogel layers and therefore accessible for proteins and cells. These methods are described in the second part of this work (***II Surface sensitive quantification***) (Figure 1). For this purpose surface plasmon resonance (SPR) and surface acoustic wave (SAW) technology (**Chapter 5**), as well as enzyme linked immunosorbent assay (ELISA) and enzyme linked lectin assay (ELLA) (**Chapter 6**) were applied on the functionalized hydrogel coatings. Additionally, cell adhesion was quantified depending on the ligand concentration on the hydrogel coatings (**Chapter 7**). In **Chapter 8**, all quantification approaches were correlated.

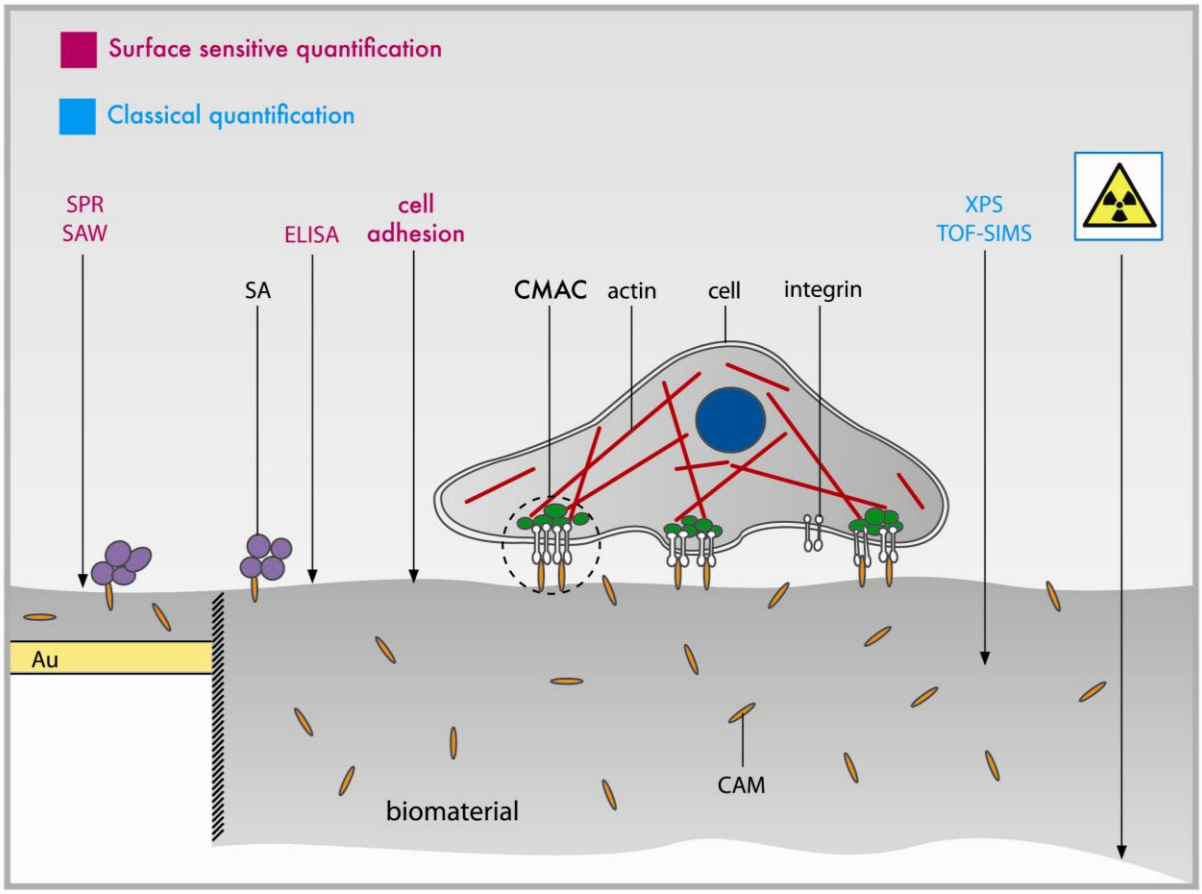

Figure 1: Ligand quantification in and on biomaterials.

CAMs immobilized to biomaterials need to be quantified. Therefore, classical as well as surface sensitive methods can be applied. Classical methods: While radiolabeling detects ligands in the bulk biomaterial, XPS and TOF-SIMS only penetrate the surface near regions depending on the experimental set-up and the material characteristics. Surface sensitive methods: SPR and SAW detect surface presented CAMs, e.g. with streptavidin (SA) as interaction partner, however, they can only be applied on ultrathin coatings on e.g. gold (Au). In contrast, ELSIA and cell adhesion have the advantage to combine surface sensitivity and the ability to be applied on all kinds of biomaterials.

In the third part of this dissertation (***III Advanced ECM engineering***), the biochemical and structural mimicry of the ECM was investigated. A biomimetic construction of the ECM was achieved via sugar-lectin mediated binding of the ECM protein fibronectin (FN) (**Chapter 9**). In the last Chapter, an approach to mimic the three-dimensional structure of the ECM is presented via the generation of hydrogel coated, nonwoven fiber meshes with controlled surfaces (**Chapter 10**). The influence of these two ECM mimetic biomaterials on cells was investigated.

References

1. Huebsch, N. and Mooney, D.J. Inspiration and application in the evolution of biomaterials. *Nature* **2009**, 462 (7272) 426-32.
2. Peppas, N.A. and Langer, R. New challanges in biomaterials. *Science* **1994**, 263 (5154) 1715-20.
3. Peppas, N.A.; Hilt, J.Z.; Khademhosseini, A. and Langer, R. Hydrogels in biology and medicine: From molecular principles to bionanotechnology. *Advanced Materials* **2006**, 18 (11) 1345-60.
4. Binnebösel, M.; vonTrotha, K.T.; Jansen, P.L.; Conze, J.; Neumann, U.P. and Junge, K. Biocompatibility of prosthetic meshes in abdominal surgery. *Seminars in Immunopathology* **2011**, 33 (3) 235-43.
5. Klinge, U.; Klosterhafen, B.; Öttinger, A.P.; Junge, K. and Schumpelick, V. PVDF as a new polymer for the construction of surgical meshes. *Biomaterials* **2002**, 23 (16) 3487-93.
6. Leber, G.E.; Garb, J.L.; Albert, I.A.A., A. I. and Reed, W.P. Long-term complications associated with prosthetic repair of incisional hernias. *Archieves of Surgery* **1998**, 133 (4) 378-82.
7. Ratner, B.D. and Bryant, S.J. Biomaterials: Where we have been and where we are going. *Annual Review of Biomedical Engineering* **2004**, 6 (1) 41-75.
8. Williams, D.F. On the mechanisms of biocompatibility. *Biomaterials* **2008**, 29 (20) 2941-53.
9. Groll, J.; Fiedler, J.; Engelhard, E.; Ameringer, T.; Tugulu, S.; Klok, H.A.; Brenner, R.E. and Moeller, M. A novel star PEG-derived surface coating for specific cell adhesion. *Journal of Biomedical Materials Research Part A* **2005**, 74A (4) 607-17.
10. Massia, S.P. and Hubbell, J.A. An RGD spacing of 440nm is sufficient for integrin alpha-V-beta-3-mediated fibroblast spreading and 140nm for focal contact and stress fiber formation. *Journal of Cell Biology* **1991**, 114 (5) 1089-100.

CHAPTER 2

Introduction

There are various definitions of biomaterials that can be found in literature. Williams defines a biomaterial as "*… a substance that has been engineered to take a form which, alone or as part of a complex system, is used to direct, by control of interactions with components of living systems, the course of any therapeutic or diagnostic procedure, in human or veterinary medicine*" [1]. To control interactions of a biomaterial with a living system and for the intelligent design of biomaterials, the *in vivo* environment of cells in the tissue of interest needs to be understood and mimicked as precisely as possible. The human body consists of functional tissues; each differently organized to fulfill specialized functions. Therefore, each tissue contains its characteristic cell types incorporated in its characteristic extracellular matrix (ECM). This Chapter summarizes relevant background information important to develop and characterize two-dimensional as well as three-dimensional biomaterials.

1. The *in vivo* environment of cells – The ECM

Tissue does not only consist of different cell types but to a great extent of the ECM, the matrix that surrounds the cells. This complex matrix is mainly composed of proteins and polysaccharides, forming a highly hydrated gel-like meshwork that is interwoven with a scaffold of fiber proteins (Figure 1). The ECM is composed of three main groups of macromolecules that can be distinguished into hydrophilic proteoglycans, adhesive glycoproteins and fibrous proteins with collagen as the most abundant one [2]. This complex scaffold provides mechanical stability for the tissue, a matrix for cell anchorage and forms the microenvironment of cells [3]. It can be seen as a communication platform storing growth factors and guiding cell adhesion, survival, differentiation, migration, proliferation, shape, and function [3-5]. Resident cells synthesize, secrete, and reorganize ECM compounds [6] and are involved in degradation of the ECM by synthesizing enzymes like the matrix metalloproteinase, elastase, and plasmin [7]. This process is important in terms of adaption to environmental changes, cell migration, and tissue repair [8, 9].

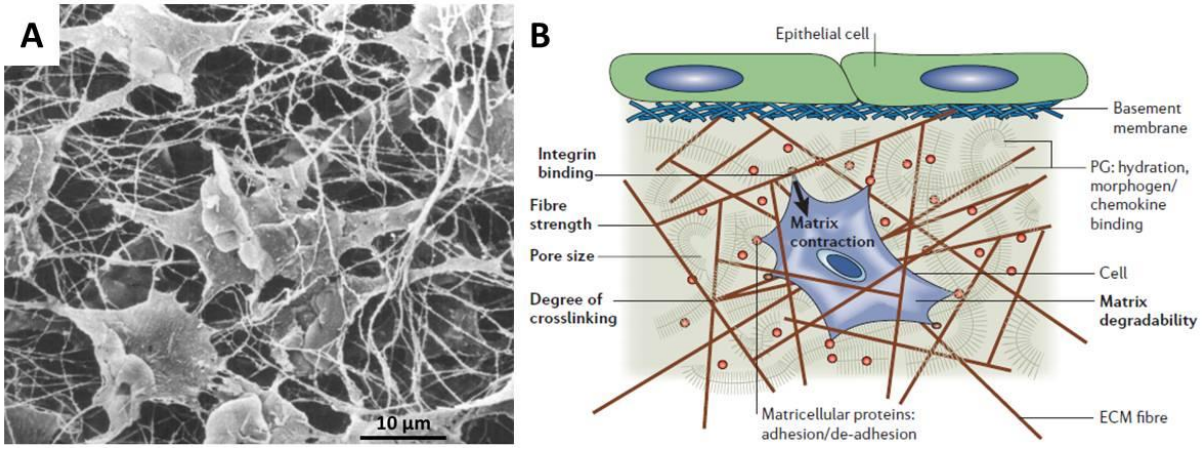

Figure 1: Fibroblasts in their *in vivo* environment.

A: Rat corneal fibroblasts in their ECM illustrated by scanning electron microscopy. The ECM consists of a hydrated, gel-like matrix and a fibrous scaffold. Image taken from reference [10] with permission from the Association for Research in Vision and Ophthalmology. B: The ECM fulfills various functions providing a scaffold for cell survival and function. Image taken from reference [11] with permission from the Nature Publishing Group.

1.1. Hydrated matrix of the ECM

The main fraction of the hydrogel matrix of the ECM consists of proteoglycans, a class of structurally diverse macromolecules that are composed of glycosaminoglycan (GAG) chains which are mostly bound to protein cores [4]. These diverse macromolecules are composed of different groups of unbranched polysaccharide chains such as sulfated chondroitin, dermatan,

heparin, and keratin, as well as non-sulfated hyaluronan [4, 12]. Sulfated GAGs bind to serine rich proteins, and form the so called proteoglycans [13], forming a negatively charged porous gel-like matrix [14], that stores signaling molecules [7]. Due to the porous structure and the hydrophilicity, this hydrogel part of the ECM can take up big amounts of water and therefore protect the tissue from compressive forces [4].

1.2. Fibrous scaffold of the ECM

The hydrogel matrix of the ECM is interwoven with a fibrous network consisting mainly of collagen I, II, III, V, and XI fibers, providing strength, stability, and integrity for the tissue [6, 15, 16]. Additionally, these collagen fibers serve as a scaffold for cell adhesion, spreading, and migration [17]. Beside collagen fibers with diameters of up to a few 100 nm [5] providing strength and stiffness, also more elastic fibers can be found. Responsible for elasticity and resilience are e.g. highly crosslinked elastin fibers interwoven within the collagen matrix [2, 15]. Cell adhesion mediating proteins like FN and laminin are also found as fibrous structures interconnecting cells and collagen [5] (Figure 2).

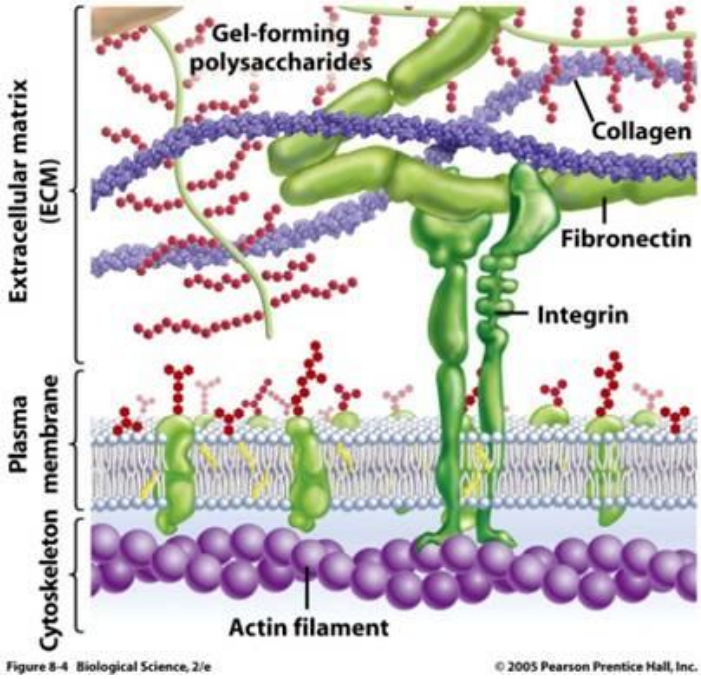

Figure 2: Interaction of integrins with the ECM.

A: Integrins bind to ECM glycoproteins like FN connected to collagen fibers, allowing the crosstalk between ECM and intracellular actin filaments. Image taken from: http://www.uic.edu/classes/bios/bios100/f06pm/integrin.jpg.

2. Interaction of cells and their ECM

2.1. Integrins: Cell adhesion receptors

The binding of anchorage dependent cells to the ECM is important to maintain a functional tissue [18]. Cell receptors like integrins, selectins, syndecans, and CD44 connect cells with their ECM [7]. Integrins play a key role in this adhesion process and are expressed on most cells of the human body [19, 20]. They are transmembrane receptors that connect the inside of the cell with its extracellular space (Figure 2), affecting both cell behavior and ECM reorganization [3, 19]. Integrins consist of one α and one β subunit [20]. There exist several α/β subunit combinations allowing binding specificity to different proteins [20] (Figure 3A). These non-covalently associated and glycosylated α/β-heterodimers form a big family of cell adhesion receptors each specialized to bind specific ligands (often more than one) in the ECM [18, 19, 21]. With their extracellular N-terminal domain they function as general adhesion receptors connecting cells to ECM proteins like fibronectin (FN), fibrinogen, laminins, collagens, and vitronectin [3, 19, 22]. In the cytoplasm, the rather small C-terminal part of the integrin receptor [23] recruits proteins including talin, vinculin, and paxilin forming multi-protein complexes that allow the integrins to interact with the actin cytoskeleton, cytoplasmic kinases, and transmembrane growth factor receptors [21, 24-27]. This process is associated with the clustering of several integrin receptors in the cell membrane forming so called cell-matrix adhesion complexes (CMAC) that promote the assembly and reorganization of actin filaments in the cell lumen [3, 18, 21, 24, 28]. CMACs are the strongest connections between cells and their ECM [29, 30] and lead to spreading and flattening of cells on the surface, which is important for the coherence of tissues [18].

Integrins transduce signals in both directions: outside-in to influence intracellular pathways and inside-out to regulate the ECM reassembly [19]. Outside-in signaling is additionally regulated by signaling molecules present in the ECM network [7] and can influence cells even on the gene expression level [27]. Thus, integrin receptors can be seen as sensors recognizing extracellular changes [31]. Inside-out signaling of integrins is most likely initiated by cytoskeletal forces acting on the integrin conformation, allowing the cell to remodel their environment maintaining the functionality of tissue. Zhu et al. proposed an integrin model explaining the ligand binding events on a molecular level [23]. In a bent conformation, integrin receptors are in a so called low affinity state. Binding of actin filaments at the cytoplasmic domain to the β-subunit and further binding to ECM ligands stretches the integrin conformation into a high affinity state thus additionally regulating cell-matrix interactions.

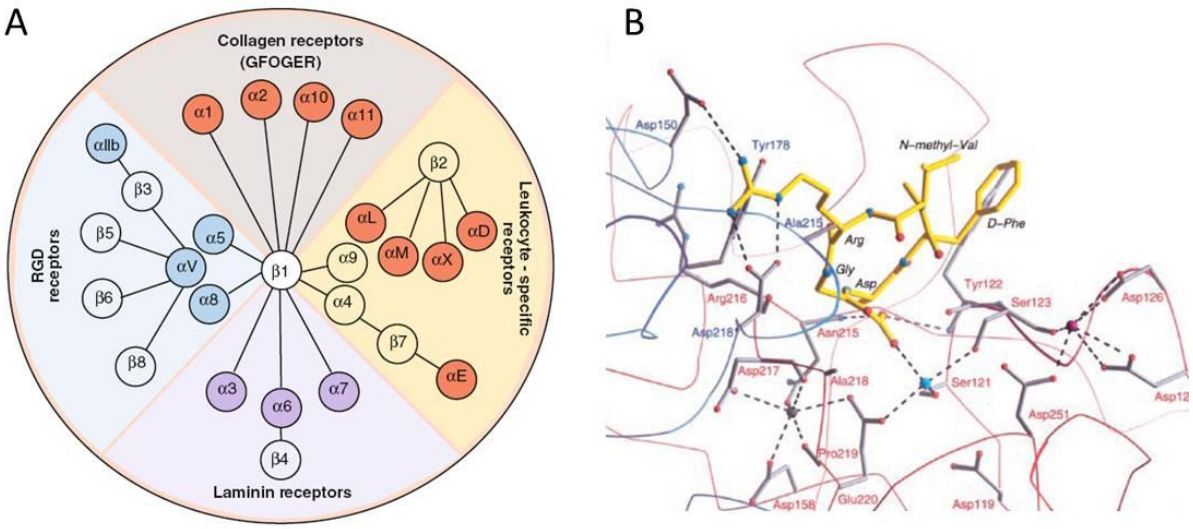

Figure 3: Integrin families and RGD binding.

A: α/β-integrin receptors are specialized to bind to various ECM proteins like RGD containing proteins, collagen, or laminin. Image taken from reference [32] with permission from Springer. B: Crystal structure of the extracellular segment of the integrin receptor $\alpha_v\beta_3$ (blue and red) bind to the peptide sequence RGD (yellow) that is the cell adhesion mediating sequence in the ECM protein FN. Image taken from reference [33] with permission from the American Association for the Advancement of Science.

2.2. Cell adhesion sites

Looking closer at the binding of integrin receptors to ECM adhesion sites, special adhesion domains can be found in the rather big ECM proteins. Many integrins recognize the tripeptide sequence arginine-glycine-aspartic acid (RGD) that can be found in various ECM proteins like FN [34, 35], vitronectin, fibrinogen, laminin, and collagen [35, 36]. RGD is located in the FN repeat III10 [37] and is known as the major cell adhesion promoting sequence of FN which was first discovered by Pierschbacher and Ruoslahti [38]. The amino acid arginine in the RGD sequence binds to a β-propeller secondary structure of the integrin α-subunit, while the aspartic acid binds to the β-subunit of the integrin [39] (Figure 3B). The binding process of integrins to the RGD sequence is influenced by the three-dimensional presentation of the peptide sequence as well as by additional residues flanking the tripeptide [37, 40].

2.3. Influence on anchorage dependant cells

A special form of outside-in signalling in anchorage dependant cells is the programmed cell death. Anchorage dependant cells like fibroblasts need cell adhesion molecules (CAM) to bind to the matrix in order to survive [41]. Only the adhesion and spreading of these cells on surfaces enables maximal DNA synthesis in these cells [42]. In suspension or in an ECM with incorrect or no adhesion signals these cells have a round shape and often undergo a special form of cell death, called anoikis [43]. Thus, the presence of suitable ligands in the ECM is

crucial for the survival of these cell types [31]. The characteristics of the complex and not yet fully understood mechanism of anoikis vary from one to another cell type and are necessary to keep tissues intact [43]. Chen et al. cultured human endothelial cells on planar surfaces with differently sized adhesive FN islands and could show that a minimum area of cell-FN contact was necessary for cell survival [44]. FN conformation and therefore the characteristic presentation of binding sequences influences integrin binding and has an impact on cell proliferation and differentiation [45]. These findings imply that the presence of tissue specific ECM is indispensable for appropriate cell adhesion and survival.

3. Biomaterials in tissue engineering

Tissue engineering is a complex and interdisciplinary research field combining the knowledge of medical, biological and material scientists. In order to repair non-functional or missing tissue, cells are implanted in combination with biomaterial scaffolds that can be of natural or synthetic origin [46]. As the material applied for this purpose builds the basis for all following cellular interactions and reactions, the appropriate material design is crucial for the success of tissue engineering approaches [47].

3.1. Biocompatibility

Biomaterials are used in a wide range of applications [48] and should cause no unacceptable degree of harm in contact with tissue [49]. Nowadays, synthetic polymers, ceramics, glasses, carbons, and metal alloys are widely used as materials for medical applications [50, 51]. Still, foreign body reactions are a significant complication, that usually occur within the first 2-3 weeks after implantation [52, 53]. Therefore, research aims at the design of more biocompatible materials, but the definition of biocompatibility is not clear as there are various definitions found in literature. Williams defined biocompatibility as *"… the ability of a biomaterial to perform its desired function with respect to a medical therapy, without eliciting any undesirable local or systemic effects in the recipient or beneficiary of that therapy, but generating the most appropriate beneficial cellular or tissue response in that specific situation, and optimizing the clinically relevant performance of that therapy*" [49]. Before a biomaterial can be applied, materials have to be tested in *in vitro* and animal *in vivo* studies, as well as in human clinical trials [54] to ensure best biocompatibility.

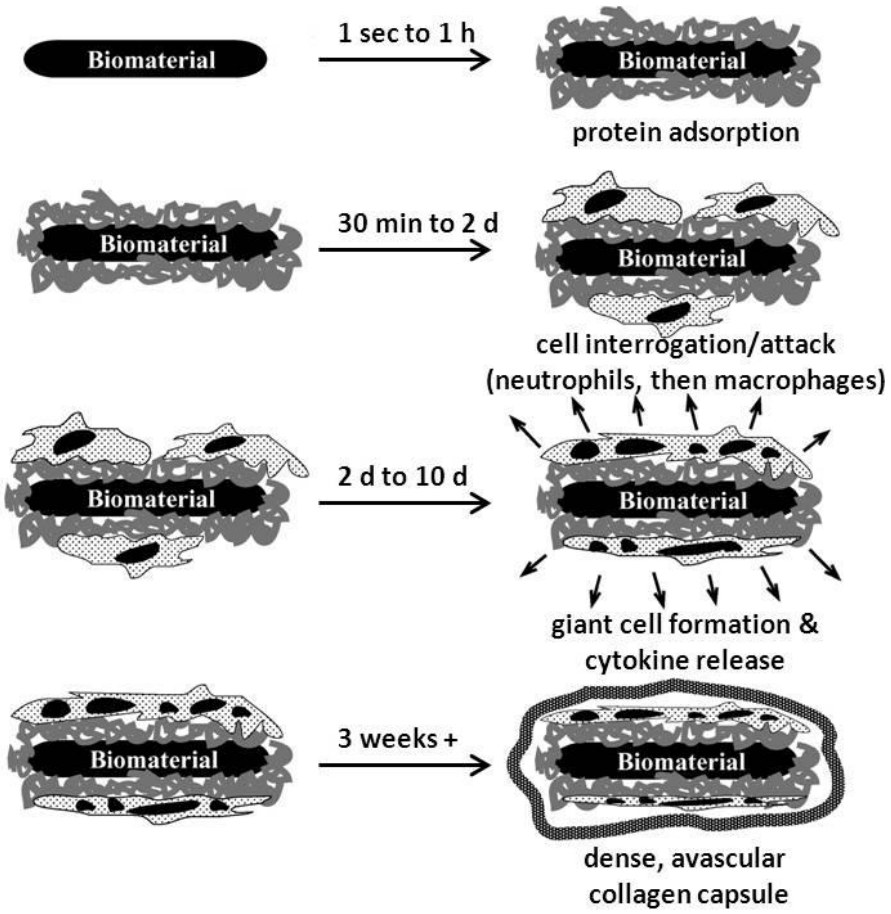

Figure 4: Immune response to a non-biocompatible material after implantation.
During implantation, biomaterials get into contact with body fluids like blood containing huge quantities of different proteins. These proteins adsorb on the surface leading to a cascade of immune reactions. Immune cells like macrophages attach to the layer of adsorbed proteins releasing signal molecules and the formation of giant cells. In the worst case, this results in the encapsulation and rejection of the material. Image modified from reference [55] with permission from Annual Reviews.

In a 'normal' wound the body has its effective mechanisms for healing, including macrophage activation. However, in presence of most biomaterials this healthy process is turned off, resulting in macrophage adhesion to the foreign material, activating unhealthy immune responses [48]. To gain control over cell-material interactions, one has to look at the interface of a material where these interactions with the biological system take place [48]. After injury, which is the first process to get a material in contact with a tissue, the material's surface gets in contact with body fluids like blood containing a mixture of more than 200 proteins [50, 52]. The almost immediate event occurring after implantation is the adsorption of proteins to the interface of the implant [48, 56] via hydrophobic interactions, followed by possible denaturation of the proteins [57], and subsequent attachment of cells [53] (Figure 4). The adsorption of proteins on surfaces depends on material characteristics such as wettability, surface charge, and structure [58]. Cell adhesion is thus rather mediated by the layer of surface adsorbed proteins than the material surface itself. Therefore, cells do not sense the material

surface anymore, but rather the protein layer on top of the material [59]. Immune cells like macrophages are attracted by the layer of non-specifically bound proteins triggering intra- and extracellular cascades of inflammation, like activation of the complement system and aggregation of platelets [48, 60]. As macrophages, which are responsible for the uptake and transport of constituents foreign to the body do not manage the uptake of large solids, this can lead to chronic inflammation and fibrous encapsulation of the material in collagen secreted by fibroblasts [48, 52]. In conclusion, biocompatibility of biomaterials highly depends on the inhibition of non-specific protein adsorption as a first step in a reaction cascade leading to inflammation [48].

3.2. Interfacial surface properties

Most biological reactions take place at surfaces [48]. The chemical as well as physical nature of a biomaterial should match the characteristics of the *in vivo* ECM in order to cause no harm at the site of implantation [5] and to fulfill the functions of the ECM. Cells adhere via integrins to surfaces, pull on the material and react with their cytoskeletal reorganization and phenotype to the surface properties [61]. Biomaterials with all kinds of surface properties are used nowadays including hyrophilic, hydrophobic, soft, or stiff materials [48]. In this paragraph some surface properties will be introduced to understand the complexity and variety of parameters influencing biocompatibility as well as cell fate.

One important parameter having an influence on cellular behavior is elasticity [41]. Tissue cells like fibroblasts sense matrix elasticity and adapt to the surface with e.g. changes in adhesion and cytoskeleton organization [41]. Engler et al. could show that matrix elasticity determines differentiation of stem cells [62]. They showed that soft matrices with an elastic modulus of around 1 kPa imitating brain tissue, directed mesenchymal stem cells (MSC) to differentiate into neuronal cells, whereas substrates with an elastic modulus of around 10 kPa led MSCs to differentiate into muscle cells [62]. On stiffer substrates (100 kPa) MSCs differentiated into osteoblasts [62].

Physical surface features like roughness and topographical structures (e.g. anisotropic lines, isotopic pits) are also known to have an impact on cellular reactions such as adhesion, spreading and cytoskeletal organization [63] as these surface parameters change the area of cell-surface interaction [64]. Already in the 1960s, nanoscale structures were shown to influence cell behavior [65]. Surface roughness of titanium and titanium-alloy were shown to

affect proliferation, differentiation, as well as protein synthesis of osteoblast-like cells [66]. The nano structuring of poly(lactic-*co*-glycolic acid) (PLGA) was shown to improve endothelial and smooth muscle cells adhesion [67].

It is important to consider, that the interaction of the material and the biological system takes place at the interface and that surface chemistry of materials is a major criterion that determines compatibility with the immune system [68]. It has been shown, that mammalian cells adhered better to hydrophilic than to hydrophobic surfaces [69]. Hydrophilic surfaces were shown to allow enhanced adhesion, spreading, and matrix secretion of osteoblast cells [70]. Additionally, a dependency of fibroblast adhesion on hydrophilicity was observed [71]. The distribution of CAMs that can be introduced to a surface via micro contact printing (MCP) has an impact on cell behavior, as well. Chen and coworkers showed, that flat surfaces with FN islands applied via MCP had a huge impact on human endothelial cell survival and DNA synthesis [44].

By only briefly introducing this great variety of surface characteristics which influence cell behavior, the complexity of the physical, cellular, and molecular processes important for biomaterial design and the study of cell-material interactions, is highlighted. This thesis focused on the control over surface chemistry. Hydrogels were used that prevent non-specific protein adsorption, which is the first step in a cascade of reactions that lead to undesired foreign body reactions [56]. Furthermore, it is necessary to think beyond chemical and biological inertness of the materials, which has been the focus in biocompatibility research for a long time [49]. Natural surfaces *in vivo* always interact via the specific presentation of interacting ligands such as proteins or polysaccharides [50]. Modern biomaterials require the mimicry of these specific interactions between cells and biomaterials in order to fulfill the high demands required for the application in tissue engineering [49]. Therefore, in a second step, specifically interacting molecules such as CAMs or signalling molecules have to be bound to per se inert surfaces in a way that preserves their biological function to allow specific interactions with the cells of interest.

3.3. Bioinert and bioactivated coatings

One strategy for the prevention of non-specific protein adsorption in order to achieve better biocompatibility is the coating of materials with inert layers. It has been shown that coatings such as self-assembled monolayers (SAMs) of alkanethiols on gold [57, 72-74] and hydrogels

[75] reduced or resisted non-specific protein adsorption. High grafting densities could be achieved with highly ordered SAMs on metal substrates (e.g. gold) resulting in excellent protein repellant surfaces [72-74]. Ostuni et al. screened SAMs bearing different functional groups for protein adsorption [76]. Those surfaces preventing non-specific protein adsorption were hydrophilic, acceptors for hydrogen-bonds, and electrically neutral [76]. Protein adsorption could also be prevented with linear poly(ethylene oxid) (PEO) chains at grafting densities where the chains stretch away from the surface (polymer brushes) [77]. Bioinert polymers have been investigated for the use as biomaterials such as the stable and transparent poly(hydroxyethyl methacrylate) (PHEMA) [78, 79] or the stable and elastic poly(vinyl alcohol) (PVA) [80]. PEO on glass was shown to inhibit platelet adsorption [81]. Higher grafting densities could be achieved by the use of star shaped PEO molecules as a result of a higher density of the molecules and a higher amount of reactive groups [82]. These molecules have been synthesized with various arm lengths and number of arms per molecule. The densest packing of star-shaped PEO could be achieved with low molecular weight molecules containing low numbers of arms [77]. Also poly(ethylene glycol) (PEG) has been intensely studied as an inert biomaterial as it is non-toxic, non-immunogenic and approved by the American food and drug administration (FDA) [68] and effectively reduced protein adsorption and cell adhesion [83].

To achieve specifically interacting surfaces, per se inert hydrogel coatings need to be functionalized with CAMs. The amount and type of CAMs presented on the surface determines the strength of cell adhesion [84]. PEG and PVA hydrogels have been chemically modified with specific cell adhesion mediating peptides to induce specific cell adhesion, proliferation, and migration [80, 85, 86]. In this thesis, coatings made of six arm star shaped amphiphilic polymers developed by Groll et al. were used to prevent non-specific protein adsorption and to induce specific interactions by functionalization the coatings with a variety of different cell adhesion mediating ligands [87].

3.4. Bioinert and bioactivated fibers

Many physiological cellular processes occur exclusively when cells are organized in a three-dimensional fashion [22]. Beside all the different characteristics, the dimensionality of a biomaterial determines cellular behavior to a great extend [14]. A two-dimensional substrate leads to a polarity of the adhering cells that is not found in the *in vivo* environment and often changes adhesion characteristics [88]. Ochsner et al. could show, that the third dimension in biomaterials altered fibroblast cytoskeleton assembly and metabolic activities, as well as

survival [61]. Therefore, research aims at the mimicry of the ECM by designing three-dimensional materials. Three-dimensional scaffolds should be highly porous, enabling cell growth and migration inside the pore network as well as allowing transport of nutrients and metabolic wastes to and from the inside of the scaffold [89]. With regard to the application as an implant, the scaffold should be degradable and should match the mechanical properties of the tissues at the site of implantation [89]. Different scientific approaches concerning the structural mimicry of the complex ECM fiber scaffold regarding to all mentioned requests have been investigated. A promising attempt is the fabrication of synthetic nanofiber meshes from biologically inert polymers by electrospinning [90]. Nanofibrous scaffolds could be produced by electrospinning that mimicked the structures found in the natural ECM of many cells that are important for cellular functions [91, 92]. Electrospun fiber scaffolds consist of fine and continuous fibers forming a highly porous scaffold with a high surface to volume ratio and tunable fiber diameter and pore size [91], thus enabling enhanced cell adhesion and proliferation as well as enhanced transport of nutrients [92]. Biodegradable as well as non-degradable fibers have been investigated for the fabrication of scaffolds for tissue engineering constructs [93-96]. Also, natural materials have been successfully electrospun into fibers [97, 98]. Poly(ε-caprolactone) fibers allowed bone marrow derived MSCs to differentiate into adipogenic, chondrogenic, and osteogenic lineages indicating the potential of three-dimensional fiber scaffolds for the use as biomaterials in tissue engineering [99].

As for two-dimensional materials or coatings, a major challenge for the fabrication of fiber scaffolds is the construction of a synthetic framework that combines the property of preventing undesired non-specific protein adsorption with a suitable surface chemistry for specific cell adhesion and proliferation. For two-dimensional substrates, the fabrication of protein repellent materials has been studied extensively [77] while the mentioned principles have often been neglected when designing three-dimensional fibrous scaffolds. Bioinert fibers with the potential to be functionalized for cell adhesion have been fabricated out of poly(ethylene glycol)-*block*-poly(D,L-lactide) by electrospinning, using a rather complicated set-up [100]. Chapter 10 will focus on the details of fiber scaffold research and describe a straight forward design of specifically interacting electrospun fibers [101].

4. Quantification of functionalization

For the design and fabrication of functional scaffolds, specific cell adhesion mediating ligands do not only need to be immobilized on a per se inert surface, but parameters such as ligand density [102] and distribution [103] have to be determined as they have an impact on cellular behavior. Addressing this important aspect, the subsequent part of this Chapter focuses on the quantification of ligands with classical as well as surface sensitive quantification methods and cell adhesion assays. Table 1 gives an overview about the advantages and disadvantages of the different quantification methods presented in this Chapter. None of the methods fulfills all requirements needed to allow profound quantification, namely being (1) fully quantitative, (2) surface sensitive, and (3) applicable to all kinds of biomaterials disregarding the material's characteristics like geometry. Therefore, the combination and comparison of different quantification methods as well as the correlation with cell adhesion experiments is indispensable.

Table 1: Methods for ligand quantification on biomaterials.

The optimal quantification method for ligands on biomaterials would fulfill three characteristics: being (1) fully quantitative, (2) surface sensitive, and (3) applicable to 'real' biomaterials. 'Real' biomaterials in this context, means all kinds of materials disregarding substrate and geometry properties. 7 methods introduced in this Chapter are compared with regard to these characteristics.

Quantification method	Quantitative?	Surface sensitive?	'Real' biomaterials?
Radiolabeling	+	-	+
XPS	semi	semi	+
TOF-SIMS	semi	semi	+
SPR	+	+	-
QCM	+	+	-
SAW	+	+	-
ELISA	semi	+	+
Cell adhesion	-	+	+

4.1. Classical quantification methods

The classical quantification methods which can be applied to determine ligand densities in biomaterials, presented in the scope of this thesis are radiolabeling, X-ray photoelectron spectroscopy (XPS), and time-of-flight secondary ion mass spectrometry (TOF-SIMS). While radiolabeling allows the determination of ligands throughout the bulk of the coating, XPS and TOF-SIMS measure surface near regions of materials. In this case, the penetration depth depends on the experimental set-up and the material characteristics.

4.1.1. Radiolabeling

Radiolabeling is a quantification method based on the substitution of an atom or ion by a stable radioactive isotope of the same element such as ^{131}I, ^{125}I, ^{14}C, and ^{3}H. The most common element that is used for labeling of proteins and peptides is the gamma emitter ^{125}I that can be introduced into tyrosine or imidazole residues. The subsequent detection of emitted gamma irradiation allows a precise conclusions about the amount of labeled ligands. Advantages of this method are its high selectivity and high sensitivity. The time consuming procedure and the quite risky work with radioactive materials are the drawbacks.

In 1962, Hunter and Greenwood developed a facile method for radiolabeling proteins [104]. This quantitative method allowed the analysis of protein adsorption on materials, e.g. the adsorption of peptides and proteins on plastic surfaces [105, 106] and SAMs [107], or the adsorption of ^{125}I labeled fibrinogen on PHEMA surfaces [108]. Poly(ethylene terephthalate) surfaces were modified with ^{125}I labeled collagen for surface concentration determination [109].

4.1.2. XPS

By means of XPS, the elemental and chemical composition as well as the electronic state of the elements in the first few nanometers of a material's surface can be semi-quantitatively analyzed [110]. During exposition of the surface to a monochromatic X-ray beam, electrons of the atoms present at the surface are activated and, when overcoming their characteristic binding energy, emitted from the material [111]. The detection and analysis of the energetic profile of the electrons allows conclusions about the surface chemistry [110, 112]. Using angle dependent measurements, depth profiles can be obtained.

XPS is a useful tool in biomaterial research. The step by step layer formation of PEG based polymer coatings on SAMs as well as the adsorption of proteins on top of these layers was observed with XPS [113]. XPS was also used to quantify carbohydrates immobilized on SAMs in various concentrations [114]. Proteins and peptides can be detected by determination of the amount of an atom, which is only present in the ligand molecule but not in the material itself. The adsorption and suppression of serum and ECM proteins like albumin, fibrinogen, or FN to different surfaces has already been determined by means of XPS [82, 105, 115]. Furthermore, ligands such as the ECM proteins FN and collagen were immobilized on polymer surfaces have

been detected by XPS [116]. Immobilization of RGD peptides on silicon, aluminia surfaces or PEO containing triblock copolymers has also been proven by XPS [117-119].

4.1.3. TOF-SIMS

TOF-SIMS is a sensitive, semi-quantitative technique analyzing elemental and chemical composition of the outermost molecular or atomic layers of a solid surface [112]. Beams of primary ions in the range of a few hundred eV to several keV (He^+, Ne^+, Ar^+, and Xe^+) are focused on a sample leading to fragmentation and bond breaking near the collision site, which results in the release of secondary molecular fragments including atoms, molecules, electrons, and ions from the upper two to three monolayers of the surface [120]. The information depth can be varied from 10 to 15 Å [50] by using different primary ions since smaller ions penetrate deeper into the material's surface compared to bigger ions. Additionally, the angle of the primary ion beam in relation to the surface and the material's composition determine the penetration depths of the ions. Secondary ions which are released from the material with specific mass to charge ratios, positively and negatively charged, allow the mapping of positive, as well as negative mass spectra [120]. These secondary ions can be detected by a TOF analyzing system providing significant information about surface chemistry [112, 120].

SIMS allowed determination of spectra specific for the material's surface [121]. Conformation and orientation of immobilized streptavidin (SA) on surfaces could be determined using TOF-SIMS [122]. Similarly, TOF-SIMS allowed conclusions about conformation of FN adsorbed on plastic surfaces [105]. The synthesis of RGD peptides on PEG monolayers to create enzyme-reactive surfaces was also monitored by TOF-SIMS [123]. Imaging TOF-SIMS was used to show antibody orientation on chemically patterned surfaces [124] and FN patterns on polymer surfaces [125]. Furthermore, the RGD concentration on PEO containing block copolymers was determined with TOF-SIMS [119].

4.2. Surface sensitive quantification methods

It is the surface of a biomaterial that determines cell fate as it is the interface between the substrate, proteins and cells that establishes the complex adhesion process. Surface plasmon resonance (SPR), quartz crystal microbalance (QCM), and surface acoustic wave (SAW) are techniques allowing the labeling free, surface sensitive, time resolved, and fully quantitative detection of protein binding to surfaces (Figure 5). Additionally, the enzyme linked immunosorbent assay (ELISA) will be introduced as promising, yet only semi-quantitative

method for ligand quantification on biomaterials. Last but not least, an insight into cell adhesion as a direct sensor of ligand densities will be given.

4.2.1. SPR

SPR provides a powerful tool for the surface characterization by optically monitoring molecular binding interactions between ligands immobilized on a metal surface such as gold or silver and a binding partner in a fluid environment [126] (Figure 5). Polarized light is focused on a gold layer in a specific angle, leading to the excitation of plasmons (free oscillating electrons) in the gold layer causing a loss of energy meaning that the reflected light is less energetic [127]. Total internal reflection and changes in the refractive index at the solvent/metal interface in correlation with adsorption of mass at the metal surface can be detected [127]. Dynamic interactions of any biological system with a surface can be measured in real-time without any need for labeling or complex sample preparation [127]. The change of the refractive index measured in reference units (RU) results from the binding of mass to the metal surface (gold, silver) or binding of mass to the coating on top of the metal surface [126]. SPR is suitable for the determination of association/dissociation kinetics and affinity constants.

With regard to biological applications, SPR has been demonstrated to be a useful technique for the establishment of biosensors as well as for characterization of any ligand interactions [126]. Dhayal and Ratner quantified glycan densities on SAMs via concanavalin A binding using SPR [114]. Mrksich et al. effectively demonstrated protein resistance of oligo(ethylene glycol) terminated SAMs on gold [128]. The influence of surface chemistry of SAMs on the adsorption of different proteins was compared using SPR and it could be shown, that PEG grafting on SAMs reduced protein adsorption from human plasma [129, 130]. Nevertheless, this method can only be applied to very thin model surfaces on metals like gold and is not suitable for biomaterials fabricated for *in vitro* or *in vivo* applications that cannot be produced as ultrathin films.

4.2.2. QCM

An acoustic quantification method that can be used for the surface sensitive quantification of ligands is QCM (Figure 5). A QCM can be seen as a bulk acoustic wave biosensor that can detect mass [131]. Due to the oscillation of a quartz plate (crystal), any mass binding on the surface can be detected as a frequency shift. As in SPR measurements, the distance of the interacting molecule, binding to the coating on the crystal surface, influences the sensitivity of the method. Therefore, coatings on the crystal need to by ultrathin. Even though this is an accepted method

for the sensitive detection of adsorption events [132], QCM has a rather low sensitivity of around 5 to 30 MHz, due to the low frequency used in this method [131].

Using QCM, Spangler et al. detected toxins with antibodies and used hydrazide terminated SAMs on gold to immobilize immunoglobulins capturing and detecting *Escherichia coli* [133]. Scott et al. revealed protein resistance of PEG coatings using QCM with dissipation monitoring (QCM-D) [134]. Different 2-hydroxylethylmethacrylate and poly(methyl-methacrylate) based hydrogels were checked for non-specific interaction with tear protein analogues, mucin, and cholesterol, using QCM-D and indicateed the suitability of these materials for the application as contact lenses [135]. Serizawa et al. followed the stepwise assembly of poly(vinylamine-*co*-*N*-vinylisobutyramide) and poly(acrylic acid) to form thermo-responsive hydrogels with QCM [136]. QCM was also used to quantify annexin A1 binding to phosphatidylserine containing lipid layers depending on the calcium ion concentration [137]. PEG functionalized SAM layers on gold surfaces were proven to resist proteins out of serum [138]. Even cell adhesion was followed in real-time using QCM [132, 139, 140].

4.2.3. SAW

Another possibility for surface sensitive quantification is the SAW technology (Figure 5). In principle, an acoustic wave propagates into a piezoelectric material and interactions at the sensor surface (binding of interacting molecules) change the frequency of the acoustic wave [131]. This acoustic method works at high frequencies of around 148 MHz and detects a shift in phase and amplitude. It has been reported to be more sensitive compared to QCM [131] since SAW functions with higher frequencies [141], thus, reducing the penetration of the acoustic wave into the liquid phase [142]. Still, one drawback is the need of ultrathin layers on e.g. gold, which may not be possible for all biomaterials.

Detections of proteins, carbohydrates, DNA, viruses, bacteria, and cells on surfaces was realized by SAW [131]. SAMs of alkanethiols with carboxy head groups on gold were functionalized with SA by carbodiimide chemistry detected by SAW [143]. Even hybridization of 20 base pair long DNA fragments could be detected with higher sensitivity compared to SPR [144].

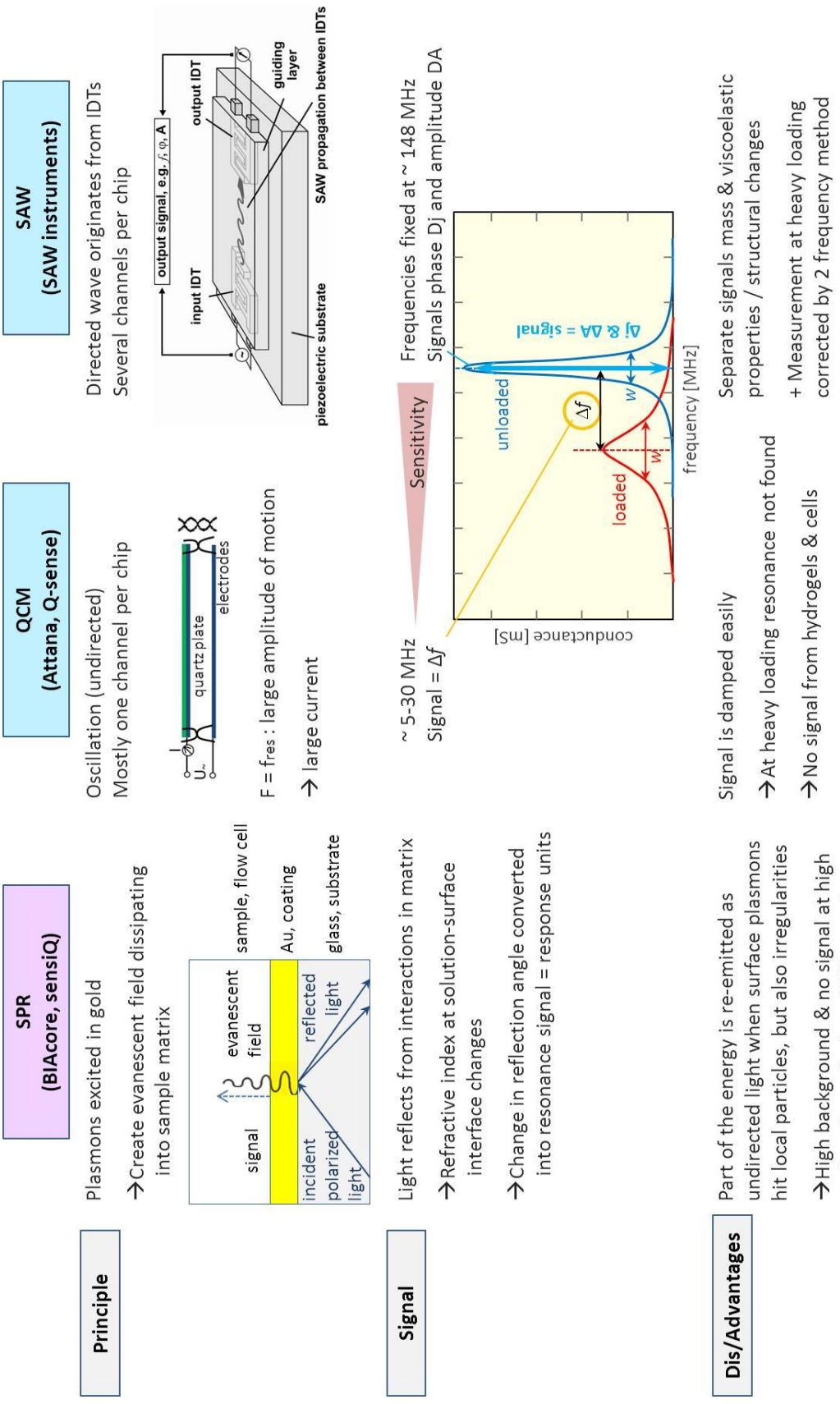

Figure 5: Comparison of surface sensitive quantification methods.

SPR, QCM and SAW are optical and acoustic surface sensitive quantification methods that can be applied on thin biomaterials on sensor surfaces. Here, the methods are compared regarding their technique, kind of signal and dis/advantages. Figure modified from a scheme that was kindly provided from SAW Instruments (Bonn, Germany).

4.2.4. ELISA

ELISA is a well-studied, surface sensitive, but semi-quantitative method that is based on specific binding interactions between antigens and antibodies. In comparison to QCM, SPR, and SAW, the substrate and geometry independent surface sensitive quantification of ligands is possible. In a first step, primary antibodies selectively bind with high affinity to ligands such as proteins or peptides that are immobilized on a surface. In a second step, these primary antibodies are detected via selective binding of a secondary antibody that is coupled to an enzyme such as phosphatase or peroxidase (POD). Finally, an enzymatic reaction results in the conversion of a substrate into a chromophore, that can be measured photometrically. Since antibodies provide a high affinity to their antigens, ELISA is highly selective and sensitive, but it is also cost intensive.

Vallières et al. used ELISA to determine the amount of FN bound to poly(tetrafluoroethylene) (teflon) surfaces [145]. Behravesh et al. quantified biotin surface concentrations on hydrogels using an anti-biotin antibody too big to diffuse into the hydrogel pores [146]. Bovine serum albumin (BSA) and bovine gamma globulin on titanium and stainless steel were also quantified using ELISA [147].

4.2.5. Cell adhesion

In order to obtain biomaterial surfaces with optimal cell adhesive properties, cell adhesion experiments on the established surfaces are of great importance. Cell adhesion experiments are not a direct quantification method in the sense that amounts of ligands bound to a surface can be measured. Still, it is important to correlate quantification results with the effect the ligands have on cell adhesion, spreading, proliferation, and vitality. The highest ligand density measured by surface sensitive quantification methods may not be the optimal concentration for cell adhesion and survival. The optimal ligand density could vary for different cell types or cells from different species. In addition, one has to consider that cells may not only bind to one ligand but spread and flatten out during the attachment process covering multiple ligands underneath one cell body.

Numerous studies aimed at the determination of minimal ligand concentrations or maximal ligand spacing on biomaterials for the best possible design of biomaterials. One has to keep in mind, that the use of different types of biomaterials, as well as ligands, and cells influence the outcome of these studies. In the 1980s, Hughes et al. determined a minimal FN spacing (FN

adsorbed on plastic) for fibroblast adhesion and spreading of 80 nm [148]. In contrast to this, in the 1990s, Underwood et al. determined a lower maximal FN spacing (FN adsorbed on plastic) of 37 nm necessary for endothelial and fibroblast cell adhesion [149]. Around the same time, RGD peptides on plastic were investigated and a minimal peptide spacing of only 16 and 22 nm was determined for fibroblast adhesion [106, 150]. Massia and Hubbell investigated RGD on glass and determined a maximal spacing of 440 nm for fibroblast adhesion and 140 nm for CMAC and stress fiber formation [103]. Investigation of cyclic RGD peptides on gold nanodots separated by inert PEG revealed a maximal spacing of 110 nm for fibroblast adhesion and 58 nm for CMAC formation [151]. A more detailed analysis of previous work in this field can be found in Chapter 7.

The introduced classical quantification methods are feasible techniques to quantify ligand densities on biomaterials. These methods were used for ligand quantification in functionalized hydrogel layers in **Chapter 3** and **4**. However these methods do not exclusively measure the amount of ligands accessible for cells at the material interface. Hence, surface sensitive quantification methods as well as cell adhesion experiments needed to be performed to fully characterize the functionalized hydrogels used in this thesis. These approaches were applied on functionalized hydrogels in **Chapter 5**, **6** and **7**. A comparison of all quantification approaches is given in **Chapter 8**. **Chapter 9** and **10** present a biochemical and structural ways of ECM mimicry to make another step towards optimal and ECM mimetic biomaterials.

5. References

1. Williams, D.F. On the nature of biomaterials. *Biomaterials* **2009**, 30 (30) 5897-909.
2. Tanzer, M.L. Current concepts of extracellular matrix. *Journal of Orthopaedic Science* **2006**, 11 (3) 326-31.
3. Geiger, B.; Bershadsky, A.; Pankov, R. and Yamada, K.M. Transmembrane extracellular matrix-cytoskeleton crosstalk. *Nature Reviews Molecular Cell Biology* **2001**, 2 (11) 793-805.
4. Alberts, B.; Johnson, A. and Lewis, J. Molecular Biology of the Cell. *Garland Science* New York **2002**.
5. Ma, Z.W.; Kotaki, M.; Inai, R. and Ramakrishna, S. Potential of nanofiber matrix as tissue-engineering scaffolds. *Tissue Engineering* **2005**, 11 (1-2) 101-09.
6. Aumailley, M. and Gayraud, B. Structure and biological activity of the extracellular matrix. *Journal of Molecular Medicine-Jmm* **1998**, 76 (3-4) 253-65.
7. Franz, S.; Rammelt, S.; Scharnweber, D. and Simon, J.C. Immune responses to implants - A review of the implications for the design of immunomodulatory biomaterials. *Biomaterials* **2011**, 32 (28) 6692-709.
8. Daley, W.P.; Peters, S.B. and Larsen, M. Extracellular matrix dynamics in development and regenerative medicine. *Journal of Cell Science* **2008**, 121 (3) 255-64.
9. Raeber, G.P.; Lutolf, M.P. and Hubbell, J.A. Molecularly engineered PEG hydrogels: A novel model system for proteolytically mediated cell migration. *Biophysical Journal* **2005**, 89 (2) 1374-88.
10. Nishida, T.; Yasumoto, K.; Otori, T. and Desaki, J. The network structure of corneal fibroblasts in the rat as revealed by scanning electron-microscopy. *Investigative Ophthalmology & Visual Science* **1988**, 29 (12) 1887-90.
11. Griffith, L.G. and Swartz, M.A. Capturing complex 3D tissue physiology in vitro. *Nature Reviews Molecular Cell Biology* **2006**, 7 (3) 211-24.
12. Varki, A.; Cummings, R.D.; Esko, J.D.; Freeze, H.H.; Stanley, P.; Bertozzi, C.R.; Hart, G.W. and Etzler, M.E. Essentials of glycobiology. *Cold Spring Harbor Laboratory Press* Cold Spring Harbor (NY) **2009**.
13. Dudhia, J. Aggrecan, aging and assembly in articular cartilage. *Cellular and Molecular Life Sciences* **2005**, 62 (19-20) 2241-56.
14. Badylak, S.F. Regenerative medicine and developmental biology: The role of the extracellular matrix. *Anat Rec B New Anat* **2005**, 287 (1) 36-41.
15. von der Mark, K.; Park, J.; Bauer, S. and Schmuki, P. Nanoscale engineering of biomimetic surfaces: cues from the extracellular matrix. *Cell and Tissue Research* **2009**, 339 (1) 131-53.
16. Poole, K.; Khairy, K.; Friedrichs, J.; Franz, C.; Cisneros, D.A.; Howard, J. and Mueller, D. Molecular-scale topographic cues induce the orientation and directional movement of fibroblasts on two-dimensional collagen surfaces. *Journal of Molecular Biology* **2005**, 349 (2) 380-86.
17. Rosso, F.; Giordano, A.; Barbarisi, M. and Barbarisi, A. From cell–ECM interactions to tissue engineering. *Journal of Cellular Physiology* **2004**, 199 (2) 174-80.
18. Gumbiner, B.M. Cell adhesion: The molecular basis of tissue architecture and morphogenesis. *Cell* **1996**, 84 (3) 345-57.

19. Hynes, R.O. Integrins: Versatility, modulation, and signaling in cell adhesion. *Cell* **1992**, 69 (1) 11-25.

20. Hynes, R.O. Integrins: A family of cell surface receptors. *Cell* **1987**, 48 (4) 549-54.

21. Giancotti, F.G. and Ruoslahti, E. Transduction - Integrin signaling. *Science* **1999**, 285 (5430) 1028-32.

22. Lutolf, M.P. and Hubbell, J.A. Synthetic biomaterials as instructive extracellular microenvironments for morphogenesis in tissue engineering. *Nature Biotechnology* **2005**, 23 (1) 47-55.

23. Zhu, J.H.; Luo, B.H.; Xiao, T.; Zhang, C.Z.; Nishida, N. and Springer, T.A. Structure of a complete integrin ectodomain in a physiologic resting state and activation and deactivation by applied forces. *Molecular Cell* **2008**, 32 (6) 849-61.

24. Geiger, B.; Spatz, J.P. and Bershadsky, A.D. Environmental sensing through focal adhesions. *Nature Reviews Molecular Cell Biology* **2009**, 10 (1) 21-33.

25. Hynes, R.O. Integrins: Bidirectional, allosteric signaling machines. *Cell* **2002**, 110 (6) 673-87.

26. Zamir, E. and Geiger, B. Molecular complexity and dynamics of cell-matrix adhesions. *Journal of Cell Science* **2001**, 114 (20) 3583-90.

27. Miyamoto, S.; Teramoto, H.; Coso, O.A.; Gutkind, J.S.; Burbelo, P.D.; Akiyama, S.K. and Yamada, K.M. Integrin function - Molecular hierarchies of cytoskeletal and signaling molecules. *Journal of Cell Biology* **1995**, 131 (3) 791-805.

28. Lock, J.G.; Wehrel-Haller, B. and Strömblad, S. Cell-matrix adhesion complexes: Master control machinery of cell migration. *Seminars in Cancer Biology* **2008**, 18 (1) 65-76.

29. Duband, J.L.; Rocher, S.; Chen, W.T.; Yamada, K.M. and Thiery, J.P. Cell-adhesion and migration in the early vertebrate emryo - Location and possible role of the putative fibronectin receptor complex. *Journal of Cell Biology* **1986**, 102 (1) 160-78.

30. Izzard, C.S. and Lochner, L.R. Cell-to-substrate contacts in living fibroblasts - Interference reflection study with an evaluation of technique. *Journal of Cell Science* **1976**, 21 (1) 129-59.

31. Stupack, D.G. and Cheresh, D.A. Get a ligand, get a life: integrins, signaling and cell survival. *Journal of Cell Science* **2002**, 115 (19) 3729-38.

32. Malgorzata, B.; Carracedo, S. and Gullberg, D. Integrins. *Cell and Tissue Research* **2010**, 339 (1) 269-80.

33. Xiong, J.-P.; Stehle, T.; Zhang, R.; Joachimiak, A.; Frech, M.; Goodman, S.L. and Arnaout, M.A. Crystal structure of the axtracellular segment of integrin αvβ3 in complex with an Arg-Gly-Asp ligand. *Science* **2002**, 296 (5565) 151-55.

34. Buck, C.A. and Horwitz, A.F. Cell surface receptors for extracellular matrix molecules. *Annual Review of Cell Biology* **1987**, 3 179-205.

35. Plow, E.F.; Haas, T.K.; Zhang, L.; Loftus, J. and Smith, J.W. Ligand binding to integrins. *Journal of Biological Chemistry* **2000**, 275 (29) 21785-88.

36. Ruoslahti, E. RGD and other recognition sequences for integrins. *Annual Review of Cell and Developmental Biology* **1996**, 12 (1) 697-715.

37. Pankov, R. and Yamada, K.M. Fibronectin at a glance. *Journal of Cell Science* **2002**, 115 (20) 3861-63.

38. Pierschbacher, M.D. and Ruoslahti, E. Cell Attachment Activity of Fibronectin Can Be Duplicated by Small Synthetic Fragments of the Molecule. *Nature* **1984**, 309 (5963) 30-33.

39. Humphries, J.D.; Byron, A. and Humphries, M.J. Integrin ligands at a glance. *Journal of Cell Science* **2006**, 119 (19) 3901-03.

40. Haas, T.A. and Plow, E.F. Integrin ligand interactions - A year in review. *Current Opinion in Cell Biology* **1994**, 6 (5) 656-62.

41. Discher, D.E.; Janmey, P. and Wang, Y.L. Tissue cells feel and respond to the stiffness of their substrate. *Science* **2005**, 310 (5751) 1139-43.

42. Folkman, J. and Moscona, A. Role of cell-shape on growth-control. *Nature* **1978**, 273 (5661) 345-49.

43. Gilmore, A.P. Anoikis. *Cell Death and Differentiation* **2005**, 12 1473-77.

44. Chen, C.S.; Mrksich, M.; Huang, S.; Whitesides, G.M. and Ingber, D.E. Geometric control of cell life and death. *Science* **1997**, 276 (5317) 1425-28.

45. Garcia, A.J.; Vega, M.D. and Boettiger, D. Modulation of cell proliferation and differentiation through substrate-dependent changes in fibronectin conformation. *Molecular Biology of the Cell* **1999**, 10 (3) 785-98.

46. Nerem, R.M. Cellular engineering. *Annals of Biomedical Engineering* **1991**, 19 (5) 529-45.

47. Langer, R. and Vacanti, J.P. Tissue engineering. *Science* **1993**, 260 (5110) 920-26.

48. Castner, D.G. and Ratner, B.D. Biomedical surface science: Foundations to frontiers. *Surface Science* **2002**, 500 (1-3) 28-60.

49. Williams, D.F. On the mechanisms of biocompatibility. *Biomaterials* **2008**, 29 (20) 2941-53.

50. Ratner, B.D. The engineering of biomaterials exhibiting recognition and specificity. *Journal of Molecular Recognition* **1996**, 9 (5-6) 617-25.

51. Huebsch, N. and Mooney, D.J. Inspiration and application in the evolution of biomaterials. *Nature* **2009**, 462 (7272) 426-32.

52. Anderson, J.M. Biological responses to materials. *Annual Review of Materials Research* **2001**, 31 81-110.

53. Puleo, D.A. and Nanci, A. Understanding and controlling the bone-implant interface. *Biomaterials* **1999**, 20 (23-24) 2311-21.

54. Peppas, N.A. and Langer, R. New challanges in biomaterials. *Science* **1994**, 263 (5154) 1715-20.

55. Ratner, B.D. and Bryant, S.J. Biomaterials: Where we have been and where we are going. *Annual Review of Biomedical Engineering* **2004**, 6 41-75.

56. Ratner, B.D. and Bryant, S.J. Biomaterials: Where we have been and where we are going. *Annual Review of Biomedical Engineering* **2004**, 6 (1) 41-75.

57. Ostuni, E.; Yan, L. and Whitesides, G.M. The interaction of proteins and cells with self-assembled monolayers of alkanethiolates on gold and silver. *Colloids and Surfaces B-Biointerfaces* **1999**, 15 (1) 3-30.

58. Altankov, G.; Grinnell, F. and Groth, T. Studies on the biocompatibility of materials: Fibroblast reorganization of substratum-bound fibronectin on surfaces varying in wettability. *Journal of Biomedical Materials Research* **1996**, 30 (3) 385-91.

59. Wilson, C.J.; Clegg, R.E.; Leavesley, D.I. and Pearcy, M.J. Mediation of biomaterial-cell interactions by adsorbed proteins: A review. *Tissue Engineering* **2005**, 11 (1-2) 1-18.

60. Hoffmann, J.; Groll, J.; Heuts, J.; Rong, H.; Klee, D.; Ziemer, G.; Moeller, M. and Wendel, J.P. Blood cell and plasma protein repellent properties of Star-PEG-modified surfaces. *Journal of Biomaterials Science, Polymer Edition* **2006**, 17 985-96.

61. Ochsner, M.; Textor, M.; Vogel, V. and Smith, M.L. Dimensionality controls cytoskeleton assembly and metabolism of fibroblast cells in response to rigidity and shape. *Plos One* **2010**, 5 (3) e9445.

62. Engler, A.J.; Sen, S.; Sweeney, H.L. and Discher, D.E. Matrix elasticity directs stem cell lineage specification. *Cell* **2006**, 126 (4) 677-89.

63. Lim, J.Y. and Donahue, H.J. Cell sensing and response to micro- and nanostructured surfaces produced by chemical and topographic patterning. *Tissue Engineering* **2007**, 13 (8) 1879-91.

64. Schwartz, Z. and Boyan, B.D. Underlying mechanisms at the bone-biomaterial interface. *Journal of Cellular Biochemistry* **1994**, 56 (3) 340-47.

65. Rosenberg, M.D. Cell guidance by alterations in monomolecular films. *Science* **1963**, 139 (355) 411-&.

66. Lincks, J.; Boyan, B.D.; Blanchard, C.R.; Lohmann, C.H.; Liu, Y.; Cochran, D.L.; Dean, D.D. and Schwartz, Z. Response of MG63 osteoblast-like cells to titanium and titanium alloy is dependent on surface roughness and composition. *Biomaterials* **1998**, 19 (23) 2219-32.

67. Miller, D.C.; Thapa, A.; Haberstroh, K.M. and Webster, T.J. Endothelial and vascular smooth muscle cell function on poly(lactic-co-glycolic acid) with nano-structured surface features. *Biomaterials* **2004**, 25 (1) 53-61.

68. Peppas, N.A.; Hilt, J.Z.; Khademhosseini, A. and Langer, R. Hydrogels in biology and medicine: From molecular principles to bionanotechnology. *Advanced Materials* **2006**, 18 (11) 1345-60.

69. Grinnell, F.; Milam, M. and Srere, P.A. Studies on cell adhesion. 2. Adhesion of cells to surfaces of diverse chemical composition and inhibition of adhesion by sulfhydryl binding reagents. *Archives of Biochemistry and Biophysics* **1972**, 153 (1) 193-&.

70. Redey, S.A.; Nardin, M.; Bernache-Assolant, D.; Rey, C.; Delannoy, P.; Sedel, L. and Marie, P.J. Behavior of human osteoblastic cells on stoichiometric hydroxyapatite and type A carbonate apatite: Role of surface energy. *Journal of Biomedical Materials Research* **2000**, 50 (3) 353-64.

71. Hallab, N.J.; Bundy, K.J.; O'Connor, K.; Moses, R.L. and Jacobs, J.J. Evaluation of metallic and polymeric biomaterial surface energy and surface roughness characteristics for directed cell adhesion. *Tissue Engineering* **2001**, 7 (1) 55-71.

72. Mrksich, M. and Whitesides, G.M. Using self-assembled monolayers to understand the interactions of man-made surfaces with proteins and cells. *Annual Review of Biophysics and Biomolecular Structure* **1996**, 25 55-78.

73. Prime, K.L. and Whitesides, G.M. Self-assembled organic monolayers - Model systems for studying adsorption of proteins at surfaces. *Science* **1991**, 252 (5009) 1164-67.

74. Prime, K.L. and Whitesides, G.M. Adsorption of proteins onto surfaces containing end-attached oligo(ethylene oxide) - a model system using self-assembled monolayers. *Journal of the American Chemical Society* **1993**, 115 (23) 10714-21.

75. Lee, K.Y. and Mooney, D.J. Hydrogels for tissue engineering. *Chemical Reviews* **2001**, 101 (7) 1869-79.

76. Ostuni, E.; Chapman, R.G.; Holmlin, R.E.; Takayama, S. and Whitesides, G.M. A survey of structure-property relationships of surfaces that resist the adsorption of protein. *Langmuir* **2001**, 17 (18) 5605-20.

77. Gasteier, P.; Reska, A.; Schulte, P.; Salber, J.; Offenhausser, A.; Moeller, M. and Groll, J. Surface grafting of PEO-based star-shaped molecules for bioanalytical and biomedical applications. *Macromolecular Bioscience* **2007**, 7 (8) 1010-23.

78. Kidane, A.; Szabocsik, J.M. and Park, K. Accelerated study on lysozyme deposition on poly(HEMA) contact lenses. *Biomaterials* **1998**, 19 (22) 2051-55.

79. Lu, S.X. and Anseth, K.S. Photopolymerization of multilaminated poly(HEMA) hydrogels for controlled release. *Journal of Controlled Release* **1999**, 57 (3) 291-300.

80. Nuttelman, C.R.; Mortisen, D.J.; Henry, S.M. and Anseth, K.S. Attachment of fibronectin to poly(vinyl alcohol) hydrogels promotes NIH3T3 cell adhesion, proliferation, and migration. *Journal of Biomedical Materials Research* **2001**, 57 (2) 217-23.

81. Merrill, E.W.; Salzman, E.W.; Wan, S.; Mahmud, N.; Kushner, L.; Lindon, J.N. and Curme, J. Platelet-compatible hydrophilic segmented polyurethanes from polyethylene glycols and cyclohexane diisocyanate. *Transactions American Society for Artificial Internal Organs* **1982**, 28 482-87.

82. Sofia, S.J.; Premnath, V. and Merrill, E.W. Poly(ethylene oxide) grafted to silicon surfaces: Grafting density and protein adsorption. *Macromolecules* **1998**, 31 (15) 5059-70.

83. Zhang, M.; Desai, T. and Ferrari, M. Proteins and cells on PEG immobilized silicon surfaces. *Biomaterials* **1998**, 19 (10) 953-60.

84. Rezania, A.; Thomas, C.H.; Branger, A.B.; Waters, C.M. and Healy, K.E. The detachment strength and morphology of bone cells contacting materials modified with a peptide sequence found within bone sialoprotein. *Journal of Biomedical Materials Research* **1997**, 37 (1) 9-19.

85. Hern, D.L. and Hubbell, J.A. Incorporation of adhesion peptides into nonadhesive hydrogels useful for tissue resurfacing. *Journal of Biomedical Materials Research* **1998**, 39 (2) 266-76.

86. Temenoff, J.S. and Mikos, A.G. Injectable biodegradable materials for orthopedic tissue engineering. *Biomaterials* **2000**, 21 (23) 2405-12.

87. Groll, J.; Fiedler, J.; Engelhard, E.; Ameringer, T.; Tugulu, S.; Klok, H.A.; Brenner, R.E. and Moeller, M. A novel star PEG-derived surface coating for specific cell adhesion. *Journal of Biomedical Materials Research Part A* **2005**, 74A (4) 607-17.

88. Cukierman, E.; Pankov, R.; Stevens, D.R. and Yamada, K.M. Taking cell-matrix adhesions to the third dimension. *Science* **2001**, 294 (5547) 1708-12.

89. Hutmacher, D.W. Scaffolds in tissue engineering bone and cartilage. *Biomaterials* **2000**, 21 (24) 2529-43.

90. Pham, Q.P.; Sharma, U. and Mikos, A.G. Electrospinning of polymeric nanofibers for tissue engineering applications: A review. *Tissue Engineering* **2006**, 12 (5) 1197-211.

91. Kumbar, S.G.; James, R.; Nukavarapu, S.P. and Laurencin, C.T. Electrospun nanofiber scaffolds: Engineering soft tissues. *Biomedical Materials* **2008**, 3 (3) 1-15.

92. Sill, T.J. and von Recum, H.A. Electro spinning: Applications in drug delivery and tissue engineering. *Biomaterials* **2008**, 29 (13) 1989-2006.

93. Kim, K.; Yu, M.; Zong, X.H.; Chiu, J.; Fang, D.F.; Seo, Y.S.; Hsiao, B.S.; Chu, B. and Hadjiargyrou, M. Control of degradation rate and hydrophilicity in electrospun non-woven poly(D,L-lactide) nanofiber scaffolds for biomedical applications. *Biomaterials* **2003**, 24 (27) 4977-85.

94. Henry, J.A.; Simonet, M.; Pandit, A. and Neuenschwander, P. Characterization of a slowly degrading biodegradable polyesterurethane for tissue engineering scaffolds. *Journal of Biomedical Materials Research Part A* **2007**, 82A (3) 669-79.

95. Chuangchote, S. and Supaphol, P. Fabrication of aligned poly(vinyl alcohol) nanofibers by electrospinning. *Journal of Nanoscience and Nanotechnology* **2006**, 6 (1) 125-29.

96. Kenawy, E.R.; Layman, J.M.; Watkins, J.R.; Bowlin, G.L.; Matthews, J.A.; Simpson, D.G. and Wnek, G.E. Electrospinning of poly(ethylene-co-vinyl alcohol) fibers. *Biomaterials* **2003**, 24 (6) 907-13.

97. Zhong, S.P.; Teo, W.E.; Zhu, X.; Beuerman, R.W.; Ramakrishna, S. and Yung, L.Y.L. An aligned nanofibrous collagen scaffold by electrospinning and its effects on in vitro fibroblast culture. *Journal of Biomedical Materials Research Part A* **2006**, 79A (3) 456-63.

98. Ji, Y.; Ghosh, K.; Shu, X.Z.; Li, B.Q.; Sokolov, J.C.; Prestwich, G.D.; Clark, R.A.F. and Rafailovich, M.H. Electrospun three-dimensional hyaluronic acid nanofibrous scaffolds. *Biomaterials* **2006**, 27 (20) 3782-92.

99. Li, W.J.; Tuli, R.; Huang, X.X.; Laquerriere, P. and Tuan, R.S. Multilineage differentiation of human mesenchymal stem cells in a three-dimensional nanofibrous scaffold. *Biomaterials* **2005**, 26 (25) 5158-66.

100. Grafahrend, D.; Calvet, J.L.; Klinkhammer, K.; Salber, J.; Dalton, P.D.; Moller, M. and Klee, D. Control of protein adsorption on functionalized electrospun fibers. *Biotechnology and Bioengineering* **2008**, 101 (3) 609-21.

101. Grafahrend, D.; Heffels, K.-H.; Beer, M.V.; Gasteier, P.; Möller, M.; Boehm, G.; Dalton, P.D. and Groll, J. Degradable polyester scaffolds with controlled surface chemistry combining minimal protein adsorption with specific bioactivation. *Nat Mater* **2011**, 10 (1) 67-73.

102. Palecek, S.P.; Loftus, J.C.; Ginsberg, M.H.; Lauffenburger, D.A. and Horwitz, A.F. Integrin-ligand binding properties govern cell migration speed through cell-substratum adhesiveness. *Nature* **1997**, 385 (6616) 537-40.

103. Massia, S.P. and Hubbell, J.A. An RGD spacing of 440nm is sufficient for integrin alpha-V-beta-3-mediated fibroblast spreading and 140nm for focal contact and stress fiber formation. *Journal of Cell Biology* **1991**, 114 (5) 1089-100.

104. Hunter, W.M. and Greenwood, F.C. Preparation of iodine-131 labelled human growth hormone of high specific activity. *Nature* **1962**, 194 (4827) 495-96.

105. Lhoest, J.B.; Detrait, E.; van den Bosch de Aguilar, P. and Bertrand, P. Fibronectin adsorption, conformation, and orientation on polystyrene substrates studied by radiolabeling, XPS, and ToF SIMS. *Journal of Biomedical Materials Research* **1998**, 41 (1) 95-103.

106. Danilov, Y.N. and Juliano, R.L. (Arg-Gly-Asp)n-albumin conjugates as a model substratum for integrin-mediated cell-adhesion. *Experimental Cell Research* **1989**, 182 (1) 186-96.

107. Capadona, J.R.; Collard, D.M. and Garcia, A.J. Fibronectin adsorption and cell adhesion to mixed monolayers of tri(ethylene glycol)- and methyl-terminated alkanethiols. *Langmuir* **2003**, 19 (5) 1847-52.

108. Lopez, G.P.; Ratner, B.D.; Rapoza, R.J. and Horbett, T.A. Plasma deposition of ultrathin films of poly(2-hydroxyethyl methacrylate) - Surface analysis and protein adsoprtion measurements. *Macromolecules* **1993**, 26 (13) 3247-53.

109. Bisson, I.; Kosinski, M.; Ruault, S.; Gupta, B.; Hilborn, J.; Wurm, F. and Frey, P. Acrylic acid grafting and collagen immobilization on poly(ethylene terephthalate) surfaces for adherence and growth of human bladder smooth muscle cells. *Biomaterials* **2002**, 23 (15) 3149-58.

110. Hauert, R. and Keller, B.A. Chemical surface analysis with nanometer depth resolution. *Chimia* **2006**, 60 (11) A800-A04.

111. Merrett, K.; Cornelius, R.M.; Mcclung, W.G.; Unsworth, L.D. and Sheardown, H. Surface analysis methods for characterizing polymeric biomaterials. *Journal of Biomaterial Science - Polymer Edition* **2002**, 13 (6) 593-621.

112. Liu, H. and Webster, T.J. Nanomedicine for implants: A review of studies and necessary experimental tools. *Biomaterials* **2007**, 28 (2) 354-69.

113. Beyer, M.; Felgenhauer, T.; Bischoff, F.R.; Breitling, F. and Stadler, V. A novel glass slide-based peptide array support with high functionality resisting non-specific protein adsorption. *Biomaterials* **2006**, 27 (18) 3505-14.

114. Dhayal, M. and Ratner, D.A. XPS and SPR analysis of glycoarray surface density. *Langmuir* **2009**, 25 (4) 2181-87.

115. Michel, R.; Pasche, S.; Textor, M. and Castner, D.G. Influence of PEG architecture on protein adsorption and conformation. *Langmuir* **2005**, 21 (26) 12327-32.

116. Zhu, Y.B.; Chian, K.S.; Chan-Park, M.B.; Mhaisalkar, P.S. and Ratner, B.D. Protein bonding on biodegradable poly(L-lactide-co-caprolactone) membrane for esophageal tissue engineering. *Biomaterials* **2006**, 27 (1) 68-78.

117. Davis, D.H.; Giannoulis, C.S.; Johnson, R.W. and Desai, T.A. Immobilization of RGD to < 111 > silicon surfaces for enhanced cell adhesion and proliferation. *Biomaterials* **2002**, 23 (19) 4019-27.

118. Popat, K.C.; Swan, E.E.L. and Desai, T.A. Modeling of RGDC film parameters using X-ray photoelectron spectroscopy. *Langmuir* **2005**, 21 (16) 7061-65.

119. Neff, J.A.; Tresco, P.A. and Caldwell, K.D. Surface modification for controlled studies of cell-ligand interactions. *Biomaterials* **1999**, 20 (23-24) 2377-93.

120. Belu, A.M.; Graham, D.J. and Castner, D.G. Time-of-flight secondary ion mass spectrometry: Techniques and applications for the characterization of biomaterial surfaces. *Biomaterials* **2003**, 24 (21) 3635-53.

121. Perez-Luna, V.H.; Hooper, K.A.; Kohn, J. and Ratner, B.D. Surface characterization of tyrosine-derived polycarbonates. *Journal of Applied Polymer Science* **1997**, 63 (11) 1467-79.

122. Kim, Y.P.; Hong, M.Y.; Kim, J.; Oh, E.; Shon, H.K.; Moon, D.W.; Kim, H.S. and Lee, T.G. Quantitative analysis of surface-immobilized protein by TOF-SIMS: Effects of protein orientation and trehalose additive. *Analytical Chemistry* **2007**, 79 (4) 1377-85.

123. Todd, S.J.; Scurr, D.J.; Gough, J.E.; Alexander, M.R. and Ulijn, R.V. Enzyme-activated RGD ligands on functionalized poly(ethylene glycol) monolayers: Surface analysis and cellular response. *Langmuir* **2009**, 25 (13) 7533-39.

124. Liu, F.; Dubey, M.; Takahashi, H.; Castner, D.G. and Grainger, D.W. Immobilized antibody orientation analysis using secondary ion mass spectrometry and fluorescence imaging of affinity-generated patterns. *Analytical Chemistry* 82 (7) 2947-58.

125. Zhang, Z.P.; Yoo, R.; Wells, M.; Beebe, T.P.; Biran, R. and Tresco, P. Neurite outgrowth on well-characterized surfaces: preparation and characterization of chemically and spatially controlled fibronectin and RGD substrates with good bioactivity. *Biomaterials* **2005**, 26 (1) 47-61.

126. Rich, R.L. and Myszka, D.G. Advances in surface plasmon resonance biosensor analysis. *Current Opinion in Biotechnology* **2000**, 11 (1) 54-61.

127. Green, R.J.; Frazier, R.A.; Shakesheff, K.M.; Davies, M.C.; Roberts, C.J. and Tendler, S.J.B. Surface plasmon resonance analysis of dynamic biological interactions with biomaterials. *Biomaterials* **2000**, 21 (18) 1823-35.

128. Mrksich, M.; Sigal, G.B. and Whitesides, G.M. Surface plasmon resonance permits in situ measurement of protein adsorption on self-assembled monolayers of alkanethiolates on gold *Langmuir* **1995**, 11 (11) 4383-85.

129. Servoli, E.; Maniglio, D.; Aguilar, M.R.; Motta, A.; Roman, J.S.; Belfiore, L.A. and Migliaresi, C. Quantitative analysis of protein adsorption via atomic force microscopy and surface plasmon resonance. *Macromolecular Bioscience* **2008**, 8 (12) 1126-34.

130. Emmenegger, C.R.; Brynda, E.; Riedel, T.; Sedlakova, Z.; Houska, M. and Alles, A.B. Interaction of blood plasma with antifouling surfaces. *Langmuir* **2009**, 25 (11) 6328-33.

131. Rocha-Gaso, M.-I.; March-Iborra, C.; Montoya-Baides, Á. and Arnau-VIves, A. Surface generated acoustic wave biosensors for the detection of pathogens: A review *Sensors* **2009**, 9 (7) 5740-69.

132. Wegener, J.; Janshoff, A. and Galla, H.J. Cell adhesion monitoring using a quartz crystal microbalance: comparative analysis of different mammalian cell lines. *European Biophysics Journal with Biophysics Letters* **1998**, 28 (1) 26-37.

133. Spangler, B.D. and Tyler, B.J. Capture agents for a quartz crystal microbalance-continuous flow biosensor: functionalized self-assembled monolayers on gold. *Analytica Chimica Acta* **1999**, 399 (1-2) 51-62.

134. Scott, J.E. Extracellular-Matrix, Supramolecular Organization and Shape. *Journal of Anatomy* **1995**, 187 259-69.

135. Lord, M.S.; Stenzel, M.H.; Simmons, A. and Milthorpe, B.K. The effect of charged groups on protein interactions with poly(HEMA) hydrogels. *Biomaterials* **2006**, 27 (4) 567-75.

136. Serizawa, T.; Nanameki, K.; Yamamoto, K. and Akashi, M. Thermoresponsive ultrathin hydrogels prepared by sequential chemical reactions. *Macromolecules* **2002**, 35 (6) 2184-89.

137. Kastl, K.; Ross, M.; Gerke, V. and Steinem, C. Kinetics and thermodynamics of annexin A1 binding to solid-supported membranes: A QCM study. *Biochemistry* **2002**, 41 (31) 10087-94.

138. Menz, B.; Knerr, R.; Gopferich, A. and Steinem, C. Impedance and QCM analysis of the protein resistance of self-assembled PEGylated alkanethiol layers on gold. *Biomaterials* **2005**, 26 (20) 4237-43.

139. Knerr, R.; Weiser, B.; Drotleff, S.; Steinem, C. and Gopferich, A. Measuring cell adhesion on RGD-modified, self-assembled PEG monolayers using the quartz crystal microbalance technique. *Macromolecular Bioscience* **2006**, 6 (10) 827-38.

140. Li, J.; Thielemann, C.; Reuning, U. and Johannsmann, D. Monitoring of integrin-mediated adhesion of human ovarian cancer cells to model protein surfaces by quartz crystal resonators: evaluation in the impedance analysis mode. *Biosensors & Bioelectronics* **2005**, 20 (7) 1333-40.

141. Länge, K.; Rapp, B.E. and Rapp, M. Surface acoustic wave biosensors: A review. *Analytical and Bioanalytical Chemistry* **2008**, 391 (5) 1509-19.

142. Smith, J.P. and Hinson-Smith, V. The new era of SAW devices. Commercial SAW sensors move beyond military and security applications. *Analytical Chemistry* **2006**, 78 (11) 3505-07.

143. SAW-Instruments Alkanethiol Surfaces: 2D surfaces with reactive head groups. *SAW instruments application note* **2010**, 7 1-2.

144. SAW-Instruments Properties of DNA: Biochemical characterization using phase and amplitude signal. *SAW instruments application note* **2010**, 12 1-2.

145. Vallieres, K.; Petitclerc, E. and Laroche, G. Covalent grafting of fibronectin onto plasma-treated PTFE: Influence of the conjugation strategy on fibronectin biological activity. *Macromolecular Bioscience* **2007**, 7 (5) 738-45.

146. Behravesh, E.; Sikavitsas, V.I. and Mikos, A.G. Quantification of ligand surface concentration of bulk-modified biomimetic hydrogels. *Biomaterials* **2003**, 24 (24) 4365-74.

147. Merritt, K.; Edwards, C.R. and Brown, S.A. Use of an enzyme linked immunosorbent assay (ELISA) for quantification of proteins on the surface of materials. *Journal of Biomedical Materials Research* **1988**, 22 (2) 99-109.

148. Hughes, R.C.; Pena, S.D.J.; Clark, J. and Dourmashkin, R.R. Molecular requirements for the adhesion and spreading of hamster fibroblasts. *Experimental Cell Research* **1979**, 121 (2) 307-14.

149. Underwood, P.A. and Bennett, F.A. A comparison of the biological-activities of the cell-adhesive proteins vitronectin and fibronectin. *Journal of Cell Science* **1989**, 93 641-49.

150. Singer, II; Kawka, D.W.; Scott, S.; Mumford, R.A. and Lark, M.W. The fibronectin cell attachment sequence Arg-Gly-Asp-Ser promotes focal contact formation during early fibroblast attachment and spreading. *Journal of Cell Biology* **1987**, 104 (3) 573-84.

151. Cavalcanti-Adam, E.A.; Micoulet, A.; Blummel, J.; Auernheimer, J.; Kessler, H. and Spatz, J.P. Lateral spacing of integrin ligands influences cell spreading and focal adhesion assembly. *European Journal of Cell Biology* **2006**, 85 (3-4) 219-24.

I Classical quantification

Detailed characterization of biomaterials is very important in order to understand and control their interactions with biological systems. In case of bioactivated, per se inert biomaterials, the ligand concentration needs to be quantified as it is known that this parameter is critical for cellular behavior. In this part of the thesis, three classical methods for the quantification of ligands in NCO-sP(EO-*stat*-PO) hydrogel coatings will be presented: radiolabeling (Chapter 3), X-ray photoelectron spectrometry (XPS), and time of flight secondary ion mass spectroscopy (TOF-SIMS) (Chapter 4). This first part of this thesis focused on 'classical' quantification methods that are not surface sensitive.

CHAPTER 3

Peptide binding capacities as determined by radiolabeling

Interaction of biomaterials with cells and tissue is a highly sensitive interplay depending on a variety of factors. It is well known that non-specific interaction with proteins needs to be minimized on materials getting in contact with body fluids to prevent undesired immune responses. Nevertheless, specifically interacting ligands need to be presented on such inert surfaces to allow specific interactions with cells and the tissue of interest. Best possible characterization of materials is necessary to gain control over the cell-material interactions. One key parameter of this characterization is the determination of ligand concentration in and on the biomaterial. This Chapter focused on the determination of the RGD peptide binding capacity of NCO-sP(EO-*stat*-PO) hydrogel films in 96-well plates as well as on glass. Small aliquots of ^{125}I-YRGDS mixed with GRGDS peptides were covalently immobilized in the hydrogels by incubation of fresh coatings or by mixing the peptides with the prepolymer solution before the coating process. Radiodetection of the peptides indicated a maximal binding capacity when coatings were incubated with ligand solution of 600 µg/mL, while no saturation could be reached using the mix-in method.

1. Introduction

As the RGD ligand concentration determines cell adhesion in contact with the material [1-6], the quantification of ligand concentration is extremely important and a variety of methods can be used for this purpose. Radiolabeling is a highly sensitive and fully quantitative method [7] and enables quantification of the ligands in a biomaterial throughout the whole depth. Additionally, this method is very useful for biomaterial research as the characteristics of the material, such as thickness, softness, or roughness do not have an impact on the method. Radiolabeling was often used to determine protein adsorption on surfaces [8-10]. Also, cell adhesion mediating ligands immobilized to biomaterials have been quantified using radiolabeling [5, 11-13].

The NCO-sP(EO-*stat*-PO) hydrogel system used in this thesis was established and characterized before [14]. Nevertheless, the ligand concentration after functionalization has not been determined so far. Here, the focus lay on the determination of the ligand binding capacity of NCO-sP(EO-*stat*-PO) hydrogels using radiolabeling. This implies the detection of ligands in the bulk hydrogel coating. The transfer of the coating procedure on glass and silicon [14] to amino functionalized CovaLink^{TM} 96-well plates was done as reported before [15]. Hydrogels were functionalized with different GRGDS concentrations by incubation of aqueous GRGDS solutions on fresh coatings still containing functional isocyanate groups, as well as by mixing GRGDS with the aqueous prepolymer solution before the coating procedure. Adding small aliquots of ^{125}I-YRGDS to the GRGDS solutions allowed the detection of irradiation in a gamma counter. Functionalization by incubation reached a maximum of GRGDS binding at GRGDS concentrations of around 600 µg/mL. Using different molar GRGDS to prepolymer ratios, no maximal ligand binding was reached.

2. Experimental section

2.1. Hydrogel coatings

2.1.1. NCO-sP(EO-stat-PO) synthesis

Isocyanate terminated prepolymers (NCO-sP(EO-*stat*-PO)) were synthesized as described in detail elsewhere [16]. In short, the prepolymer was fabricated by the reaction of hydroxyl terminated star shaped polyether polyole with isophorone diisocyanate (IPDI).

2.1.2. Preparation of glass surfaces

Glass substrates (Ø 15 mm, Paul Marienfeld, Lauda-Königshofen, Germany) were polished with isopropanol and successively cleaned in acetone, distilled water, and isopropanol in an ultrasonic bath for 5 min each followed by drying in a stream of nitrogen. Solvents were purchased from Prolabo (Darmstadt, Germany). Glass substrates were activated by O_2-plasma treatment in the plasma process plant AK 330 (Roth & Rau, Hohenstein-Ernstthal, Germany) for 15 min (400 W, 50 sccm, 0.4 mbar). Afterwards, glass substrates were left in a desiccator containing 100 µl 3-aminopropyl-trimethoxysilan (AS) at 5 mbar for 60 min. After removal of AS, the glass substrates were left in a vacuum of minimum 10^{-2} mbar for 1 h and stored at 250 mbar.

2.1.3. NCO-sP(EO-stat-PO) coating

In 96-well plates

The coating procedure has been described earlier [15]. Prepolymers were dissolved in tetrahydrofuran (THF, dried over sodium, VWR, Darmstadt, Germany). After adding water to the solution (9/1 v/v mixture of water/THF, prepolymer concentration 10 mg/mL), prepolymers crosslinked for 5 min. For the coating procedure, 400 µL of the solution were filled in each well of a CovaLink^{TM}NH 96-well plate (NUNC, Langenselbold, Germany). After 10 min incubation at room temperature, leftover polymer solution was removed.

On glass

The coating procedure has been described earlier [14]. Prepolymers were solubilized in tetrahydrofuran (THF, dried over sodium, Prolabo, Darmstadt, Germany). After adding water to the solution (9/1 v/v water/THF, prepolymer concentration 10 mg/ml), prepolymers were left for crosslinking for 5 min. Two droplets of the solution were placed on the aminosilanized surface of a glass substrate after filtration through a 0.2 µm syringe filter (Whatman, Dassel,

Germany). The coating process was carried out in the spin coater WS-400-B-6NPP/LITE (Laurell Technologies, North Wales, USA) at 2,500 rpm for 40 sec with an acceleration time of 5 sec. Each prepolymer solution was used to coat a maximum of 6 substrates. Coated substrates were stored at room temperature for at least 12 h to ensure complete crosslinking of the coating.

2.1.4. Radioisotopic labeling

YRGDS (Bachem, Bubendorf, Switzerland) was radiolabeled with carrier-free $Na^{125}I$ (NEZ0033A, PerkinElmer, Rodgau, Germany) using a modified chloramine T procedure [17]. 10 µg YRGDS in 10 µg 0.4 M sodium phosphate buffer (pH 7.5) and 300 µCi $Na^{125}I$ were combined in a 1.5 mL plastic tube. Iodination was started by adding 1 µg of chloramine T in 5 µL 0.04 M sodium phosphate buffer and stirring for 5 min at room temperature. After this time another 1 µg chloramine T was added and the reaction was continued for 25 min. Subsequently, the reaction was transferred to a Sep-Pak C18 cartridge (Waters Corporation, Eschborn, Germany) that had been equilibrated with TFA/CH_3CN (9/1). After washing, the radioiodinated derivative was eluted with 50% CH_3CN in 0.1% TFA in fractions of 1 mL. The radiochemical purity was 99.5% by analytical RP-HPLC and the isolated yield of desired product was 176 µCi. Typical specific activity of the labeled peptide was between 0.2 x $1,0^{16}$ and 2 x $1,0^{16}$ cpm/mol. ^{125}I-YRGDS was stored at -20°C in the dark until needed. Under these conditions, no radiolytic decomposition was observed.

2.1.5. Functionalization

Incubation method

GRGDS peptide was purchased from Bachem (Bubendorf, Switzerland). GRGDS was solubilized in sodium carbonate buffer (0.02 M Na_2CO_3/$NaHCO_3$, pH 9.4). Small aliquots of radiolabeled ^{125}I-YRGDS were added to each solution. 50 µL ligand solution were incubated on coated wells and 100 µL on coated glass substrates (1 h after preparation of the coatings) with ligand concentrations of 100 to 1,000 µg/mL. Coatings were washed 3 times with deionized water.

Mix-in method

Prior to the coating procedure, GRGDS and small aliquots of radiolabeled ^{125}I-YRGDS were added to the prepolymer solution in different molar peptide to prepolymer ratios and the coating process was performed as described above. GRGDS was used in molar ligand to prepolymer ratios of 1/10 to 2/1.

2.2. Coating characterization by radioisotopic measurement

Coatings were washed 3 times with distilled water and measured in a LB 2111 Multi Crystal Gamma Counter (Berthold Technologies, Bad Wildbach, Germany).

3. Results and discussion

Coating of glass slides, silicon substrates [14], or silicone rubbers [18] with NCO-sP(EO-*stat*-PO) require surface pre-treatment steps such as activation with UV/O_3 or oxygen plasma and amino functionalization through reaction with AS. Therefore, coatings were transferred to commercially available amino functional 96-well plates as described before [15]. Without any further surface treatment of the well plates, wells could be coated by facile incubation of the prepolymer solution in the wells for 10 min. Coatings were shown to minimize non-specific protein adsorption and cell adhesion of primary human dermal fibroblasts (HDF). With this coating system for glass surfaces and well plates at hands, various studies on this inert system in different formats, presenting different ligands, can be performed.

Radiolabeling is a straight forward method allowing the absolute quantification of labeled substances in a biomaterial. Additionally, it is extremely sensitive, detecting labeled ligands in small amounts throughout the whole depth of the material and therefore, small aliquots of ^{125}I-YRGDS mixed with GRGDS were sufficient for detection in the hydrogel. Both peptides bound to the isocyanate groups of the fresh hydrogel coatings (incubation method) or of the prepolymers in solution prior to the coating procedure (mix-in method) respectively via their N-terminal amino groups. With known molar ratios of the ^{125}I-YRGDS to GRGDS, the amount of bound peptide can be calculated after Radiodetection of the labeled peptide in the coatings. Nevertheless, relative peptide amounts in the hydrogels are shown in Figure 1, to indicate maximal binding capacity of the hydrogels.

In this Chapter, NCO-sP(EO-*stat*-PO) hydrogel coatings in 96-well plates and on glass were functionalized by incubation of fresh coatings with ligand solutions of different concentration (incubation method) and by mixing the peptides with the prepolymer solution before coating in different molar peptide to prepolymer ratios (mix-in method). Using the incubation method on coatings in well plates, a slight increase in peptide amount could be detected (Figure 1A). Still, standard deviations were quite high allowing only the estimation of a maximum reached between 300 and 700 µg/mL. On glass substrates, an increase in peptide binding could be measured as well, reaching a maximum at 600 µg/mL (Figure 1B). Previously, coatings on glass have been well characterized with coating thicknesses of 30 +/- 5 nm [19]. Thicknesses of coatings in the well plates have not been determined so far. Additionally to the possible difference in thickness, the structure of the crosslinked hydrogel coatings could vary on glass compared to coatings in plastic wells. Peptides incubated on fresh coatings (1 h after

preparation), which were not fully crosslinked yet, bound to remaining isocyanate groups. The rather small peptides could diffuse into the coatings during the incubation of 1 h. Different hydrogel characteristics could explain an earlier maximum reached for coatings in well plates due to thicker or less crosslinked coatings allowing more peptides to diffuse into the hydrogels.

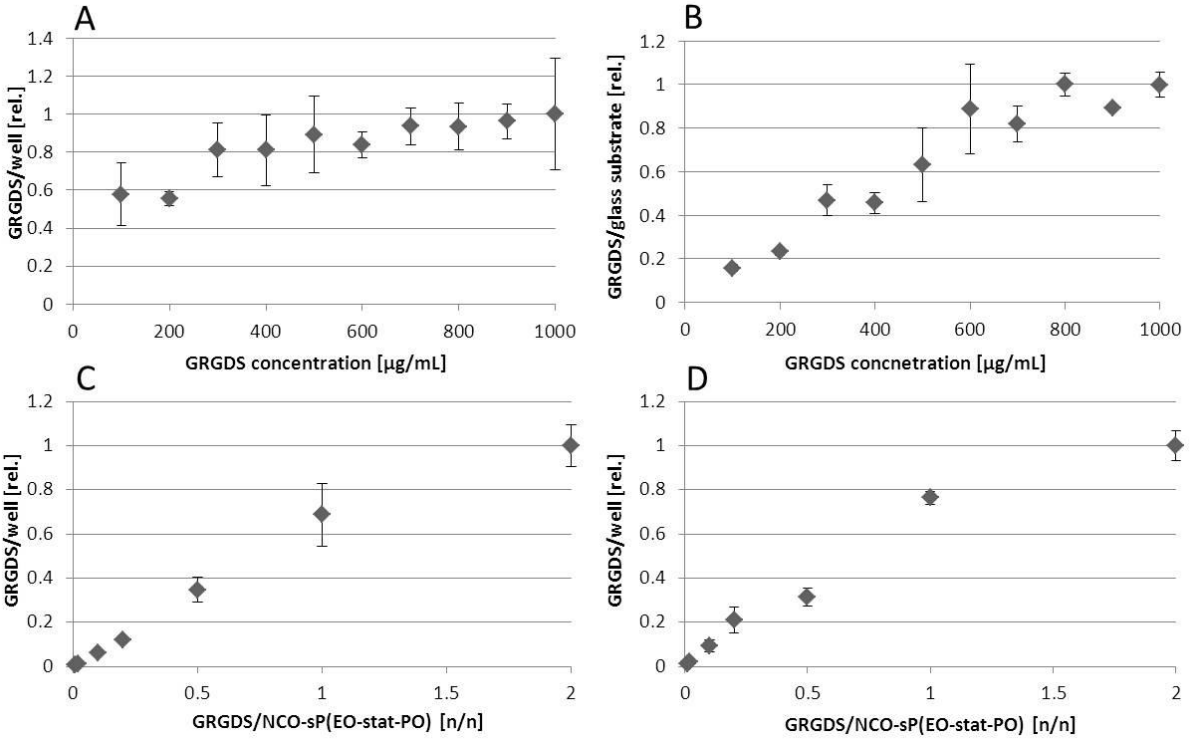

Figure 1: Radioisotopic quantification of ligands in hydrogels.

Relative comparison of GRGDS amounts on NCO-sP(EO-*stat*-PO) hydrogel coatings by radioisotopic measurement. Coatings in 96-well plates (A, C) and on glass (B, D) were functionalized by the incubation method (A, B) and the mix-in method (C, D) using different concentrations of GRGDS and small aliquots of ^{125}I-YRGDS.

Using the mix-in method, an increase of peptide binding could be measured with increasing peptide to prepolymer ratio (1/10 – 2/1). The maximal ligand to prepolymer ratio of 2/1 means that statistically 2 arms of each prepolymer were occupied with a peptide and 4 arms per prepolymer were left for crosslinking. Even though no maximal ligand concentration was reached in coatings in well plates and on glass, higher ligand concentrations were not used to ensure that complete crosslinking of the hydrogels was not affected.

4. Conclusions

Radiodetection of ^{125}I labeled peptide ligands in NCO-sP(EO-*stat*-PO) hydrogel coatings allowed the straight forward determination of ligand binding capacities of the hydrogel system. Functionalizing the hydrogel coatings in well plates and on glass by incubation of fresh coatings, a maximal ligand binding was reached for peptide solutions of around 600 µg/mL. Using the mix-in method for functionalization with different peptide to prepolymer ratios, no maximal ligand binding capacity was reached.

Even though, handling radiolabeled materials requires extreme care, the possibilities of this quantification method justify the time consuming procedure. This quantification method can be transferred to other biomaterial functionalized with any kind of radiolabeled ligand. Nevertheless, biomaterial research requires the quantification of ligands at the interface, thus accessible for cells and proteins because this interface determines biocompatibility of biomaterials. After ligand quantification of surface near regions in Chapter 4, Chapter 5 to 7 will present surface sensitive quantification methods including direct cell studies. A comparison of the different methods will be shown in Chapter 8, where radiolabeling will be used for fully quantitative ligand detection at the interface of amino reactive well plates.

5. References

1. Liu, J.C. and Tirrell, D.A. Cell response to RGD density in cross-linked artificial extracellular matrix protein films. *Biomacromolecules* **2008**, 9 (11) 2984-88.
2. Hughes, R.C.; Pena, S.D.J.; Clark, J. and Dourmashkin, R.R. Molecular requirements for the adhesion and spreading of hamster fibroblasts. *Experimental Cell Research* **1979**, 121 (2) 307-14.
3. Humphries, M.J.; Akiyama, S.K.; Komoriya, A.; Olden, K. and Yamada, K.M. Identification of an alternatively spliced site in human-plasma fibronectin that mediates cell type-specific adhesion. *Journal of Cell Biology* **1986**, 103 (6) 2637-47.
4. Massia, S.P. and Hubbell, J.A. An RGD spacing of 440nm is sufficient for integrin alpha-V-beta-3-mediated fibroblast spreading and 140nm for focal contact and stress fiber formation. *Journal of Cell Biology* **1991**, 114 (5) 1089-100.
5. Neff, J.A.; Tresco, P.A. and Caldwell, K.D. Surface modification for controlled studies of cell-ligand interactions. *Biomaterials* **1999**, 20 (23-24) 2377-93.
6. Cavalcanti-Adam, E.A.; Volberg, T.; Micoulet, A.; Kessler, H.; Geiger, B. and Spatz, J.P. Cell spreading and focal adhesion dynamics are regulated by spacing of integrin ligands. *Biophysical Journal* **2007**, 92 (8) 2964-74.
7. Dawids, S.G. Test procedures for the blood compatibility of biomaterials. *Springer Netherlands* **1993**, 317.
8. Lhoest, J.B.; Detrait, E.; van den Bosch de Aguilar, P. and Bertrand, P. Fibronectin adsorption, conformation, and orientation on polystyrene substrates studied by radiolabeling, XPS, and ToF SIMS. *Journal of Biomedical Materials Research* **1998**, 41 (1) 95-103.
9. Capadona, J.R.; Collard, D.M. and Garcia, A.J. Fibronectin adsorption and cell adhesion to mixed monolayers of tri(ethylene glycol)- and methyl-terminated alkanethiols. *Langmuir* **2003**, 19 (5) 1847-52.
10. Lopez, G.P.; Ratner, B.D.; Rapoza, R.J. and Horbett, T.A. Plasma deposition of ultrathin films of poly(2-hydroxyethyl methacrylate) - Surface analysis and protein adsoprtion measurements. *Macromolecules* **1993**, 26 (13) 3247-53.
11. Hern, D.L. and Hubbell, J.A. Incorporation of adhesion peptides into nonadhesive hydrogels useful for tissue resurfacing. *Journal of Biomedical Materials Research* **1998**, 39 (2) 266-76.
12. Bisson, I.; Kosinski, M.; Ruault, S.; Gupta, B.; Hilborn, J.; Wurm, F. and Frey, P. Acrylic acid grafting and collagen immobilization on poly(ethylene terephthalate) surfaces for adherence and growth of human bladder smooth muscle cells. *Biomaterials* **2002**, 23 (15) 3149-58.
13. Barber, T.A.; Harbers, G.M.; Park, S.; Gilbert, M. and Healy, K.E. Ligand density characterization of peptide-modified biomaterials. *Biomaterials* **2005**, 26 (34) 6897-905.
14. Groll, J.; Ameringer, T.; Spatz, J.P. and Moeller, M. Ultrathin coatings from isocyanate-terminated star PEG prepolymers: Layer formation and characterization. *Langmuir* **2005**, 21 (5) 1991-99.
15. Kasten, A.; Müller, P.; Bulnheim, U.; Groll, J.; Bruellhoff, K.; Beck, U.; Steinhoff, G.; Möller, M. and Rychly, J. Mechanical integrin stress and magnetic forces induce biological responses in mesenchymal stem cells which depend on environmental factors. *Journal of Cellular Biochemistry* **2010**, 111 (6) 1586-97.
16. Götz, H.; Beginn, U.; Bartelink, C.F.; Grünbauer, H.J.M. and Möller, M. Preparation of isophorone diisocyanate terminated star polyethers. *Macromolecular Materials and Engineering* **2002**, 287 (4) 223-30.

17. Hunter, W.M. and Greenwood, F.C. Preparation of iodine-131 labelled human growth hormone of high specific activity. *Nature* **1962**, 194 (4827) 495-96.

18. Salber, J.; Grater, S.; Harwardt, M.; Hofmann, M.; Klee, D.; Dujic, J.; Huang, J.H.; Ding, J.D.; Kippenberger, S.; Bernd, A.; Groll, J.; Spatz, J.P. and Moller, M. Influence of different ECM mimetic peptide sequences embedded in a nonfouling environment on the specific adhesion of human-skin keratinocytes and fibroblasts on deformable substrates. *Small* **2007**, 3 (6) 1023-31.

19. Groll, J.; Fiedler, J.; Engelhard, E.; Ameringer, T.; Tugulu, S.; Klok, H.A.; Brenner, R.E. and Moeller, M. A novel star PEG-derived surface coating for specific cell adhesion. *Journal of Biomedical Materials Research Part A* **2005**, 74A (4) 607-17.

CHAPTER 4

Ligand density determination in hydrogels by XPS and TOF-SIMS

After the bulk quantification using radiolabling, this Chapter focused on XPS and TOF-SIMS, which are more surface sensitive compared to radiolabeling but still have a certain penetration depth into materials depending on the experimental set-up and characteristics (e.g. softness) of the material. XPS and TOF-SIMS are sensitive analytical methods, however not fully quantitative. They were successfully applied on functionalized NCO-sP(EO-*stat*-PO) hydrogel coatings to detect maximum ligand binding capacities of the hydrogel system. It is advantageous, that these methods can be applied to all kinds of biomaterials disregarding the material's characteristics.

1. Introduction

The determination of ligand densities has been subject to biomaterial research for a long time in order to characterize biomaterials and control cell-material interactions. Different quantification methods can be used for this purpose. As described in Chapter 2, most quantification methods do not fulfill all requirements necessary for optimal biomaterial characterization. On the one hand, methods should be fully quantitative like radiolabeling (Chapter 3), on the other hand, they should be surface sensitive like surface plasmon resonance (SPR), surface acoustic wave technology (SAW), or enzyme linked immunosorbent assay (ELISA) (Chapter 5 and 6). Additionally, they should be applicable to all kinds of biomaterials, which is the case for XPS and TOF-SIMS. Even though, XPS and TOF-SIMS are not fully quantitative or surface sensitive, they are important methods to compare. Having a much lower penetration depth into materials compared to radiolabeling without being completely surface sensitive [1], they can give an insight into the ligand distribution in the bulk hydrogel when comparing with other quantification methods.

Surface spectroscopic XPS is a well-established method for biomaterial analysis [2]. By measuring the elemental composition of the upper 5 to 10 nm of a material [1, 3], conclusions about chemical composition of the material can be drawn. The formation of self-assembled monolayers (SAM) was followed by XPS [4]. Also, resistance of inert surfaces towards serum and ECM proteins like albumin, fibrinogen, lysozyme, and fibronectin adsorption could be shown [5-9]. Not only the adsorption of proteins, but also the immobilization of protein or peptide ligands to materials can be detected. Immobilized RGD peptides were identified on poly(caprolactone) (PCL), dextran, silicon, and poly(ethylene oyxid) (PEO) triblock copolymers using XPS by increased nitrogen to carbon ratio [10-16].

TOF-SIMS, which probes only around 1 nm into a surface [1], depending on the material characteristics and the experimental set-up, is sensitive enough to detect physical and chemical changes at a material's surface [17]. Resistance of poly(ethylene glycol) surfaces towards lysozyme and fibronectin protein adsorption was probed by XPS as well as TOF-SIMS [5]. Even though XPS showed resistance toward protein adsorption, TOF-SIMS could detect very low, but significant protein adsorption in positive spectra indicating the higher sensitivity of TOF-SIMS compared to XPS. Also, immobilized RGD peptides were identified on PEO containing block copolymers [15]. Not only the presence of proteins or peptides was possible, even

conformational changes of immobilized streptavidin (SA) on surfaces could be shown by TOF-SIMS [18].

In this Chapter, XPS and TOF-SIMS were presented as suitable methods for the determination of maximum ligand binding capacities of the NCO-sP(EO-*stat*-PO) hydrogel system. As ligands, a fluorinated amino acid and an iodinated peptide were covalently immobilized to the hydrogel coatings in molar ligand to prepolymer ratios of 1/2, 1/1, and 2/1. Both methods revealed the same maximal ligand binding capacity of the hydrogels at molar ligand to prepolymer ratios of 1/1.

2. Experimental section

2.1. Hydrogel coatings

2.1.1. NCO-sP(EO-stat-PO) synthesis

Isocyanate terminated prepolymers (NCO-sP(EO-*stat*-PO)) were synthesized as described in detail elsewhere [19]. In short, the prepolymer was fabricated by the reaction of hydroxyl terminated star shaped polyether polyole with isophorone diisocyanate (IPDI).

2.1.2. Preparation of silicon surfaces

1 cm^2 silicon wafer (CrysTecKristall-technologie, n-Type, Berlin, Germany) were successively cleaned in acetone, distilled water, and isopropanol in an ultrasonic bath for 5 min each followed by drying in a stream of nitrogen. Solvents were purchased from Prolabo (Darmstadt, Germany). Glass substrates were activated by O_2-plasma treatment in the plasma process plant AK 330 (Roth & Rau, Hohenstein-Ernstthal, Germany) for 15 min (400 W, 50 sccm, 0.4 mbar). Afterwards, glass substrates were left in a desiccator containing 100 µl 3-aminopropyl-trimethoxysilan (AS) at 5 mbar for 60 min. After removal of AS, the glass substrates were left in a vacuum of minimum 10^{-2} mbar for 1 h and stored at 250 mbar.

2.1.3. NCO-sP(EO-stat-PO) coatings

The coating procedure has been described earlier [20]. Prepolymers were solubilized in tetrahydrofuran (THF, dried over sodium, Prolabo, Darmstadt, Germany). After adding water to the solution (9/1 v/v water/THF, prepolymer concentration 10 mg/ml), prepolymers were left for crosslinking for 5 min. Two droplets of the solution were placed on the aminosilanized surface of a glass substrate after filtration through a 0.2 µm syringe filter (Whatman, Dassel, Germany). The coating process was carried out in the spin coater WS-400-B-6NPP/LITE (Laurell Technologies, North Wales, USA) at 2,500 rpm for 40 sec with an acceleration time of 5 sec. Each prepolymer solution was used to coat a maximum of 6 substrates. Coated substrates were stored at room temperature for at least 12 h to ensure complete crosslinking of the coating.

2.1.4. Functionalization

Ligands were solubilized in water and mixed with the NCO-sP(EO-*stat*-PO) solution in THF to a final prepolymer concentration of 10 mg/mL. The 4-(trifluoromethyl)-DL-phenylalanine (fluorinated amino acid) from Fluorochem (Derbyshire, England) and the peptide KGRGDSP-3,5-diiodo-Y (iodinated peptide) from Bachem (Bubendorf, Switzerland) were used in ligand to

prepolymer ratios of 1/2, 1/1, and 2/1. Coatings were stored for at least 12 h at room temperature to assure complete crosslinking before further usage.

2.2. Coating characterization

2.2.1. Ellipsometry

For determination of coating thicknesses on silicon, the spectroscopic ellipsometer M2000D (J.A. Woollam Co., Lincoln, England) was used with a wave length between 195 and 1700 nm and an angle of incidence of 67, 70 and 75°.

2.2.2. XPS

Elemental composition of hydrogel coatings on silicon was measured with the X-ray photoelectron spectrometer AXIS ULTRA (Kratos, Manchester, England) using a monochromatic Al K (alpha) X-ray source with an energy of 1486.7 eV and an angle of 60° (compared to the perpendicular of the surface). The X-ray anode was used with a potential of 15 kV and an emission of 15 mA (225 W). A magnetic lens was placed under the sample to efficiently collect photoelectrons into the analyzer. The concentrical, half-spherical analyzer had a constant transmission modulus. Measurements were performed in ultra-high vacuum.

2.2.3. TOF-SIMS

Mass spectra of hydrogel coatings on silicon were measured with the TOF-SIMS spectrometer IV (IONTOF, Münster, Germany). A Bi ion source was used with an angle of 45° relative to the sample surface with Bi_3^+ primary ions of 25 keV. The TOF analyzer was installed at an angle of 90 ° to the sample surface. Negative spectra were used for analysis.

3. Results and discussion

The aim of this Chapter was the quantification of ligand densities by XPS and TOF-SIMS, two non-surface sensitive quantification methods. As ligands, a fluorinated amino acid (Figure 1A) and an iodinated peptide (Figure 1B) were used in three different molar ligand to prepolymer ratios (1/2, 1/1 and 2/1). Ellipsometry measurements were applied to determine the thickness of the hydrogel coatings and to ensure that it was sufficient for analysis with XPS and TOF-SIMS (Figure 1C). UV/O_3 activated silicon wafer formed a layer of silicium oxide on the surface of around 2.2 nm thickness. The aminosilan layer on top of the silicium oxide layer had a thickness of 0.5 +/- 0.1 nm. This corresponds to a monolayer of aminosilan. The superimposed hydrogel coating was 40.7 +/- 5.2 nm and the functionalized hydrogel coating 25.4 +/- 3.5 nm thick, which was sufficient for XPS and TOF-SIMS analysis. The loss of coating thickness in case of functionalization can be explained by lower amounts of arms of the prepolymers available for crosslinking as they were occupied by ligands.

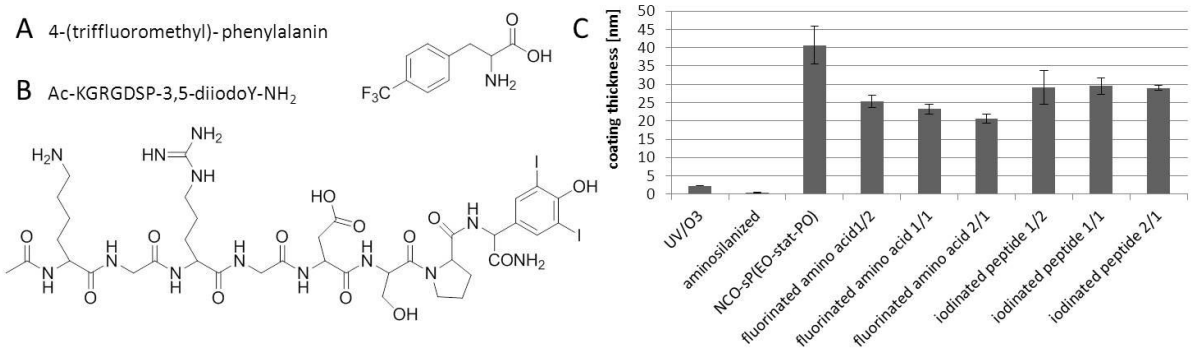

Figure 1: Ligands for functionalization and coating thickness determined by ellipsometry.

Ligands mixed with prepolymer solutions for functionalization of NCO-sP(EO-*stat*-PO) hydrogel coatings. As ligands, a fluorinated amino acid (A) and an iodinated peptide (B) were used. Thickness of activated, aminosilanized and NCO-sP(EO-*stat*-PO) hydrogel coated silicon wafers, determined by ellipsometry (C).

Table 1 gives an overview of theoretically calculated percentual elemental composition and elemental composition measured by XPS. For calculation, a homogeneous distribution and complete binding of the ligands to the prepolymers prior to spin coating was assumed. In case of pure hydrogel coatings the measured C 1s, O 1s and N 1s data lay in the range of the sensitivity of the method and confirmed calculated data. In case of functionalization with fluorinated amino acid the amount of nitrogen did not increase significantly due to the presence of only one nitrogen atom in the ligand molecule. As expected, the amount of nitrogen increased significantly in case of functionalization with iodinated peptide containing 13 nitrogen atoms per peptide.

Table 1: XPS calculations and measurements of elemental composition of coatings.

Calculated (gray) and measured (white) elemental composition of pure and functionalized NCO-sP(EO-*stat*-PO) hydrogel coatings with fluorinated amino acid and iodinated peptide in molar ligand to prepolymer ratios of 1/2, 1/1 and 2/1.

Elements	**C 1s**	**O 1s**	**N 1s**	**F 1s**	**I 3d $_{5/2}$**
Binding energy [eV]	280-290	528-530	395-400	683-696	617-620
Calculated elemental composition in NCO-sP(EO-*stat*-PO) coatings					
NCO-sP(EO-*stat*-PO)	69.6	29	1.5	-	-
Measured elemental composition in NCO-sP(EO-*stat*-PO) coatings					
NCO-sP(EO-*stat*-PO)	71.6	26.9	1,4	-	-
Calculated elemental composition in NCO-sP(EO-*stat*-PO) coatings functionalized with…					
…fluorinated amino acid 1/2	69.5	28.8	1.5	0.2	-
…fluorinated amino acid 1/1	69.4	28.7	1.6	0.4	-
…fluorinated amino acid 2/1	69.2	28.4	1.7	0.7	-
…iodinated peptide 1/2	69.1	28.6	2.2	-	0.1
…iodinated peptide 1/1	68.6	28.3	2.8	-	0.2
…iodinated peptide 2/1	67.9	27.7	4	-	0.4
Measured elemental composition in NCO-sP(EO-*stat*-PO) coatings functionalized with…					
…fluorinated amino acid 1/2	71.6	27.2	1.2	0.28	-
…fluorinated amino acid 1/1	71	27.6	1.4	0.69	-
…fluorinated amino acid 2/1	71.2	27.3	1.4	0.64	-
…iodinated peptide 1/2	71.5	27.2	1.4	-	0.02
…iodinated peptide 1/1	71.8	26.5	1.7	-	0.07
…iodinated peptide 2/1	71.4	26.9	1.7	-	0.07

Functionalizing the hydrogel with the iodinated peptide, a decrease in organic bound iodine signal over time during XPS measurements was observed, shown for coatings with the highest content of iodinated peptide (2/1) in Figure 2. The peak was transferred to lower kinetic energies indicating that organic bound iodine was detached and detected as iodide (Figure 2A). This was most likely due to the attachment of iodide to ammonium groups of a polymer arm or an ammonium group of a peptide before it evaporated as HI. With this time-resolved

measurement, the amount of organic bound iodine before XPS measurement was recalculated for all samples (Figure 2B, Table 1). XPS measurements of NCO-sP(EO-*stat*-PO) coatings functionalized with fluorinated amino acid showed the same phenomenon of fluorine unbinding over time allowing the calculation of fluorine amount in the coating before measurement according to the measurements with iodine (Table 1).

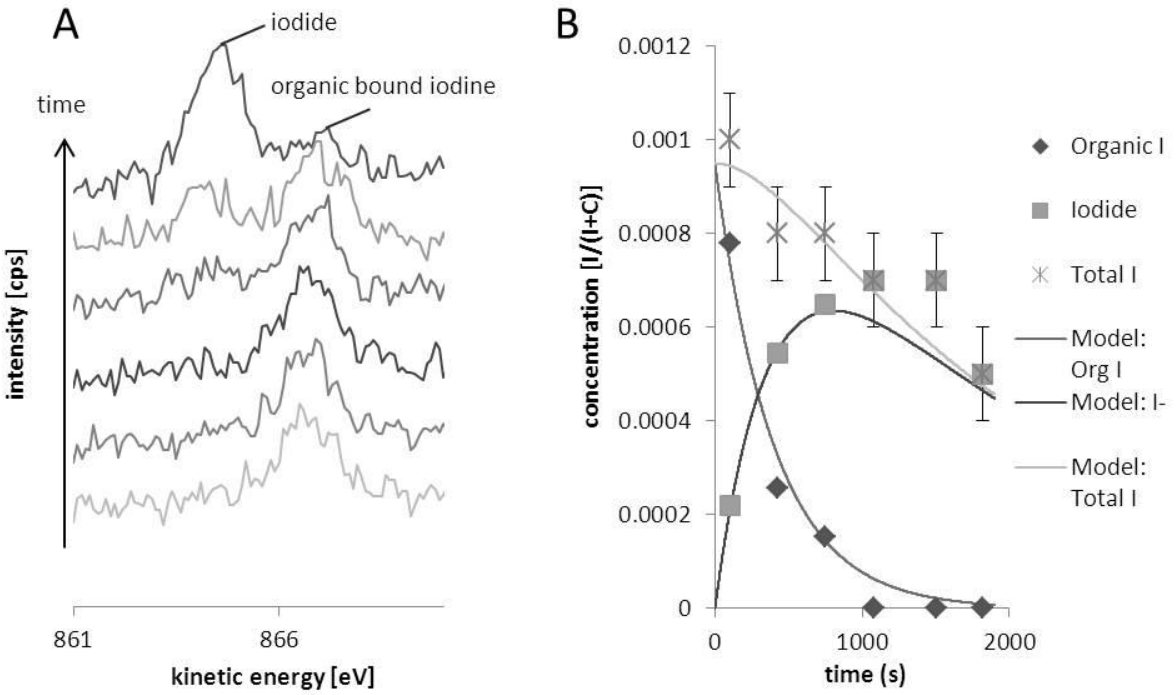

Figure 2: Decrease of iodine signal during XPS measurement.

Decrease of iodine signal during XPS measurement of NCO-sP(EO-*stat*-PO) coatings functionalized with iodinated peptide (2/1). Loss of bound iodine signal over time (A) was observed and recalculation of the amount of bound iodine before the measurement was possible (B).

Comparison of calculated and measured elemental composition in Table 1 shows, that the binding of ligands to prepolymers was not 100% efficient as assumed in theoretical calculations. Hydrogels functionalized with the highest amount of fluorinated amino acid (2/1) almost reached the theoretically calculated amount of 0.7 atom % (Figure 3A). In case of two iodinated peptides per prepolymer (2/1) a maximum amount of 0.4 atom % was theoretically possible but only an amount of 0.07 atom % was reached (Figure 3B). This indicates that the binding was not 100% efficient and one cannot assume that all ligands used were actually bound in the coating. Figure 3B shows that in case of two iodinated peptides per prepolymer (2/1) and one iodinated peptide per prepolymer (1/1) about 50% of the theoretically possible peptides bound to the prepolymers. In case of one peptide per 2 prepolymers (1/2) even less than 50% of the binding capacity was reached. Modification with the small amino acid seemed more effective compared to the rather big iodinated peptide. Fluorinated phenylalanine is a rather small molecule

compared to the iodinated peptide containing 8 amino acids. The small amino acid could have more space moving in the prepolymer solution prior to spin coating which led to a higher binding chance. Additionally, the fluorinated phenylalanine is more hydrophobic making it more likely to bind to hydrophobic isocyanate groups at the ends of the prepolymer arms. In case of 1/2 and 1/1, the measured atom % was higher than the calculated possible amount assuming homogeneous distribution of the ligand in the coating. If the fluorinated amino acids bound quickly to the prepolymers, an accumulation of a few amino acids on one prepolymer could have been possible.

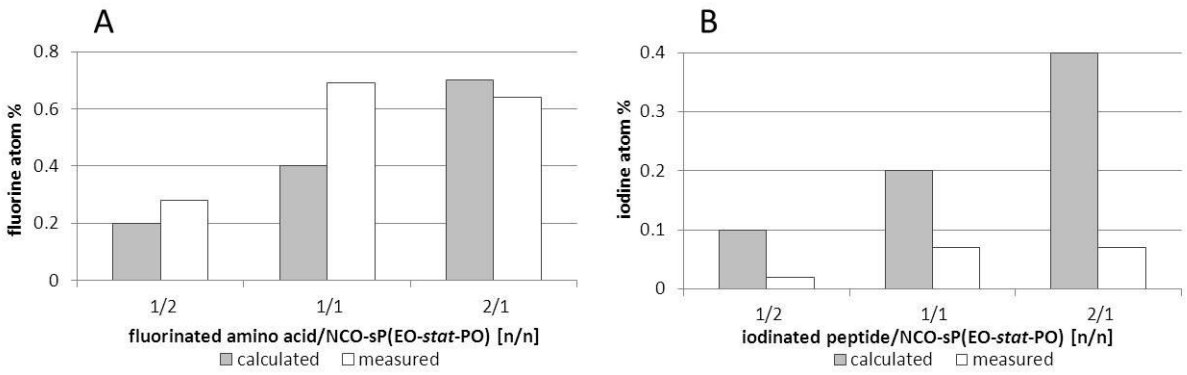

Figure 3: XPS calculations and measurements of F and I in coatings.

Calculated (gray) and measured (white) amounts of fluorine (A) and iodine (B) atom % of NCO-sP(EO-*stat*-PO) coatings functionalized with fluorinated amino acid and iodinated peptide in molar ligand to prepolymer ratios of 1/2, 1/1 and 2/1.

The upper nm of the pure and functionalized hydrogel coatings were analyzed with TOF-SIMS measuring negative and positive spectra. Negative spectra showed much higher intensities and more peaks were clearly related to the fluorinated amino acid and the iodinated peptide compared to positive spectra (not shown). Therefore, negative spectra were used for the analysis and ligand specific ions were detected in all functionalized coatings. Functionalized coatings showed the same amounts of ligand specific ions in case of the two higher ligand concentrations (1/1 and 2/1) (Figure 4A, C). This leads to the conclusion that a maximum binding capacity of ligands to the prepolymers was reached when prepolymer and ligand were mixed in the molar ratio of 1/1. Peaks of the hydrogel coatings were slightly influenced by the functionalization (Figure 4B, D) where some peak intensities increased with higher number of ligands, others decreased, and others stayed the same. This effect was independent of the concentration of ligands.

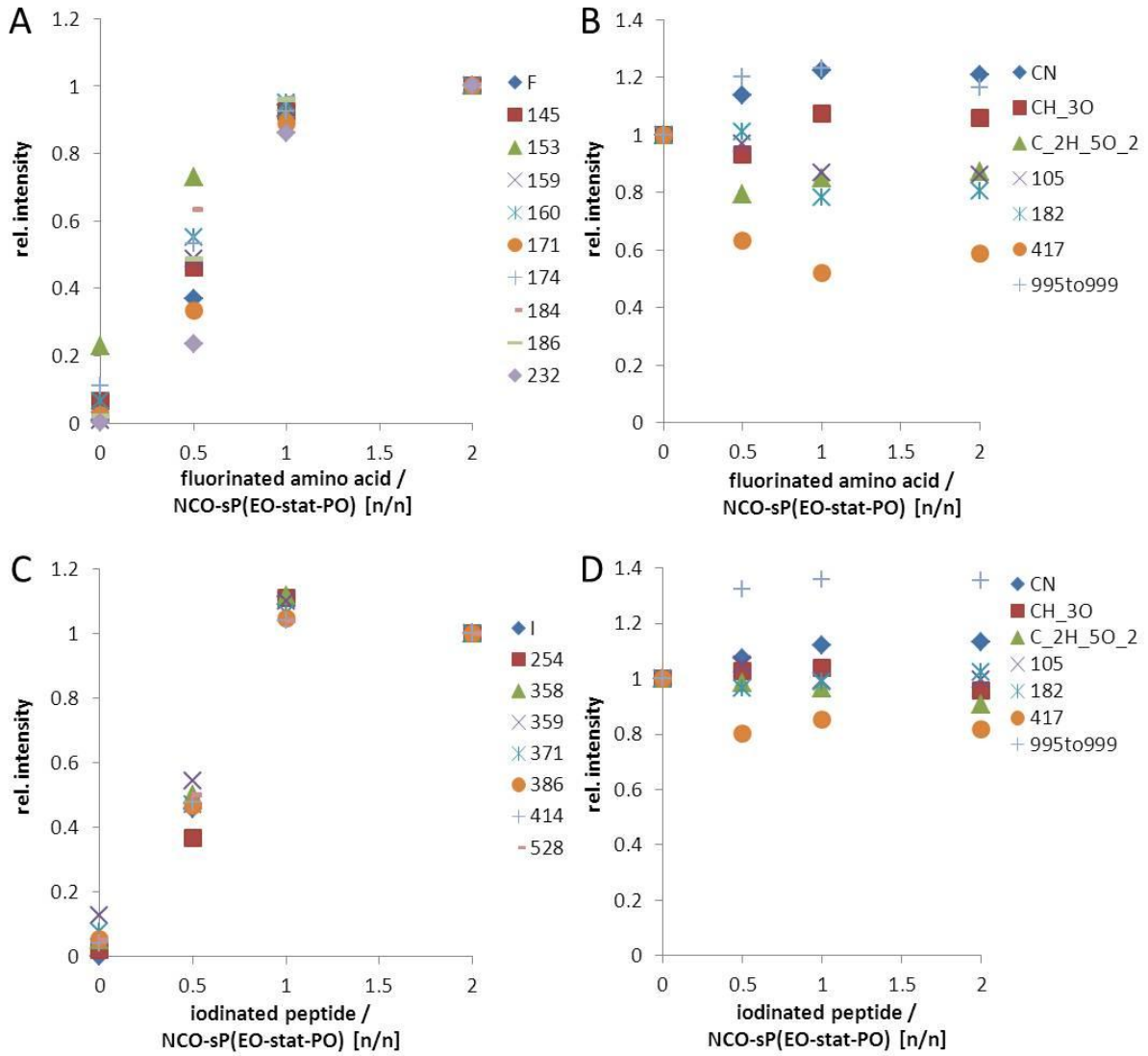

Figure 4: TOF-SIMS measurement of functionalized coatings.

TOF-SIMS data of NCO-sP(EO-*stat*-PO) hydrogel coatings functionalized with fluorinated amino acid (A, B) and iodinated peptide (C, D) in molar ligand to prepolymer ratios of 1/2, 1/1 and 2/1. Relative intensities of ligand specific ions (A, C) and hydrogel specific ions (B, D) are shown.

TOF-SIMS was 1,000 times more sensitive compared to XPS measurements. Intensities of ligand specific signals detected by both methods were therefore compared relatively in Figure 5. Both methods detected maximum ligand amounts when a molar ligand to prepolymer ratios of 1/1 was used. Higher ligand concentrations in the prepolymer solution before spin coating did not lead to additional ligands immobilized in the crosslinked hydrogel.

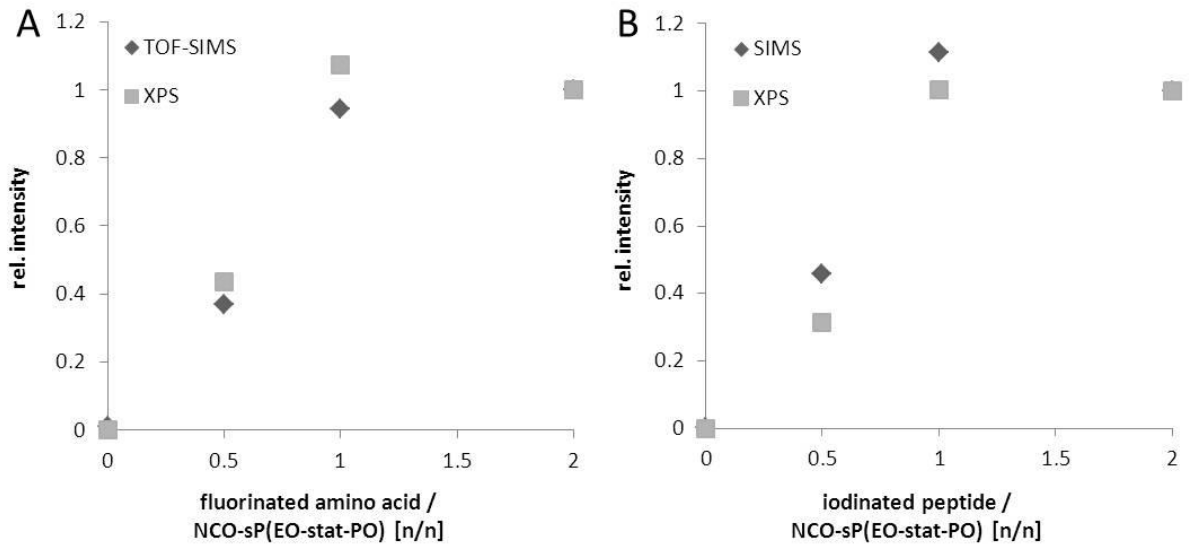

Figure 5: Relative comparison of XPS and TOF-SIMS.

Relative ligand intensities in NCO-sP(EO-*stat*-PO) hydrogel functionalized with fluorinated amino acid (A) and iodinated peptide (B) in molar ligand to prepolymer ratios of 1/2, 1/1 and 2/1, determined by XPS and TOF-SIMS.

4. Conclusions

In this Chapter, NCO-sP(EO-*stat*-PO) hydrogel coatings were functionalized with a fluorinated amino acid and an iodinated peptide in different molar ligand to prepolymer ratios (1/2, 1/1 and 2/1) before spin coating on silicon surfaces. Functionalized coatings were 25.4 +/- 3.5 nm thick, as measured by ellipsometry, and therefore suitable for characterization with XPS and TOF-SIMS. A maximum ligand binding capacity of the hydrogels was reached at ligand to prepolymer ratios of 1/1. Higher ratios did not lead to higher ligand amounts immobilized in the hydrogels.

In the first part of this thesis, NCO-sP(EO-*stat*-PO) hydrogels were analyzed with regard to ligand concentrations in the bulk and surface near regions (Chapter 3 and 4). Still, for biological applications, the amount of ligands accessible for proteins and cells at the interface needs to be determined. Therefore, the next part of this thesis aimed at the surface sensitive quantification of ligands on the hydrogels (Chapter 5-7). A complete comparison of classical and surface sensitive quantification methods will be presented in Chapter 8.

5. References

1. Norrman, K.; Haugshoj, K.B. and Larsen, N.B. Lateral and vertical quantification of spin-coated polymer films on silicon by TOF-SIMS, XPS, and AFM. *Journal of Physical Chemistry B* **2002**, 106 (51) 13114-21.
2. Kasemo, B. Biological surface science. *Surface Science* **2002**, 500 (1-3) 656-77.
3. Hauert, R. and Keller, B.A. Chemical surface analysis with nanometer depth resolution. *Chimia* **2006**, 60 (11) A800-A04.
4. Briand, E.; Salmain, M.; Compere, C. and Pradier, C.M. Immobilization of protein A on SAMs for the elaboration of immunosensors. *Colloids and Surfaces B-Biointerfaces* **2006**, 53 (2) 215-24.
5. Kingshott, P.; McArthur, S.; Thissen, H.; Castner, D.G. and Griesser, H.J. Ultrasensitive probing of the protein resistance of PEG surfaces by secondary ion mass spectrometry. *Biomaterials* **2002**, 23 (24) 4775-85.
6. Sofia, S.J.; Premnath, V. and Merrill, E.W. Poly(ethylene oxide) grafted to silicon surfaces: Grafting density and protein adsorption. *Macromolecules* **1998**, 31 (15) 5059-70.
7. Michel, R.; Pasche, S.; Textor, M. and Castner, D.G. Influence of PEG architecture on protein adsorption and conformation. *Langmuir* **2005**, 21 (26) 12327-32.
8. Lhoest, J.B.; Detrait, E.; van den Bosch de Aguilar, P. and Bertrand, P. Fibronectin adsorption, conformation, and orientation on polystyrene substrates studied by radiolabeling, XPS, and ToF SIMS. *Journal of Biomedical Materials Research* **1998**, 41 (1) 95-103.
9. Sung, D.; Park, S. and Jon, S. Facile method for selective immobilization of biomolecules on plastic surfaces. *Langmuir* **2009**, 25 (19) 11289-94.
10. Santiago, L.Y.; Nowak, R.W.; Rubin, J.P. and Marra, K.G. Peptide-surface modification of poly(caprolactone) with laminin-derived sequences for adipose-derived stem cell applications. *Biomaterials* **2006**, 27 (15) 2962-69.
11. Massia, S.P. and Stark, J. Immobilized RGD peptides on surface-grafted dextran promote biospecific cell attachment. *Journal of Biomedical Materials Research* **2001**, 56 (3) 390-99.
12. Tong, Y.W. and Soichet, M.S. Peptide surface modification of poly(tetrafluoroethylene-co-hexafluoropropylene) enhances its interaction with central nervous system neurons. *Journal of Biomedical Materials Research* **1998**, 42 (1) 85-95.
13. Davis, D.H.; Giannoulis, C.S.; Johnson, R.W. and Desai, T.A. Immobilization of RGD to < 111 > silicon surfaces for enhanced cell adhesion and proliferation. *Biomaterials* **2002**, 23 (19) 4019-27.
14. Popat, K.C.; Swan, E.E.L. and Desai, T.A. Modeling of RGDC film parameters using X-ray photoelectron spectroscopy. *Langmuir* **2005**, 21 (16) 7061-65.
15. Neff, J.A.; Tresco, P.A. and Caldwell, K.D. Surface modification for controlled studies of cell-ligand interactions. *Biomaterials* **1999**, 20 (23-24) 2377-93.
16. Cook, A.D.; Hrkach, J.S.; Gao, N.N.; Johnson, I.M.; Pajvani, U.B.; Cannizzaro, S.M. and Langer, R. Characterization and development of RGD-peptide-modified poly(lactic acid-co-lysine) as an interactive, resorbable biomaterial. *Journal of Biomedical Materials Research* **1997**, 35 (4) 513-23.
17. Norrman, K.; Papra, A.; Kamounah, F.S.; Gadegaard, N. and Larsen, N.B. Quantification of grafted poly(ethylene glycol)-silanes on silicon by time-of-flight secondary ion mass spectrometry. *Journal of Mass Spectrometry* **2002**, 37 (7) 699-708.

18. Kim, Y.P.; Hong, M.Y.; Kim, J.; Oh, E.; Shon, H.K.; Moon, D.W.; Kim, H.S. and Lee, T.G. Quantitative analysis of surface-immobilized protein by TOF-SIMS: Effects of protein orientation and trehalose additive. *Analytical Chemistry* **2007**, 79 (4) 1377-85.

19. Gotz, H.; Beginn, U.; Bartelink, C.F.; Grunbauer, H.J.M. and Moller, M. Preparation of isophorone diisocyanate terminated star polyethers. *Macromolecular Materials and Engineering* **2002**, 287 (4) 223-30.

20. Groll, J.; Ameringer, T.; Spatz, J.P. and Moeller, M. Ultrathin coatings from isocyanate-terminated star PEG prepolymers: Layer formation and characterization. *Langmuir* **2005**, 21 (5) 1991-99.

II Surface sensitive quantification

Artificial materials used in research fields such as biosensors or tissue engineering need to be characterized and controlled at their interface that is in direct contact with proteins and cells. After classical quantification methods described in the first part of my thesis, this second part focuses on the surface sensitive quantification of ligands at the interface of NCO-sP(EO-*stat*-PO) hydrogel layers using surface plasmon resonance (SPR), surface acoustic wave technology (SAW) (Chapter 5), and enzyme linked immunosorbent assay (ELISA) (Chapter 6). To control cellular behavior at the hydrogel interface, the ligand concentration needs to be correlated to cellular responses. Therefore, cell adhesion, proliferation, and vitality were measured dependent on the concentration of cell adhesion mediating ligands on the hydrogel surface (Chapter 7). In Chapter 8, classical and surface sensitive quantification methods were compared.

CHAPTER 5

SPR and SAW for surface sensitive quantification of ligands on hydrogels

Regarding the quantification of ligands at the surface of hydrogel coatings, quantitative optical and acoustic methods can be used to measure the interaction of surface presented ligands to binding partners in solution in real time. Within this Chapter, surface plasmon resonance (SPR) was chosen as optical, and surface acoustic wave (SAW) technology as acoustic method. For both methods, the NCO-sP(EO-*stat*-PO) hydrogel coating procedure needed to be transferred from standard glass or silicon to gold surfaces. Coatings on gold showed more inhomogeneities and were thinner as compared to standard coatings on glass and silicon as shown by atomic force microscopy (AFM) and ellipsometry, respectively. Nevertheless, first attempts at implementing SPR and SAW experiments for the surface sensitive quantification of ligands on the hydrogels promised a high potential of these two quantification methods.

1. Introduction

Quantification of ligands on functionalized biomaterials is crucial for the proper characterization of a material interfaces to control cell behavior dependent on the ligand concentration [1], to later on, design functional biomaterials with optimal ligand concentrations. One optical quantification method that is frequently used for surface sensitive quantification of interactions at interface is SPR. The excitation of plasmons in a gold layer leads to the loss of energy of the reflected light [2] and the refractive index changes dependent on the mass binding to the gold surface [2]. Using ultrathin coatings on gold allows the analysis of interaction of binding partners on top of this coating. The resistance of self-assembled monolayers (SAM) on gold against non-specific protein adsorption of fibrinogen, lysozyme or human plasma was shown by SPR [3, 4]. Mrksich et al. investigated the adsorption of RNase, lysozyme, fibrinogen, and pyruvate kinase on SAMs with hexa(ethylene glycol) and methyl groups and could determine a value of functional group ratios preventing non-specific adsorption [5]. Also, carbonic anhydrase binding to SAMs consisting of tri(ethylene glycol) presenting benzenesulfonamide ligands was quantified by SPR [6]. Roberts et al. investigated mixed SAMs of alkanethiols on gold with regard to protein adsorption and cell adhesion as well as detachment by presenting a mixture of RGD peptides and oligo(ethylene glycol) and could determine the RGD content necessary to prevent protein adsorption and allow cell adhesion [7].

SAW, a surface sensitive quantification method applicable to ultrathin coatings on gold, can detect mass binding on the surface of a gold layer by changes in frequency [8]. Using acoustic SAW technology, the interaction of surfaces with proteins, carbohydrates, DNA, viruses, and cells on surfaces was shown [8]. Even the hybridization of DNA fragments with a length of 20 base pairs was successfully detected by SAW with an even higher sensitivity compared to SPR [9].

In this Chapter, gold was coated with the pure and functionalized NCO-sP(EO-*stat*-PO) hydrogel layers. To achieve covalent binding of the NCO-sP(EO-*stat*-PO) prepolymers to the gold surfaces, cystamine was covalently bound on UV/O_3 activated gold surfaces. Coating thicknesses were determined with ellipsometry and homogeneity with AFM measurements. Unfortunately, cystamine formed an inhomogeneous multilayer of around 20 nm on gold. The hydrogel coating on top was rather thin with around 10 nm and inhomogeneous as well. SPR revealed resistance of the pure hydrogel coatings against protein adsorption out of undiluted

serum and specific streptavidin (SA) binding to coatings functionalized with the model ligand biocytin. Using SAW, the inert properties of the non-functionalized coatings was confirmed. Additionally, specific SA binding was shown to be dependent on the amount of biocytin and GRGDSK-biotin immobilized on the hydrogel coatings.

2. Experimental section

2.1. Hydrogel coatings

2.1.1. NCO-sP(EO-stat-PO) synthesis

Isocyanate terminated prepolymers (NCO-sP(EO-*stat*-PO)) were synthesized as described in detail elsewhere [10]. In short, the prepolymer was fabricated by the reaction of hydroxyl terminated star shaped polyether polyole with isophorone diisocyanate (IPDI).

2.1.2. Preparation of gold surfaces

The coating procedure for NCO-sP(EO-*stat*-PO) hydrogels on gold was developed earlier [11]. For SPR measurements, glass substrates sputtered with gold were purchased from Mivitec (Sinzig near Regensburg, Germany). For SAW measurements, SAW chips from SAW Instruments (Bonn, Germany) were used. Gold surfaces were cleaned for 15 min in 40 vol-% H_2SO_4 and activated in UV/O_3 for 15 min. After incubation in 10 mM cystamine dihydrochloride (Alfa Asear, Karlsruhe, Germany) for 4 h, gold substrates were incubated in 0.05 mM $NaHCO_3$ (Prolabo, Darmstadt, Germany) for 15 min and dried in a stream of nitrogen.

2.1.3. NCO-sP(EO-stat-PO) coating

Prepolymers were solubilized in tetrahydrofuran (THF, dried over sodium, Prolabo, Darmstadt, Germany). After adding water to the solution (9/1 v/v water/THF, prepolymer concentration 10 mg/mL), prepolymers were left for crosslinking for 5 min. For SPR gold surfaces, 2 droplets of the prepolymer solution were placed on gold surfaces after filtration through a 0.2 µm syringe filter (Whatman, Dassel, Germany). The coating process was carried out in the spin coater WS-400-B-6NPP/LITE (Laurell Technologies, North Wales, USA) at 2,500 rpm for 40 sec with an acceleration time of 5 sec. Each prepolymer solution was used to coat a maximum of 6 substrates. Coated substrates were stored at room temperature for at least 12 h to ensure complete crosslinking of the coating. For SAW chip coating, equipment was kindly provided from SAW Instruments (Bonn, Germany). The gold chip was placed in the sam®5 coating device with 5 chambers and 30 µL of the prepolymer solution in water/THF (5 min after addition of water) were incubated in each chamber. After 10 min incubation at room temperature, leftover polymer solution was removed.

2.1.4. Functionalization

Biocytin was purchased from Sigma-Aldrich (Steinheim, Germany) and GRGDSK-biotin from Bachem (Bubendorf, Switzerland). Coatings on SPR gold chips were functionalized using the mix-in method. Prior to coating, biocytin was added to the prepolymer solution with molar biocytin to prepolymer ratios of 1/1. The coating process was performed as described above. Coatings were washed 3 times with water. Coatings on gold in the SAW coating device (1 h after preparation) were incubated with 30 µL biocytin or GRGDSK-biotin solution (100 and 500 µg/mL in 0.02 M Na_2CO_3/$NaHCO_3$, pH 9.4) for 1 h. Coatings were washed 3 times with water.

2.2. Coating characterization

2.2.1. Ellipsometry

For determination of the coating thickness, the spectroscopic ellipsometer model OMT-RTE-3501 NM30 (OMT, Ulm, Germany) was used with a wavelength range of 450-800 nm under an angle of incidence of 70°. The system was operated in high resolution mode. The calculation of the layer thickness was based on a model for hydrogel layers on gold. For determination of the layer thickness, three gold layers with cystamine and three gold layers with cystamine and the hydrogel layer were measured. The difference of the mean deviations was calculated as the thickness of the hydrogel coating.

2.2.1. AFM

AFM was performed in tapping mode in air with OTESPA tips (Veeco, Mannheim, Germany) in a Dimension® ICON® instrument (Bruker AXS, Mannheim, Germany). Measurements were performed in air at room temperature. A spring constant of 12 - 103 N/m and scan rates of 278 – 357 kHz were applied. Analysis was performed with the NanoScope™ software (version 8.10 R1.60476).

2.2.2. SPR

SPR equipment was kindly provided by Prof. Offenhäuser (FZ Jülich, Germany). SPR measurements were performed at room temperature. Coated gold substrates were placed into a BIO-Suplar 3 apparatus (Mivitec, Sinzig near Regensburg, Germany) by fixing the backside of the substrate with SPR-oil series A (Cargille Labs, Cedar Grove, USA) to the prism. Surfaces were rinsed with PBS buffer (0.01 M, pH 7.4) using a flow chamber and peristaltic pump with a flow rate of 0,255 mL/min. After a stable baseline of the reference units (RU), non-functionalized coatings were treated with pure serum (PAA, Cölbe, Germany) and coatings functionalized with

biocytin were treated with SA (50 µg/mL, in PBS). After saturation (stable baseline), samples were rinsed with PBS until all loosely attached serum/SA was washed away (stable baseline). Results were analyzed using the software Plasmon version 5.3.

2.2.3. SAW

Equipment for SAW measurements was kindly provided by SAW Instruments (Bonn, Germany). The coated SAW chip was placed into the fluidic cell of the SAW system sam®5 and equilibrated in running buffer (PBS) for 15 h till a stable base line was reached. SA solution (2.5 µg/mL, in PBS) was injected 4 times (160 µL) to achieve saturation of the SA binding. After injections, coatings were rinsed with PBS buffer.

3. Results and discussion

For the use of SPR and SAW, gold surfaces needed to be coated with NCO-sP(EO-*stat*-PO). Therefore, a coating procedure developed by Sinn et al. was used [11]. After activation of the gold surfaces with UV/O_3, cystamine was bound to the gold surface by incubation for 4 h at room temperature. The thickness of the cystamine layer on activated gold was 20.3 +/- 4.8 nm as determined by ellipsometry. This corresponds to a multilayer of cystamine instead of the expected monolayer. Nevertheless, NCO-sP(EO-*stat*-PO) coatings were spin coated on the cystamine covered gold surfaces using standard spin coating parameters applied for NCO-sP(EO-*stat*-PO) coatings on glass and silicon [12]. NCO-sP(EO-*stat*-PO) hydrogel layers covalently bound to the cystamine on gold and showed a thickness of 10.8 +/- 0.6 nm. This was a very thin layer compared to hydrogel coatings on glass and silicon of 30 +/- 5 nm [13] and could be due to less amino groups on the cystamine functionalized gold surface being available for binding of the isocyanate terminated prepolymers.

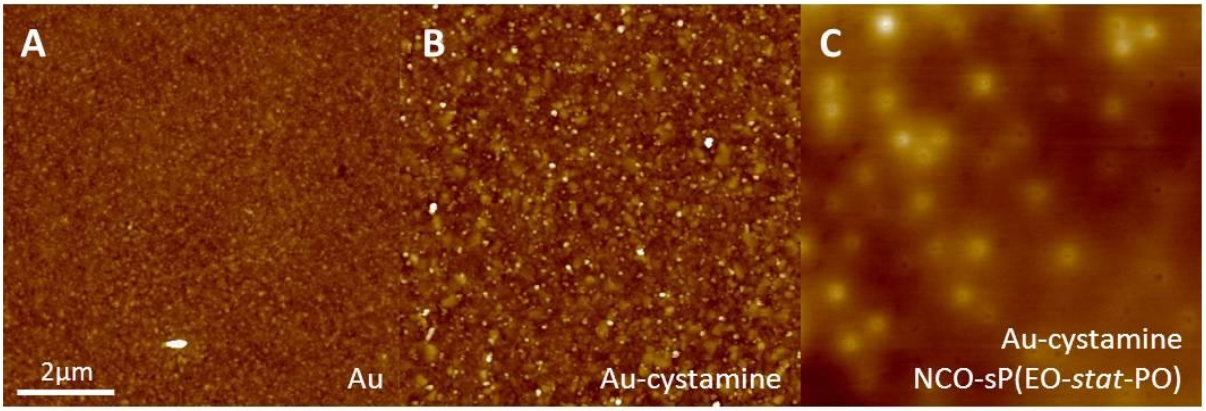

Figure 1: AFM measurements on gold surfaces during hydrogel coating procedure.
Gold surfaces were cleaned with 40% H_2SO_4 (A), coated with cystamine (B) and subsequently coated with NCO-sP(EO-stat-PO) by spin coating (C). After each step of this coating procedure, AFM images (A-C) were taken.

For the determination of coating homogeneity, coatings were analyzed with AFM in the tapping mode. Cleaned gold surfaces, gold surfaces coupled to cystamine as well as NCO-sP(EO-*stat*-PO) coatings on gold were analyzed. Cleaned gold surfaces were homogeneous with a surface roughness of 15 nm (Figure 1A). Cystamine binding to the gold surfaces changed the surface structure and the AFM image revealed an increased roughness (Figure 1B). After coating with NCO-sP(EO-*stat*-PO), surfaces were even less homogeneous with a surface roughness of 40 nm (Figure 1C). The quality of the coatings was not as good as standard coatings on glass or silicon and needs to be optimized, which was not possible as it would go beyond the scope of this thesis. Nevertheless, these coatings were used for preliminary tests with SPR and SAW.

SPR showed in a series of studies that SAMs resist non-specific protein adsorption [4, 5, 14]. For NCO-sP(EO-*stat*-PO) coatings, protein resistance was only shown via adsorption of fluorescently labeled proteins analyzed via fluorescence microscopy so far [13]. Even though ellipsometry and AFM showed the need to optimize NCO-sP(EO-*stat*-PO) coatings on gold, first SPR experiments showed satisfying results (Figure 2). During equilibration with water, RUs diminished over time. This was most probably due to swelling and thickening of the hydrogel, which had an effect on the sensitivity of the SPR measurement. The effect minimized over time but never stopped completely during measurements. Therefore, calculations of differences of RUs were always the best possible estimation. To test protein resistance of non-functionalized coatings, pure serum was chosen as it is a concentrated mixture of different proteins getting in contact with a material's surface during implantation. Even if RUs increased during serum treatment, this was not due to adsorption of the proteins to the hydrogel surface, as RU reached the previous level after PBS washing (Figure 2A). This experiment led to the conclusion, that NCO-sP(EO-*stat*-PO) coatings on gold resisted non-specific protein adsorption during a serum treatment of 30 min.

Biocytin was chosen as a small molecule that can be covalently immobilized on the hydrogel coating system via its amino group and can be easily detected with SA. NCO-sP(EO-*stat*-PO) hydrogel coatings functionalized with biocytin were tested for specific SA binding (Figure 2B). Therefore, coatings were equilibrated with PBS buffer and treated with SA solution leading to an increase of RU. To wash away all non-specifically attached SA on the surface, coatings were washed with PBS buffer until a stable baseline was reached. With a sensitivity of the SPR instrument of 10 RU = 1 ng/cm^2, the difference of RU before and after SA treatment of 110 RU corresponds to a specific SA binding of 11 ng SA/cm^2. These measurements demonstrated, that quantification of ligands on the hydrogel system were possible using a binding partner in the mobile phase that has a binding constant high enough to resist shear stress in the flow chamber.

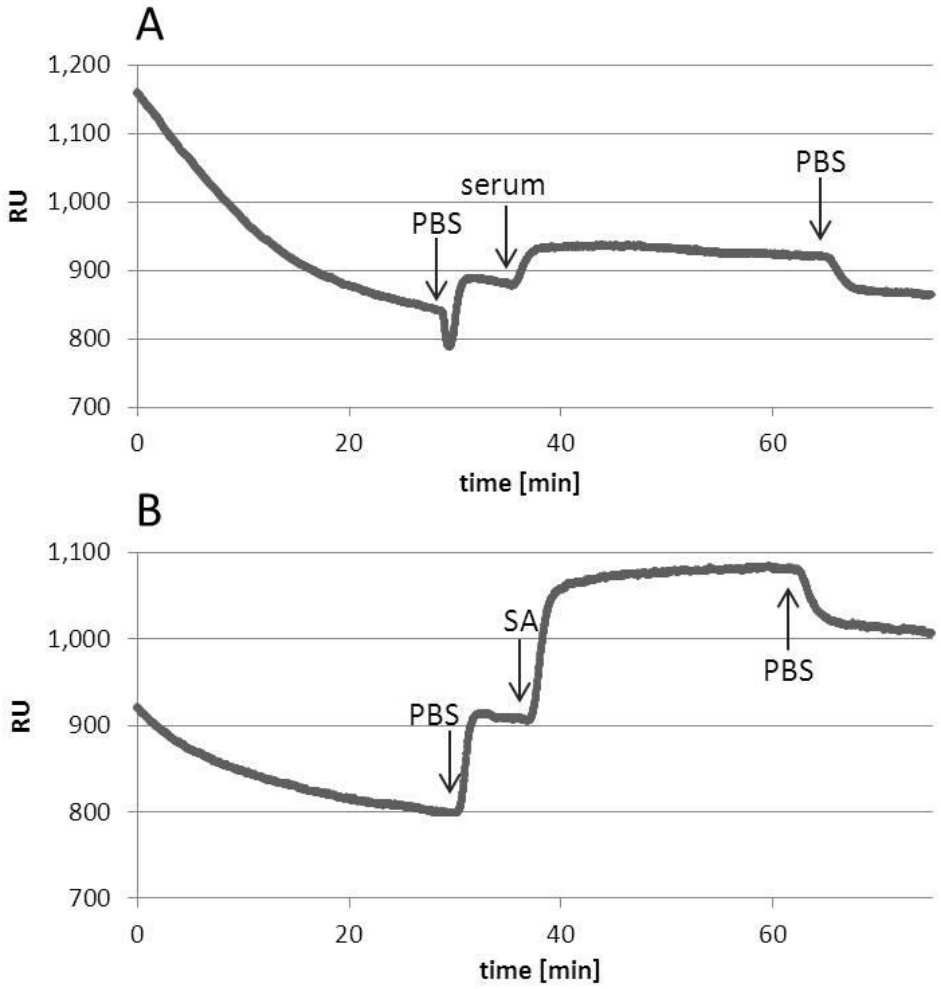

Figure 2: SPR measurements on pure and functionalized hydrogel coatings.

SPR analysis of serum on pure NCO-sP(EO-*stat*-PO) coatings (A) showed resistance of the coatings toward protein adsorption. Coatings functionalized with biocytin (B) specifically bound SA.

SAW measurements on pure and functionalized hydrogel coatings on gold chips were promising even though the coatings were not as homogeneous as on glass or silicon surfaces. The coating procedure of 96-well plates developed for amino functionalized 96-well plates [15] was transferred to SAW gold chips previously coated with a layer of cystamine for binding of isocyanate terminated NCO-sP(EO-*stat*-PO) prepolymers. The sam®5 SAW technology allowed the parallel measurement of 5 chambers on one chip, each being individually functionalized. As a reference, one chamber was coated with the hydrogel layer and left non-functionalized. After 15 h equilibration in PBS buffer, a stable baseline was reached (Figure 3, time point zero). The drift during this initial contact with a liquid ('negative' time points) was most likely due to the water uptake of the hydrogel. This swelling effect of the hydrogel coating had less impact on the SAW measurements as compared to SPR measurements, where the impact of the effect was significantly higher. For SPR measurements, the increase of the hydrogel layer thickness strongly diminished the sensitivity since the size of the drift signal was in the range of the target

signal. This effect was observed and described earlier [9]. On pure hydrogel coatings, almost no SA could bind revealing the inert properties of the hydrogel system (Figure 3, Table 1). The small phase shift of 0.11° can be seen as a background signal and could possibly be diminished by further optimization of the coating procedure on gold.

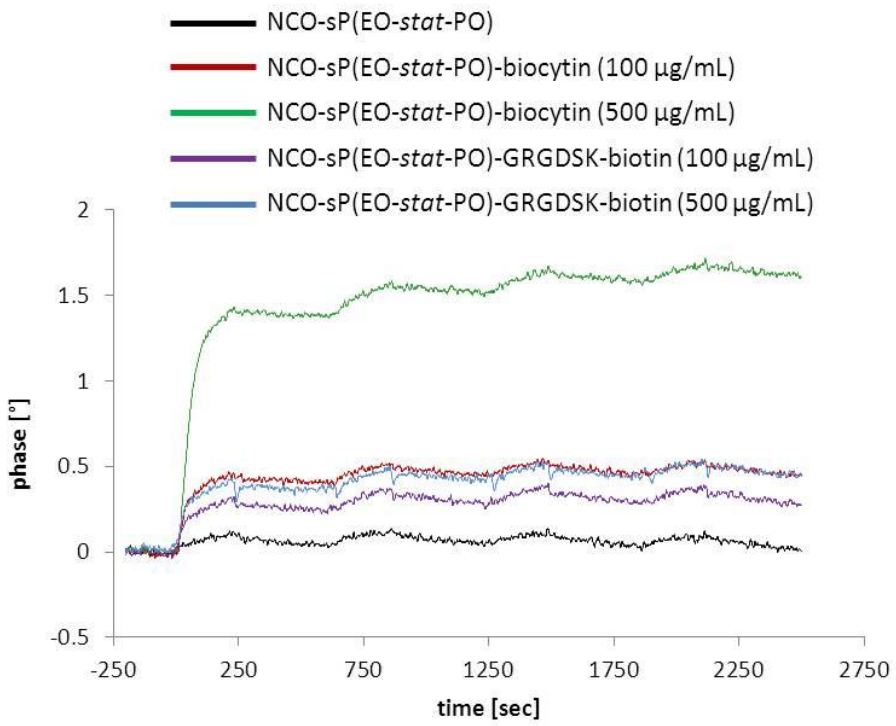

Figure 3: SAW measurements on pure and functionalized hydrogel coatings

SAW gold chips were coated with NCO-sP(EO-*stat*-PO) and functionalized with 100 and 500 µg/mL biocytin and 100 and 500 µg/mL GRGDSK-biotin. SA binding was measured in a sam®5 SAW instrument.

Four chambers of the coated gold chip were functionalized with two different ligands in two different concentrations each. Biocytin was used as small molecule interacting with SA as already shown in SPR measurements. Additionally, the biotinylated peptide GRGDSK-biotin was immobilized on the coatings, allowing the detection of a peptide on the hydrogel with SA as binding partner in the mobile phase. In principle, peptide biotinylation, which can also be achieved via terminal cysteins and Michael addition to avoid interference with lysines in the functional sequence of longer peptides, can be used for any peptide sequence of interest allowing the screening of a variety of peptides using the same experimental procedure. After quadruplicate injection of 160 µL SA, the functionalized surfaces were saturated with SA (Figure 3, Table 1). The phase shift after the fourth injection was used for the calculation of SA mass on the surface using the apparatus specific sensitivity factor of 515 [° cm^2 μg^{-1}]. Incubation of 100 µg/mL GRGDSK-biotin allowed 0.62 ng SA to bind per cm^2, while incubation of 500 µg/mL GRGDSK-biotin and 100 µg/mL biocytin led to binding of 0.91 ng SA per cm^2. The highest SA

binding of 3.15 ng/cm^2 occurred on hydrogels functionalized with 500 µg/mL biocytin. Due to the smaller molecular weight of biocytin (372.48 g/mol) compared to GRGDSK-biotin (843.96 g/mol) more biocytin ligands were in an e.g. 100 µg/mL solution compared to the bigger protein allowing more ligands to bind to the fresh coating. Additionally, the biotinylated peptide was more flexible compared to the small biocytin and thus more likely presented in a way that prevents access of the SA to the biotin recognition sequence. Most importantly, it could be shown that the sensitivity of the SAW technology on the functionalized hydrogel coatings was sufficient to detect differences in ligand concentration of the coatings.

Table 1: SAW measurements on hydrogel coatings.

NCO-sP(EO-stat-PO) hydrogel coatings on gold chips were functionalized with biocytin and GRGDSK-biotin. Binding of SA after 4 injections was measured as a phase shift and bound SA amount per area calculated with the apparatus specific sensitivity factor of 515 [° cm^2 µg^{-1}].

	Phase shift per injection [°]				
	Injection				
Coating	1	2	3	4	Bound SA [ng/cm^2]
NCO-sP(EO-*stat*-PO)	0.11	0.13	0.09	0.11	0.21
NCO-sP(EO-*stat*-PO)-biocytin, 100µg/mL	0.39	0.47	0.48	0.47	0.91
NCO-sP(EO-*stat*-PO)-biocytin, 500µg/mL	1.14	1.57	1.65	1.62	3.15
NCO-sP(EO-*stat*-PO)-GRGDSK-biotin, 100µg/mL	0.30	0.26	0.31	0.32	0.62
NCO-sP(EO-*stat*-PO)-GRGDSK-biotin, 500µg/mL	0.37	0.40	0.42	0.47	0.91

4. Conclusions

In summary, NCO-sP(EO-*stat*-PO) coatings were applied on gold surfaces, however, this coating procedure needs to be optimized as AFM and ellipsometry revealed inhomogeneous and thick cystamine layers on gold leading to thin and inhomogeneous hydrogel coatings on top. Nevertheless, it could be shown, that pure hydrogel coatings resisted serum adsorption comparable to the capacity of SAMs. Additionally, functionalization of the coatings with biocytin and GRGDSK-biotin induced specific SA binding.

For further analysis of different ligand concentrations on the coatings as well as the detection of a variety of different ligands, the coating procedure on gold surfaces needs to be optimized. Therefore, the cystamine layer on the activated gold surfaces should be minimized, optimally achieving a monolayer. This will most probably change the coating thickness of NCO-sP(EO-*stat*-PO) layers which was so far much thinner compared to standard coatings on glass or silicon.

SPR and SAW are optimal methods for the on-line analysis of binding events on surfaces. Still, one needs to keep in mind that both methods can only be applied on ultrathin model coatings on gold but biomaterials cannot always be transferred as ultrathin coatings on gold. To develop a surface sensitive ligand quantification method applicable to all biomaterials disregarding the substrate or geometry, ELISA might be the method of choice. This approach will be presented in the next Chapter.

5. References

1. Palecek, S.P.; Loftus, J.C.; Ginsberg, M.H.; Lauffenburger, D.A. and Horwitz, A.F. Integrin-ligand binding properties govern cell migration speed through cell-substratum adhesiveness. *Nature* **1997**, 385 (6616) 537-40.
2. Green, R.J.; Frazier, R.A.; Shakesheff, K.M.; Davies, M.C.; Roberts, C.J. and Tendler, S.J.B. Surface plasmon resonance analysis of dynamic biological interactions with biomaterials. *Biomaterials* **2000**, 21 (18) 1823-35.
3. Li, L.Y.; Chen, S.F.; Zheng, J.; Ratner, B.D. and Jiang, S.Y. Protein adsorption on oligo(ethylene glycol)-terminated alkanethiolate self-assembled monolayers: The molecular basis for nonfouling behavior. *Journal of Physical Chemistry B* **2005**, 109 (7) 2934-41.
4. Emmenegger, C.R.; Brynda, E.; Riedel, T.; Sedlakova, Z.; Houska, M. and Alles, A.B. Interaction of blood plasma with antifouling surfaces. *Langmuir* **2009**, 25 (11) 6328-33.
5. Mrksich, M.; Sigal, G.B. and Whitesides, G.M. Surface plasmon resonance permits in situ measurement of protein adsorption on self-assembled monolayers of alkanethiolates on gold *Langmuir* **1995**, 11 (11) 4383-85.
6. Lahiri, J.; Isaacs, L.; Grzybowski, B.; Carbeck, J.D. and Whitesides, G.M. Biospecific binding of carbonic anhydrase to mixed SAMs presenting benzenesulfonamide ligands: A model system for studying lateral steric effects. *Langmuir* **1999**, 15 (21) 7186-98.
7. Roberts, C.; Chen, C.S.; Mrksich, M.; Martichonok, V.; Ingber, D.E. and Whitesides, G.M. Using mixed self-assembled monolayers presenting RGD and (EG)(3)OH groups to characterize long-term attachment of bovine capillary endothelial cells to surfaces. *Journal of the American Chemical Society* **1998**, 120 (26) 6548-55.
8. Rocha-Gaso, M.-I.; March-Iborra, C.; Montoya-Baides, Á. and Arnau-VIves, A. Surface generated acoustic wave biosensors for the detection of pathogens: A review *Sensors* **2009**, 9 (7) 5740-69.
9. SAW-Instruments Properties of DNA: Biochemical characterization using phase and amplitude signal. *SAW instruments application note* **2010**, 12 1-2.
10. Götz, H.; Beginn, U.; Bartelink, C.F.; Grünbauer, H.J.M. and Möller, M. Preparation of isophorone diisocyanate terminated star polyethers. *Macromolecular Materials and Engineering* **2002**, 287 (4) 223-30.
11. Sinn, S.; Müller, L.; Drechsel, H.; Wandel, M.; Northoff, H.; Ziemer, G.; Wendel, H.P. and Gehring, F.K. Platelet aggregation monitoring with a newly developed quartz crystal microbalance system as an alternative to optical platelet aggregometry. *Analyst* **2010**, 135 (11) 2930-38.
12. Groll, J.; Ameringer, T.; Spatz, J.P. and Moeller, M. Ultrathin coatings from isocyanate-terminated star PEG prepolymers: Layer formation and characterization. *Langmuir* **2005**, 21 (5) 1991-99.
13. Groll, J.; Fiedler, J.; Engelhard, E.; Ameringer, T.; Tugulu, S.; Klok, H.A.; Brenner, R.E. and Moeller, M. A novel star PEG-derived surface coating for specific cell adhesion. *Journal of Biomedical Materials Research Part A* **2005**, 74A (4) 607-17.
14. Servoli, E.; Maniglio, D.; Aguilar, M.R.; Motta, A.; Roman, J.S.; Belfiore, L.A. and Migliaresi, C. Quantitative analysis of protein adsorption via atomic force microscopy and surface plasmon resonance. *Macromolecular Bioscience* **2008**, 8 (12) 1126-34.
15. Kasten, A.; Müller, P.; Bulnheim, U.; Groll, J.; Bruellhoff, K.; Beck, U.; Steinhoff, G.; Möller, M. and Rychly, J. Mechanical integrin stress and magnetic forces induce biological responses in mesenchymal stem cells which depend on environmental factors. *Journal of Cellular Biochemistry* **2010**, 111 (6) 1586-97.

CHAPTER 6

ELISA for substrate and geometry independent surface sensitive quantification of ligands on hydrogels

Precise determination of biomolecular interactions at the biointerface is crucial for biomaterial characterization. In the previous Chapters, ligand quantification methods applied on functionalized hydrogel films were not surface sensitive or not applicable to all kinds of biomaterials. In this Chapter, functionalized NCO-sP(EO-*stat*-PO) hydrogels in 96-well plates and on glass were used and functionalized with a broad range of ligands, which were quantified via surface sensitive enzyme linked immunosorbent assay (ELISA) and enzyme linked lectin assay (ELLA). As ligands, the peptide GRGDSK-biotin, the broadly applicable coupler molecule biocytin, the protein fibronectin (FN), and the carbohydrates N-acetylglucosamine (GlcNAc) and N-acetyllactosamine (LacNAc) were covalently coupled to the hydrogels using the incubation as well as the mix-in method.

This Chapter represents a cooperative work with Claudia Rech.

1. Introduction

Most surface sensitive ligand quantification techniques, such as surface plasmon resonance (SPR) or surface acoustic wave (SAW) technology, that were used in the previous Chapter, are restricted to specialized sensors or model substrates and cannot be easily transferred to standard biomaterials or 96-well plate format. Ligand densities and accessibility on surfaces is crucial for the evaluation of interaction efficiency. Immobilization of biotin on the surface of hydrogels was optimized and quantified by ELISA before [1, 2]. It becomes clear that the polymer composition of the hydrogel determines the surface concentration of accessible ligand making such surfaces highly specific for the recognition of the ligand. However, hydrogel surfaces need to be optimized separately for each new hydrogel surface/ligand combination.

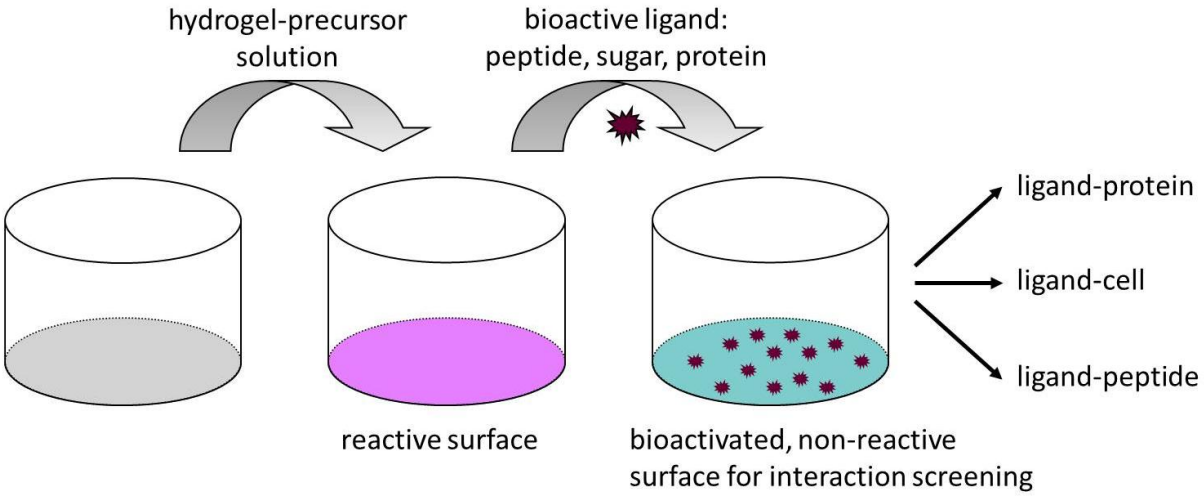

Figure 1: Principle of specific ligand presentation for interaction assays in well plate format.
Scheme of well plate coating with a functional hydrogel layer that gets functionalized with bioactive ligands (peptide, sugar, protein). This system enables the detection of specific interactions of the ligands with proteins, cells or peptides.

Figure 1 demonstrates the different interactions that can be investigated on a hydrogel system in the well plate format, either in directly hydrogel coated wells or on hydrogel coated glass slides that are placed inside the wells. To demonstrate the spectrum of ligands that can be immobilized on the NCO-sP(EO-*stat*-PO) hydrogel system, a range of molecules were covalently embedded into the layer in this Chapter. The amino functional biotin derivative biocytin was used as a widely used standard linker that specifically recognizes streptavidin (SA) with high affinity. Additionally, the ECM protein FN, the FN derived cell adhesion mediating peptide sequence GRGDSK-biotin, and the amino functionalized carbohydrates GlcNAc as well as LacNAc were immobilized on the hydrogel coatings. While GlcNAc served as mere proof of principle for the immobilization and detection of a sugar ligand, LacNAc was selected because

of its important role *in vivo* as basic component for biological relevant epitopes like blood group ABO or Lex on glycoproteins and glycolipids [3-8]. Furthermore, LacNAc is a ligand for galectins, a family of galactose binding proteins, which mediates cell-cell and cell-matrix interactions [9, 10]. ELISA and ELLA protocols were established for the different molecules bound to the hydrogels to determine different ligand densities on top of the hydrogel surfaces.

2. Experimental section

2.1. Hydrogel coatings

2.1.1. NCO-sP(EO-stat-PO) synthesis

Isocyanate terminated prepolymers (NCO-sP(EO-*stat*-PO)) were synthesized as described in detail elsewhere [11]. In short, the prepolymer was fabricated by the reaction of hydroxyl terminated star shaped polyether polyole with isophorone diisocyanate (IPDI).

2.1.2. Preparation of glass surfaces

Glass substrates (Ø 15 mm, Paul Marienfeld, Lauda-Königshofen, Germany) were polished with isopropanol and successively cleaned in acetone, distilled water, and isopropanol in an ultrasonic bath for 5 min each followed by drying in a stream of nitrogen. Solvents were purchased from Prolabo (Darmstadt, Germany). Glass substrates were activated by O_2-plasma treatment in the plasma process plant AK 330 (Roth & Rau, Hohenstein-Ernstthal, Germany) for 15 min (400 W, 50 sccm, 0.4 mbar). Afterwards, glass substrates were left in a desiccator containing 100 µl 3-aminopropyl-trimethoxysilan (AS) at 5 mbar for 60 min. After removal of AS, the glass substrates were left in a vacuum of minimum 10^{-2} mbar for 1 h and stored at 250 mbar.

2.1.3. NCO-sP(EO-stat-PO) coating

In 96-well plates

The coating procedure has been described earlier [12]. Prepolymers were dissolved in tetrahydrofuran (THF, dried over sodium, VWR, Darmstadt, Germany). After adding water to the solution (9/1 v/v mixture of water/THF, prepolymer concentration 10 mg/mL), prepolymers crosslinked for 5 min. For the coating procedure, 400 µL of the solution were filled in each well of a CovaLink^{TM}NH 96-well microtiter plate (NUNC, Langenselbold, Germany). After 10 min incubation at room temperature, leftover polymer solution was removed.

On glass

The coating procedure has been described earlier [13]. Prepolymers were solubilized in tetrahydrofuran (THF, dried over sodium, Prolabo, Darmstadt, Germany). After adding water to the solution (9/1 v/v water/THF, prepolymer concentration 10 mg/ml), prepolymers were left for crosslinking for 5 min. Two droplets of the solution were placed on the aminosilanized surface of a glass substrate after filtration through a 0.2 µm syringe filter (Whatman, Dassel,

Germany). The coating process was carried out in the spin coater WS-400-B-6NPP/LITE (Laurell Technologies, North Wales, USA) at 2,500 rpm for 40 sec with an acceleration time of 5 sec. Each prepolymer solution was used to coat a maximum of 6 substrates. Coated substrates were stored at room temperature for at least 12 h to ensure complete crosslinking of the coating.

2.1.4. Functionalization

Incubation method

Biocytin and human plasma fibronectin (FN) were purchased from Sigma-Aldrich (Steinheim, Germany). The peptide GRGDSK-biotin was bought from Bachem (Bubendorf, Switzerland). Amino functionalized GlcNAc and LacNAc structures were synthesized as described earlier [14, 15]. Biocytin, GRGDSK-biotin and carbohydrates were solubilized in sodium carbonate buffer (0.02 M Na_2CO_3/$NaHCO_3$, pH 9.4), FN was dissolved in deionized water.

Coatings in 96-well plates

50 µL ligand solutions were incubated on coated wells (1 h after preparation of the coatings). Ligand concentrations were varied as follows: 0 – 500 µg/mL (biocytin, GRGDSK-biotin), 0 - 20 µg/mL (FN), and 0 - 10 mM (GlcNAc, LacNAc). After 1 h incubation, coatings were washed 3 times with deionized water.

Coatings on glass

100 µL ligand solutions were incubated as a droplet on coatings (1 h after preparation of the coatings). Ligand concentrations were varied as follows: 0 – 200 µg/mL (biocytin), 1 - 1,000 µg/mL (GRGDSK-biotin) and 0 – 20 µg/mL (FN). After 1 h incubation, coatings were washed 3 times with deionized water.

Mix-in method

Coatings in 96-well plates

Prior to the coating preocedure, ligands were added to the prepolymer solution in different molar ligand to prepolymer ratios and coating was performed as described above. Biocytin was used in molar ratios of 1/200 - 1/2 and GRGDSK-biotin in molar ratios of 1/200 – 1/1.

Coatings on glass

Prior to the coating procedure, ligands were added to the prepolymer solution in different molar ligand to prepolymer ratios and coating was performed as described above. Biocytin and GRGDSK-biotin were used in the molar ratios 1/200 – 1/1.

2.2. ELISA

2.2.1. ELISA in coated 96-well plates

Wells were coated and functionalized as described above. Incubation of the wells with 300 µL deionized water for 60 min was followed by a washing step (three times) with 300 µL PBS-Tween (0.05 vol-% Tween-20 in PBS (0.01 M, pH 7.4), Roth, Karlsruhe, Germany).

Biocytin and GRGDSK-biotin

Wells were incubated with 300 µL glycidol solution (2.23 mg/mL in 0.2 M bicarbonate buffer) for 60 min followed by washing 3 times with 300 µL PBS-Tween. Ligands were detected by incubation with 50 µL streptavidin-peroxidase (SA-POD, 1/3000 in PBS, Roche, Mannheim, Germany) for 60 min. Wells were washed again with PBS-Tween. After dissolving one OPD tablet (Dako, Hamburg, Germany) in 3 mL deionized water and 1.25 µL H_2O_2 (30 vol-%), 100 µL of the OPD solution were added to each well. After 1 min incubation, the reaction was stopped by adding 100 µL 3 M HCl. Optical density (OD) of each well was measured in the microplate reader model Sunrise (Tecan, Maennedorf, Switzerland) at a wavelength of 492 nm. Results are shown on a logarithmic scale.

FN

Primary rabbit-anti-human FN antibody and goat-anti-rabbit IgG-POD were purchased from Sigma-Aldrich (Steinheim, Germany). After coating, functionalization, and incubation in deionized water as described above, wells were incubated with 50 µL of a 1/1000 dilution of rabbit-anti-FN antibody in PBS for 60 min and washed 3 times with 300 µL PBS-Tween. 50 µL of a 1/1000 dilution of goat-anti-rabbit IgG-POD in PBS were added to each well for 60 min. Afterwards, wells were washed with PBS-Tween again. Detection with OPD solution and OD measurement were carried out as described above.

Carbohydrates

Lectin II from *Griffonia simplicifolia* (GSII) was purchased from Vector Laboratories (Burlingame, USA). The recombinant lectin His_6CGL2 was produced in *E. coli* BL21 (DE3), purified as described earlier [15], and stored in PBS. Coatings functionalized with the sugar GlcNAc were incubated with glycidol solution as described above. After three times washing with 300 µL PBS-Tween, GlcNAc was detected with 50 µL of the biotinylated lectin GSII (10 µg/mL in 10 mM HEPES, pH 7.5). Coatings presenting the carbohydrate LacNAc were incubated with 50 µL of the recombinant galectin His_6CGL2 (50 µg/mL, in PBS) with subsequent washing for three times with 300 µL PBS-Tween. The detection of the lectins was carried out by incubation with 50 µL SA-POD (1/1000 in PBS) for biotinylated GSII bound to GlcNAc and 50 µL anti-His_6-POD from mouse IgG2a (1/4000 in PBS, Roche, Mannheim, Germany) for the recombinant galectin His_6CGL2 bound to LacNAc for 60 min. After washing, the detection with OPD solution and OD measurement were carried out as described above with 2 min incubation of the OPD substrate.

2.2.2. ELISA on coated glass

Glass substrates were coated and functionalized as described above. Coatings on glass were placed into a 24-well polystyrene plate (PS, Greiner Bio-One, Frickenhausen, Germany) and incubated with distilled water for 60 min.

Biocytin and GRGDSK-biotin

Coatings were incubated with 300 µl glycidol solution for 60 min and were washed 3 times with 300 µL PBS-Tween. The uncoated side of the substrates was blocked with PBS-BSA (1 wt-% bovine serum albumin in PBS, Servia Electrophoresis, Heidelberg, Germany) for 60 min followed by a washing step with PBS-Tween. 200 µL SA-POD (1/5000 in PBS) were incubated on coatings for 60 min and washed with PBS-Tween. After dissolving one OPD tablet in 6 mL deionized water and 2.5 µL H_2O_2 (30 vol-%), 200 µL of the OPD solution were added to each well. After 1 min incubation, the reaction was stopped by adding 100 µL 3 M HCl. OD measurements were carried out as described above.

FN

Primary rabbit-anti-FN antibody and goat-anti-rabbit IgG-POD were purchased from Sigma-Aldrich (Steinheim, Germany). After coating, functionalization and incubation with deionized water as described above, wells were incubated with 200 µL of a 1/1000 dilution of anti-FN antibody in PBS-BSA for 60 min and washed 3 times with PBS-Tween. 200 µL of a 1/1000

dilution of goat-anti-rabbit IgG-POD in PBS-BSA were added in each well for 60 min. Afterwards, wells were washed with PBS-Tween again. Detection with OPD solution and OD measurement were carried out as described above.

3. Results and discussion

ELISA and ELLA are promising surface sensitive quantification methods, which were applied to functionalized NCO-sP(EO-*stat*-PO) coatings in well plates and on glass in this Chapter. Due to the high functionality of the hydrogel, specific ligands could be easily introduced by incubation of fresh coatings (incubation method) or mixing the ligands with the prepolymers before the coating procedure (mix-in method). The coatings in well plates did not require blocking of non-specific binding sites since the coatings intrinsically resisted non-specific protein adsorption. However, in ELISAs using SA-POD, non-specific binding of SA-POD to the coatings was observed, which could be completely prevented by incubation with glycidol, which converted amino groups of the coatings into hydrophilic diols. One explanation for the SA binding to non-functionalized coatings could be the structural similarity of the biotin molecule and the isophorone ring of the IPDI as part of the hydrogel coating which may have been recognized by the SA. In case of ELISAs using antibodies instead of SA, glycidol incubation was not necessary. For coatings on glass placed in PS 24-well plates, an additional blocking step with BSA was necessary to block the uncoated side of the glass substrate and the PS well plate.

Biocytin was chosen as a model and standard molecule to prove the ability to detect even small molecules immobilized on the coatings. With its amino group it could covalently bind to fresh NCO-sP(EO-*stat*-PO) coatings still containing isocyanate groups. Figure 2A shows that a maximum biocytin binding to the coating in well plates was reached at 100 µg/mL. For coatings on glass approximately the same maximum binding concentration was determined (Figure 2B), even though standard deviations were much higher compared to ELISAs in well plates. This could be due to the back of the glass substrates and the PS well being blocked with BSA, which was probably not as efficient as the hydrogel coating of 96-well plates where the entire well was intrinsically blocked by the coating.

The biotin technology was also used for the detection of peptide sequences immobilized on the hydrogel coating. Biotin was coupled to the cell adhesion mediating peptide GRGDS via an additional C-terminal lysine residue (GRGDSK-biotin) that could be easily detected by SA. In principle, peptide biotinylation, which can also be achieved via terminal cysteins and Michael addition to avoid interference with lysines in the functional sequence of longer peptides, can be used for any peptide sequence of interest allowing the screening of a variety of peptides using the same ELISA procedure. Figure 2C shows a maximal binding of GRGDSK-biotin to the coating in well plates at concentrations of 200 µg/mL. This resembles the results for the

functionalization with biocytin, indicating that the binding mechanism is similar. Functionalized coatings on glass reached the maximum later at around 1000 µg/mL (Figure 2D).

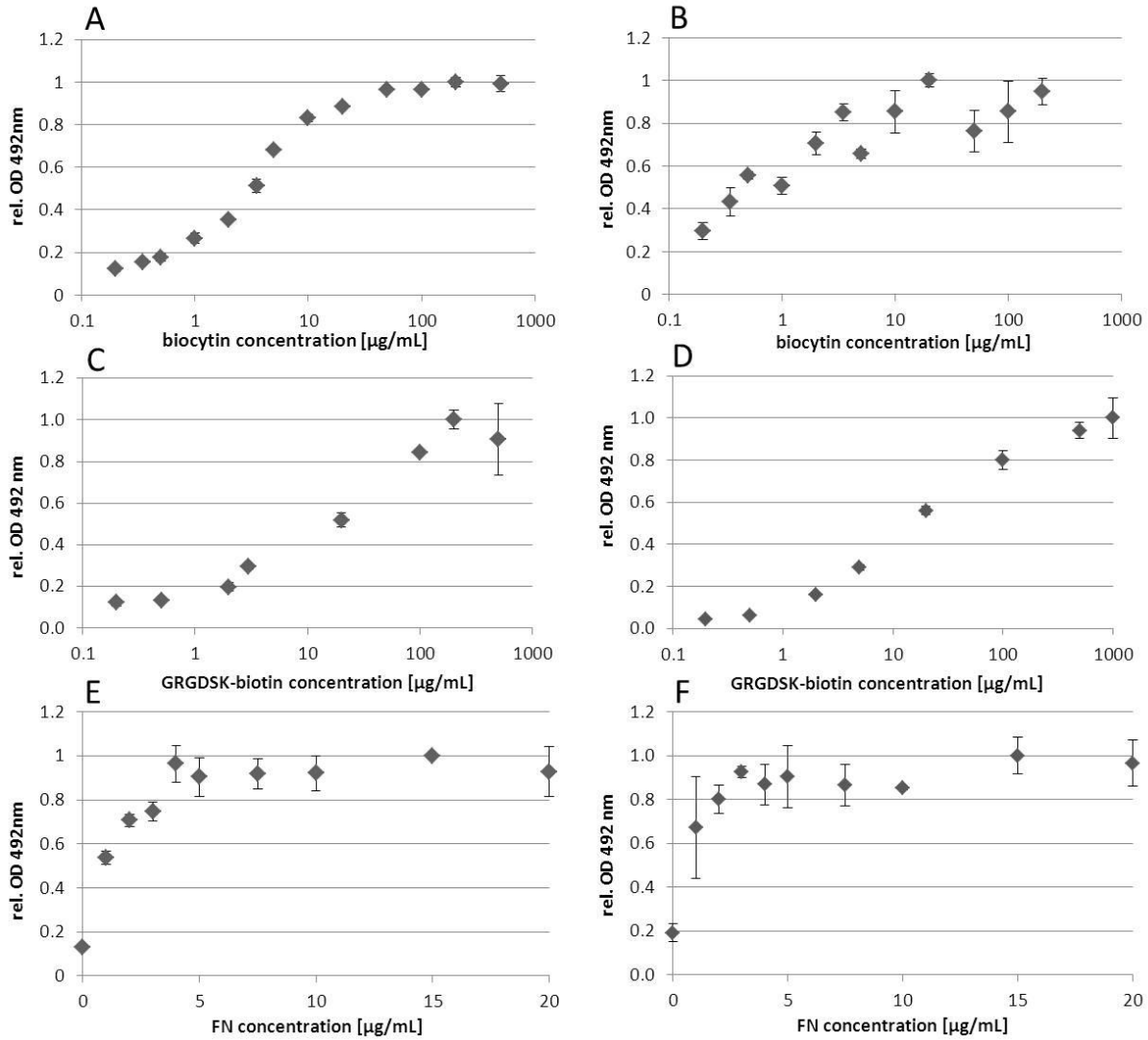

Figure 2: ELISA on hydrogels functionalized via incubation method.

Relative ODs of ELISAs on NCO-sP(EO-*stat*-PO) coatings in 96-well plates (A, C, E) and on glass (B, D, F) functionalized with different concentrations of biocytin (A, B), GRGDSK-biotin (C, D), and FN (E, F). Biocytin and GRGDSK-biotin were detected by SA-POD conjugate. FN was detected by rabbit-anti-human FN antibody and goat-anti-rabbit IgG-POD.

It can be noticed that the ligand concentration on top of the coating rose faster in case of biocytin as ligand compared to GRGDSK-biotin (Figure 2A-D). This can be explained by different molecular weights of the two ligands. Biocytin, having a molecular weight of 372.48 g/mol, is a smaller molecule compared to GRGDSK-biotin that has a molecular weight of 843.96 g/mol. Hence, a biocytin solution contained more ligand molecules that can bind to coatings than a GRGDSK-biotin solution of the same mass concentration and the same volume.

The ECM protein FN was also immobilized on the hydrogel coatings and detected via ELISA using a rabbit-anti-human antibody and a goat-anti-rabbit antibody conjugated to POD. A maximum binding capacity of coatings in well plates and on glass was reached at a FN concentration of 5 µg/mL (Figure 2E, F).

Hydrogel coating of well plates with NCO-sP(EO-*stat*-PO) was also utilized for the immobilization of amino functionalized carbohydrates. The sugars GlcNAc and LacNAc (Figure 3A, B) were chosen to demonstrate proof of principle for lectin recognition and interaction with a galectin, respectively. LacNAc was chosen because of its importance for galectin mediated cell-cell and cell-matrix interactions *in vivo*. Immobilizing LacNAc glycan structures on an inert surface would allow a more natural presentation of ECM proteins mediated by galectins [15]. Coupling of the sugars to NCO-sP(EO-*stat*-PO) coatings was accomplished by deprotection of the amino group at a hydrophobic linker [15]. Detection of the immobilized carbohydrates was performed by ELLA using lectins, namely the GlcNAc-specific lectin II from *Griffonia simplicifolia* (GSII) and the LacNAc-specific recombinant galectin His_6CGL2 from *Coprinus cinereus* [15, 16] (Figure 3C, D). This proof-of-principle was established on the small-scale coatings in well plates exclusively due to the time-consuming and expensive synthesis of the carbohydrates.

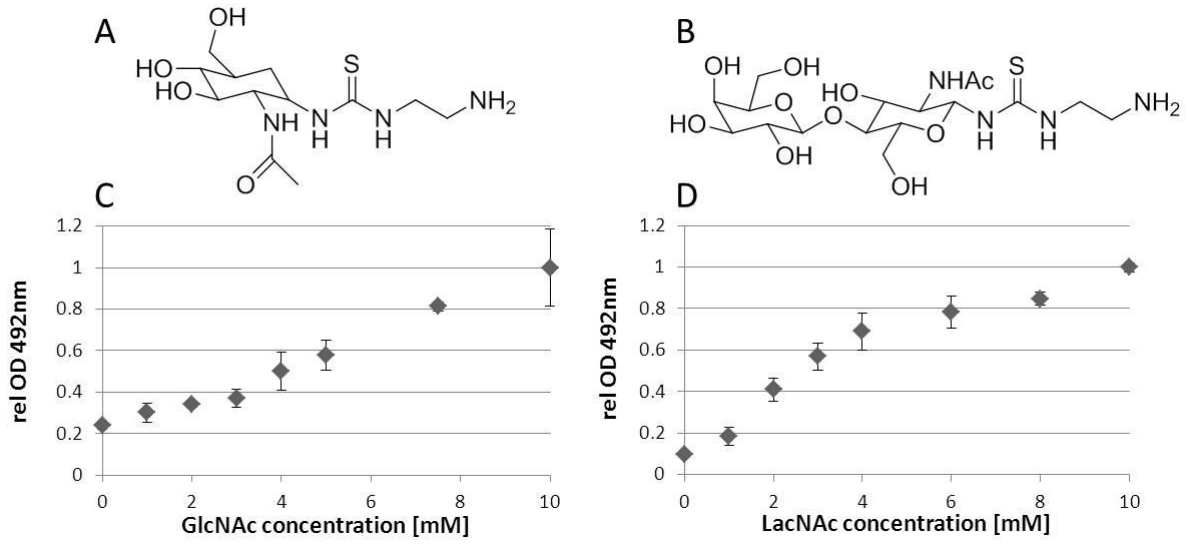

Figure 3: ELISA on hydrogels functionalized with carbohydrates via incubation method.

Rel. ODs of ELLAs on NCO-sP(EO-*stat*-PO) hydrogel coatings in 96-well plates functionalized with the sugars GlcNAc (A) and LacNAc (B). GlcNAc was detected by the biotinylated GSII and SA-POD conjugate (C). LacNAc was detected by His_6CGL2 and anti-His_6-IgG-POD (D).

Figure 3C and D show that binding of both lectins to the corresponding carbohydrates increased with higher sugar concentrations. In the case of GlcNAc, a saturation of the lectin to the immobilized monosaccharide on the coating could not be reached up to 10 mM sugar concentration (Figure 3C). This first assays shows that the binding of GlcNAc detected by GSII on the coated well plates was at least as good as optimized assays in commercial microtiter plates [15]. The disaccharide LacNAc interacting with the galectin His_6CGL2 was chosen as a more complex and relevant carbohydrate ligand. A maximal binding of the galectin His_6CGL2 was reached at incubation with 5 mM LacNAc solution in a reproducible manner (Figure 3D). The results demonstrate that immobilization and subsequent detection of the carbohydrates on hydrogel coated well plates was possible, and opens the possibility to use this platform for the screening of a variety of synthesized glycan structures. In addition, this system possesses the advantage of further construction of more complex structures on the hydrogel surface such as binding of proteins followed by cell adhesion studies which is not possible with the systems that are available so far (see Chapter 9).

Beside the incubation method, the mix-in method was used for functionalization of the hydrogel coatings using the ligands biocytin and GRGDSK-biotin. Testing expensive ligands, the incubation method is advantageous in terms of reduced consumption of the ligand. Additionally, the mix-in method is not suitable for bigger molecules like the protein FN. Human FN has a molecular weight of 450 kDa with a high number of nucleophilic residues in the periphery of the protein. Concerning the big size and the multi-functionality of the protein towards the prepolymers, the protein may covalently bind several prepolymers. In case of the mix-in method, it can be assumed that the FN acts as a crosslinker in solution, thus large aggregates of the FN molecules decorated by prepolymers are formed. Testing a coating on glass functionalized with FN via mix-in method in cell culture, the surface of the coating was as inert against cell adhesion as a pure coating (results not shown). In case of mixing biocytin with NCO-sP(EO-*stat*-PO) in molar ratios of 1/200 to 2/1 before the coating procedure in the well plates, a normal distribution with a maximum between 1/50 and 1/20 was observed via ELISA (Figure 4A). In case of coatings on glass functionalized with biocytin using the mix-in method, a plateau was reached at biocytin to prepolymer ratios of 1/5 (Figure 4B). Functionalizing the coatings with the peptide GRGDSK-biotin, a maximal binding was observed at peptide to prepolymer ratios of 1/20 and between 1/10-1/5 for coatings in well plates and on glass, respectively (Figure 4C, D).

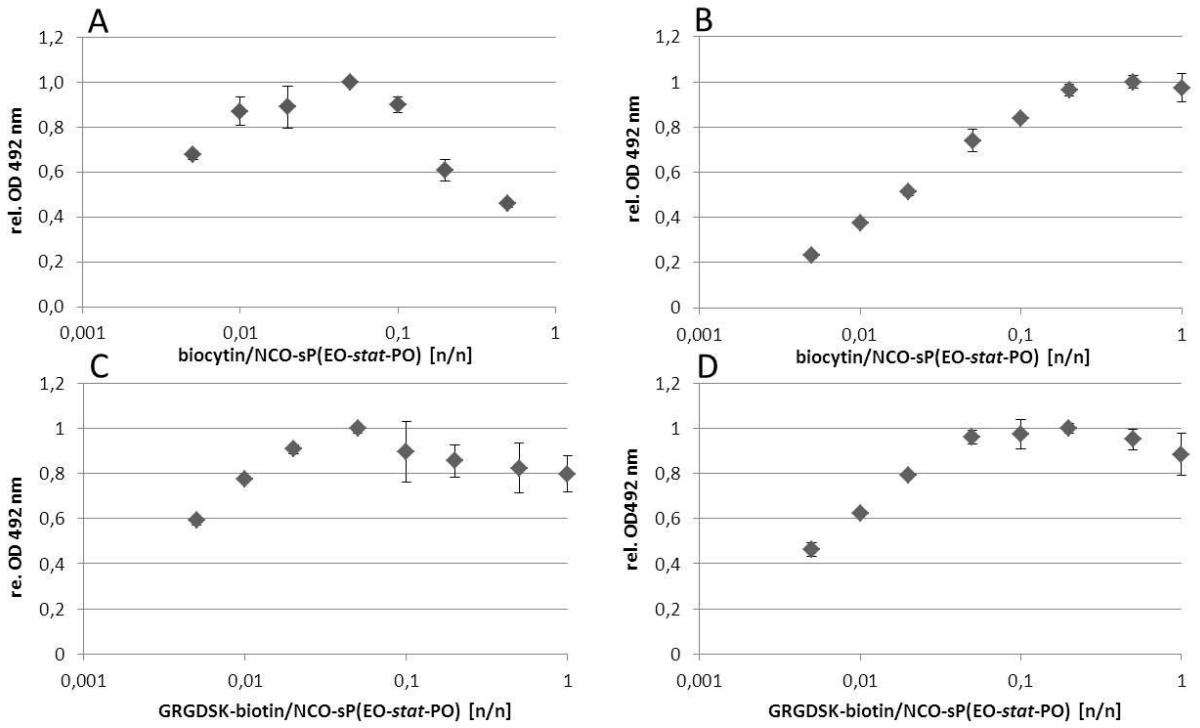

Figure 4: ELISA on hydrogels functionalized via mix-in method.

Relative ODs of ELISAs on NCO-sP(EO-*stat*-PO) coatings in 96-well plates (A, C) and on glass (B, D) functionalized with different molar ligand to prepolymer ratios using biocytin (A, B) and GRGDSK-biotin (C, D). Biocytin and GRGDSK-biotin were detected by SA-POD conjugate.

An explanation for the unexpected maximum that occurred when mixing biocytin with the prepolymer solution before the coating procedure of well plates could be the chemical structure of biocytin (Figure 5). Dankers et al. could form reversible gels by hydrogen bonding of ureido-pyrimidinone functionalized polymers [17]. These hydrogels were only formed over a critical polymer concentration, but the study demonstrated that multiple hydrogen bond formation was strong enough to yield aggregation also in water. It may be possible that the same effect was observed in the experiment explained above through dimerization of biocytin above a critical concentration. With raising biocytin concentrations in the prepolymer solution, higher biocytin concentrations were detected by ELISA at the surface of the hydrogel films. A maximum biocytin concentration was achieved at biocytin to prepolymer ratios between 1/50 and 1/20. Higher biocytin concentrations in the prepolymer solution reduced the detectable biocytin concentration on top of the crosslinked hydrogel. This could be due to the formation of hydrogen bonds between the α-amino carbonic acids of two biocytins above a critical biocytin concentration in solution (Figure 5). The fact that this effect did not occur for the biotinylated peptide (Figure 4C) supports this hypothesis.

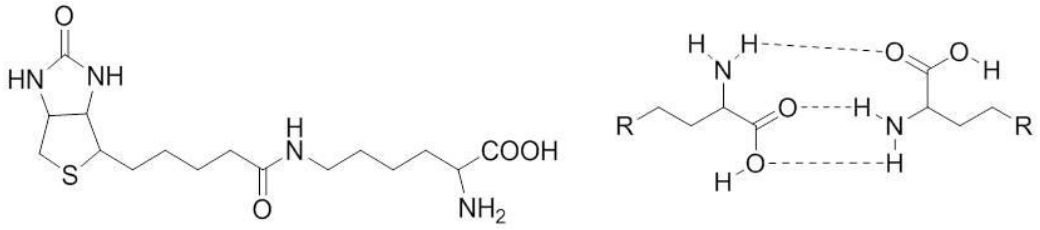

Figure 5: Biocytin and hydrogen bonding.

Chemical structure of biocytin with its α-amino carbonic acid residue (left) and possible hydrogen bonding between two α-amino carbonic acids (right).

4. Conclusions

In summary, the coated wells and glass substrates could be utilized for the screening of different ligands via ELISA and ELLA. The coatings were functionalized with a low-molecular structure (biocytin), a peptide (GRGDSK-biotin), a protein (FN), and carbohydrates (GlcNAc, LacNAc) by incubation of fresh coatings and by mixing ligands and prepolymers prior to the coating procedure. Detection and quantification of the ligands with SA, antibodies, and lectins using ELISA and ELLA techniques were possible. The great advantage of functionalized NCO-sP(EO-*stat*-PO) coatings in the well plate format is the ligand presentation on a per se inert surface, thus no need of an additional blocking step. ELISAs showed no background signal by non-specific binding to the coatings. Only SA was found to slightly bind to untreated coatings, which could be eliminated by glycidol treatment. To apply ELISA on functionalized coatings on glass, which were placed into a PS well plate, an additional blocking step with BSA was necessary, only to block the plastic of the well plate and the uncoated back of the glass substrate. Nevertheless, specific detection of the ligands was possible. Consequently, an easy applicable ELISA/ELLA method was demonstrated that has the potential to serve as a surface sensitive ligand quantification technique on hydrogel coatings with the potential to be transferred to any kind of biomaterial.

5. References

1. Behravesh, E.; Sikavitsas, V.I. and Mikos, A.G. Quantification of ligand surface concentration of bulk-modified biomimetic hydrogels. *Biomaterials* **2003**, 24 (24) 4365-74.
2. Sung, D.; Park, S. and Jon, S. Facile method for selective immobilization of biomolecules on plastic surfaces. *Langmuir* **2009**, 25 (19) 11289-94.
3. Cummings, R.D. and Kornfeld, S. The distribution of repeating [Galbeta1,4GlcNAcbeta1,3] sequences in asparagine-linked oligosaccharides of the mouse lymphoma cell-lines BW5147 and PHAR2.1 - binding of oligosaccharides containing these sequences to immobilized datura-stramonium agglutinin. *Journal of Biological Chemistry* **1984**, 259 (10) 6253-60.
4. Fukuda, M.; Carlsson, S.R.; Klock, J.C. and Dell, A. Structures of O-linked oligosaccharides isolated from nonrmal granulocytes, chronic myelogenous leukemia-cells, and acute myelogenous leukemia-cells. *Journal of Biological Chemistry* **1986**, 261 (27) 2796-806.
5. Krusius, T.; Finne, J. and Rauvala, H. Poly(glycosyl) chains of glycoproteins - Characterization of a novel type of glycoprotein saccharides from human erythrocyte-membrane. *European Journal of Biochemistry* **1978**, 92 (1) 289-300.
6. McEver, R.P.; Moore, K.L. and Cummings, R.D. Leukocyte trafficking mediated by selectin-carbohydrate interactions. *Journal of Biological Chemistry* **1995**, 270 (19) 11025-28.
7. Ujita, M.; McAuliffe, J.; Suzuki, M.; Hindsgaul, O.; Clausen, H.; Fukuda, M.N. and Fukuda, M. Regulation of I-branched poly-*N*-acetyllactosamine synthesis - Concerted actions by i-extension enzyme, I-branching enzyme, and b1,4-galactosyltransferase I. *Journal of Biological Chemistry* **1999**, 274 (14) 9296-304.
8. Zhou, D.P. Why are glycoproteins modified by poly-N-acetyllactosamine glycoconjugates? *Current Protein & Peptide Science* **2003**, 4 (1) 1-9.
9. Elola, M.T.; Wolfenstein-Todel, C.; Troncoso, M.F.; Vasta, G.R. and Rabinovich, G.A. Galectins: Matricellular glycan-binding proteins linking cell adhesion, migration, and survival. *Cellular and Molecular Life Sciences* **2007**, 64 1679 – 700.
10. Hughes, R.C. Galectins as modulators of cell adhesion. *Biochimie* **2001**, 83 (7) 667-76.
11. Gotz, H.; Beginn, U.; Bartelink, C.F.; Grunbauer, H.J.M. and Moller, M. Preparation of isophorone diisocyanate terminated star polyethers. *Macromolecular Materials and Engineering* **2002**, 287 (4) 223-30.
12. Kasten, A.; Müller, P.; Bulnheim, U.; Groll, J.; Bruellhoff, K.; Beck, U.; Steinhoff, G.; Möller, M. and Rychly, J. Mechanical integrin stress and magnetic forces induce biological responses in mesenchymal stem cells which depend on environmental factors. *Journal of Cellular Biochemistry* **2010**, 111 (6) 1586-97.
13. Groll, J.; Ameringer, T.; Spatz, J.P. and Moeller, M. Ultrathin coatings from isocyanate-terminated star PEG prepolymers: Layer formation and characterization. *Langmuir* **2005**, 21 (5) 1991-99.
14. Rech, C.; Rosencrantz, R.R.; Křenek, K.; Pelantová, H.; Bojarová, P.; Römer, C.; Hanisch, F.-G.; Křen, V. and Elling, L. Combinatorial one-pot synthesis of poly-N-acetyllactosamine oligosaccharides with leloir-glycosyltransferases. *Advanced Synthesis and Catalysis* **2011**, 353 2492-500.

15. Sauerzapfe, B.; Krenek, K.; Schmiedel, J.; Wakarchuk, W.W.; Pelantova, H.; Kren, V. and Elling, L. Chemo-enzymatic synthesis of poly-N-acetyllactosamine (poly-LacNAc) structures and their characterization for CGL2-galectin-mediated binding of ECM glycoproteins to biomaterial surfaces. *Glycoconjugate Journal* **2009**, 26 (2) 141-59.

16. Walser, P.J.; Haebel, P.W.; Kunzler, M.; Sargent, D.; Kues, U.; Aebi, M. and Ban, N. Structure and functional analysis of the fungal galectin CGL2. *Structure* **2004**, 12 (4) 689-702.

17. Dankers, P.Y.W.; Harmsen, M.C.; Brouwer, L.A.; Van Luyn, M.J.A. and Meijer, E.W. A modular and supramolecular approach to bioactive scaffolds for tissue engineering. *Nature Materials* **2005**, 4 (7) 568-74.

CHAPTER 7

Cell behavior analysis dependent on ligand densities on hydrogels

Quantification of ligands immobilized to NCO-sP(EO-*stat*-PO) hydrogel coatings were discussed in Chapter 3 to 6, where maximal ligand densities achievable in and on the hydrogel system were determined. However, maximal ligand density is not necessarily the optimum in respect to cell-material contact. To design functional biomaterials in contact with cells and tissue, the *in vitro* analysis is of great importance to determine not only maximal but rather optimal ligand densities regarding cell adhesion, proliferation, and vitality. In this Chapter, NCO-sP(EO-*stat*-PO) hydrogel coatings were functionalized with different GRGDS concentrations below and above the maximum functionalization as determined in previous Chapters. To assure that softness of the hydrogel coatings did not negatively influence cell adhesion, atomic force microscopy (AFM) was performed and showed an approximate elasticity of 2.8 GPa of the coatings, which was hard enough for proper fibroblast adhesion. For quantification of cell adhesion, primary human dermal fibroblasts (HDF) were counted on life cell images and with a CASY® cell counter. A minimal ligand to prepolymer ratio of 1/5 and 1/2 was determined respectively. Additionally, HDF vitality was analyzed measuring different intracellular enzyme activities revealing that cell vitality did not depend on the ligand concentration. Cells that adhered to coatings with low peptide to prepolymer ratio were just as vital as cells on hydrogels with higher ratios.

In the Appendix belonging to this Chapter, cell adhesion studies using the mouse fibroblast cell line L929 are shown. Cell adhesion and proliferation on GRGDS functionalized NCO-sP(EO-*stat*-PO) hydrogel coatings were determined by cell counting on life cell images. In contrast to experiments with HDFs, the highest ligand to prepolymer ratio of 2/1 was necessary for maximal L929 cell adhesion. These results showed that optimal ligand density for cells is different for cells from different species.

1. Introduction

RGD, the cell binding mediating peptide sequence in the ECM protein fibronectin (FN), was first discovered by Pierschbacher and Rouslahti in 1984 [1]. The RGD sequence immobilized to polymer materials is recognized by the cellular transmembrane integrin receptors [2, 3]. Integrins binding to RGD peptides, cluster together in the cell membrane, forming cell-matrix adhesion complexes (CMAC) within the size range of 0.25 – 10 µm [4, 5]. This cell-ECM connection allows cells to spread over an area of various peptides. In the natural ECM, integrin ligands are available with certain distances, as ligands such as the RGD containing FN are attached to collagen fibers [6], which appear in distances of around 67 nm [7]. Various polymers have been functionalized with RGD peptides for controlled cell-material interactions (for review, see reference [8]). It was shown before, that a decrease in ligand spacing led to an increased number of $\alpha_5\beta_1$-integrin-FN binding [9], meaning, that cell adhesion was advanced with increasing RGD densities (for overview, see Table 1). However, due to integrin size and steric configurations, cells can only sense a certain amount of RGD peptides on a surface. Consequently, ligand concentrations above this maximal range will not lead to additional integrin binding. Therefore, it is very important for *in vitro* and *in vivo* applications, to not only determine the maximal loading capacities of biomaterials by physical methods like radiolabeling, X-ray photoelectron spectroscopy (XPS) or time-of-flight secondary ion mass spectrometry (TOF-SIMS) (Chapter 3 and 4), but also to sense the optimal ligand density by cells themselves.

Since 1970, various studies aimed at the determination of minimal ligand spacing allowing cell adhesion and spreading, aiming to understand cellular function, and designing optimal biomaterials. Studies with different fibroblast cells and different RGD ligands on various surfaces have been performed and the outcomes were quite different with ligand distances between 10 and 500 nm (Table 1). There are most certainly more studies concerning this issue, nevertheless, this Table should give a good overview over the research during the last decades, indicating the importance of individually analyzing each biomaterial system in contact with different cells.

To avoid undesired immune responses in the host, biomaterials should be inert, preventing non-specific protein adsorption [10]. Moreover, they should present specifically interacting cell adhesion molecules (CAM) on the per se inert background for defined cell-material interactions. For analyzing such materials to determine minimal ligand spacing necessary for

proper cell adhesion and spreading, all other influences on cell behavior need to be excluded. This can be achieved by presenting CAMs on per se inert materials such as self-assembled monolayers (SAM) or hydrogels. Many of the studies shown in Table 1, like Hughes et al. 1979 [11] or Massia and Hubbell 1991 [12] did not pay attention to present RGD peptides on a non-fouling background. Later studies from Drumheller et al. [13], Hern and Hubbel [14], Neff et al. [15], Cavalcanti-Adam et al. [16], or George et al. [17] presented RGD ligands on inert backgrounds allowing the exclusive analysis of the effect of ligand distances. Nevertheless, ligand spacing determined by Hern and Hubbell was only an assumption. Even though, RGD ligands were presented on an inert 10 nm hydrogel, Hern and Hubbell quantified peptides in the bulk hydrogel and only assumed that 10% were sterically available for cell receptors. George et al. immobilized ligands on SAMs and no absolute ligand spacing for cell adhesion or spreading could be given, only the tendency that fibroblast spreading was increased with reduced lateral spacing of the RGD ligands. Different studies, which revealed different ligand distances ranging from 2 to 110 nm determined on non-fouling backgrounds show the complexity of the influences. Even though, RGD peptides were immobilized to inert biomaterials, influences such as surface chemistry, e.g. hydrophilicity, determined cell behavior beside the ligand spacing [18]. Due to the variety of influences investigating different biomaterials, each biomaterial system needs to be analyzed individually.

NCO-sP(EO-*stat*-PO) hydrogels used in this study have been introduced a few years ago [24] and were shown to inhibit non-specific protein adsorption [25]. Specific cell adhesion could be introduced by immobilizing RGD peptides [25]. So far, RGD immobilized to the hydrogels was not quantified and cell adhesion on these surfaces was not analyzed in a RGD concentration dependent manner. To assure that softness of the hydrogel coatings did not negatively influence cell adhesion, an elasticity of 2.8 GPa was determined for the coatings by AFM, which was hard enough for proper fibroblast adhesion. In this Chapter, the proliferation of HDFs and L929 cells was observed on NCO-sP(EO-*stat*-PO) hydrogel coatings functionalized with different GRGDS to prepolymer ratios. Cell populations were determined by counting adherent cells on life cell images. While a minimal ligand to prepolymer ratio of 1/5 was sufficient for HDF adhesion, a higher ratios of 2/1 was necessary for maximal L929 cell adhesion. Additionally, HDFs were counted using a CASY® cell counter revealing different results compared to HDFs counted on life cell images. This method revealed a minimal GRGDS to prepolymer ratio of 1/2 necessary for proper cell adhesion. Also, HDF vitality on the GRGDS functionalized hydrogels was investigated measuring the activity of different intracellular enzymes. Unfortunately, no clear correlation of RGD content to cell vitality could be observed.

Table 1: RGD spacing on surfaces for fibroblast adhesion.

Literature overview of determined minimal RGD spacing necessary for sufficient fibroblast adhesion, spreading, or CMAC formation. Table modified and actualized from reference [12] with permission from the Rockefeller University Press.

Reference	Year	Surface	Spacing [nm]	Cell behavior analyzed
Hughes et al. [11]	1979	FN on TCPS	80	Hamster kidney fibroblast (BHK) adhesion and spreading
Humphries et al. [19]	1986	RGDS on PS	10	Hamster kidney fibroblast (BHK) adhesion and spreading
		FN on PS	12	
Singer et al. [20]	1987	RGDS on PS	16	Rat (NRK), hamster (Nil 8), and mouse (Balb/c 3T3) fibroblast adhesion
Brandley et al. [21]	1988	YAVTGRGD on polyacrylamide gel	76*	Balb/c 3T3 mouse fibroblast adhesion
Danilov and Juliano [22]	1989	GRGDSP–BSA conjugate	22	CHO fibroblast adhesion and spreading
		vitronectin	22	
		FN (all on TCPS)	42	
Underwood and Bennett [23]	1989	FN on plastic	37	Hamster kidney fibroblast (BHK-21) adhesion
		Vitronectin	20	
Massi and Hubbell [12]	1991	GRGDY on glass	440 / 140	Human foreskin fibroblast adhesion / CMAC and stress fiber formation
Drumheller et al. [13]	1994	GRGDS on PAA hydrogel with PEG spacer	4 / 2*	Fibroblast adhesion / CMAC formation
Hern and Hubbell [14]	1998	PEG diacrylate hydrogles with GRGDS on a spacer (MW 3400)	14*	Human foreskin fibroblasts spreading
Neff et al. [15]	1999	GRGDSY on PEO/PPO/PEO triblock copolymers	12*	Mouse embryonic fibroblast (NIH 3T3) adhesion and spreading
Cavalcanti-Adam et al. [16]	2007	Cyclic-RGD gold nanodots in between PEG	110 / 58	Rat embryo fibrolast (REF52) adhesion / spreading
George et al. [17]	2009	PS-PEO block copolymers with CGRGDS	44 to 62	Mouse embryonic fibroblast (NIH 3T3) spreading

* Values were not given in the publications or in reference [12]. Therefore, ligands were assumed to be distributed homogeneously on the surfaces in a hexagonal pattern and the spacing calculated from the ligand concentration given in the publications.

2. Experimental section

2.1. Hydrogel coatings

2.1.1. NCO-sP(EO-stat-PO) synthesis

Isocyanate terminated prepolymers (NCO-sP(EO-*stat*-PO)) were synthesized as described in detail elsewhere [26]. In short, the prepolymer was fabricated by the reaction of hydroxyl terminated star shaped polyether polyole with isophorone diisocyanate (IPDI).

2.1.2. Preparation of silicon and glass surfaces

Glass substrates (Ø 15 mm, Paul Marienfeld, Lauda-Königshofen, Germany) were polished with isopropanol. Glass substrates and 1 cm^2 silicon wafer (CrysTecKristall-technologie, n-Type, Berlin, Germany) were successively cleaned in acetone, distilled water, and isopropanol in an ultrasonic bath for 5 min each followed by drying in a stream of nitrogen. Solvents were purchased from Prolabo (Darmstadt, Germany). Substrates were activated by O_2-plasma treatment in the plasma process plant AK 330 (Roth & Rau, Hohenstein-Ernstthal, Germany) for 15 min (400 W, 50 sccm, 0.4 mbar). Afterwards, substrates were left in a desiccator containing 100 µl 3-aminopropyl-trimethoxysilan (AS) at 5 mbar for 60 min. After removal of AS, the glass substrates were left in a vacuum of minimum 10^{-2} mbar for 1 h and stored at 250 mbar.

2.1.3. NCO-sP(EO-*stat*-PO) c*oating*

The coating procedure has been described earlier [27]. Prepolymers were solubilized in tetrahydrofuran (THF, dried over sodium, Prolabo, Darmstadt, Germany). After adding water to the solution (9/1 v/v water/THF, prepolymer concentration 10 mg/ml), prepolymers were left for crosslinking for 5 min. Two droplets of the solution were placed on the amino-silanized surface of a glass substrate after filtration through a 0.2 µm syringe filter (Whatman, Dassel, Germany). The coating process was carried out in the spin coater WS-400-B-6NPP/LITE (Laurell Technologies, North Wales, USA) at 2,500 rpm for 40 sec with an acceleration time of 5 sec. Each prepolymer solution was used to coat a maximum of 6 substrates. Coated substrates were stored at room temperature for at least 12 h to ensure complete crosslinking of the coating.

2.1.4. Functionalization

Prior to the coating procedure, GRGDS (Bachem, Bubendorf, Switzerland) was added to the prepolymer solution in molar GRGDS to prepolymer ratios of 1/20, 1/10, 1/5, 1/2, 1/1, and 2/1. Coating was performed as described above.

2.2. Coating characterization

2.2.1. Ellipsometry

The spectroscopic ellipsometer model OMT-RTE-3501 NM30 (OMT, Ulm, Germany) was used with a wavelength-range of 450 - 800 nm under an angle of incidence of 70°. The system was operated in high resolution mode. The calculation of the layer thickness was based on a model for hydrogel layers on silicon. For the determination of the layer thickness, the heights of 3 aminosilanized and 3 coated silicon substrates were measured. The difference of the mean values resulted in the thickness of the hydrogel coating.

2.2.2. AFM

Coatings on silicon were scratched with a needle. At the border of silicon and coating, the height and the elasticity of the coating were determined with the Dimension® ICON® atomic force microscope (Bruker AXS, Mannheim, Germany). Measurements were performed in air at room temperature using the PeakForce QNM modus and OTESPA tips (Veeco, Mannheim, Germany). A force constant of around 50 N/m and a resonance frequency of 325.6 kHz were applied and areas measured were sized 10 x 10 µm. Analysis was performed with NanoScope™ software (version 8.10 R1.60476).

2.3. *In vitro* cell experiments

2.3.1. Cell culture

HDFs (max. passage 8) isolated from human foreskin were kindly provided by Prof. Baron (Department of Dermatology and Allergology, University Hospital of the RWTH Aachen University, Germany). HDFs were cultured in DMEM medium (Invitrogen Karlsruhe, Germany) supplemented with 10 vol-% fetal bovine serum (Biowest, Nuaillé, France) and 1 vol-% penicillin/streptomycin (PAA, Cölbe, Germany) at standard cell culture conditions (37°C, 5% CO_2, 95% humidity).

2.3.2. Sample preparation and cell seeding

Coated glass substrates in 24-well polystyrene plate (PS, Greiner Bio-One, Frickenhausen, Germany) were washed thoroughly with sterile water and PBS buffer (0.01 M, pH 7.4) for sterilization. HDFs were harvested by incubation with accutase (PAA, Cölbe, Germany) for 16 min at 37°C. The reaction was stopped by adding DMEM. 1 mL cell suspension (20,000 cells/mL in DMEM) was seeded on each coated glass substrate and in a tissue culture polystyrene 24-well plate

(TCPS, Greiner Bio-One, Frickenhausen, Germany) and incubated under standard cell culture conditions.

2.3.3. Cell adhesion

Counting of adherent cells on life images

Cell adhesion was monitored up to 24 h by optical microscopy using an inverted Axiovert 100A imaging microscope (Carl Zeiss, Göttingen, Germany) and adherent cells counted after 0.25, 0.5, 1, 2, 3, 24 h.

Counting of adherent cells with CASY® cell counter

Cells were cultured on coatings up to 1 week. For cell number determination they were washed 2 times with 1 mL PBS buffer and detached from the surface by incubation with 0.5 mL accutase for 16 min at 37°C. 0.5 mL DMEM medium were added and the cells were pipetted up and down 20 times to dissolve cell clusters and get a homogenous cell suspension. 100 µL of the cell suspension were diluted in 10 mL Coulter® Isoton® III diluent (Beckmann Coulter, Krefeld, Germany) and cells in the range of 12 to 30 µm were counted immediately in the CASY® cell counter (Schärfe System, Reutlingen, Germany).

2.3.4. Cell viability

CellTiter-Blue® cell viability assay

Medium and Cell Titer-Blue Reagent (protected from light) were heated up to 37°C. For measurement of the cell vitality up to 96 h, the medium was discarded and 400 µL fresh medium were filled into each well. 80 µL CellTiter-Blue® Reagent from the CellTiter-Blue® cell viability assay (Promega, Mannheim, Germany) were added without exposure to light. The well plate was shaken for 10 sec and incubated for 60 min under standard cell culture conditions. 100 µL of the sample supernatants and 50 µL SDS solution (3 wt-%) were filled into a black 96-well plate. The fluorescence intensity was determined in a Tecan Infinite 200 micro-plate reader (Crailsheim, Germany) with an excitation wavelength of 560 nm and an emission wavelength of 590 nm.

WST-1 cell proliferation assay

Cell proliferation reagent WST-1 (Roche Diagnostics, Mannheim, Germany) was diluted in DMEM (10 vol-%). Cells were cultivated up to 1 week. The medium in each well was replaced by 500 µL WST-1 solution and incubated at 37°C for 30 min. Afterwards, 2 times 200 µL solution of

each well were filled into a 96-well plate and the absorbance was measured by a Tecan Spectra Fluor plus micro-plate reader (Crailsheim, Germany) at a wavelength of 450 nm.

3. Results and discussion

Even-Ram et al. showed that cell fate strongly depended on the stiffness of a material [28]. Additionally, fibroblast adhesion was observed to depend on the material's stiffness. It was shown that fibroblasts adhered better to stiffer substrates with an elasticity of 30 - 100 kPa compared to soft materials with 1 kPa [29]. On stiffer surfaces, fibroblasts built up more organized actin filaments, which are important for cell adhesion and spreading [30]. To ensure that NCO-sP(EO-*stat*-PO) hydrogel coatings of 30 nm thickness were stiff enough to support HDF adhesion by suppressing the soft hydrogel character via the thin coating, the elastic modulus of the coatings was determined by AFM. Therefore, coatings on silicon were scratched with a needle to create a border between the silicon and the coating and to determine height and elasticity of the coating. With an elastic modulus of 2.8 GPa (Figure 1), the coatings were clearly over the favored 30 – 100 kPa [29], and therefore, stiff enough to promote strong fibroblast adhesion. It needs to be mentioned, that ellipsometry determined a coating thickness of 46.8 +/- 4.2 nm (results not shown). In contrast, coating thickness determines by AFM using the PeakForce QNM modus was only 10 nm (Figure 1). During the AFM measurement in the tapping mode, the hydrogel was most likely pressed against the silicon surface, most certainly causing the compression of the coating. Therefore, the measured elasticity was just an approximate value and may have been slightly lower in reality. Nevertheless, the measurements pointed out, that the soft character of a thick and swollen hydrogel was suppressed, when applied as thin coating on a stiff surface.

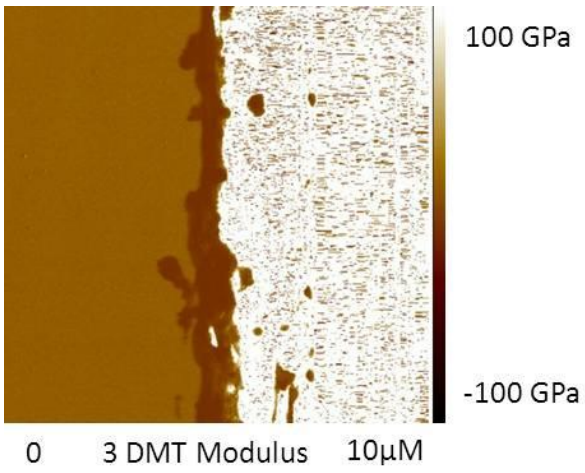

Figure 1: Stiffness of NCO-sP(EO-*stat*-PO) coatings.

AFM image of a NCO-sP(EO-*stat*-PO) coating on silicon scratched with a needle (left: coating, right: silicon). An elastic modus of 2.8 GPa and a thickness of 10 nm were determined using the PeakForce QNM modus.

Figure 2 presents results of cell adhesion studies with primary HDFs on NCO-sP(EO-*stat*-PO) coatings functionalized with different GRGDS to prepolymer ratios. As a first method, life cell images were taken after different time points and adherent cells were counted (Figure 2A). Hydrophobic TCPS served as positive control for cell adhesion. Proteins out of the medium adsorb on TCPS [10] leading to the adhesion of cells on top of the protein layer. On non-functionalized hydrogel coatings, no cell adhesion was observed. At initial time points up to 1 h, more HDFs adhered to coatings with higher GRGDS to prepolymer ratios. Coatings with GRGDS contents of peptide to prepolymer ratio of 1/1 and 2/1 enabled even more cells to adhere compared to TCPS. After 3 and 24 h of cultivation, the amount of cells that adhered to coatings functionalized with molar GRGDS to prepolymer ratios of 1/5 to 2/1 was comparable. On coatings functionalized with lower molar ratios of 1/10, significantly lower numbers of cells adhered and proliferated compared to coatings functionalized with higher amounts of GRGDS or TCPS. HDFs grown on coatings with high GRGDS amounts were nearly confluent after 24 h with about 10,000 to 14,000 cells/cm^2. The results of the cell kinetic studies revealed that the minimum threshold of GRGDS to prepolymer ratio allowing efficient cell adhesion was 1/5. To allow HDFs to adhere efficiently already after 30 min to 1 h, a molar ratio of 1/1 and 2/1 was necessary.

On the basis of these results, one can speculate that cells which adhered in an non-specific way to hydrophobic TCPS needed to build their own ECM and therefore, adhered slower at initial time points. Cells on inert coatings functionalized with GRGDS recognized the RGD peptide as a part of the natural ECM, which enabled them to adhere faster at initial time points. This hypothesis has to be proven by staining different ECM proteins on the surfaces at the initial time points to validate increased ECM secretion of cells on TCPS. The investigation would allow a better insight into cellular reactions to the surface to find an explanation for the observed phenomenon.

Additionally, adherent HDFs were counted after the detachment with accutase using a CASY® cell counter. Figure 2B shows that HDFs adhered faster on TCPS at initial time points up to 24 h compared to GRGDS functionalized hydrogels. All functionalized hydrogel coatings with different amounts of GRGDS showed slightly lower cell growth. However, after one week of cell culture, coatings functionalized with molar GRGDS to prepolymer ratios of 1/20, 1/10, and 1/5 showed significantly lower amounts of adherent cells compared to TCPS. In case of functionalized coatings with ratios of 1/2 and 1/1, significantly higher cell densities were measured compared to all other surfaces. The results of cell adhesion studies with the CASY®

cell counter indicate that a minimum threshold of GRGDS to prepolymer of 1/2 was necessary for efficient HDF adhesion.

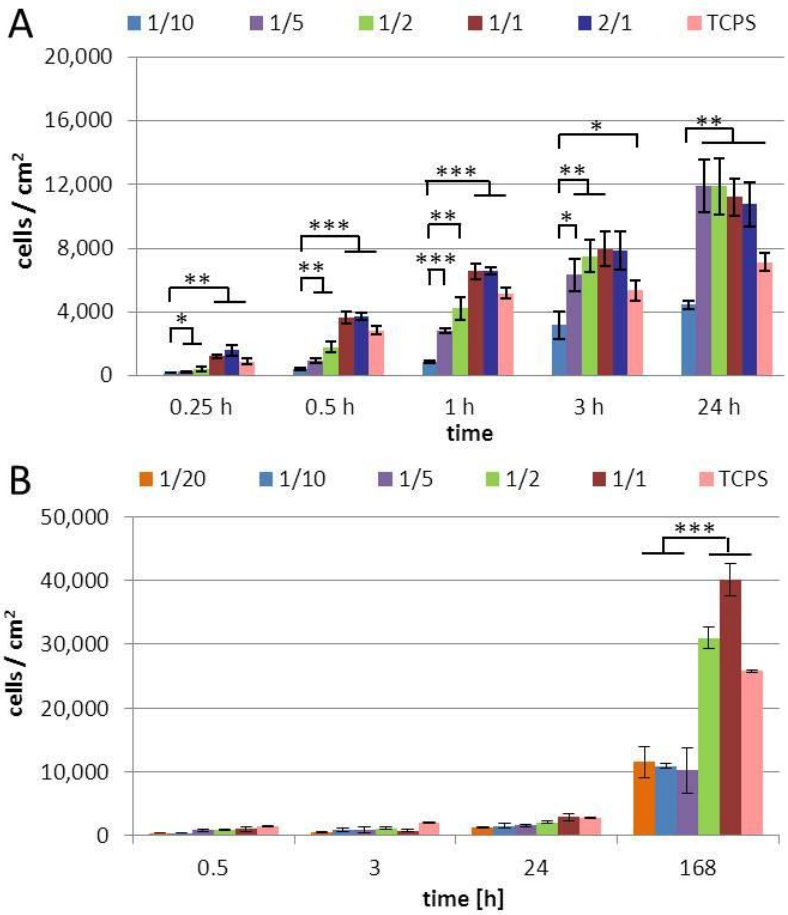

Figure 2: HDF adhesion on functionalized hydrogel coatings.

HDF adhesion was determined on NCO-sP(EO-*stat*-PO) coatings functionalized with different molar GRGDS to prepolymer ratios. Adherent cells were counted on life cell images after 0.25, 0.5, 1, 3 and 24 h (A). Additionally, cells were harvested with accutase and cells counted with a CASY® cell counter after 0.5, 1, 3, 24 h and 1 week (B).

In comparison to cell counting of life cell images, cell quantification using the CASY® cell counter did not confirm the hypothesis of preferred adhesion to GRGDS functionalized hydrogels at initial time points compared to TCPS. Whereas initial cell adhesion was faster on GRGDS functionalized coatings compared to TCPS using cell counting on life cell images, cells adhered faster on TCPS using the CASY® cell counter. Additionally, results of the cell adhesion studies revealed different minimum thresholds of GRGDS to prepolymer ratios for efficient cell adhesion. Counting cells on life cell images revealed a threshold of 1/5, whereas counting cells with CASY® cell counter revealed a threshold of 1/2. For cell counting on life cell images, representative pictures were taken in the middle of the substrates. Adherent cells were probably not distributed homogeneously on the surfaces and the life cell image of only a part of the substrate may not have been representative for the whole coating. Using the CASY® cell

counter, more cells adhered to the coatings compared to cell numbers counted on life cell images. Cells were detached from the substrates with accutase and counted in the size range of 12 to 30 µm in solution. Cells cultivated on coated glass in 24-well plates could adhere to the plastic at the thin border between the glass substrate and the well, influencing the result to higher cell numbers using the CASY® cell counter because these cells were also detached by accutase. Counting cells on life cell images, these cells adhering off the hydrogel, were not affecting the results explaining the different cell numbers. Another variable in these two experiments were the donors of the foreskin fibroblasts. As experiments were performed at different time points, cells from different donors were used, without knowing age or healthiness of the donors. Varying age of the donors could explain different ligand to prepolymer ratios obtained for optimal cell adhesion, since age and healthiness of the donors have an impact on cell behavior *in vitro* [31, 32]. For further comparison of cell numbers with other ligand quantification methods in Chapter 8, cell counting experiments of life cell images were used.

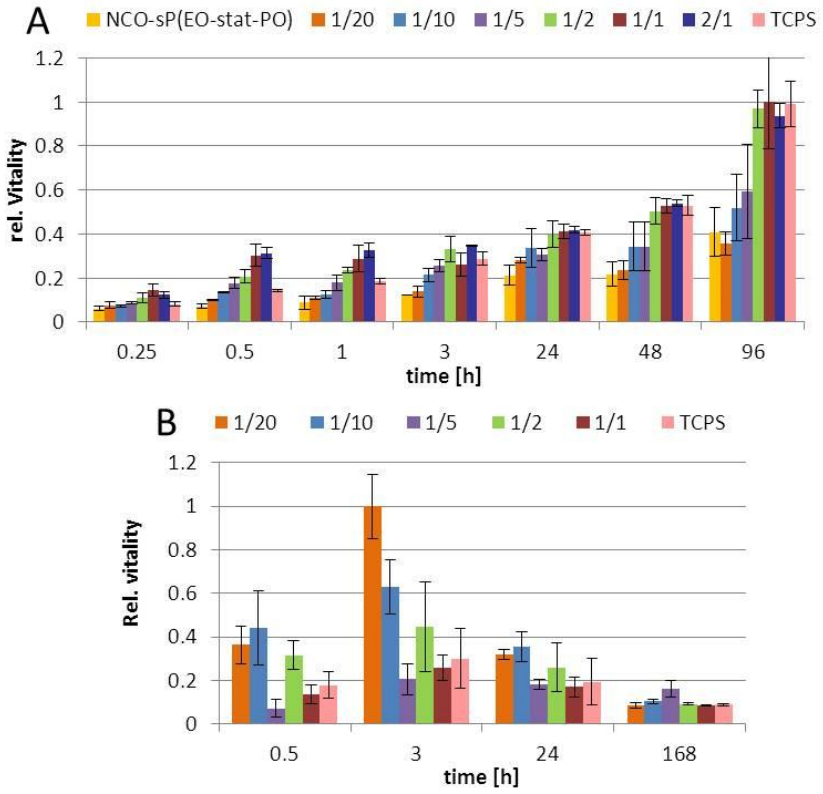

Figure 3: Vitality of adherent HDFs on functionalized hydrogel coatings.

HDF were cultivated on TCPS, pure NCO-sP(EO-*stat*-PO) coatings and coatings functionalized with molar GRGDS to prepolymer ratios of 20/1 to 1/2. A: Vitality of adherent HDFs was determined using the CellTiter-Blue® cell viability assay measuring the activity of several intracellular redox enzymes after 0.25, 0.5, 1, 3, 24, 48 and 96 h. B: Cell activity was measured using the WST-1 cell proliferation assay measuring intracellular succinate dehydrogenase activity after 0.5, 1, 3, 24 h and 1 week. WST intensities are given in relation to cell numbers from CASY® cell counting experiments.

Beside cell adhesion and proliferation, cell vitality studies were performed on functionalized hydrogel coatings (Figure 3). Non-adherent cells were washed away before the analysis to ensure the measurement of enzyme activity in adherent cells, exclusively. In the CellTiter-Blue® cell viability assay, activities of several intracellular redox enzymes were measured, which reduced the dye resazurin into the fluorometrically detectable resorufin. Visually, no cells adhered to the non-functionalized coatings but some cells were able to reach the protruding plastic of the well, the outer glass rim, and the back of the glass substrates at the edges of the wells explaining the positive signal detected on these inert coatings. The thin glass substrates could not be transferred to another well plate before the measurement without breaking. Therefore, cell activity on substrates that reached the same amount as on pure hydrogel coatings should be taken as background signal. At initial time points up to 1 h, higher cell vitalities were measured for cells adhering to coatings with higher GRGDS to prepolymer ratios with a maximal vitality at ratios of 1/1 and 2/1. On coatings with GRGDS to prepolymer ratios of 1/20 to 1/2 vitality was lower compared to coatings with higher GRGDS contents. After 48 h, maximal cell vitality was reached on coatings with ratios of 1/2 to 2/1. Nevertheless, the higher the number of adherent cell, the higher the total enzymatic activity in total in the well. This means, that cell numbers influenced the outcome of the assay. Measured vitalities have to be correlated to cell numbers. This was not done for these experiments due to time running out. However, another cell vitality assay was performed, where cell vitalities and cell numbers were correlated.

Using the WST-1 cell proliferation assay to determine cell vitality, activity of the enzyme succinate dehydrogenase in mitochondria was measured (Figure 3B). The stable formazan salt WST-1 was cleaved in a NAD(P)H dependent process of the respiratory chain. As mitochondria are essentially responsible for provision of energy for various cellular processes and cell survival, the activity of succinate dehydrogenase can give evidence about the energetic state of the cells. For this assay, cell vitality as well as cell number using the CASY® cell counter, were performed on the same substrates allowing the calculation of cell vitality in correlation to cell numbers. 3 h after seeding, the cell activity rose up reaching a maximum amount. At this time point, cells were in the growth phase, where proteins were synthesized and mitochondria proliferated and therefore, a lot of energy was needed. After 24 h of cell culture, the activity decreased, reaching minimal values after 168 h, a cell state after exponential growth where cells needed less energy. Using the WST-1 cell proliferation assay, no connection of GRGDS concentration and cell vitality could be observed. Results indicated that ligand concentration

did not affect HDF vitality. Cells that managed to adhere to the RGD surfaces, even to surfaces with low RGD content, still seemed to be vital.

In this Chapter, effects of GRGDS concentration immobilized on the per se inert NCO-sP(EO-*stat*-PO) hydrogel surfaces on HDF adhesion, proliferation and vitality were analyzed. Two different cell counting methods revealed two different minimal ligand to prepolymer ratios necessary for maximal HDF adhesion (1/5 and 1/2), but could be explained by different cell donors and differences in methodology. Additionally, different enzyme activities were measured, that revealed no coherence between RGD concentration and HDF vitality. Even HDFs that adhered to coatings with low amounts of GRGDS were still vital.

4. Conclusions

Cell analysis *in vitro* is a complex research field and working with primary cells raises the number of variables that need to be controlled. Nevertheless, analysis of biomaterials with primary cells is crucial for the application in contact with cells and tissue. One cell adhesion experiment raised the hypothesis that cells on GRGDS presenting surfaces sensed the peptides as part of the ECM and therefore, adhered very fast at initial time points. On TCPS surfaces, cells did not sense an ECM but an adsorbed protein layer and therefore, started secreting their own ECM before adhesion. This hypothesis needs to be confirmed with further adhesion experiments as well as additional analysis of ECM protein secretion by the cells. Cell vitality measurements did not reveal an optimal GRGDS to prepolymer ratio necessary for maximal cell vitality. Cells adhering to hydrogel coatings with low peptide to prepolymer ratio were just as vital as cells on hydrogel with higher ratios.

Though, cell adhesion experiments could not determine real ligand concentrations but only the effect on cell behavior. Therefore, comparison with classical and surface sensitive ligand quantification methods was very important. Cell counting experiments on life cell images were used for this comparison in Chapter 8. With additional cell experiments, enzyme linked immunosorbent assays (ELISA), and combination with radiolabeling technique, the exact ligand spacing for HDF adhesion on GRGDS functionalized NCO-sP(EO-*stat*-PO) hydrogels could be determined.

5. Appendix

5.1. Introduction

Primary cell responses in *in vitro* and *in vivo* studies are important for biomaterial analysis. Therefore, HDFs were used for detailed analysis of GRGDS functionalized NCO-sP(EO-*stat*-PO) coatings in this thesis. Nevertheless, the mouse fibroblast cell line L929 is accepted for cytocompatibility assessment in the DIN EN ISO 10993. Therefore, an additional cell adhesion experiment with murine L929 fibroblasts was performed and the results presented in this Appendix.

5.2. Experimental section

5.2.1. Hydrogel coatings

NCO-sP(EO-stat-PO) synthesis

Isocyanate terminate prepolymers (NCO-sP(EO-*stat*-PO)) were synthesized as described in detail elsewhere [26]. In short, the prepolymer was fabricated by the reaction of hydroxyl terminated star shaped polyether polyole with isophorone diisocyanate (IPDI).

Preparation of glass surfaces

Glass substrates (Ø 15 mm, Paul Marienfeld, Lauda-Königshofen, Germany) were polished with isopropanol and successively cleaned in acetone, distilled water, and isopropanol in an ultrasonic bath for 5 min each followed by drying in a stream of nitrogen. Solvents were purchased from Prolabo (Darmstadt, Germany). Glass substrates were activated by O_2-plasma treatment in the plasma process plant AK 330 (Roth & Rau, Hohenstein-Ernstthal, Germany) for 15 min (400 W, 50 sccm, 0.4 mbar). Afterwards, glass substrates were left for 60 min in a desiccator containing 100 µl 3-aminopropyl-trimethoxysilan (AS) at 5 mbar. After removal of AS, the glass substrates were left in vacuum for min. 10^{-2} mbar for another hour and stored at 250 mbar.

NCO-sP(EO-stat-PO) coating

The coating procedure has been described earlier [27]. NCO-sP(EO-*stat*-PO) prepolymers were dissolved in tetrahydrofuran (THF, dried over sodium, VWR, Darmstadt, Germany). After adding water to the solution (9/1 v/v mixture of water/THF, prepolymer concentration 10 mg/mL), prepolymers crosslinked for 5 min. Two droplets of the solution were placed on the aminosilanized surface of a glass substrate after filtration through a 0.2 µm syringe filter

(Whatman, Dassel, Germany). The coating procedure was carried out in the spin coater WS-400-B-6NPP/LITE (Laurell Technologies, North Wales, USA) at 2,500 rpm for 40 sec with an acceleration time of 5 sec. Each prepolymer solution was used to coat a maximum of 6 substrates. Coated substrates were stored at room temperature for at least 12 h to ensure complete crosslinking of the coating.

Functionalization

Prior to the coating procedure, GRGDS (Bachem, Bubendorf, Switzerland) was added to the prepolymer solution in molar ligand to prepolymer ratios of 1/2, 1/1, and 2/1 and coating was performed as described above.

5.2.2. In vitro cell experiments

Cell culture

Murine connective tissue fibroblast cell line NIH L929 (L929, max. passage 10) from the German collection of microorganisms and cell cultures (DSMZ, Braunschweig, Germany) were kindly provided by Prof. Baron (Department of Dermatology and Allergology, University Hospital of the RWTH Aachen University, Germany). L929 cells were cultured in RPMI-1460 medium supplemented with 10 vol-% fetal bovine serum and 1 vol-% penicillin/streptomycin (all media ingredients were purchased from PAA, Cölbe, Germany) at standard cell culture conditions (37°C, 5% CO_2, 95% humidity).

Sample preparation and cell seeding

Coated glass substrates in 24-well polystyrene plate (PS, Greiner Bio-One, Frickenhausen, Germany) were washed thoroughly with sterile water and PBS buffer (0.01 M, pH 7.4) for sterilization. L929 cells were harvested by incubation with 0.25% trypsin/EDTA (PAA, Cölbe, Germany) at 37°C for 3 min. The reaction was stopped by adding RPMI. 1 mL cell suspension (20,000 cells/mL in RPMI) was seeded on each substrate and cells were incubated under standard cell culture conditions.

Cell adhesion

Cell adhesion was monitored by optical microscopy using an inverted Axiovert 100A imaging microscope (Carl Zeiss, Göttingen, Germany) and adherent cells were counted on life cell images after 1, 2, 3, and 22 h.

5.3. Results and discussion

NCO-sP(EO-*stat*-PO) coatings functionalized with molar GRGDS to prepolymer ratios of 1/2, 1/1, and 2/1 were seeded with L929 mouse fibroblasts and adherent cells counted on life images after 1, 2, 3, and 22 h (Figure A1). The higher the GRGDS to prepolymer ratio, the more L929 cells adhered to the coatings. At initial time points up to 3 h, more cells adhered to GRGDS functionalized coatings compared to TCPS. This confirmed the hypothesis proposed in the main part of this Chapter for HDFs, saying that cells sensed GRGDS as part of the ECM and therefore, adhered faster at initial time points compared to TCPS. On TCPS in contrast, cells sensed a layer of adsorbed proteins on the surface and started secreting their own ECM as they did not 'see' an ECM, thus slowing down the adhesion process at initial time points.

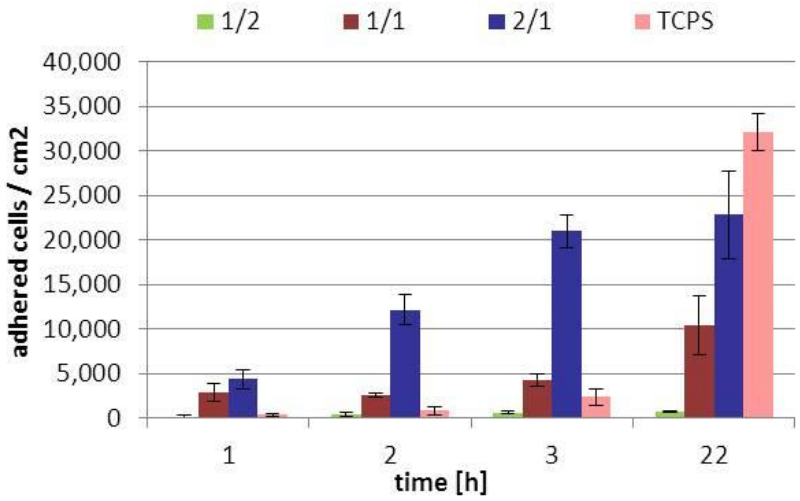

Figure A1: L929 adhesion on functionalized NCO-sP(EO-*stat*-PO) coatings.
L929 adhesion was determined on NCO-sP(EO-*stat*-PO) coatings functionalized with different molar GRGDS to prepolymer ratios. Adherent cells were counted on life cell images after 1, 2, 3, and 22 h.

20,000 L929/cm^2 were counted on GRGDS functionalized hydrogels with ratios of 2/1. In comparison, only 12,000 HDF/cm^2 adhered to GRGDS functionalized coatings of the same concentrations, even though same cell numbers (20,000 cells/substrate) were seeded in both cases. This can be explained by the smaller size of the mouse cells. A spread L929 cell covered an area of around 1,000 nm^2, whereas a HDF covered an area of around 5,000 nm^2. That means, that spread HDFs covered a bigger area and therefore more GRGDS peptides compared to spread L929 cells, allowing HDFs the adhesion at lower GRGDS concentration.

5.4. Conclusions

Cell adhesion kinetics need to be determined for each cell type and each biomaterial combination individually. Cell adhesion of HDFs and L929 cells analyzed on NCO-sP(EO-*stat*-PO) hydrogels functionalized with different amounts of GRGDS resulted in different GRGDS concentrations necessary for proper cell adhesion.

6. References

1. Pierschbacher, M.D. and Ruoslahti, E. Cell attachment activity of fibronectin can be duplicated by small synthetic fragments of the molecule. *Nature* **1984**, 309 (5963) 30-33.
2. Hynes, R.O. Integrins: A family of cell surface receptors. *Cell* **1987**, 48 (4) 549-54.
3. Hynes, R.O. Integrins: Versatility, modulation, and signaling in cell adhesion. *Cell* **1992**, 69 (1) 11-25.
4. Izzard, C.S. and Lochner, L.R. Cell-to-substrate contacts in living fibroblasts - Interference reflection study with an evaluation of technique. *Journal of Cell Science* **1976**, 21 (1) 129-59.
5. Lock, J.G.; Wehrel-Haller, B. and Strömblad, S. Cell-matrix adhesion complexes: Master control machinery of cell migration. *Seminars in Cancer Biology* **2008**, 18 (1) 65-76.
6. Ma, Z.W.; Kotaki, M.; Inai, R. and Ramakrishna, S. Potential of nanofiber matrix as tissue-engineering scaffolds. *Tissue Engineering* **2005**, 11 (1-2) 101-09.
7. Poole, K.; Khairy, K.; Friedrichs, J.; Franz, C.; Cisneros, D.A.; Howard, J. and Mueller, D. Molecular-scale topographic cues induce the orientation and directional movement of fibroblasts on two-dimensional collagen surfaces. *Journal of Molecular Biology* **2005**, 349 (2) 380-86.
8. Hersel, U.; Dahmen, C. and Kessler, H. RGD modified polymers: biomaterials for stimulated cell adhesion and beyond. *Biomaterials* **2003**, 24 (24) 4385-415.
9. Garcia, A.J. and Boettiger, D. Integrin-fibronectin interactions at the cell-material interface: initial integrin binding and signaling. *Biomaterials* **1999**, 20 (23-24) 2427-33.
10. Ratner, B.D. and Bryant, S.J. Biomaterials: Where we have been and where we are going. *Annual Review of Biomedical Engineering* **2004**, 6 (1) 41-75.
11. Hughes, R.C.; Pena, S.D.J.; Clark, J. and Dourmashkin, R.R. Molecular requirements for the adhesion and spreading of hamster fibroblasts. *Experimental Cell Research* **1979**, 121 (2) 307-14.
12. Massia, S.P. and Hubbell, J.A. An RGD spacing of 440nm is sufficient for integrin alpha-V-beta-3-mediated fibroblast spreading and 140nm for focal contact and stress fiber formation. *Journal of Cell Biology* **1991**, 114 (5) 1089-100.
13. Drumheller, P.D. and Hubbell, J.A. Polymer networks with grafted cell-adhesion peptides for highly biospecific cell adhesive substrates. *Analytical Biochemistry* **1994**, 222 (2) 380-88.
14. Hern, D.L. and Hubbell, J.A. Incorporation of adhesion peptides into nonadhesive hydrogels useful for tissue resurfacing. *Journal of Biomedical Materials Research* **1998**, 39 (2) 266-76.
15. Neff, J.A.; Tresco, P.A. and Caldwell, K.D. Surface modification for controlled studies of cell-ligand interactions. *Biomaterials* **1999**, 20 (23-24) 2377-93.
16. Cavalcanti-Adam, E.A.; Volberg, T.; Micoulet, A.; Kessler, H.; Geiger, B. and Spatz, J.P. Cell spreading and focal adhesion dynamics are regulated by spacing of integrin ligands. *Biophysical Journal* **2007**, 92 (8) 2964-74.
17. George, P.A.; Doran, M.R.; Croll, T.I.; Munro, T.P. and Cooper-White, J.J. Nanoscale presentation of cell adhesive molecules via block copolymer self-assembly. *Biomaterials* **2009**, 30 (27) 4732-37.
18. Shin, H.; Jo, S. and Mikos, A.G. Biomimetic materials for tissue engineering. *Biomaterials* **2003**, 24 (24) 4353-64.

19. Humphries, M.J.; Akiyama, S.K.; Komoriya, A.; Olden, K. and Yamada, K.M. Identification of an alternatively spliced site in human-plasma fibronectin that mediates cell type-specific adhesion. *Journal of Cell Biology* **1986**, 103 (6) 2637-47.

20. Singer, II; Kawka, D.W.; Scott, S.; Mumford, R.A. and Lark, M.W. The fibronectin cell attachment sequence Arg-Gly-Asp-Ser promotes focal contact formation during early fibroblast attachment and spreading. *Journal of Cell Biology* **1987**, 104 (3) 573-84.

21. Brandley, B.K. and Schnaar, R.L. Covalent attachment of an Arg-Gly-Asp sequence peptide to derivatizable polyacrylamide surfaces - support of fibroblast adhesion and long-term growth. *Analytical Biochemistry* **1988**, 172 (1) 270-78.

22. Danilov, Y.N. and Juliano, R.L. (Arg-Gly-Asp)n-albumin conjugates as a model substratum for integrin-mediated cell-adhesion. *Experimental Cell Research* **1989**, 182 (1) 186-96.

23. Underwood, P.A. and Bennett, F.A. A comparison of the biological-activities of the cell-adhesive proteins vitronectin and fibronectin. *Journal of Cell Science* **1989**, 93 641-49.

24. Götz, H.; Beginn, U.; Bartelink, C.F.; Grünbauer, H.J.M. and Möller, M. Preparation of isophorone diisocyanate terminated star polyethers. *Macromolecular Materials and Engineering* **2002**, 287 (4) 223-30.

25. Groll, J.; Fiedler, J.; Engelhard, E.; Ameringer, T.; Tugulu, S.; Klok, H.A.; Brenner, R.E. and Moeller, M. A novel star PEG-derived surface coating for specific cell adhesion. *Journal of Biomedical Materials Research Part A* **2005**, 74A (4) 607-17.

26. Gotz, H.; Beginn, U.; Bartelink, C.F.; Grunbauer, H.J.M. and Moller, M. Preparation of isophorone diisocyanate terminated star polyethers. *Macromolecular Materials and Engineering* **2002**, 287 (4) 223-30.

27. Groll, J.; Ameringer, T.; Spatz, J.P. and Moeller, M. Ultrathin coatings from isocyanate-terminated star PEG prepolymers: Layer formation and characterization. *Langmuir* **2005**, 21 (5) 1991-99.

28. Even-Ram, S.; Artym, V. and Yamada, K.M. Matrix control of stem cell fate. *Cell* **2006**, 126 (4) 645-47.

29. Pelham, R.J. and Wang, Y.L. Cell locomotion and focal adhesions are regulated by substrate flexibility. *Proceedings of the National Academy of Sciences of the United States of America* **1997**, 94 (25) 13661-65.

30. Discher, D.E.; Janmey, P. and Wang, Y.L. Tissue cells feel and respond to the stiffness of their substrate. *Science* **2005**, 310 (5751) 1139-43.

31. Chen, X. and Thibeault, S.L. Characteristics of age-related changes in cultured human vocal fold fibroblasts. *Laryngoscope* **2008**, 118 (9) 1700-04.

32. Wang, Y.-C.; Yu, S.-Q.; Wang, X.-H.; Han, B.-M.; Zhao, F.-J.; Zhu, G.-H.; Hong, Y. and Xia, S.-J. Differences in phenotype and gene expression of prostate stromal cells from patients of varying ages and their influence on tumor formation by prostate epithelial cells. *Asian Journal of Andrology* **2011**, 13 (5) 732-41.

CHAPTER 8

Comparison of the quantification methods and correlation with cell adhesion

Hydrogels provide an excellent basis for the production of functional and biocompatible coatings on materials and are increasingly used for this purpose. However, their three-dimensional nature makes it important to distinguish between the bioactive ligand density on the hydrogel surface that is thus able to interact with cells and the ligands immobilized inside the hydrogel and therefore inaccessible for cells, which occurs even in ultrathin films. Here, a comparison of different quantification methods used in the previous Chapters is presented. This multi-technique analysis comparison was necessary to gain best possible insight into ligand distributions in the hydrogels which were functionalized with different molar ligand to prepolymer ratios. Ligands in and on functionalized hydrogel coatings were quantified with radiolabeling (Chapter 3), X-ray photoelectron spectrometry (XPS), time-of-flight secondary ion mass spectroscopy (TOF-SIMS) (Chapter 4), enzyme linked immunosorbent assay (ELISA) (Chapter 6), and direct cell adhesion studies using primary human dermal fibroblasts (HDF) (Chapter 7). Most importantly, radioisotopic measurements, ELISA, and cell adhesion studies on amine reactive well plates that were directly functionalized with peptides could be used to quantify the absolute ligand density necessary to allow cell adhesion on hydrogel films. Optimal ligand spacing for HDF adhesion and proliferation was 6-18 nm.

1. Introduction

One key aspect of the characterization of material surfaces intended for the application as biomaterials or sensitive sensor surfaces is the quantification of the amount of ligands. Although many hydrogel systems have already been functionalized with ligands such as cell adhesion mediating peptides and proteins [1, 2], the quantification of the ligand concentration at the hydrogel interface was often disregarded. Multiple quantification methods such as radiolabeling [3-5], XPS [6] and TOF-SIMS [5], ELISA [7], quartz crystal microbalance (QCM) [8], ellipsometry [4], surface plasmon resonance (SPR) [4, 9], total internal reflection fluorescence (TIRF) [4], and attenuated total reflectance-FTIR [7] were used for this purpose. In these studies that hardly drew comparisons between the different methods and to the obtained results, some methods like radiolabeling, XPS and TOF-SIMS were used despite not being surface sensitive. Some methods such as SPR, TIRF, ATR-FTIR, and QCM were employed even though they are only applicable to ultraflat model substrates and not to 'real' biomaterials which are often rough and made of materials that cannot be properly analyzed by these methods. Controlling the nanoscale spacing of cell adhesion mediating ligands and advancing the technologies for the determination of ligand spacing at the interface would allow further understanding and control of cellular behavior which is an important factor for biomaterial research [10]. The effect of the ligand spacing on cell adhesion was previously described without presenting the ligands on a per se inert background and therefore without excluding influences on cell behavior stemming from the substrate itself rather than the ligand spacing [11-14]. Only in later studies concerning the influence of the ligand spacing on cell adhesion were the ligands presented on per se inert backgrounds [3, 5, 10, 15, 16].

In this study, NCO-sP(EO-*stat*-PO) hydrogel coatings on silicon and glass surfaces were used. Even though this hydrogel coating system was often used and applied, a throughout ligand quantification has so far not been performed. The hydrogel films were functionalized with ligands traceable by the different quantification methods by mixing different molar ligand to prepolymer ratios before the coating procedure. The study showed that radiolabeling revealed no maximal ligand binding in the hydrogel coatings, whereas XPS and TOF-SIMS revealed a maximal ligand concentration in the surface near regions of the hydrogel coatings at ligand to prepolymer ratios of 1/1. However, this did not correlate with the amount of peptide needed at the surface for induction of maximal cell adhesion, which was achieved at lower ratios of 1/5. This value could be correctly measured by the ELISA technique. Using radiolabeling, ELISA and cell adhesion as control measurements on flat substrates allowed absolute quantification of

ligand densities. Therefore, amine reactive 96-well plates were functionalized with RGD peptides and non-functionalized plastic was blocked with thiol functionalized poly(glycidol) (PG-SH). Maximal ELISA intensities and maximal HDF adhesion were achieved at a ligand spacing ranging between 6 and 18 nm.

2. Experimental section

2.1. Substrate preparation

2.1.1. NCO-sP(EO-stat-PO) coating and functionalization

Coatings were prepared as described in Chapter 3, 4, 6 and 7. In this Chapter results on coatings functionalized by the mix-in method were compared.

2.1.2. Functionalization of amine reactive well pates

50 µL GRGDS or GRGDSK-biotin solution (0.2 – 500 µg/mL in 0.02 M Na_2CO_3/$NaHCO_3$ buffer, pH 9.4) were incubated in each well of an amine reactive 96-well plate (Immobilizer™ Amine Module, Nunc, Wiesbaden, Germany) for 1 h. For radioisotopic measurements, small aliquots of radiolabelled ^{125}I-YRGDS were added to each GRGDS solution (100 – 1,000 µg/mL in 0.02 M Na_2CO_3/$NaHCO_3$, pH 9.4). Functionalized wells were rinsed 3 times with 1 wt-% SDS (Bio-Rad, Munich, Germany) and 3 times with PBS buffer (0.01 M, pH 7.4). Thiol functionalized poly(glycidol) (4.5 kDa, PG-SH, 13 thiol groups) was synthesized as described earlier [19]. For ELISA and cell experiments, the plastic background of the wells was blocked by incubating 200 µL PG-SH solution (1 mM, in 0.05 M $NaHCO_3$/NaOH buffer, pH 11) in each well for 1 h followed by rinsing with distilled water thrice. After 3 times washing with 2-hydroxyethylacrylat (10 mM, in 0.01 M PBS, pH 7.4, Sigma-Aldrich, Steinheim, Germany), wells were rinsed 3 times with distilled water. For cell experiments, wells were sterilized 20 min with UV light.

2.1. Ligand quantification

2.1.1. On functionalized NCO-P(EO-stat-PO) coatings

Radiolabeling, XPS, TOF-SIMS, ELISA and cell experiments on hydrogel coatings were performed as described in Chapter 3, 4, 6 and 7.

2.1.2. On functionalized amine reactive well plates

Radioisotopic measurement

Coatings in well plates were measured in a LB 2111 Multi Crystal Gamma Counter (Berthold Technologies, Bad Wildbach, Germany).

ELISA

ELISA protocols for use on NCO-sP(EO-*stat*-PO) coatings in well plates were developed in Chapter 6 and refined for amine reactive 96-well plates for this study. 50 µL streptavidin-peroxidase (SA-POD, 1/3000 in PBS, Roche, Mannheim, Germany) were incubated in the wells for 60 min and washed with PBS-Tween (0.05 vol-% Tween-20 in PBS, Roth, Karlsruhe, Germany). After dissolving one OPD tablet (Dako, Hamburg, Germany) in 6 mL deionized water and 2.5 µL H_2O_2 (30 vol-%), 100 µL of the OPD solution were added to each well. After 1 min incubation, the reaction was stopped by adding 100 µL 3 M HCl. Optical density (OD) of each well was measured in the microplate reader model Sunrise (Tecan, Maennedorf, Switzerland) at a wavelength of 492 nm. Results are shown on a logarithmic scale.

Cell adhesion

300 µL HDF suspension (20,000 cells/mL) were seeded in each 96-well and incubated under standard cell culture conditions (37°C, 5% CO_2, 95% humidity). Life cell images were taken with an Axiovert 100A imaging microscope (Carl Zeiss, Göttingen, Germany) after 3 h of cell culture and cells were counted on the images. Additionally, pictures of cells in non-treated amine reactive wells and on wells blocked with PG-SH that were washed with 2-hydroxyethylacrylat were taken with a magnification of 10x.

3. Results and discussion

Various methods were applied to quantify maximal and optimal ligand densities in and on the NCO-sP(EO-*stat*-PO) hydrogel layers. In this Chapter, results from radioisotopic measurements, XPS, TOF-SIMS, ELISA and direct cell adhesion studies were compared. For functionalization, ligands were mixed with the prepolymer solution prior to the coating procedure (Chapter 3, 4, 6, and 7). As ligands, ^{125}I-YRGDS and GRGDS were used for radiolabeling, a fluorinated amino acid and an iodinated peptide for XPS and TOF-SIMS measurements, GRGDSK-biotin for ELISA detection, and GRGDS for cell adhesion assays (Figure 1B-F).

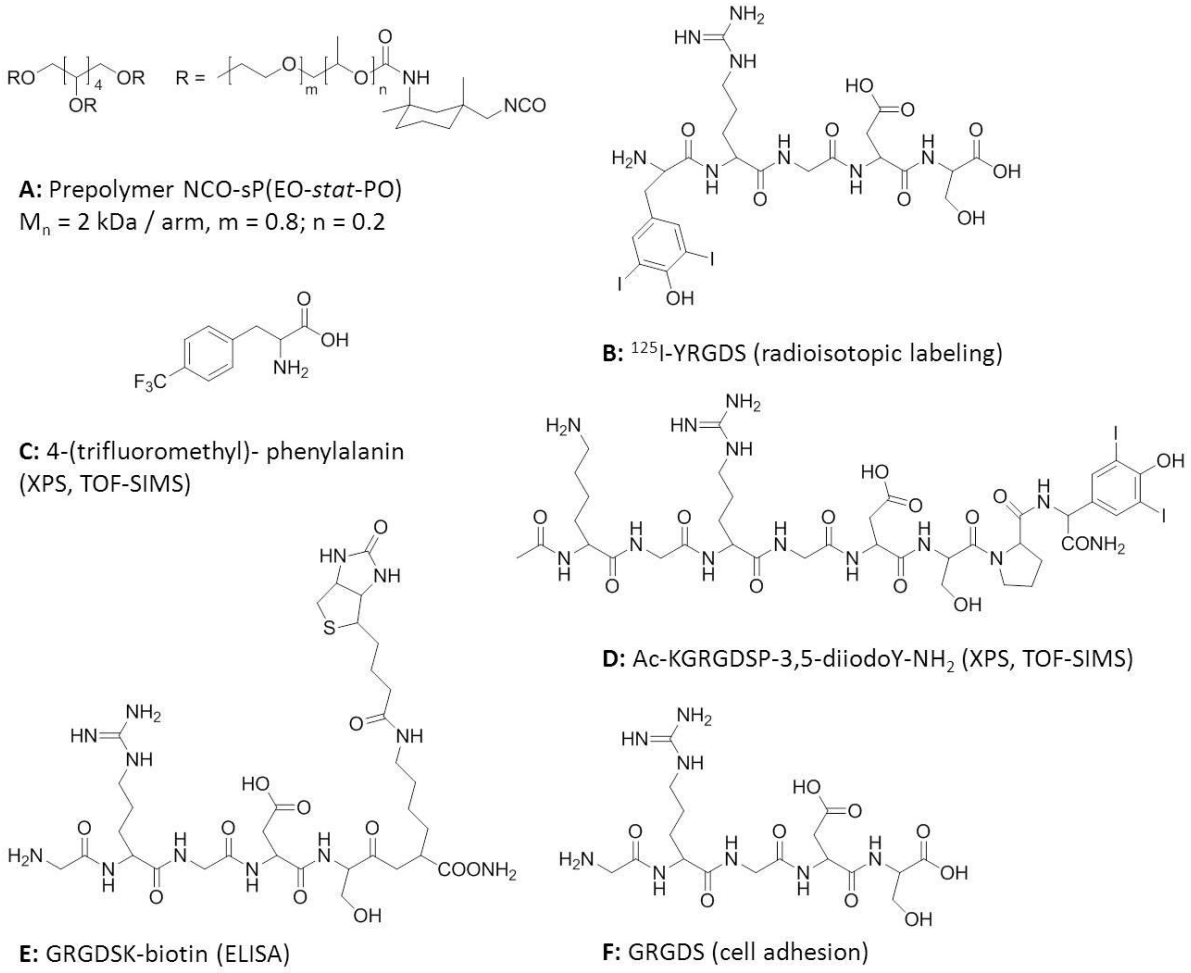

Figure 1: Prepolymer NCO-sP(EO-*stat*-PO) and ligands for functionalization.

The prepolymer (A) consists of a backbone out of PEO and PPO and its 6 arms are functionalized with isocyanate groups. Ligands: ^{125}I-YRGDS (B) for radioisotopic measurement, a fluorinated amino acid (C) and an iodinated peptide (D) for XPS and TOF-SIMS, GRGDSK-biotin (E) for ELISA detection and GRGDS (F) for cell adhesion quantification were used for functionalization of NCO-sP(EO-stat-PO) hydrogels.

Figure 2 gives an overview over the five different quantification methods used in the previous Chapters (relative intensities were compared). Radioisotopic labeling gave information about the ligand concentrations throughout the whole hydrogel but no maximal amount of ligands could be detected when increasing the peptide to prepolymer ratio. Even though no maximal ligand concentration was detected in the coatings, higher ligand to prepolymer ratios than 2/1 were not used to ensure that the complete crosslinking of the hydrogels was not affected. In contrast, XPS and TOF-SIMS which only penetrated the surface near regions of the coating and revealed a maximal ligand density at molar ligand to prepolymer ratios of 1/1. Surface sensitive quantification methods (ELISA and cell adhesion) already detected a maximum SA binding and HDF adhesion at ratios of 1/5. This led to the conclusion, that a maximal ligand concentration was necessary for maximal cell adhesion, but that the maximal ligand concentration at the surface was reached at lower ligand to prepolymer ratios (1/5) compared to the surface near regions of the hydrogel where a maximal loading was already reached at ratios of 1/1 (XPS, TOF-SIMS). These results indicate the importance of the right choice of quantification method and suggest that the ligands were not distributed homogeneously throughout the coatings. For determination of the optimal ligand concentration at the surface of a material, surface sensitive quantification methods are indispensable.

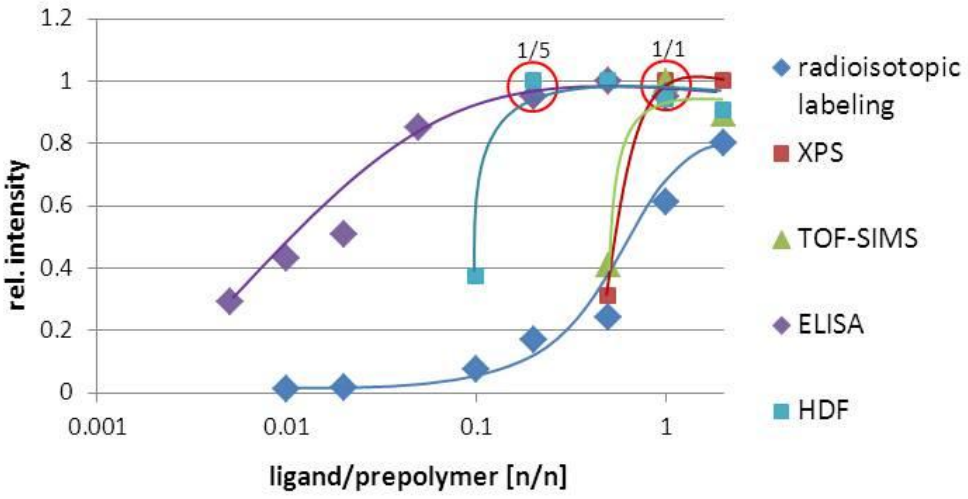

Figure 2: Relative comparison of ligand quantification.

Comparison of relative intensities of ligand concentrations in and on NCO-sP(EO-stat-PO) coatings. Radiolabeling did not reach a maximum; a maximum of 80% was assumed for this graphic. XPS and TOF-SIMS reached a maximal ligand concentration at ligand to prepolymer ratios of 1/1 (results of iodinated peptide are shown). Surface sensitive quantification via ELISA and cell adhesion (24h) reached a maximum at lower ligand to prepolymer rations of 1/5.

Deviations of the results obtained by XPS and TOF-SIMS on the one and radioactive quantification on the other hand concerning at which peptide to prepolymer ratio maximal peptide binding occurred may be explained through reactivity differences between GRGDS and ^{125}I-YRGDS peptides used for the radioactive quantification. The iodinated peptide could only be used in small amounts and was thus supplemented to GRGDS, with both peptides together yielding the aimed peptide to prepolymer ratio. Both peptides bound to the isocyanate groups of the prepolymers with their amino group at the N-terminus (G and Y, respectively). However, the amino group of the radiolabeled peptide was sterically restricted due to the iodinated tyrosine residue. This may have reduced the binding affinity of the labeled peptide in comparison to GRGDS. Since GRGDS was always present in excess (around 30,000/1 GRGDS/^{125}I-YRGDS), the two peptides might not bind to the prepolymers in the same molar ratio that was present in the solution but rather GRGDS would bind preferentially. The labeled peptide would thus be underrepresented in the coatings as compared to the molar ratio in the solution, so that the measured values were lower than the real values. Hence, a maximal ligand binding capacity of the hydrogel may have already been reached at peptide to prepolymer ratios used in the experiments, but due to the shift of the actual amount with regard to the labeled peptide, this could not be measured. XPS and TOF-SIMS measurements that were conform in their data support in this model, so that it can be concluded that the maximum binding capacity as detected by XPS and TOF-SIMS showed the real situation.

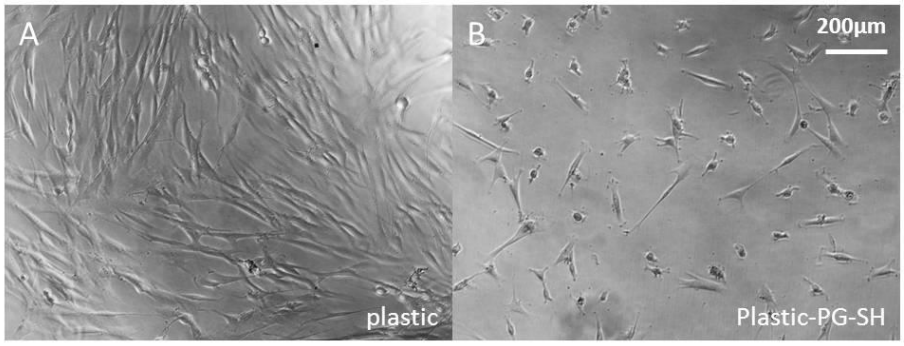

Figure 3: HDF adhesion on amine reactive surfaces.

HDF adhesion after 24 h of cell culture on non-treated amine reactive 96-well plates (A) and in wells that were blocked with PG-SH and treated with 2-hydroxyethylacrylat . Pictures were taken with a magnification of 10x.

Unfortunately, the surface sensitive ELISA technique and cell adhesion are not a fully quantitative and allowed only comparison of SA binding intensities and number of adherent HDFs. Therefore, amine reactive 96-well plates were incubated with RGD peptides in different concentrations and non-covalently bound peptides were detached with SDS and PBS. Incubation of hydrogel coatings with peptides may result in the diffusion of the peptides into

the hydrogel and therefore, radioisotopic measurement cannot distinguish between peptides at the surface and peptides inside the hydrogel layer. When peptides were incubated on the amine reactive wells, no diffusion could occur so that radioisotopic measurements detected only peptides presented at the surface. For radioisotopic measurements, the ^{125}I-YRGDS peptide was mixed with the peptide GRGDS. Radioisotopic measurements detected a maximum ligand density at peptide concentrations of 741 µg/mL (Figure 4A). For ELISA and cell experiments, the non-functionalized plastic space in between the peptides was blocked with PG-SH, a 4.5 kDa poly(glycidol) containing 13 thiol groups that bound flat to the plastic surface in between the RGD peptides with high certainty. To ensure that no free thiols remained, wells were washed 3 times with 2-hydroxyethylacrylat. As a control, non-functionalized amine reactive wells were blocked with PG-SH and washed with 2-hydroxyethylacrylat to show the potential of these blocked surfaces to significantly reduce cell adhesion. Since cell adhesion was significantly reduced on the blocked wells (Figure 3B) compared to cells on the pure plastic wells (Figure 3A), this blocking procedure was seen suitable for ELISA and cell experiments. On the wells that were functionalized with peptides and blocked subsequently, a maximal ELISA signal and maximal HDF adhesion were reached on surfaces incubated with peptide solutions of 50 µg/mL (Figure 4B, C). With radioisotopic measurements, all peptides on the surface disregarding their orientation were measured, while ELISA and cell adhesion only detected peptides accessible for SA (ELISA) and integrins in the cell membrane of HDFs and therefore, the orientation of the peptides influenced the outcome. Additionally, both SA and a cell cover a certain area on the surface that may be presenting several peptides. Increasing the ligand density beyond a certain threshold may therefore not be necessary for maximal ELISA signal or cell adhesion.

Peptides on amine reactive surfaces did not form a brush-like structure but rather lay flat on the surface. Therefore, the peptide size diminished the maximal possible peptide density on the amine reactive well plates. With an approximate GRGDS size of 1 x 2 nm, a maximal peptide density on the surfaces of 2.5×10^{13} GRGDS/cm^2 was possible which corresponds to the maximal gamma irradiation reached when incubated with GRGDS concentrations of 741 µg/mL (Figure 4C). This peptide density was possible on amine reactive plates since, according to the manufacturer's information, these well plates had a reactive group density of 10^{14} reactive groups/cm^2. Assuming a linear increase of GRGDS binding to the well surface with increasing GRGDS concentration in the solutions, incubating 50 µg/mL GRGDS (maximum of ELISA and cell adhesion experiments) resulted in a peptide density of 2×10^{12} GRGDS/cm^2. When homogeneously distributed, this corresponded to a peptide distance of 6 nm.

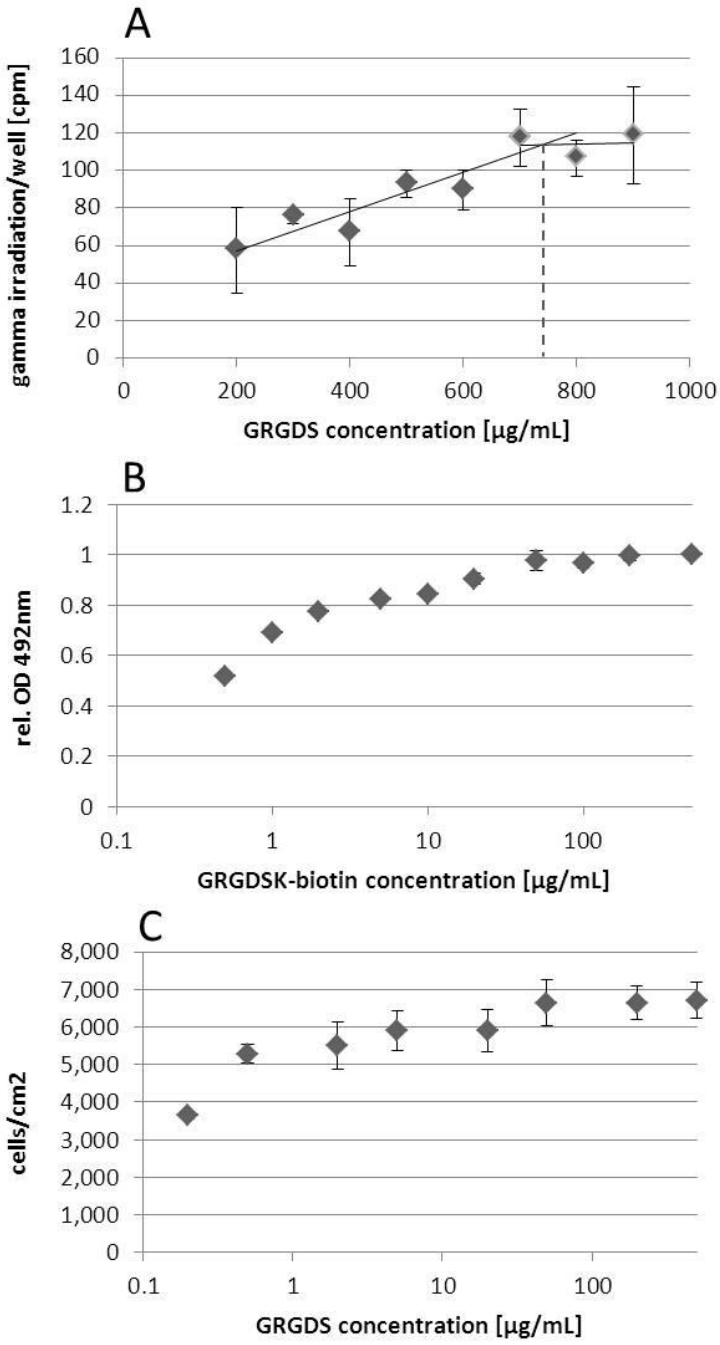

Figure 4: Quantification of ligand density on amine reactive well plates.

Amine reactive 96-well plates were functionalized with RGD peptides and were quantified using radioisotopic measurements (A), ELISA (B), and cell adhesion of HDFs (C).

For ELISA experiments, another factor had to be taken into account. The tetrameric SA used for the detection of the biotinylated peptide had a diameter of 24 nm (calculated from the given surface area of a tetrameric SA of 17,780 square Å given from the European Bioinformatics Institute (EBI) www.ebi.ac.uk). Assuming a dense packing of the SA on the surface in a hexagonal ordering, the diameter of the SA corresponded to the distance of the centers of the SA. A maximal loading of the surface of 1.77×10^{11} SA/cm^2 would be possible. SA has 4 biotin

binding sites. Assuming that two of them were oriented toward the surface thus being able to bind to the biotinylated peptides, this corresponded to a ligand density of 3.54 x 10^{11} GRGDSK-biotin/cm^2 with a distance of 18 nm.

Due to several assumptions made in these calculations, the minimal RGD spacing necessary for proper HDF adhesion can be seen to range between 6 and 18 nm. This is in the range of previously detected ligand spacing using fibroblasts on RGD functionalized hydrogels [3, 5] and indicates the potential of the NCO-sP(EO-*stat*-PO) hydrogel system for cell studies with different ligands. Other studies using different hydrogels and different fibroblasts revealed slightly different RGD spacing optimal for fibroblast adhesion and spreading [10, 16, 17]. Therefore, each interaction of a special cell type with a ligand on a hydrogel system needs to be analysed individually.

4. Conclusions

Aim of this Chapter was to demonstrate the importance of comparing different quantification methods for the determination of the optimal ligand concentration on hydrogels needed for the intelligent design of functional biomaterials. Optimal ligand concentrations do not necessarily equal the maximal ligand concentration achievable in the hydrogel system of choice. With straight forward quantification methods it was demonstrated that ligands were not homogeneously distributed in the hydrogel coatings. Using XPS and TOF-SIMS with certain penetration depths into the hydrogels revealed a maximal ligand load at higher ligand to prepolymer ratios (1/1) compared to surface sensitive quantification using ELISA and direct cell adhesion (1/5). Using radiolabeling technique, ELISA and cell adhesion on RGD-functionalized amine reactive well plates enabled the determination of the optimal RGD spacing for hydrogels functionalized with ligand to prepolymer ratios of 1/5 being between 6-18 nm.

These reliable quantification methods demonstrated here can easily be transferred to other hydrogel systems functionalized with a variety of ligands. This material based knowledge is indispensable for the more detailed analysis of hydrogel systems which enables the use as biomaterials coming in contact with special cell types or tissue.

5. References

1. Temenoff, J.S. and Mikos, A.G. Injectable biodegradable materials for orthopedic tissue engineering. *Biomaterials* **2000**, 21 (23) 2405-12.
2. Nuttelman, C.R.; Mortisen, D.J.; Henry, S.M. and Anseth, K.S. Attachment of fibronectin to poly(vinyl alcohol) hydrogels promotes NIH3T3 cell adhesion, proliferation, and migration. *Journal of Biomedical Materials Research* **2001**, 57 (2) 217-23.
3. Hern, D.L. and Hubbell, J.A. Incorporation of adhesion peptides into nonadhesive hydrogels useful for tissue resurfacing. *Journal of Biomedical Materials Research* **1998**, 39 (2) 266-76.
4. Barber, T.A.; Harbers, G.M.; Park, S.; Gilbert, M. and Healy, K.E. Ligand density characterization of peptide-modified biomaterials. *Biomaterials* **2005**, 26 (34) 6897-905.
5. Neff, J.A.; Tresco, P.A. and Caldwell, K.D. Surface modification for controlled studies of cell-ligand interactions. *Biomaterials* **1999**, 20 (23-24) 2377-93.
6. Cook, A.D.; Hrkach, J.S.; Gao, N.N.; Johnson, I.M.; Pajvani, U.B.; Cannizzaro, S.M. and Langer, R. Characterization and development of RGD-peptide-modified poly(lactic acid-co-lysine) as an interactive, resorbable biomaterial. *Journal of Biomedical Materials Research* **1997**, 35 (4) 513-23.
7. Hersel, U.; Dahmen, C. and Kessler, H. RGD modified polymers: biomaterials for stimulated cell adhesion and beyond. *Biomaterials* **2003**, 24 (24) 4385-415.
8. Lord, M.S.; Cousins, B.G.; Doherty, P.J.; Whitelock, J.M.; Simmons, A.; Williams, R.L. and Milthorpe, B.K. The effect of silica nanoparticulate coatings on serum protein adsorption and cellular response. *Biomaterials* **2006**, 27 (28) 4856-62.
9. Uchida, K.; Otsuka, H.; Kaneko, M.; Kataoka, K. and Nagasaki, Y. A reactive poly(ethylene glycol) layer to achieve specific surface plasmon resonance sensing with a high S/N ratio: The substantial role of a short underbrushed PEG layer in minimizing nonspecific adsorption. *Analytical Chemistry* **2005**, 77 (4) 1075-80.
10. George, P.A.; Doran, M.R.; Croll, T.I.; Munro, T.P. and Cooper-White, J.J. Nanoscale presentation of cell adhesive molecules via block copolymer self-assembly. *Biomaterials* **2009**, 30 (27) 4732-37.
11. Hughes, R.C.; Pena, S.D.J.; Clark, J. and Dourmashkin, R.R. Molecular requirements for the adhesion and spreading of hamster fibroblasts. *Experimental Cell Research* **1979**, 121 (2) 307-14.
12. Singer, II; Kawka, D.W.; Scott, S.; Mumford, R.A. and Lark, M.W. The fibronectin cell attachment sequence Arg-Gly-Asp-Ser promotes focal contact formation during early fibroblast attachment and spreading. *Journal of Cell Biology* **1987**, 104 (3) 573-84.
13. Underwood, P.A. and Bennett, F.A. A comparison of the biological-activities of the cell-adhesive proteins vitronectin and fibronectin. *Journal of Cell Science* **1989**, 93 641-49.
14. Massia, S.P. and Hubbell, J.A. An RGD spacing of 440nm is sufficient for integrin alpha-V-beta-3-mediated fibroblast spreading and 140nm for focal contact and stress fiber formation. *Journal of Cell Biology* **1991**, 114 (5) 1089-100.
15. Cavalcanti-Adam, E.A.; Micoulet, A.; Blummel, J.; Auernheimer, J.; Kessler, H. and Spatz, J.P. Lateral spacing of integrin ligands influences cell spreading and focal adhesion assembly. *European Journal of Cell Biology* **2006**, 85 (3-4) 219-24.
16. Drumheller, P.D. and Hubbell, J.A. Polymer networks with grafted cell-adhesion peptides for highly biospecific cell adhesive substrates. *Analytical Biochemistry* **1994**, 222 (2) 380-88.

17. Cavalcanti-Adam, E.A.; Volberg, T.; Micoulet, A.; Kessler, H.; Geiger, B. and Spatz, J.P. Cell spreading and focal adhesion dynamics are regulated by spacing of integrin ligands. *Biophysical Journal* **2007**, 92 (8) 2964-74.

III Advanced ECM engineering

Biomaterials in contact with tissue still cause significant complications after implantation. The optimal biomaterial would be a reconstruction of the *in vivo* environment of cells and thus be fully accepted by the host. This could not be achieved so far since the complexity of the extracellular matrix (ECM) is not yet fully understood. However, research needs to aim at the reconstruction of parts of this complex matrix system. In this third and last part of this thesis, two approaches to biochemically and structurally mimic the ECM were investigated. Chapter 9 focused on the biochemical surface set-up of two-dimensional coatings by presenting the ECM glycoprotein fibronectin (FN) in a more biomimetic and non-covalent manner via sugar-lectin mediated binding. Chapter 10 aimed at the structural reconstruction of the three-dimensional fibrous network of the ECM by electrospun fiber scaffolds with controlled surfaces.

CHAPTER 9

Biochemical ECM mimicry through sugar-lectin mediated biomimetic presentation of ECM components

In order to achieve better outcomes for biomaterials in contact with human tissue, the complex structures found *in vivo* need to be presented at the interface. The mere attachment of cell adhesion molecules (CAM) on per se inert surfaces is not sufficient to control the complex interactions of cells with their environment, e.g. in case of an implant that is coated with a biomaterial. For the mimicry of the *in vivo* environment of cells, biochemical mimicry of the extracellular matrix (ECM) is necessary, an approach which is presented in this Chapter. A galectin mediated presentation of the ECM glycoprotein fibronectin (FN) for a more flexible, non-covalent, and biomimetic presentation was performed. For this purpose, the carbohydrate poly-N-acetyllactosamine (polyLacNAc) was covalently immobilized on a per se inert hydrogel coating via micro contact printing (MCP) and incubation. The fungal galectin His_6CGL2 was bound to the carbohydrate on the surface and due to its tetrameric structure allows the non-covalent attachment of FN to the surface. This layer build-up was proven with fluorescent staining. Optimal concentrations for the incubation of the sugar and galectin layer were obtained using an enzyme linked lectin assay (ELLA) while for the determination of the optimal concentration for FN incubation, an enzyme linked immunosorbent assay (ELISA) was employed. Primary human dermal fibroblasts (HDF) could adhere efficiently only to complete layer build-ups (hydrogel-polyLacNAc-His_6CGL2-FN). Additionally, cells were able to spread faster at initial time points and more cells adhered on the ECM mimetic substrates after 3 h compared to standard tissue culture polystyrene (TCPS). Subsequently, HDFs rearranged FN only on ECM mimetic surfaces, indicating that FN was presented in a more biomimetic and flexible way compared to FN adsorbed on glass and FN covalently immobilized on hydrogel layers, where no rearrangement by the cells was possible. With this ECM mimetic system a new path for more biomimetic presentation of ECM proteins for biomimetic materials and tissue engineering was introduced.

This Chapter represents a cooperative work with Claudia Rech.

1. Introduction

In vivo, lectins, ß-galactosides binding proteins, mediate cell adhesion to the ECM by connecting glycol structures on cell surfaces, the so called glycocalix, with sugars on ECM glycoproteins like FN, collagen, and laminin (Figure 1A). Such non-covalent and flexible presentation of proteins allows cells to rearrange their surrounding *in vivo* [1]. Only few lectin mediated bindings of proteins to glycan structures have been described in literature for biomaterial functionalization or tissue engineering. Macron et al. revealed a higher expression of naturally occurring galectin-1 in pig chondrocytes cultured on lactose modified chitosan [2]. They concluded that galectin-1 must act as a linker between chondrocytes and the scaffold. As a next step, Chen et al. increased cell adhesion and growth of rat chondrocytes by coating galectin-1 on chitosan-poly(D,L-lactide-*co*-glycolide) scaffolds or by enhancing the expression of galectin-1 in the cells [3]. Furthermore, these galectin-1 coatings promoted cell-cell aggregation and migration on the scaffold resulting in the conclusion that galectin-1 could be a potential building block in biomaterials for cartilage reconstruction. More often, the binding of the monosaccharide galactose to synthetic and natural polymers was used for liver tissue engineering [4]. The initial adhesion of the hematocytes occurred by the cell membrane bound C-type lectinasialoglycoprotein receptor to the immobilized galactose. However, ECM glycoprotein binding is usually mediated by oligomeric and polymeric carbohydrates rather than monosaccharides (Figure 1A).

Furthermore, there were attempts to bind lectins covalently or adsorptive to polymers and promote cell adhesion in this way. Wang et al. suggested that lectins enhance cell-material interaction via oligosaccharide mediated cell adhesion and could improve human skin fibroblast adhesion and proliferation via the interaction of the plant lectin WGA to the polysaccharide chitosan [5]. Reska and Gasteier et al. immobilized the plant lectin concanavalin A covalently on hydrogel coatings and could induce insect neutron adhesion on the per se inert hydrogels [6, 7].

The fundamental hypothesis is, that the development of biomimetic materials requires more than irreversible binding of specifically interacting molecules to an inert surface. It rather needs a dynamic way of presenting these molecules to achieve a better similarity with the complex structures found *in vivo*. Glycan-lectin mediated binding of ECM proteins is a flexible and biomimetic approach for binding glycoproteins on biomaterial surfaces. This would allow the non-covalent and flexible presentation of ECM proteins which, by time, may be rearranged by adherent cells in a tissue specific manner due to the reversibility of the protein attachment.

2. Experimental section

2.1. Hydrogel coatings

2.1.1. NCO-sP(EO-stat-PO) synthesis

Isocyanate terminated prepolymers (NCO-sP(EO-*stat*-PO)) were synthesized as described in detail elsewhere [8]. In short, the prepolymer was fabricated by the reaction of hydroxyl terminated star shaped polyether polyole with isophorone diisocyanate (IPDI).

2.1.2. Preparation of silicon and glass surfaces

Glass substrates (Ø 15 mm, Paul Marienfeld, Lauda-Königshofen, Germany) were polished with isopropanol. Glass substrates and 1 cm^2 silicon wafers (CrysTecKristall-technologie, n-Type, Berlin, Germany) were successively cleaned in acetone, distilled water, and isopropanol in an ultrasonic bath for 5 min each followed by drying in a stream of nitrogen. Solvents were purchased from Prolabo (Darmstadt, Germany). Substrates were activated by O_2-plasma treatment in the plasma process plant AK 330 (Roth & Rau, Hohenstein-Ernstthal, Germany) for 15 min (400 W, 50 sccm, 0.4 mbar). Afterwards, substrates were left in a desiccator containing 100 µl 3-aminopropyl-trimethoxysilan (AS) at 5 mbar for 60 min. After removal of AS, the glass substrates were left in a vacuum of minimum 10^{-2} mbar for 1 h and stored at 250 mbar.

2.1.3. NCO-sP(EO-*stat*-PO) c*oating*

The coating procedure has been described earlier [9]. Prepolymers were solubilized in tetrahydrofuran (THF, dried over sodium, Prolabo, Darmstadt, Germany). After adding water to the solution (9/1 v/v water/THF, prepolymer concentration 10 mg/ml), prepolymers were left for crosslinking for 5 min. Two droplets of the solution were placed on the aminosilanized surface of a glass substrate after filtration through a 0.2 µm syringe filter (Whatman, Dassel, Germany). The coating process was carried out in the spin coater WS-400-B-6NPP/LITE (Laurell Technologies, North Wales, USA) at 2,500 rpm for 40 sec with an acceleration time of 5 sec. Each prepolymer solution was used to coat a maximum of 6 substrates. Coated substrates were stored at room temperature for at least 12 h to ensure complete crosslinking of the coating.

2.1.4. Functionalization

MCP of polyLacNAc

PDMS stamps with lines and dots as patterns were prepared as described earlier [10]. The carbohydrate poly-*N*-acetyllactosamine (polyLacNAc) was synthesized as described before [11].

Stamps were covered with polyLacNAc solution (2.5 mM, in water) and incubated for 1 h. Afterwards, stamps were dried with nitrogen and gently pressed on hydrogel coatings (1 h after preparation) for 1 h. Substrates were washed 2 times with water and coatings left for complete crosslinking at room temperature for 24 h.

Incubation of polyLacNAc

PolyLacNAc was dissolved in Na_2CO_3/$NaHCO_3$ buffer (0.02 M, pH 9.4) in a concentration of 2.5 mM. Hydrogel coatings on glass (1 h after preparation) were incubated with 100 µL polyLacNAc solution for 1 h. Afterwards, substrates were washed 2 times with distilled water. For ELISA experiments, hydrogel coated well plates were incubated with 50 µL polyLacNAc (0 - 5 mM) solution for 1 h and washed 2 times with distilled water. Coatings were left for complete crosslinking at room temperature for 24 h.

Layer build-up with His_6CGL2 and FN

The recombinant lectin His_6CGL2 was produced in *E. coli* BL21 (DE3), purified as described earlier [12], and stored in PBS. FN was bought from Sigma-Aldrich (Steinheim, Germany). Coatings functionalized with polyLacNAc were incubated with a His_6CGL2 solution (in water) for 60 min. Coatings on glass were incubated with 100 µL His_6CGL2 solution (50 µg/mL) and coatings in well plates with 50 µL His_6CGL2 solution (0 - 112 µg/mL). After washing the coatings with distilled water twice, the coatings were incubated with FN solution (in water). Glass substrates were incubated with 100 µL FN solution (50 µg/mL) and coatings in well plates with 50 µL FN solution (0 - 10 µg/mL). Coatings were washed with water twice and used immediately for further experiments.

For control experiments, FN was adsorbed non-specifically on glass and directly on hydrogel coatings. Therefore, 100 µL FN solution (50 µg/mL, in water) were incubated on glass substrates and hydrogel coated glass (1 h after preparation) for 1 h.

2.2. Coating characterization

2.2.1. Fluorescent staining of MCP substrates

BSA was purchased from Serva Electrophoresis (Heidelberg, Germany). Substrates were blocked by incubation with PBS-BSA (1 wt-% bovine serum albumin in PBS (0.01 M, pH 7.4)) for 30 min. Primary and secondary antibodies were incubated for 1 h each with a washing step with PBS buffer in between. For His_6CGL2 staining, anti-His_6 antibody conjugated to Alexa Fluor

488 (Penta-His^{TM} Alexa Fluor 488 conjugate, Quiagen, Hilden, Germany) were diluted 1/1000 in PBS-BSA. For FN staining, primary rabbit-anti-FN antibody and secondary goat-anti-rabbit antibody conjugated to Atto 594 (Sigma-Aldrich, Steinheim, Germany) were diluted 1/1000 in PBS-BSA. Fluorescent microscopy was carried out with the inverted Axiovert 100A imaging microscope, pictures taken with an AxioCam MRc digital camera and analyzed using the AxioVisionV4.7 software. Hard- and software were from Carl Zeiss (Göttingen, Germany).

2.2.1. ELISA

Wells were incubated with 400 µL deionized water for 60 min. Subsequently, they were washed three times with 300 µL PBS-Tween (50 mM Na_2HPO_4, 150 mM NaCl, 0.01 M, pH 7.5, 0.05 vol-% Tween-20, Roth, Karlsruhe, Germany). ELLA and ELISA on coatings functionalized with polyLacNAc were performed as described in Chapter 6. PolyLacNAc was detected by incubation of 50 µL His_6CGL2 (50 µg/mL in PBS) for 1 h. After washing three times with 250 µL PBS-Tween, 50 µL anti-His_6-POD from mouse IgG2a (1/4000 in PBS, Roche, Mannheim, Germany) were incubated in the wells for 1 h. Coatings functionalized with polyLacNAc and different concentrations of His_6CGL2 were detected analogous with the anti-His_6-POD antibody. Coatings functionalized with polyLacNAc-His_6CGL2 and different concentrations of FN were detected with 50 µL primary rabbit-anti-FN antibody and secondary goat-anti-rabbit-POD antibody (both from Sigma-Aldrich, Steinheim, Germany). Each antibody (1/1000 in PBS) was incubated for 1 h in the wells with PBS-Tween washing steps in between. After dissolving one OPD tablet (Dako, Hamburg, Germany) in 3 mL deionized water and 1.25 µL H_2O_2 (30 vol-%), 100 µL of the OPD solution were added to each well. After 1 min of incubation, the reaction was stopped with 100 µL 3 M HCl. Optical density (OD) of each well was measured in the microplate reader (Tecan, Maennedorf, Switzerland) at a wavelength of 492 nm. Results are shown on a logarithmic scale.

2.3. *In vitro* cell experiments

2.3.1. Cell culture

HDFs with a maximal passage of 8 were isolated from foreskin (kindly provided by Prof. Baron, Department of Dermatology and Allergology, University Hospital of the RWTH Aachen University, Germany). HDFs were cultured in DMEM medium (Invitrogen Karlsruhe, Germany) supplemented with 10 vol-% fetal bovine serum (Biowest, Nuaillé, France) and 1 vol-% penicillin/streptomycin (PAA, Cölbe, Germany) at standard cell culture conditions (37°C, 5% CO_2, 95% humidity).

2.3.2. Sample preparation and cell seeding

After fabrication, glass substrates were placed in 24-well suspension culture plates (Greiner Bio-One, Frickenhausen, Germany) and washed thoroughly with sterile water and PBS buffer for sterilization. HDFs were harvested by incubation with accutase (PAA, Cölbe, Germany) at 37°C for 16 min. The reaction was stopped by adding DMEM. 1 mL cell suspensions (20,000 cells/mL in DMEM) was seeded on each substrate and incubated under standard cell culture conditions. As control surfaces, TCPS 24-well plates (Greiner Bio-One, Frickenhausen, Germany) were used.

2.3.3. Cell size

Life cell images were taken after 15 min, 30 min and 1 h. The diameter of adherent cells was measured and the mean value and standard deviation calculated.

2.3.4. Cell proliferation

Cells were washed 2 times with PBS buffer (37°C) and incubated with 500 µL accutase (PAA, Cölbe, Germany) for 16 min. 500 µL medium were added and cells suspended by mixing thoroughly. 100 µL of the cell suspension were added to 10 mL Coulter Isoton III Diluent (Beckman Coulter, Krefeld, Germany) and cells counted in a Casy® Cell Counter TTC (Schärfe System, Reutlingen, Germany).

2.3.5. Fluorescent staining of cell substrates

After 48 h of cell culture, cells were fixed with 4 wt-% paraformaldehyde (Roth, Karlsruhe, Germany), followed by 4 times washing with distilled water and permeabilization with 0,1 vol-% Triton X-100 (Sigma-Aldrich, Steinheim, Germany) in PBS. After washing with PBS thrice, samples were blocked with PBS-BSA for 30 min. FN was stained as described above. Cell nuclei were stained with 4',6-diamidino-2-phenylindole (DAPI, 1/1000 in PBS-BSA). DAPI was taken from the Actin Cytoskeleton and Focal Adhesion Staining Kit (Chemicon, Schwalbach, Germany). After staining, samples were washed with PBS buffer thrice and analyzed by fluorescence microscopy.

2.3.6. Microscopy

Optical and fluorescent microscopy were carried out with the inverted Axiovert 100A imaging microscope, pictures taken with an AxioCam MRc digital camera and analyzed using the AxioVisionV4.7 software. Hard- and software were from Carl Zeiss (Göttingen, Germany).

3. Results and discussion

In this study, a closer mimicry of the *in vivo* environment of cells was introduced by a more flexible, non-covalent, and biomimetic presentation of the ECM glycoprotein FN on non-interacting hydrogels using the carbohydrate polyLacNAc (Figure 1B). PolyLacNAc is an important oligosaccharide structure on cell and protein surfaces and serves as ligand for galectin mediated cell adhesion to ECM glycoproteins (Figure 1A) [13-15]. It has been reported before, that coatings prepared from six arm star shaped PEO based prepolymers with isocyanate endgroups (NCO-sP(EO-*stat*-PO)) prevent the adsorption of proteins and the adhesion of cells [16] but can be modified with CAMs to enable specific cell adhesion [16, 17]. Thus, this system was used as basis for the biomimetic strategy followed in this Chapter (Figure 1C). First, terminally amino-functionalized polyLacNAc was coupled to the isocyanate groups of freshly prepared NCO-sP(EO-*stat*-PO) coatings. Since polyLacNAc was chemically modified with an amino linker, immobilization on fresh NCO-sP(EO-*stat*-PO) coatings could be easily achieved by MCP or by incubation with a polyLacNAc solution and selection of proper conditions ensured preferential binding of the amino group [12]. For a biomimetic presentation of FN on NCO-sP(EO-*stat*-PO) hydrogel coatings functionalized with polyLcNAc, a successful layer-by-layer build-up of sugar, galectin and protein was crucial. To achieve this, the recombinant tetrameric model galectin His_6CGL2 [12, 18] was coupled to the sugar by incubation after complete hydrolysis of the isocyanate groups in the hydrogel coating. Selective binding of the galectin to the polyLacNAc functionalized surface areas was shown by fluorescent staining with an anti-His_6 antibody, proving the specific sugar-galectin coupling on the surface (Figure 1D). In a last incubation step, the glycoprotein FN was bound to the galectin. Fluorescent staining again proved selective binding of FN to the tetrameric galectin functional areas on the substrate (Figure 1D).

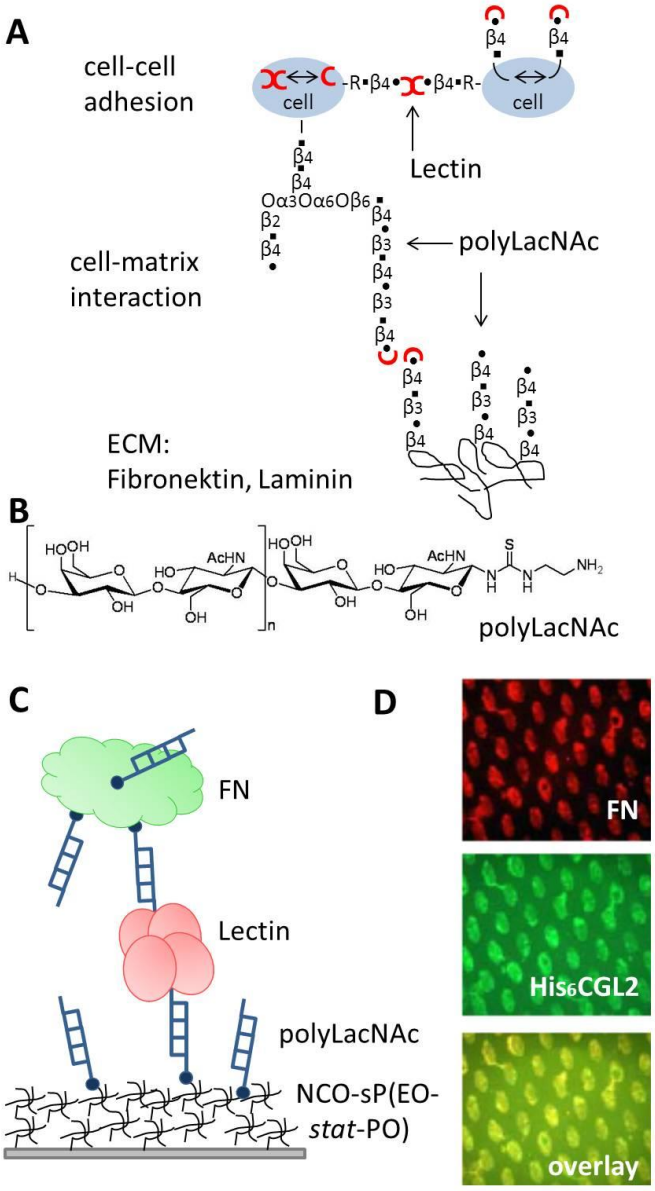

Figure 1: Role of polyLacNAc in cell-cell and cell-matrix interactions and scheme of the ECM mimetic layer build-up.

A: Lectins are of crucial importance for cell-cell and cell-matrix interactions. These sugar-binding proteins assemble to multifunctional di-, tri- or tetramers that specifically recognize sugar moieties such as the carbohydrate polyLacNAc (B). C: Scheme of the biomimetic layer build-up on NCO-sP(EO-*stat*-PO) coatings with the sugar polyLacNAc, the galectin His_6CGL2, and the ECM glycoprotein FN. D: PolyLacNAc immobilized via MCP printing in patterns on NCO-sP(EO-*stat*-PO) coatings, incubated with His_6CGL2 and stained with antibodies (green), as well as incubated with His_6CGL2 and subsequently with FN and stained with antibodies (red) and the overlay of both fluorescent pictures (yellow), as proof for the specific binding sequence. Figure 1A and 1C were adapted from reference [19].

ELLA/ELISA experiments in coated 96-well plates enabled the determination of optimal concentrations for incubation of each layer. PolyLacNAc was covalently coupled to fresh hydrogel coatings in 96-well plates by incubation of freshly NCO-sP(EO-stat-PO) coated well plates with polyLacNAc in concentrations from 0 to 5 mM. A concentration of 2.5 mM yielded a

surface density not significantly lower than for 5 mM (Figure 2A), so that this concentration was chosen for further experiments. His_6CGL2 was incubated on polyLacNAc functionalized coatings, revealing a maximum surface density at 25 µg/mL (Figure 2B). For further experiments, a concentration of 50 µg/mL was chosen to guarantee a maximal galectin binding since this concentration was decisive for successive binding of the ECM glycoprotein. FN was incubated on the sugar-galectin construct in concentrations from 0 to 10 µg/mL and ELISA experiments showed a maximum surface concentration at 10 µg/mL (Figure 2C). Again, a higher concentration of 50 µg/mL was selected for further experiments to ensure maximal FN surface density.

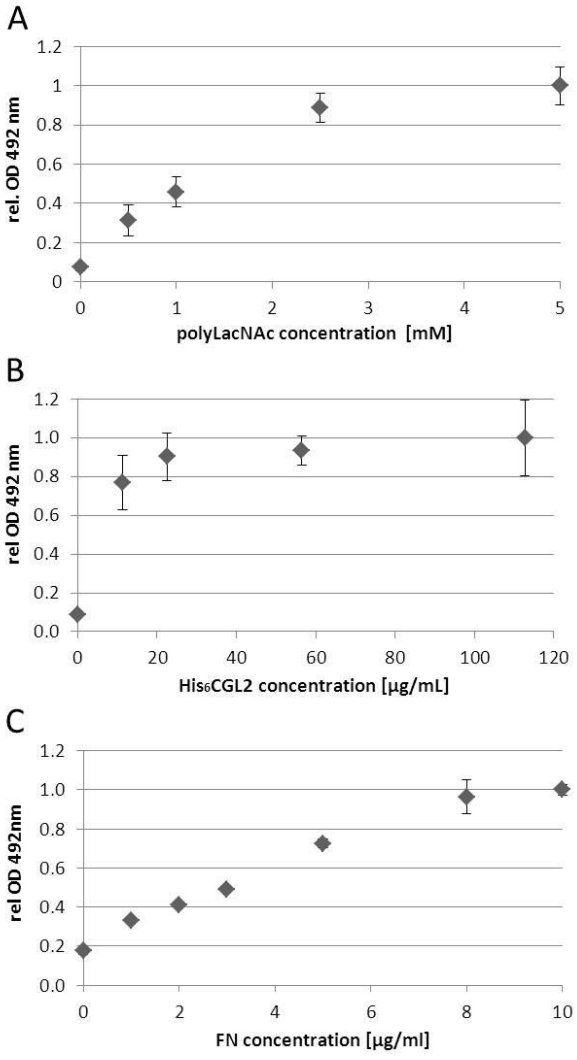

Figure 2: ELLA and ELISA for the different stages in ECM build-up on functionalized hydrogels.

ELLAs and ELISAs were performed on hydrogel coatings in 96-well plates were carried out with different concentrations of polyLacNAc (A), His_6CGL2 (B) and FN (C) to determine optimal concentrations for incubation. A: Different concentrations of polyLacNAc were detected by incubating 50 µg/mL His_6CGL2 and anti-His_6-POD. C: His_6CGL2 was bound on 2.5 mM polyLacNAc on NCO-sP(EO-*stat*-PO) and detected by anti-His_6-POD. E: Different concentrations of FN on 50 µg/mL His_6CGL2 on 2.5 mM polyLacNAc on NCO-sP(EO-*stat*-PO) were detected by rabbit-anti-FN and goat-anti-rabbit-POD antibodies.

HDF cells were cultured on surfaces representing all steps of the ECM layer construction: hydrogel coatings functionalized with polyLacNAc only, polyLacNAc-His_6CGL2, polyLacNAc-FN and the complete layer build-up of polyLacNAc-His_6CGL2-FN (Figure 3). As expected, non-functionalized NCO-sP(EO-*stat*-PO) coatings prevented cell adhesion [16]. Also, coatings functionalized with polyLacNAc alone did not induce HDF adhesion after 24 h (Figure 3A). However, when the galectin layer of His_6CGL2 was bound on the sugar layer, some cells could adhere after 24 h (Figure 3B). During cell culture, glycoproteins out from the medium which contained 10 vol-% serum, and proteins produced by the HDFs during cell culture could bind to the galectins and therefore serve as cell adhesion ligands. This protein binding to the sugar-galectin surface was not as efficient as incubation with concentrated FN solutions, so that the surface density of the proteins was low and only a few cells managed to adhere. Yet, these results again emphasize the binding capacity of these sugar-galectin surfaces for glycoproteins. It is known, that FN can bind to polyLacNAc, though ineffectively [20], and it is therefore not surprising that some HDFs could adhere to polyLacNAc functionalized coatings incubated with FN (Figure 3C). Still, only a few cells could adhere to these incomplete layers. In contrary, on the complete ECM mimetic surfaces (NCO-sP(EO-*stat*-PO)-polyLacNAc-His_6CGL2-FN), HDFs could adhere rapidly and in great numbers after 24 h of cell culture (Figure 3D). This demonstrated, that this biomimetic artificial ECM construct with galectin mediated immobilization of FN on polyLacNAc was well accepted by HDFs.

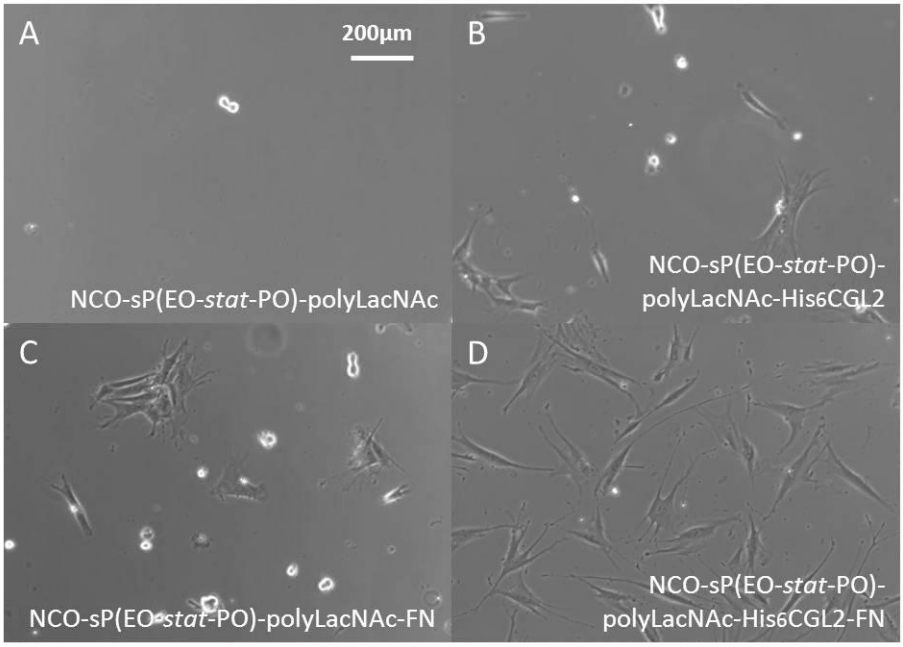

Figure 3: HDF adhesion on the different stages in ECM build-up on functionalized hydrogels.

HDFs were cultivated on NCO-sP(EO-*stat*-PO) coatings functionalized with polyLacNAc (A), polyLacNAc and His_6CGL2 (B), polyLacNAc and FN (C), and polyLacNAc with His_6CGL2 and FN (D). Pictures were taken after 24 h of cell culture with a magnification of 10x.

For evaluation of the biomimetic ECM construction, the constructs were compared with TCPS as a well-accepted surface for cell adhesion regarding spreading and proliferation. In the first hour of cell culture, cell adhesion on TCPS and NCO-sP(EO-*stat*-PO)-polyLacNAc-His_6CGL2-FN showed similar trends, with tendentiously but not significantly faster spreading of HDFs on the ECM mimetic surfaces (Figure 4A). As possible explanation it can be hypothesized that, on TCPS, cells first had to produce a sufficient amount of ECM proteins that subsequently adhered non-specifically on the hydrophobic surface to yield a density on the surface that allowed cell adhesion. This can be explained by the potential for the active replacement of initially presented FN by cell secreted glycoproteins in a manner that allowed the cells the reversible and dynamic shape of their environment.

In order to assess long term effects, HDFs on TCPS and NCO-sP(EO-*stat*-PO)-polyLacNAc-His_6CGL2-FN were observed over a period of 1 week. After different time points, cells were harvested and counted (Figure 4B). At time points up to 1 h, HDFs adhered in comparable numbers on both surfaces. However, after 1 week of cell culture, HDFs proliferated more rapidly on the biomimetic constructs and adhered in significant higher numbers as compared to cells on TCPS. This can be explained by the possibility of the cells to actively replace the initially presented FN by secreted glycoproteins in a manner that allowed the cells the reversible and dynamic conditioning of their environment.

To prove this hypothesis, the difference in the ability of cells to sense and react on the more flexible and non-covalent presentation of FN on the sugar-galectin construct compared to FN adsorbed on glass (glass-FN) and FN covalently bound to hydrogel coatings (NCO-sP(EO-*stat*-PO)-FN) was analyzed. Therefore, HDFs were seeded on these three different surfaces. Adhesion and spreading of HDFs was similar on all three surfaces regarding life cell images (results not shown). For more detailed information about the dynamic nature of the surfaces, FN was fluorescently stained on the surfaces before and after 48 h of cell culture (Figure 4 C-H). On all surfaces, FN was homogeneously distributed before cell culture. After 48 h of cell culture on glass-FN, FN was only found located under spread HDFs (Figure 4F). This indicated that FN adsorbed on glass desorbed during cell culture and only the cells fixed it to the surface. Covalently immobilized FN on hydrogels neither desorbed during cell culture, nor could the cells rearrange FN during the spreading process (Figure 4G). In contrast, cells on NCO-sP(EO-*stat*-PO)-polyLacNAc-His_6CGL2-FN were able to rearrange the homogeneously bound FN into fibrillar structures (Figure 4H). These experiments gave a first experimental proof corroborating

the hypothesis that the biomimetically presented FN may be rearranged by the cells in a dynamic and *in vivo* like manner.

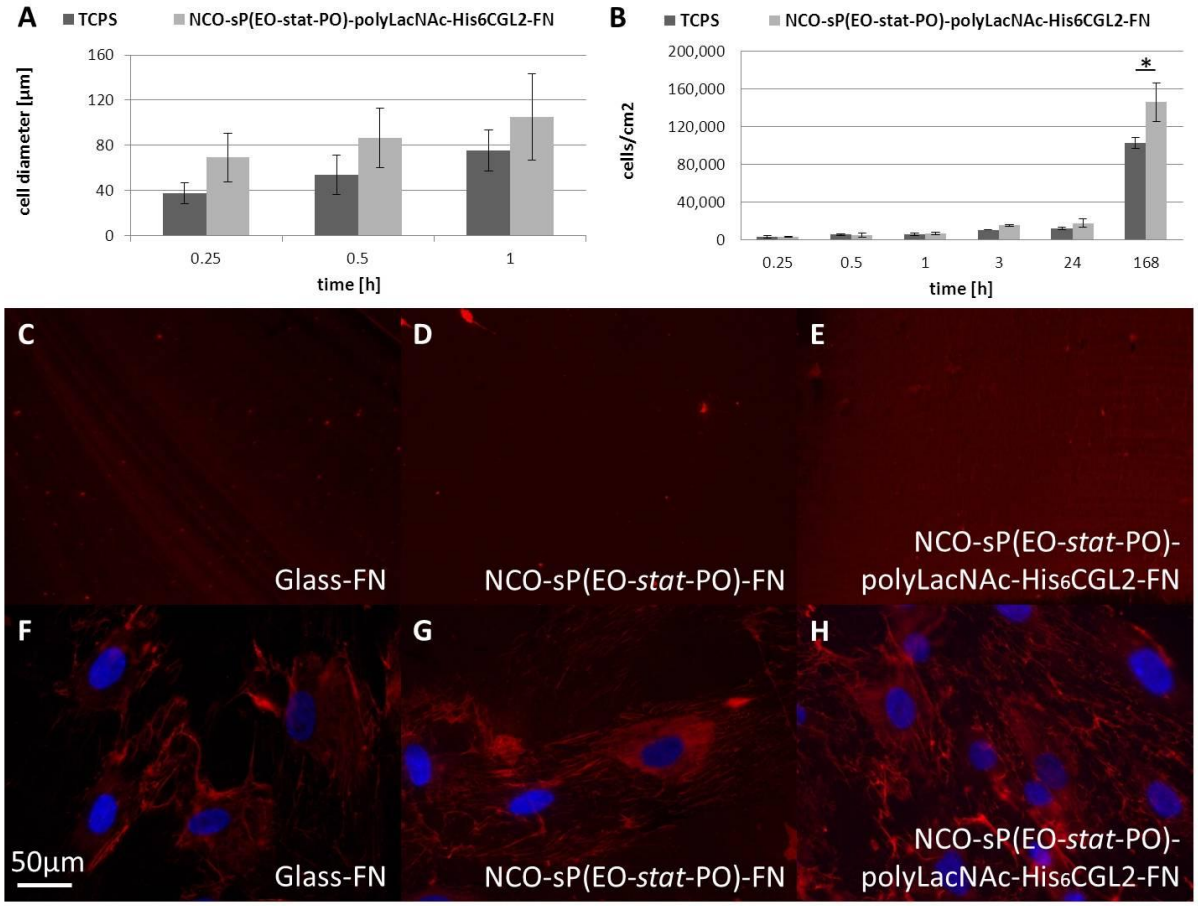

Figure 4: HDF spreading, proliferation and FN rearrangement.

Cell diameter of adherent HDFs was measured after the initial seeding process at 15, 30 and 60 min on TCPS and NCO-sP(EO-*stat*-PO)-polyLacNAc-His_6CGL2-FN (A). HDF adhesion was observed on TCPS and NCO-sP(EO-*stat*-PO)-polyLacNAc-His_6CGL2-FN over a period of 1 week (B), * $p < 0.05$. Cells showed a clear but not significant trend for faster spreading on the biomimetic ECM. With increasing time, the number of adherent cells became significantly higher on the biomimetic ECM. FN staining of substrates before cell culture (C-E) and FN and DAPI staining of cells cultured 24 h on substrates (F-H) showed that rearrangement of the FN on the reversible biomimetic layer build up was possible but not on covalently immobilized or physically adsorbed FN. As substrates, FN adsorbed on glass (C, F), FN covalently bound on NCO-sP(EO-stat-PO) hydrogel coatings (D, G) and the ECM mimetic layer build-up (E, H) were used. Pictures were taken with a magnification of 40x.

It is known, that the spreading of fibroblasts is affected by the environment of the cells [21] and that cells actively build-up and degrade their microenvironment [22]. The ECM glycoprotein FN contains 4 – 9 % carbohydrates and is part of the natural environment of cells, functioning in form of insoluble fibrils [23]. Cultured cells can rearrange FN into fibrils [24]. It was already shown, that higher densities of adhesion signals on a surface facilitate better spreading of fibroblasts [25, 26], but not only is the density of adhesion signals of importance for cell adhesion and function, Garcia et al. also showed that the conformation of adsorbed FN on

different surfaces influenced the cell adhesion of myoblasts [27]. In the *in vivo* environment, FN is bound to the ECM / collagen fibers via galectins [28]. The experiments in this Chapter indicated that the biomimetic galectin mediated presentation of FN made a significant difference in the ability of HDFs to rearrange FN on the surfaces as compared to the mere adsorption of FN on glass. Cells could adhere on both surfaces but only on ECM mimetic substrates HDFs seemed to be able to rearrange the FN into fibrils.

4. Conclusion

In summary, a way to construct a biomimetic cellular microenvironment on materials surfaces based on reversible carbohydrate / galectin mediated binding of ECM glycoproteins was presented in this Chapter. Specific recognition of the subsequent layer construction was proven by fluorescent staining on micro-patterned substrates that showed selective binding to the functionalized areas. With ELLAs and ELISAs, the maximum binding of the carbohydrate, the galectin and the ECM protein were determined. Consequently, a simple, easily modifiable and flexible mimicry of a natural ECM was produced. Cell experiments with HDFs as prove-of-concept demonstrated a selective binding of the cells to the full layer build-up of polyLacNAc-His_6CGL2-FN only. Compared to standard TCPS, HDFs were able to spread on the ECM mimetic surface more rapidly and proliferate better over a period of 1 week. FN staining after 48 h of cell culture gave a first hint that HDFs on the artificial ECM may have been able to rearrange the galectin bound FN, while FN adsorbed on glass and covalently bound to hydrogel coatings could not be rearranged.

Although this system needs further in depth analysis, it can be postulated that such surface functionalization proved superior for cell adhesion and function. This strategy bears great potential for biomaterials as well as for *in vitro* culture systems that allow the mimicry of the *in vivo* situation better than culture plates available today.

5. References

1. Zhu, W.B.; Iatridis, J.C.; Hlibczuk, V.; Ratcliffe, A. and Mow, V.C. Determination of collagen-proteoglycan interactions in vitro. *Journal of Biomechanics* **1996**, 29 (6) 773-83.
2. Marcon, P.; Marsich, E.; Vetere, A.; Mozetic, P.; Campa, C.; Donati, I.; Vittur, F.; Gamini, A. and Paoletti, S. The role of Galectin-1 in the interaction between chondrocytes and a lactose-modified chitosan. *Biomaterials* **2005**, 26 (24) 4975-84.
3. Chen, S.J.; Lin, C.C.; Tuan, W.C.; Tseng, C.S. and Huang, R.N. Effect of recombinant galectin-1 on the growth of immortal rat chondrocyte on chitosan-coated PLGA scaffold. *Journal of Biomedical Materials Research Part A* **2010**, 93A (4) 1482-92.
4. Kim, B.S.; Park, I.K.; Hoshiba, T.; Jiang, H.L.; Choi, Y.J.; Akaike, T. and Cho, C.S. Design of artificial extracellular matrices for tissue engineering. *Progress in Polymer Science* **2011**, 36 (2) 238-68.
5. Wang, Y.C.; Kao, S.H. and Hsieh, H.J. A chemical surface modification of chitosan by glycoconjugates to enhance the cell-biomaterial interaction. *Biomacromolecules* **2003**, 4 (2) 224-31.
6. Reska, A.; Gasteier, P.; Schulte, P.; Moeller, M.; Offenhausser, A. and Groll, J. Ultrathin coatings with change in reactivity over time enable functional in vitro networks of insect neurons. *Advanced Materials* **2008**, 20 (14) 2751-55.
7. Gasteier, P.; Reska, A.; Schulte, P.; Salber, J.; Offenhausser, A.; Moeller, M. and Groll, J. Surface grafting of PEO-Based star-shaped molecules for bioanalytical and biomedical applications. *Macromolecular Bioscience* **2007**, 7 (8) 1010-23.
8. Gotz, H.; Beginn, U.; Bartelink, C.F.; Grunbauer, H.J.M. and Moller, M. Preparation of isophorone diisocyanate terminated star polyethers. *Macromolecular Materials and Engineering* **2002**, 287 (4) 223-30.
9. Groll, J.; Ameringer, T.; Spatz, J.P. and Moeller, M. Ultrathin coatings from isocyanate-terminated star PEG prepolymers: Layer formation and characterization. *Langmuir* **2005**, 21 (5) 1991-99.
10. Groll, J.; Haubensak, W.; Ameringer, T. and Moeller, M. Ultrathin coatings from isocyanate terminated star PEG prepolymers: Patterning of proteins on the layers. *Langmuir* **2005**, 21 (7) 3076-83.
11. Rech, C.; Rosencrantz, R.R.; Křenek, K.; Pelantová, H.; Bojarová, P.; Römer, C.; Hanisch, F.-G.; Křen, V. and Elling, L. Combinatorial one-pot synthesis of poly-N-acetyllactosamine oligosaccharides with leloir-glycosyltransferases. *Advanced Synthesis and Catalysis* **2011**, 353 2492-500.
12. Sauerzapfe, B.; Krenek, K.; Schmiedel, J.; Wakarchuk, W.W.; Pelantova, H.; Kren, V. and Elling, L. Chemo-enzymatic synthesis of poly-N-acetyllactosamine (poly-LacNAc) structures and their characterization for CGL2-galectin-mediated binding of ECM glycoproteins to biomaterial surfaces. *Glycoconjugate Journal* **2009**, 26 (2) 141-59.
13. Barondes, S.H.; Cooper, D.N.W.; Gitt, M.A. and Leffler, H. Galectins - Structure and function of a large family of animal lectins. *Journal of Biological Chemistry* **1994**, 269 (33) 20807-10.
14. Hughes, R.C. Galectins as modulators of cell adhesion. *Biochimie* **2001**, 83 (7) 667-76.
15. Elola, M.T.; Wolfenstein-Todel, C.; Troncoso, M.F.; Vasta, G.R. and Rabinovich, G.A. Galectins: Matricellular glycan-binding proteins linking cell adhesion, migration, and survival. *Cellular and Molecular Life Sciences* **2007**, 64 1679 – 700.

16. Groll, J.; Fiedler, J.; Engelhard, E.; Ameringer, T.; Tugulu, S.; Klok, H.A.; Brenner, R.E. and Moeller, M. A novel star PEG-derived surface coating for specific cell adhesion. *Journal of Biomedical Materials Research Part A* **2005**, 74A (4) 607-17.

17. Kasten, A.; Müller, P.; Bulnheim, U.; Groll, J.; Bruellhoff, K.; Beck, U.; Steinhoff, G.; Möller, M. and Rychly, J. Mechanical integrin stress and magnetic forces induce biological responses in mesenchymal stem cells which depend on environmental factors. *Journal of Cellular Biochemistry* **2010**, 111 (6) 1586-97.

18. Walser, P.J.; Haebel, P.W.; Kunzler, M.; Sargent, D.; Kues, U.; Aebi, M. and Ban, N. Structure and functional analysis of the fungal galectin CGL2. *Structure* **2004**, 12 (4) 689-702.

19. Varki, A.; Cummings, R.D.; Esko, J.D.; Freeze, H.H.; Stanley, P.; Bertozzi, C.R.; Hart, G.W. and Etzler, M.E. Essentials of glycobiology. *Cold Spring Harbor Laboratory Press* Cold Spring Harbor (NY) **2009**.

20. Hoermann, H.; Jelinic, V. and Richter, H. Evidence for a Cryptic Lecton Site in the Cell Binding Domain of Plasma Fribronectin. *Hoppe-Seyler's Zeitschrift fuer Physiologische Chemie* **1984**, 365 (5) 517-24.

21. Yeung, T.; Georges, P.C.; Flanagan, L.A.; Marg, B.; Ortiz, M.; Funaki, M.; Zahir, N.; Ming, W.Y.; Weaver, V. and Janmey, P.A. Effects of substrate stiffness on cell morphology, cytoskeletal structure, and adhesion. *Cell Motility and the Cytoskeleton* **2005**, 60 (1) 24-34.

22. Zhu, J.M. Bioactive modification of poly(ethylene glycol) hydrogels for tissue engineering. *Biomaterials* **2010**, 31 (17) 4639-56.

23. Pankov, R. and Yamada, K.M. Fibronectin at a glance. *Journal of Cell Science* **2002**, 115 (20) 3861-63.

24. Pankov, R.; Cukierman, E.; Katz, B.Z.; Matsumoto, K.; Lin, D.C.; Lin, S.; Hahn, C. and Yamada, K.M. Integrin dynamics and matrix assembly: Tensin-dependent translocation of alpha(5)beta(1) integrins promotes early fibronectin fibrillogenesis. *Journal of Cell Biology* **2000**, 148 (5) 1075-90.

25. Deeg, J.A.; Louban, I.; Aydin, D.; Selhuber-Unkel, C.; Kessler, H. and Spatz, J.P. Impact of local versus global ligand density on cellular adhesion. *Nano Letters* **2011**, 11 (4) 1469-76.

26. George, P.A.; Doran, M.R.; Croll, T.I.; Munro, T.P. and Cooper-White, J.J. Nanoscale presentation of cell adhesive molecules via block copolymer self-assembly. *Biomaterials* **2009**, 30 (27) 4732-37.

27. Garcia, A.J.; Vega, M.D. and Boettiger, D. Modulation of cell proliferation and differentiation through substrate-dependent changes in fibronectin conformation. *Molecular Biology of the Cell* **1999**, 10 (3) 785-98.

28. Varki, A. Biological Roles of Oligosaccharides - All of the Theories Are Correct. *Glycobiology* **1993**, 3 (2) 97-130.

CHAPTER 10

Structural mimicry of the ECM through nanofibers with controlled surface chemistry: Ligand quantification and cell behavior

The development of advanced biomaterials and scaffolds for tissue engineering place high demands on materials and exceed the passive biocompatibility requirements previously considered acceptable for biomedical implants [1-4]. Many approaches focus on the structural mimicry of the native environment of cells, the ECM that consists partly of protein fibers which provide a mechanical scaffold for cells. Together with degradability, the activation of specific cell–material interactions and a three-dimensional environment that mimics the ECM are core challenges and prerequisites for the organization of living cells to functional tissue [5]. Although bioactive signalling combined with minimization of non-specific protein adsorption is an advanced modification technique for flat surfaces [6], it is usually not accomplished for three-dimensional fibrous scaffolds. In this Chapter a one-step preparation of fully synthetic, bioactive and degradable ECM-mimetic scaffolds by electrospinning, using poly(D,L-lactide-*co*-glycolide) (PLGA) as the matrix polymer is presented. Addition of the functional and amphiphilic macromolecule based on star-shaped poly(ethylene oxide) (NCO-sP(EO-*stat*-PO)) transformed current biomedically used degradable polyesters into hydrophilic fibers, which caused the suppression of non-specific protein adsorption on the fibers' surface. The cell adhesion mediating peptides (GRGDS), whole ECM proteins (FN) and the carbohydrate poly-N-acetyllactosamine (polyLacNAc) binding the galectin His_6CGL2 and FN were covalently attached to the hydrophilic fibers. These bioactivated scaffolds enabled human dermal fibroblasts (HDF) and human mesenchymal stem cells (MSC) adhesion, proliferation, and survival through exclusive recognition of the immobilized binding motifs. The presentation of peptides and proteins on the fibers' surface was quantified with enzyme linked immunosorbent assay (ELISA).

This Chapter represents a cooperative work with Dirk Grafahrend, Karl-Heinz Heffels and Claudia Rech.

Parts of this Chapter have been published:

Grafahrend D., Heffels K.-H., Beer M.V., Gasteier P., Möller M., Boehm G., Dalton P.D. and Groll J. Degradable polyester scaffolds with controlled surface chemistry combining minimal **protein** adsorption with specific bioactivation. *Nature Materials* **2011**, 10(1), 67-73.

1. Introduction

Cells are inherently sensitive to local meso-, micro-, and nanoscale environments [5]. Therefore, controlling bioactive functionality at different topographical scales is important for research in cell biology, tissue engineering and medical science [7]. Nanoscale fibers formed from electrostatic spinning, or electrospinning, are an increasingly important substrate for both tissue engineering and regenerative medicine [8-10]. To improve the biocompatibility, performance and function of the nanofibrous material, cell adhesion mediating proteins or peptide sequences have been either physically adsorbed [11] or covalently attached [12, 13] onto fiber surfaces so far. The strategies followed for covalent attachment are typically time consuming and involve several activation and coupling steps [14, 15].

The surface of such nanofibers is important since biocompatibility and the interactions of materials with the immune system are influenced by their surface chemistry. As a consequence of the high specific surface area of electrospun fibers, this is a decisive factor for micro- and nanoscale materials [16]. Protein adsorption occurs rapidly after a material is implanted. These proteins can denature on hydrophobic surfaces, triggering the immune system and influencing wound healing [3]. Therefore, in addition to bioactivation, prevention of non-specific protein adsorption is a key feature determining the control over a biomaterial implant. Poly(ethylene oxide) (PEO) has been used extensively as a coating material for two-dimensional substrates to generate surfaces that resist non-specific protein adsorption [17]. In contrast, attempts to reduce protein adsorption on electrospun nanofibers were often ignored in cell adhesion studies. Recently, a method has been reported for the generation of electrospun fibers coated with poly(ethylene oxide-block-ε-caprolactone) (PEO-*b*-PCL), which resisted the adsorption of proteins [18]. This approach, however, required several synthetic and time-consuming scaffold functionalization steps, so introduction of cell adhesion ligands on the fiber surface was a difficult multistep procedure. Overcoming non-specific protein adsorption while at the same time generating specific adhesion of cells remains a serious challenge for both electrospinning and scaffolds for tissue engineering in general. Nevertheless, such advanced scaffolds are expected to be necessary for the ultimate formation of functional tissue [19].

In this Chapter, a method that dramatically alterd the properties of electrospun materials by combining functional additives with existing hydrolytically degradable polymers was used. The resulting protein resistant, functionalized, electrospun fibers were formed in a single step, with a multitude of variations possible. The strategy relied on adding a functional amphiphilic

macromolecule based on star-shaped PEO to poly(D,L-lactide-*co*-glycolide) (PLGA, Figure 1A). The additive was a six arm star shaped poly(ethylene oxide-*stat*-propylene oxide) with isocyanate end groups (NCO-sP(EO-*stat*-PO)) with 80% ethylene oxide (EO) content and a molecular weight of 12 kDa (Figure 1B). It has been reported before that coatings prepared from NCO-sP(EO-*stat*-PO) prevented the adsorption of proteins and the adhesion of cells [1, 2]. In this Chapter, the transfer of this hydrogel coating on flat surfaces used in the previous Chapters of this work was transferred to three-dimensional fibers. The electrospun fibers showed protein and cell repellent properties combined with the ability to be functionalized with cell adhesion mediating ligands specifically allowing cell adhesion while still remaining biocompatible.

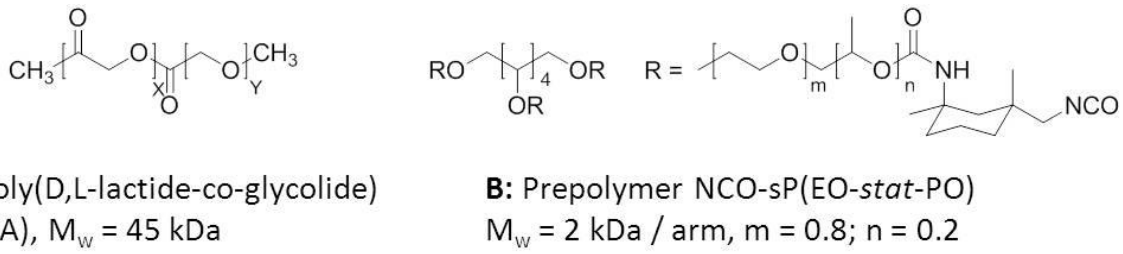

Figure 1: The two components of the elecrospun nanofibers.

Protein and cell repellent nanofibers were electrospun out of a solution containing (A) poly(D,L-lactide-*co*-glycolide) (PLGA) and (B) the six arm star shaped poly(ethylene oxide-*stat*-propylene oxide) with isocyanate end groups (NCO-sP(EO-*stat*-PO)).

PLGA/sP(EO-*stat*-PO) fibers functionalized with ligands were analysed using methods established in previous Chapters of this work for two-dimensional coatings. Determination of ligand density on the interface of the fibers was analysed using the surface sensitive ELISA technique. Therefore, the biotinylated RGD peptide GRGDSK-biotin was immobilized on the fibers for detection using streptavidin-peroxidase (SA-POD). Additionally, the protein FN was detected with a primary and secondary antibody coupled to POD. Furthermore, cell adhesion of HDFs and MSCs on fibers with different GRGDS densities was quantified allowing determination of minimal ligand concentrations necessary for proper cell adhesion. More detailed analysis of cell behaviour on the three-dimensional scaffolds was performed with HDFs regarding cell morphology, vitality, and long term survival, all of which are important factors for the development of functional scaffolds for tissue engineering or regenerative medicine. Additionally, it was proven that fibers could be functionalized with more complex molecules like the carbohydrate polyLacNAc binding the fungal galectin His_6CGL2 and FN, developed for two-dimensional surfaces in Chapter 9 and mediated a more biomimetic adhesion of HDFs.

2. Experimental section

2.1. Hydrogel coatings

2.1.1. NCO-sP(EO-stat-PO) synthesis

Isocyanate terminated prepolymers (NCO-sP(EO-*stat*-PO)) were synthesized as described in detail elsewhere [20]. In short, the prepolymer was fabricated by the reaction of hydroxyl terminated star shaped polyether polyole with isophorone diisocyanate (IPDI).

2.1.2. Preparation of glass substrates

Glass substrates (Ø 15 mm, Paul Marienfeld, Lauda-Königshofen, Germany) were polished with isopropanol and successively cleaned in acetone, distilled water, and isopropanol in an ultrasonic bath for 5 min each followed by drying in a stream of nitrogen. Solvents were purchased from Prolabo (Darmstadt, Germany). Glass substrates were activated by O_2-plasma treatment in the plasma process plant AK 330 (Roth & Rau, Hohenstein-Ernstthal, Germany) for 15 min (400 W, 50 sccm, 0.4 mbar). Afterwards, glass substrates were left in a desiccator containing 100 µl 3-aminopropyl-trimethoxysilan (AS) at 5 mbar for 60 min. After removal of AS, the glass substrates were left in a vacuum of minimum 10^{-2} mbar for 1 h and stored at 250 mbar.

2.1.3. NCO-sP(EO-stat-PO) coating

The coating procedure has been described earlier [21]. Prepolymers were solubilized in tetrahydrofuran (THF, dried over sodium, Prolabo, Darmstadt, Germany). After adding water to the solution (9/1 v/v water/THF, prepolymer concentration 10 mg/ml), prepolymers were left for crosslinking for 5 min. Two droplets of the solution were placed on the aminosilanized surface of a glass substrate after filtration through a 0.2 µm syringe filter (Whatman, Dassel, Germany). The coating process was carried out in the spin coater WS-400-B-6NPP/LITE (Laurell Technologies, North Wales, USA) at 2,500 rpm for 40 sec with an acceleration time of 5 sec. Each prepolymer solution was used to coat a maximum of 6 substrates. Coated substrates were stored at room temperature for at least 12 h to ensure complete crosslinking of the coating.

2.2. Fiber scaffolds

2.2.1. PLGA fibers

143 mg Poly-D,L-lactide-*co*-glycolide (PLGA RG 504, Boehringer Ingelheim Pharma, Ingelheim am Rhein, Germany) were dissolved in 0.45 mL dry aceton (Prolabo, Darmstadt, Germany). 50 µl dimethylsulphoxide (DMSO), and 10 µl trifluoracetic acid solution (TFA, 2 µl/ml in water) were added, the solution was stirred and immediately used for electrospinning. DMSO and TFA were bought from Sigma-Aldrich (Steinheim, Germany). Polymer solutions were fed at rates of 1 mL/h to a flat-tip stainless-steel spinneret connected to a high-voltage power supply. The high-voltage generator Eltex KNH34 (Eltex-Electrostatik, Weil am Rhein, Germany) was used to charge the solutions at 20 kV while the collector remained earthed. The solutions were pumped to an 18-gauge, flat-tipped, stainless-steel spinneret with a collection distance of 20 cm. As collectors, hydrogel coated glass substrates were fixed on a rotating aluminum drum and fibers spun for 30 to 60 sec.

2.2.2. PLGA/sP(EO-stat-PO) fibers

29 mg NCO-sP(EO-*stat*-PO) were dissolved in 0.45 ml acetone and 50 µl DMSO under mechanical stirring. After addition of 10 µl TFA and 143 mg PLGA the solution was stirred thoroughly and directly used for electrospinning under conditions described above.

2.2.3. Functionalization of PLGA/sP(EO-stat-PO) fibers

Incubation method

The peptide GRGDSK-biotin (Bachem, Bubendorf, Switzerland) and the carbohydrate polyLacNAc (synthesized as described elsewhere [22]) were dissolved in 0.02 M Na_2CO_3/$NaHCO_3$ buffer (pH 9.4) at concentrations from 0.2 to 1,000 µg/ml (GRGDSK-biotin) and 1 to 20 µg/ml (polyLacNAc). The protein FN (Sigma-Aldrich, Steinheim, Germany) was dissolved in distilled water (Carl Roth, Karlsruhe, Germany) at concentrations between 1 and 20 µg/ml. The PLGA/sP(EO-*stat*-PO) fibers were fabricated as described above. 70 min after adding water to the prepolymer solution, 100 µl of the ligand solution were incubated as a droplet on the fibers for 60 min. Afterwards, the fibers were washed 2 times with deionized water. When the fibers were functionalized with polyLacNAc, an artificial ECM was built up by incubation of the recombinant fungal galectin His_6CGL2 [23] and the human ECM protein FN (Sigma-Aldrich, Steinheim, Germany). His_6CGL2 and FN were diluted in distilled water at concentrations of

50 µg/mL and subsequently incubated on the polyLacNAc presenting surfaces at room temperature for 60 min.

Mix-in method

The peptides GRGDS and GRGES (Bachem, Bubendorf, Switzerland) were dissolved in the NCO-sP(EO-*stat*-PO) solution in molar peptide to prepolymer ratios of 1/1 (GRGES) and 1/20 to 1/1 (GRGDS). Afterwards, PLGA was added and the electrospinning process was performed as described above.

2.3. Fiber characterization

2.3.1. Calculation of fibers' surface

The fiber surface area was calculated on the basis of the fiber diameter and the relative area of the substrate covered by fibers. Fiber diameters were determined via magnified optical microscope pictures. With the image manipulation program Gimp 2.2, the optical images of the fiber substrates were converted into black/white images and the threshold was chosen for each image individually so that fibers and background were clearly separated and the percentage of area covered by fibers was determined. Under the assumption that fibers were a cylinder that lay on the surface of the substrate the surface area of the fibers was calculated.

2.3.2. Protein adsorption

Fibers were stored in deionized water for 60 min. Afterwards, the fibers were incubated with 50 µL BSA-rhodamine red conjugate (bovine serum albumin, Invitrogen, Karlsruhe, Germany) in PBS buffer (0.01 M, pH 7.4) for 20 min, immersed 5 times with PBS buffer for 20 min, washed thoroughly with deionized water, and dried in a stream of nitrogen. Protein adsorption was observed by fluorescence microscopy using an Axioplan 2 imaging microscope (Carl Zeiss, Göttingen, Germany) within the same day. Pictures were taken with an AxioCamMRc digital camera and analyzed using the AxioVisionV4.6 software. The fiber meshes were placed in 1 mL sodium dodecyl sulphate (SDS, 1 wt-%, Bio-Rad, Munich, Germany) solution for 1 hour. SDS detached the adsorbed proteins from the fiber surface, thus the fluorescence of the proteins in solution was measured with a fluorescence spectrometer. A calibration curve gave the amount of BSA per mL SDS solution.

2.3.3. ELISA

Functionalized PLGA/sP(EO-*stat*-PO) fibers on glass substrates were left at room temperature for at least 12 h to ensure complete hydrogel crosslinking. Fibers on glass were placed into a

24-well suspension culture plate (Greiner Bio-One, Frickenhausen, Germany) and incubated with distilled water for 60 min.

ELISA on GRGDSK-biotin functionalized fibers

Fibers were incubated with 300 µl glycidol solution (2.23 mg/ml in 0.2 M bicarbonate buffer) for 60 min and washed 3 times with 300 µL PBS-Tween (0.05 vol-% Tween-20 in PBS, Roth, Karlsruhe, Germany). The uncoated side of the glass substrates was blocked with PBS-BSA (1 wt-% BSA in PBS, Servia Electrophoresis, Heidelberg, Germany) in PBS for 60 min. 200 µL streptavidin-peroxidase (SA-POD, 1/5000 in PBS, Roche, Mannheim, Germany) were incubated on the fibers for 60 min and washed with PBS-Tween. After dissolving one OPD tablet (Dako, Hamburg, Germany) in 6 mL deionized water and 2.5 µL H_2O_2 (30 vol-%), 200 µL of the OPD solution were added to each well. After 1 min incubation, the reaction was stopped by adding 100 µL 3 M HCl. Optical density (OD) of each well was measured in the microplate reader Sunrise (Tecan, Maennedorf, Switzerland) at a wavelength of 492 nm.

ELISA on FN functionalized fibers

Primary rabbit-anti-human FN antibody and goat-anti-rabbit IgG-POD were purchased from Sigma-Aldrich (Steinheim, Germany). Fibers were incubated with 200 µL of a 1/1000 dilution of the anti-FN antibody in PBS-B for 60 min and washed 3 times with PBS-Tween. 200 µL of a 1/1000 dilution of goat-anti-rabbit IgG-POD in PBS-BSA were added to each well for 60 min. Afterwards, wells were washed with PBS-Tween again. Detection with OPD solution and OD measurement were carried out as described above.

2.4. *In vitro* cell experiments

2.4.1. Cell culture

Primary human dermal fibroblasts

HDFs (isolated from foreskin, maximum passage 6) were kindly provided by Prof. Baron (Department of Dermatology and Allergology, University Hospital of the RWTH Aachen, Germany). Cells were cultured in DMEM medium (Invitrogen, Karlsruhe, Germany) supplemented with 10 vol-% fetal bovine serum (Biowest, Nuaillé, France) and 1 vol-% penicillin/streptomycin under standard cell culture conditions (37°C, 5% CO_2, 95% humidity). Cells were harvested by incubation with 0.25% trypsin/EDTA (PAA, Cölbe, Germany) at 37°C for 3 min. The reaction was stopped by adding DMEM. Supplements and trypsin were from PAA (Cölbe, Germany).

Mesenchymal stem cells

MSCs (maximum passage 2) were kindly provided from PD Neuss-Stein (Department of Pathology, University Hospital of the RWTH Aachen, Germany). MSCs were collected from an anonymous donor (hip operation) and isolated according to the minimal criteria of the International Society for Cellular Therapy described in Dominici et al. [24]. MSCs were cultured under standard cell culture conditions in DMEM medium from PAN-Biotech (Aidenbach, Germany) containing 60 vol-% DMEM low glucose, 40 vol-% MCDB-201, 2 vol-% fetal bovine serum, 1 x ITS-plus (insulin-transferrin-selenic acid + BSA-linoleic acid), 1 nM dexamethasone, 100 µM ascorbic-acid-2-phosphate, and 10 ng/ml epidermal growth factor. MSCs were harvested by incubation with trypsin from Cell Systems (Kirkland, USA) at 37°C for 3 min. The reaction was stopped by adding DMEM.

2.4.2. Sample preparation and cell seeding

After fabrication, fibers were left at ambient conditions for at least 12 h. Coated glass substrates with electrospun fibers were placed in a 24-well suspension culture plate (Greiner Bio-One, Frickenhausen, Germany) and washed thoroughly with sterile PBS buffer from PAA (Cölbe, Germany) and distilled water for 5 times each to remove any contaminations. 1 ml cell suspension (20,000 cells/mL in DMEM) was seeded on each fiber substrate. Samples were incubated under standard cell culture conditions.

2.4.3. Cell adhesion

HDFs and MSCs were seeded and cultured on PLGA, PLGA/sP(EO-*stat*-PO), PLGA/sP(EO-*stat*-PO)-GRGES (1/1) and PLGA/sP(EO-*stat*-PO)-GRGDS (1/1) fibers. Additionally HDFs were seeded on PLGA/sP(EO-*stat*-PO)-GRGDS fibers with molar peptide to prepolymer ratios of 1/20, 1/10, 1/5 and 1/2. Life cell images were taken after 0.25, 0.5, 1, 2, 3, 24 and 48 h with a magnification of 10x and adherent cells counted on the life cell images.

2.4.4. Cell viability/cytotoxicity staining

For determination of cell survival, a LIVE/DEAD® viability/cytotoxicity kit for mammalian cells (Invitrogen, Karlsruhe, Germany) was used according to the manufacturer's instructions.

2.4.5. Fluorescent staining of the cytoskeleton

To observe the cell morphology, cells were fixed with 4 wt-% paraformaldehyde (Roth, Karlsruhe, Germany) and permeabilized with 0.1 vol-% Triton X-100 (Sigma-Aldrich, Steinheim, Germany) in PBS buffer. Tetramethylrhodamine isothiocyanate-conjugated phalloidin (1/500 in PBS) and 4',6-diamidino-2-phenylindole (DAPI, 1/1000 in PBS) from the Actin Cytoskeleton and Focal Adhesion Staining Kit (Chemicon, Schwalbach, Germany) were incubated subsequently on the cells for 1 h, each with washing with PBS buffer in between.

2.4.6. Microscopy

Optical and fluorescent microscopy were carried out with the inverted Axiovert 100A Imaging microscope with an AxioCam MRc digital camera and were analyzed using the AxioVisionV4.7 software. Hard- and software were from Carl Zeiss (Göttingen, Germany).

3. Results and discussion

The chemical properties of hydrogel coated fibers were analyzed by Grafahrend and Heffels [25] and are shown in this Chapter to give an idea about the fiber characteristics mainly determining cell behavior on these constructs. The wetting of electrospun materials with aqueous solutions is a relevant property for cell culture, since media exchanges and cell seeding are a key step in common protocols. Typically, electrospun PLGA fibers are hydrophobic as a consequence of the nature of the polymer and the contact angle is further increased by the porous morphology of the mesh. A water contact angle of 120° was measured on electrospun PLGA fibers, significantly higher than the value of 70° reported for bulk PLGA [26]. In contrast, a water droplet placed onto PLGA/sP(EO-*stat*-PO) fibers was absorbed within seconds. The wettability of the fibers indicates that the NCO-sP(EO-*stat*-PO) additive transformed the PLGA, rendering its surface hydrophilic. X-ray photoemission spectroscopy measurements on PLGA and PLGA/sP(EO-*stat*-PO) fibers confirmed this counterintuitive surface segregation of the hydrophilic PEO-based star molecules in the hydrophobic matrix. Defect-free and stable fibers were collected. Both PLGA and PLGA/sP(EO-*stat*-PO) fiber meshes degraded under physiological conditions (PBS buffer, pH 7.4 and 37°C), showing a lag time of three weeks and complete mass loss after three months. The hydrophilic fibers degraded significantly faster after 35 days.

For protein adsorption and *in vitro* experiments, glass substrates previously coated with an ultrathin film of NCO-sP(EO-*stat*-PO) were used as collectors. These films prevent non-specific protein adsorption and resist cell adhesion for at least four weeks under standard cell culture conditions [27]. These hydrogel films were pre-exposed to water, thus having surficial amino groups that can react with isocyanate groups on the surface of the freshly prepared PLGA/sP(EO-*stat*-PO) fibers. In this way, newly formed electrospun fibers were captured and covalently anchored to this surface. Using such 'reactive collectors' enabled the investigation of 'dilute' quantities of fibers on a protein repellent substrate. This *in vitro* test system provided insight into the responses of cells on electrospun fibers, as the fibers could be chemically modified independently of the substrate. Furthermore, possible detachment of fibers and loss of electrospun material during the frequent media changes was prevented, while preserving the protein repellency of the ultrathin film coating. To demonstrate this idea, pure PLGA and PLGA/sP(EO-*stat*-PO) electrospun fibers were collected on such coated targets and stored under ambient conditions overnight followed by incubation with fluorescently labeled BSA as a model protein. Figure 2 shows both optical (A, C) and fluorescence (B, D) microscope images of electrospun fibers after incubation with labeled BSA. Although pure PLGA electrospun fibers

induced protein adsorption resulting in strong fluorescence on the fibers (Figure 2B), the PLGA/sP(EO-*stat*-PO) electrospun fibers showed almost no detectable fluorescence (Figure 2D). This set-up also enabled the quantification of surface-adsorbed BSA by desorption of the proteins from the fiber surface using a SDS solutions. Although 41.8 +/- 14.8 ng/nm BSA adsorbed on the fiber surface in the case of PLGA, only 0.3 +/- 0.2 ng/cm BSA could adsorb on the NCO-sP(EO-*stat*-PO) modified fibers. This reduction of protein adsorption by 99.2% was a crucial step for the generation of specific cell adhesion by binding of cell adhesion mediating sequences onto such scaffolds.

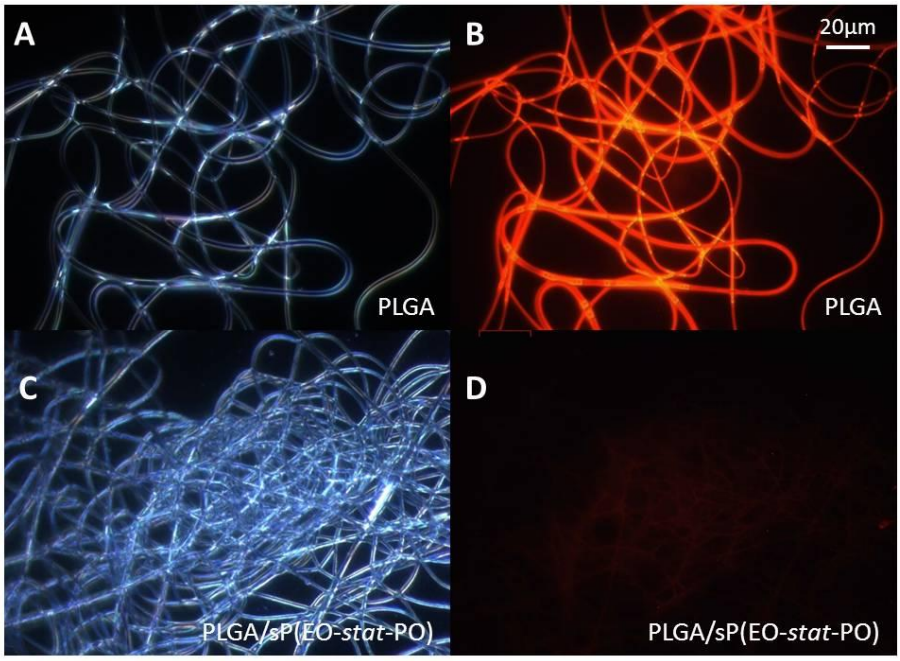

Figure 2: Protein adsorption on PLGA and PLGA/sP(EO-*stat*-PO) fibers.

Optical microscopy images (A, C) and fluorescence microscopy images (B, D) of PLGA fibers (A, B) and PLGA/sP(EO-*stat*-PO) fibers (C, D), both incubated with 25 µg/ml fluorescence labelled BSA. Insignificant protein adsorption occured even on the dense mesh area of hydrogel coated fibers displayed in panel D. Quantification of protein adsorption showed a reduction by more than 99.2% by use of the NCO-sP(EO-*stat*-PO) additive. Image modified from reference [25] with permission from the Nature Publishing Group.

To show the potential of the ELISA method described in Chapter 6 to determine ligand densities on surfaces, ELISAs were performed on functionalized fibers. For this purpose, fibers were functionalized with the peptide GRGDSK-biotin (Figure 3A) and the protein FN (Figure 3B) using the incubation method. A maximal peptide concentration on the fibers' surface was reached at a peptide concentration of 100 µg/ml, whereas a maximal protein concentration was already reached at 5 µg/ml. These experiments point out the possibility to quantify ligand densities with surface sensitive ELISA not only on flat surfaces, but even on three-dimensional fiber scaffolds and confirms that ELISA is applicable to all kinds of biomaterials.

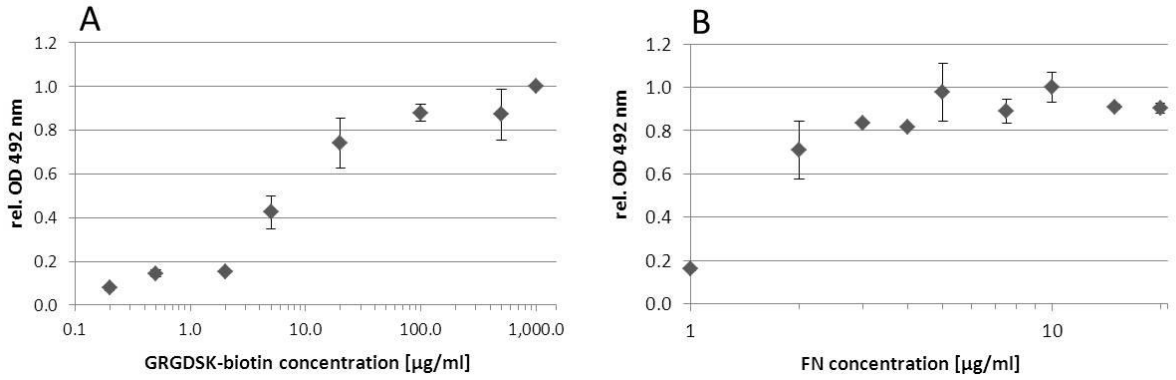

Figure 3: ELISA on functionalized PLGA/sP(EO-*stat*-PO).

Relative optical density of ELISAs on PLGA/sP(EO-*stat*-PO) fiber coatings functionalized with different concentrations of GRGDSK-biotin (A) and FN (B) via incubation method. GRGDSK-biotin was detected by streptavidin-peroxidase conjugate and FN by rabbit-anti-human FN antibody and goat-anti-rabbit IgG-peroxidase.

This fiber system was suitable for functionalization with different kinds of ligands such as peptides or proteins. For more detailed analysis of cellular responses, GRGDS was used as peptide for the preparation of cell adhesion mediating fibers since it is extensively used as a cell adhesion mediating sequence [28]. To prove that the integrity of the surface layer was not affected by addition of a peptide sequence and to demonstrate specificity of cell adhesion, the sequence GRGES, which, although very similar to GRGDS, does not act as a ligand for cell adhesion, was taken as a control sequence. In this study, functionalized fibers were prepared by addition of the peptide to the polymer solution before electrospinning (mix-in method). The peptide covalently reacted with the isocyanate groups and was, together with the star shaped molecules at the distal ends of the arms, presented at the surface of the fibers after the electrospinning process.

HDFs were seeded onto electrospun PLGA and PLGA/sP(EO-*stat*-PO) fibers as well as peptide (GRGDS as well as GRGES) functionalized PLGA/sP(EO-*stat*-PO) fibers with a molar peptide to prepolymer ratio of 1/1. Cells were cultivated for 1 week on the fibers and cells stained with a LIVE/DEAD® staining kit (Figure 4). Cells grew nicely on PLGA fibers (Figure 4A) although it has to be pointed out that this adhesion was non-specific and cells may not have adhered to the PLGA fibers directly but to a layer of adsorbed proteins of the medium on the PLGA fibers. Nevertheless, cells on PLGA fibers were green indicating their vitality. No adherent cells were observed on PLGA/sP(EO-*stat*-PO) fibers (Figure 4B). This can be explained with the protein repellent surface of the fibers. As a result of the PEO enriched surface and the hydrophilicity of the PLGA/sP(EO-*stat*-PO) fibers, neither proteins from the medium nor proteins produced and secreted by the cells adsorbed onto the fibers, so the fibroblasts were unable to adhere. Also

for GRGES modified PLGA/sP(EO-*stat*-PO) fibers no cell adhesion was observed (Figure 4C). This confirmed that attachment of a peptide sequence onto the fiber surface did not alter the ability of the fiber surface to resist non-specific cell adhesion. In contrast, the PLGA/sP(EO-*stat*-PO) fibers modified with GRGDS mediated cell adhesion and HDFs adhered and showed green fluorescence indicating their vitality (Figure 4D). With this experiment it was possible to clearly demonstrate that an non-specific adhesion on PLGA fibers was possible but could be inhibited by 'coating' the fibers with NCO-sP(EO-*stat*-PO). The immobilization of GRGES peptide verified that the hydrogel coating of the fibers was not disintegrated by the coupling of a peptide. The immobilization of the cell adhesion mediating peptide GRGDS induced specific cell adhesion and survival.

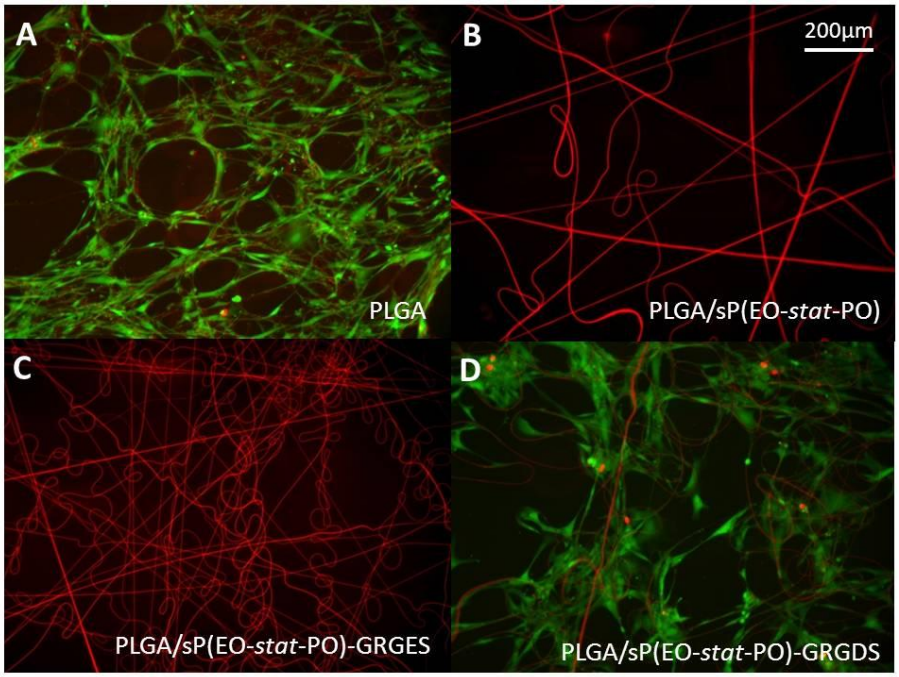

Figure 4: Viability of HDFs on fiber constructs after 1 week.

HDFs were seeded on PLGA (A), PLGA/sP(EO-*stat*-PO) (B), PLGA/sP(EO-*stat*-PO)-GRGES (1/1) (C) and PLGA/sP(EO-*stat*-PO)-GRGDS (1/1) (D) fibers for 1 week and subsequently stained with LIVE/DEAD® staining. The LIVE/DEAD® staining kit consists of Calcein AM and Ethidium homodimer-1. In viable cells, Calcein AM is taken up and converted by esterase into green fluorescent Calcein, while the red fluorescent Ethidium homodimer-1 can only enter into cells when the membrane is disintegrated. Thus, the green fluorescence of the cells that adhered to the PLGA and PLGA/sP(EO-*stat*-PO)-GRGDS (1/1) fibers indicated viability of the cells. Image modified from reference [25] with permission from the Nature Publishing Group.

HDFs on GRGDS modified PLGA/sP(EO-*stat*-PO) fibers were fixed with paraformaldehyde and the actin cytoskeleton (red) as well as the nucleus (blue) were stained fluorescently (Figure 5). Cells maintained a normal phenotypic shape, became adherent and spread in between the fibers (false color, green) already after 24 h of *in vitro* cell culture. Adherent cells bridged

between several fibers and were integrated into the surrounding mesh to form a three-dimensional network only adhering to the fibers and not to the inert hydrogel background.

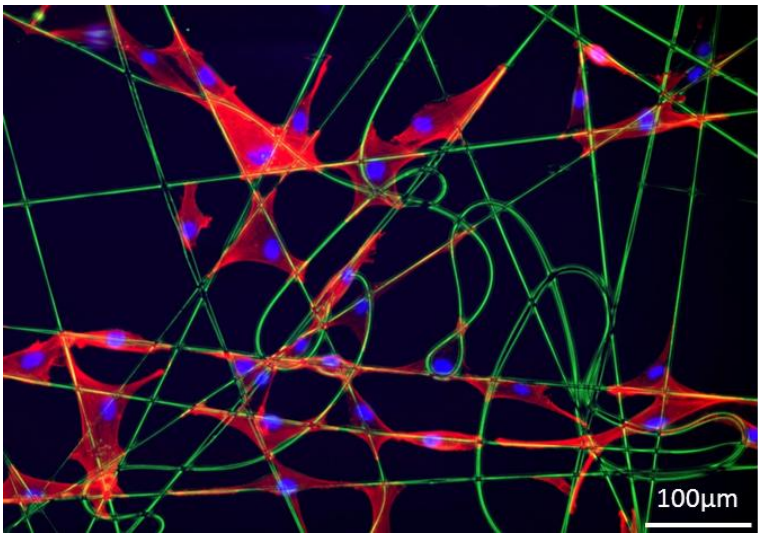

Figure 5: Morphology of HDFs on PLGA/sP(EO-*stat*-PO)-GRGDS fibers.

Fluorescence microscope image (nuclei blue, actin filaments red) of HDFs after 24 h in cell culture on GRGDS functionalized PLGA/sP(EO-*stat*-PO) fibers (fibers in false-color green from optical microscope picture overlay) with a prepolymer to peptide ratio of 1/1. The fiber diameter was 830 ± 100 nm. Image modified from reference [25] with permission from the Nature Publishing Group.

Long term *in vitro* cell culture of HDFs on GRGDS functionalized PLGA/sP(EO-*stat*-PO) fibers (1/1) showed that the cells proliferated well in the fiber meshes (Figure 6). After 2 weeks of cell culture, a confluent cell layer was formed on the fiber constructs (Figure 6 E, F). With on-going experimental time, the cells stopped proliferating due to spatial limitations (confluency), so that the experiments were stopped after 3 weeks. Interestingly, cells did not adhere to the sP(EO-*stat*-PO) coated substrates at any time throughout the experiment, underlining the efficient and sustainable cell adhesion preventing property of these coatings even in standard cell culture conditions over several weeks.

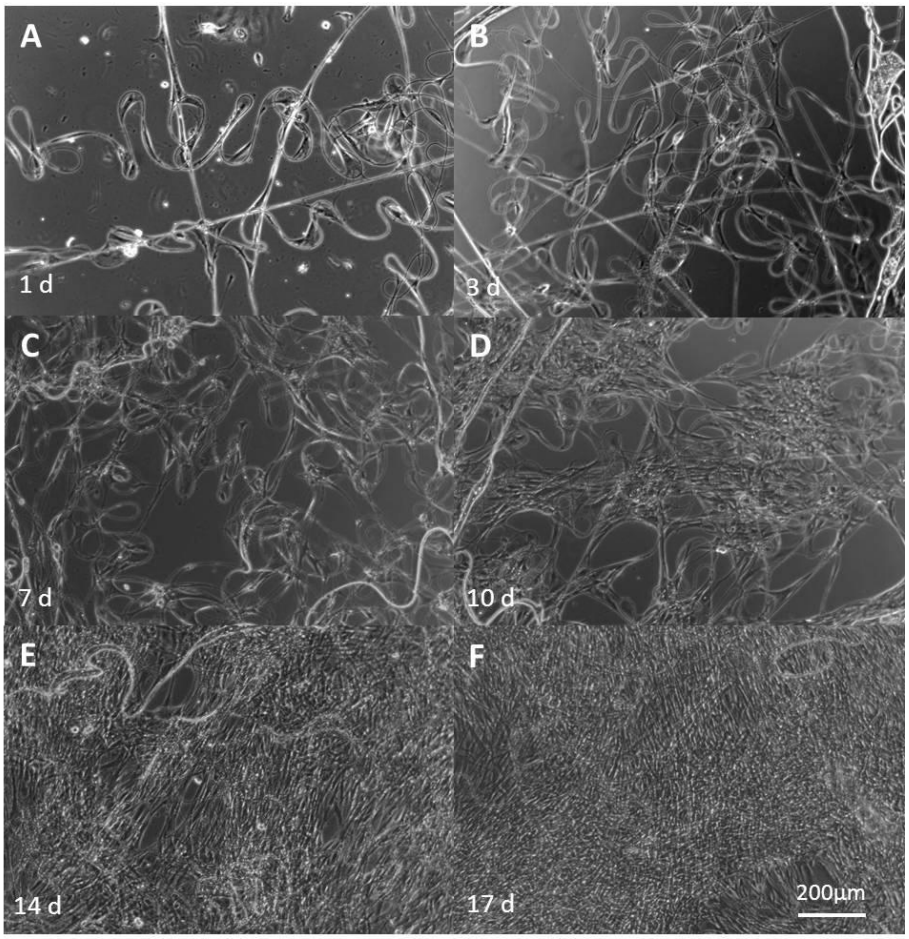

Figure 6: Long term *in vitro* cell culture of HDFs on GRGDS functionalized fibers.
HDFs were cultured on PLGA/sP(EO-*stat*-PO)-GRGDS fibers with a peptide to prepolymer ratio of 1/1. Images were taken after 1 (A), 3 (B), 7 (C), 10 (D), 14 (E) and 17 (F) days.

HDFs were seeded on pure PLGA fibers as well as PLGA/sP(EO-*stat*-PO) fibers functionalized with molar ligand to prepolymer ratios of 1/20, 1/10, 1/5, 1/2 and 1/1. Cell counting after 2, 24, and 48 h allowed determination of cell adhesion kinetics (Figure 7A). On 1/20 fibers, cells did not adhere as effectively as on fibers with higher GRGDS to prepolymer ratio. After 48 h, the medium was changed before cell counting to wash away all cells not strongly adhered to the fibers. The cell number on 1/20 fibers decreased, indicating, that cells adhered on these fibers but not strong enough to resist the forces applied by medium suction. ata suggest that a molar peptide to prepolymer ratio of 1/10 was the minimum threshold for proper cell adhesion that did not significantly increase with further increasing the amount of peptide on the fibers. Quantification of LIVE/DEAD® stainings of HDFs on fibers with different peptide contents revealed that, although a molar peptide to prepolymer ratio of 1/10 was sufficient for a high number of adherent cells, the vitality of the adherent cells was increasing with higher peptide content and was highest for a ratio of 1/1 with 97% living cells (Figure 7B). Yet, overall survival

rates of the cells in all constructs after one week of cell culture were above 88% and thus very high.

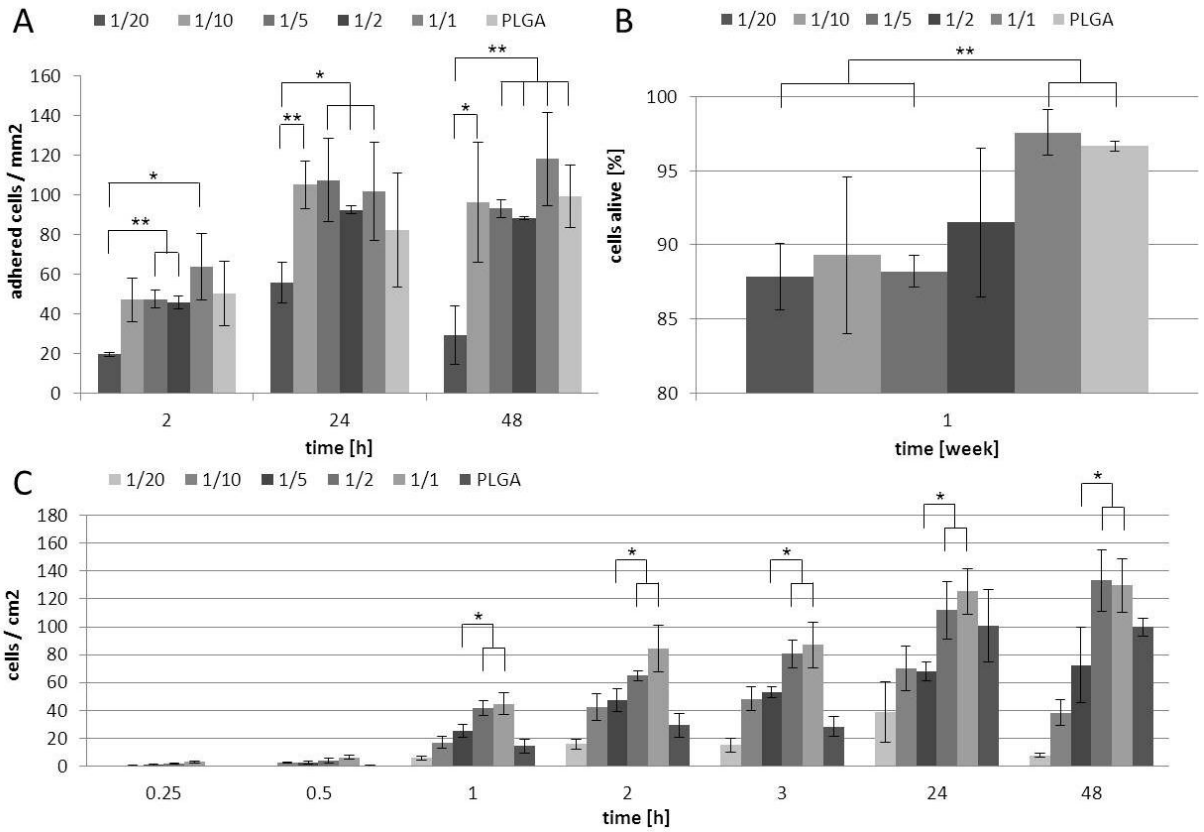

Figure 7: Quantification of HDF adhesion and vitality on fiber constructs.

Quantification of HDF adhesion was carried out on GRGDS functionalized PLGA/sP(EO-*stat*-PO) fibers with variation of peptide content (A, C) and quantification of the corresponding LIVE/DEAD® stainings (B) (* = < 0.05, ** = p < 0.01). Parts of image modified from reference [25] with permission from the Nature Publishing Group.

In a cell culture experiment conducted at a later time to determine cell adhesion kinetics, HDFs were seeded on fibers containing the same ratios of GRGDS to prepolymers and counted after 0.25, 0.5, 1, 2, 3, 24, and 48 h (Figure 7C). In this experiment, a minimum ligand concentration for strong cell adhesion that resisted medium suction was achieved with peptide to prepolymer ratios of 1/2. This higher value in comparison to the value of 1/10 in the earlier experiment was most likely due to the fiber diameters. Earlier experiments that revealed a minimum ratio of 1/10 were performed on fibers with an approximate diameter of 800 nm. Fibers, on which a GRGDS to prepolymer ratio of 1/2 was necessary, had an approximate diameter of 400 nm. A fiber scaffold covers a certain area dependent on the fiber diameter and the pore size of the scaffold. The thicker the fibers or the smaller the pore size, the more area is formed for contact with cells. In other words, a thick fiber provides more space for cell contact compared to a thin fiber. Therefore, on a mesh with thicker fibers, a lower ligand to prepolymer ratio was sufficient

for proper cell adhesion (Figure 7A). Nevertheless, the tendency of both cell adhesion kinetics was the same. A minimal ligand concentration was needed to achieve cell adhesion that was strong enough to resist forces applied during medium suction. The only difference lay in the threshold value.

Even though the focus in this Chapter lay on fibers functionalized with the peptide sequence GRGDS, some results are discussed to show the potential of these fiber constructs for functionalization with different cell adhesion mediating ligands. Due to the high concentration of isocyanate groups on the surface of freshly electrospun fibers, ligands containing e.g. amino groups can covalently bind to the fiber surface by simple incubation. Additionally, such ligands can be mixed with the PLGA/prepolymer solution prior to electrospinning thus resulting in fibers with covalently bound ligands presented at the surface of the fibers. The ECM protein FN exhibiting various amino groups at the surface was bound to fresh fibers using the incubation method. The mix-in method was not suitable for such a big ligand since the prepolymers in solution could bind to the amino groups distributed on the surface of the protein with their isocyanate groups, thus covering the protein with a cell repellent polymer layer leading to the covering of the cell adhesion mediating peptide sequence RGD and therefore preventing cell adhesion. Still, the functionalization via incubation successfully converted the inert fibers into cell adhesion mediating fibers (Figure 8A).

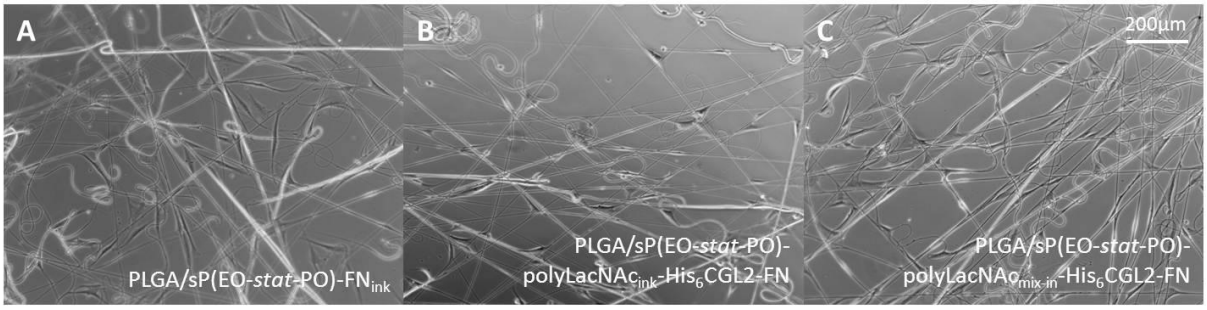

Figure 8: Fibers functionalized with FN and carbohydrates.

PLGA/sP(EO-stat-PO) fibers were functionalized by incubation of fresh fibers with FN (A) and polyLacNAc and subsequent incubation with the fungal galectin His_6CGL2 and FN (B). Additionally, polyLacNAc was mixed with the prepolymer solution before electrospinning with subsequent incubation of His_6CGL2 and FN. HDFs are shown after cultivation on fibers after 24 h.

The mimicry of the complex structures found in the natural ECM is a complex research field. In Chapter 9, a more biomimetic way to present FN on surfaces was introduced. This principle of sugar-lectin mediated presentation of FN was transferred from two-dimensional surfaces to PLGA/sP(EO-*stat*-PO) fibers. Therefore, the sugar polyLacNAc was covalently bound to

PLGA/sP(EO-*stat*-PO) fibers by incubation (Figure 8B) and by mixing the sugar with the prepolymer solution before electrospinning (Figure 8C). The fungal galectin His_6CGL2 and the protein FN were bound to this covalently immobilized sugar, leading to a non-covalent and flexible presentation of the protein. This non-covalent FN presentation on the three-dimensional scaffolds mediated HDF adhesion and spreading (Figure 8B, C). Fibers with incomplete layer build-up did not lead to cell adhesion (results not shown) confirming the results of two-dimensional studies.

To confirm applicability of the fiber scaffolds to other cell types, experiments with MSCs have been carried out on GRGDS modified PLGA/sP(EO-*stat*-PO) fibers (1/1) (Figure 9). MSCs are found e.g. in bone marrow and can differentiate into different lineages such as bone, muscle, tendon, or cartilage [29, 30]. Due to their multi-lineage potential and autologous source they are appropriate candidates for tissue engineering applications [31]. These cells behaved very similarly to HDFs on the fibers. After 2 h, cells only became adherent on the PLGA/sP(EO-*stat*-PO)-GRGDS fibers, indicating a faster adhesion kinetic of these cells on the peptide modified specifically interacting fibers in comparison to the fibers prepared from pure PLGA (Figure 9A, G). However, after 24 hours, MSCs adhered and formed a confluent cell layer both on the PLGA/sP(EO-*stat*-PO)-GRGDS (Figure 9H) and on the PLGA fiber constructs (Figure 9B). Although the stem cells did not adhere on the sP(EO-*stat*-PO) surface of the substrate the fibers were spun onto, some of them managed to punctually adhere to PLGA/sP(EO-*stat*-PO) (Figure 9C, D) and to PLGA/sP(EO-*stat*-PO)-GRGES fibers (Figure 9E, F) without the ability to fully spread. Additionally, counting of adherent cells on the different fiber constructs after 24 h revealed significantly higher numbers of adherent cells on PLGA fibers and GRGDS functionalized fibers compared to PLGA/sP(EO-*stat*-PO) fibers or GRGES functionalized fibers (Figure 9I). HDFs did not adhere on these fibers at all, indicating a basically similar but more complex behavior of the MSCs in comparison to the HDFs.

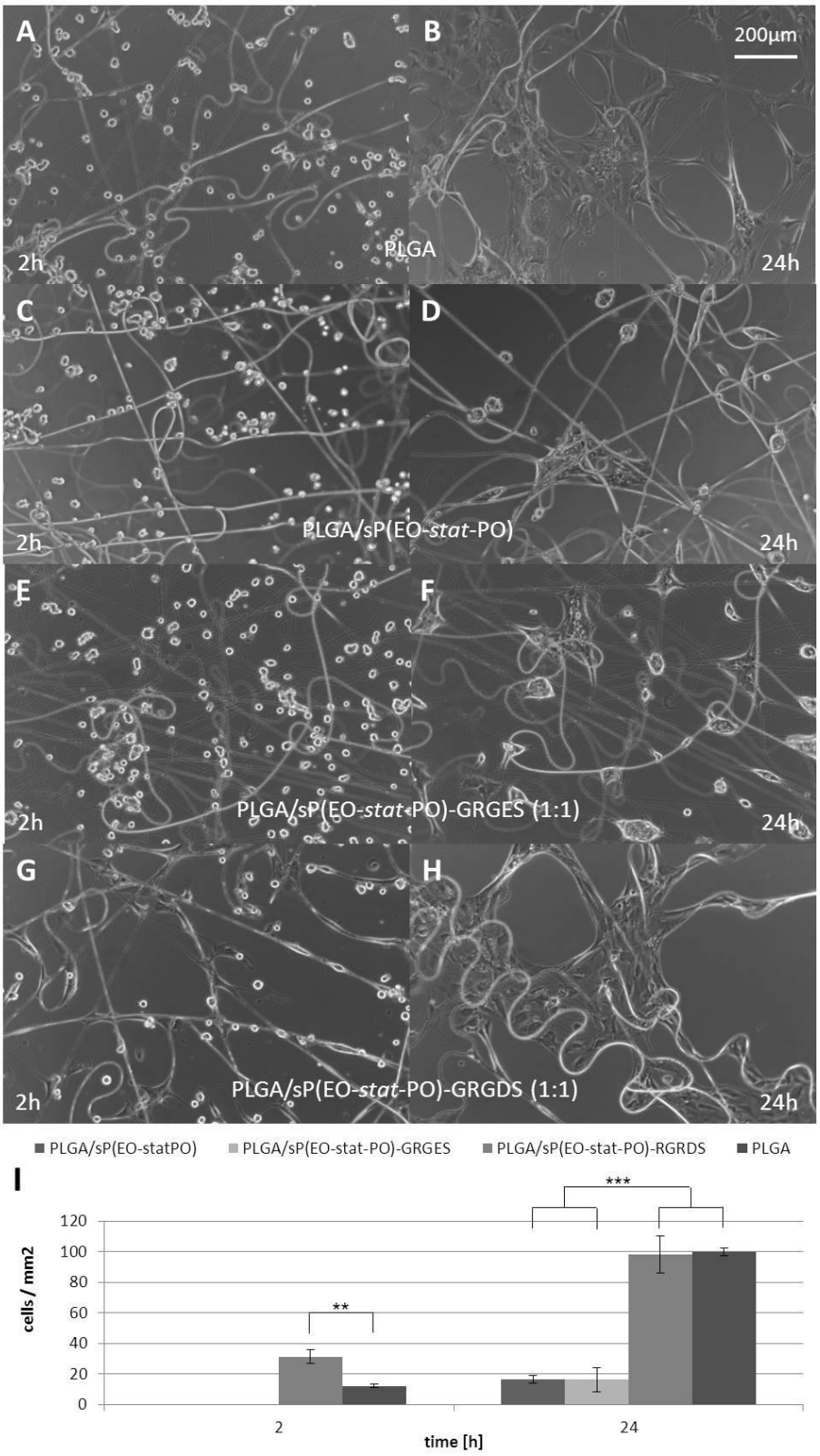

Figure 9: MSC adhesion on fiber constructs.

MSCs were cultured for 2 h (A, C, E, G) and 24 h (B, D, F, H) on PLGA (A, B), PLGA/sP(EO-*stat*-PO) (C, D), PLGA/sP(EO-*stat*-PO)-GRGES (1/1) (E, F) and PLGA/sP(EO-*stat*-PO)-GRGDS (1/1) (G, H) fibers. Quantification of MSC adhesion was carried out on the same fiber constructs after 24 h (I). (** = $p < 0.01$, *** = $p < 0.001$). Parts of image modified from reference [25] with permission from the Nature Publishing Group.

4. Conclusions

The electrospinning of common biomedical polyesters was advanced with a one-step preparation of fully degradable bioactivated fiber meshes with controlled surface chemistry and functionality. By using the multifunctional amphiphilic macromolecular additive NCO-sP(EO-*stat*-PO) and functionalizing these scaffolds with cell adhesion mediating ligands led to specific cell-material interactions while reducing protein adsorption. The hydrophilic PLGA/sP(EO-*stat*-PO) fibers significantly reduced non-specific protein adsorption compared to pure PLGA fibers, prevented cell adhesion of HDFs, and significantly reduced cell adhesion of MSCs. To allow specific cell adhesion to such cell repulsive hydrogel coated fibers, the peptide GRGDS and the protein FN were covalently immobilized on the fibers' surface and could be quantified by ELISA. As negative control, GRGES peptides were attached to the fibers. While the suppression of non-specific protein adsorption was preserved for fibers modified with either of the peptides, only the GRGDS functionalized fibers allowed strong adhesion of HDFs as well as MSCs, allowing spreading and proliferation of the cells, building a confluent cell layer on the fibers after two weeks. LIVE/DEAD® stainings proved vitality of the cells. Additionally, FN was directly immobilized on the fibers as well as presented via sugar-lectin mediated binding, in both cases introducing HDF adhesion.

These fiber scaffolds need to be further characterized and ligand distances on the fibers need to be determined to understand cell responses on these constructs and even on fibrous scaffolds in general. Surface sensitive quantification methods such as SPR and SAW can only be used for ultraflat model films on gold. Here, surface sensitive quantification methods like ELISA need to be used for such three-dimensional biomaterials. Calculation of exact amounts of ligands and calculation of ligand distances would be possible by comparison with radiolabeling experiments described for two-dimensional materials in Chapters 8 for two-dimensional substrates.

With these fibers, systematic variation of specifically bioactivated fiber scaffolds can be achieved. A multitude of cellular responses to the scaffolds can be triggered, and this feasibility of constructing complex sets of cellular interactions with synthetic fibers is an important step towards biomimetic *in vitro* cell culture systems and specifically interacting tissue engineering scaffolds. This approach will enable the layered construction of bipolar membranes for *in vitro* co-culture systems and more complex artificial basal membranes.

5. References

1. Pham, Q.P.; Sharma, U. and Mikos, A.G. Electrospinning of polymeric nanofibers for tissue engineering applications: A review. *Tissue Engineering* **2006**, 12 (5) 1197-211.
2. Hutmacher, D.W. Scaffolds in tissue engineering bone and cartilage. *Biomaterials* **2000**, 21 (24) 2529-43.
3. Ratner, B.D. and Bryant, S.J. Biomaterials: Where we have been and where we are going. *Annual Review of Biomedical Engineering* **2004**, 6 (1) 41-75.
4. Hollister, S.J. Porous scaffold design for tissue engineering. *Nature Materials* **2005**, 4 (7) 518-24.
5. Stevens, M.M. and George, J.H. Exploring and engineering the cell surface interface. *Science* **2005**, 310 (5751) 1135-38.
6. Bearinger, J.P.; Terrettaz, S.; Michel, R.; Tirelli, N.; Vogel, H.; Textor, M. and Hubbell, J.A. Chemisorbed poly(propylene sulphide)-based copolymers resist biomolecular interactions. *Nature Materials* **2003**, 2 (4) 259-64.
7. Nie, Z.H. and Kumacheva, E. Patterning surfaces with functional polymers. *Nature Materials* **2008**, 7 (4) 277-90.
8. Huang, Z.M.; Zhang, Y.Z.; Kotaki, M. and Ramakrishna, S. A review on polymer nanofibers by electrospinning and their applications in nanocomposites. *Composites Science and Technology* **2003**, 63 (15) 2223-53.
9. Greiner, A. and Wendorff, J.H. Electrospinning: A fascinating method for the preparation of ultrathin fibres. *Angewandte Chemie-International Edition* **2007**, 46 (30) 5670-703.
10. Lee, J.; Cuddihy, M.J. and Kotov, N.A. Three-dimensional cell culture matrices: State of the art. *Tissue Engineering Part B-Reviews* **2008**, 14 (1) 61-86.
11. Ma, Z.W.; Gao, C.Y.; Ji, J.A. and Shen, J.C. Protein immobilization on the surface of poly-L-lactic acid films for improvement of cellular interactions. *European Polymer Journal* **2002**, 38 (11) 2279-84.
12. Steffens, G.C.M.; Nothdurft, L.; Buse, G.; Thissen, H.; Hocker, H. and Klee, D. High density binding of proteins and peptides to poly(D,L-lactide) grafted with polyacrylic acid. *Biomaterials* **2002**, 23 (16) 3523-31.
13. Ma, Z.; Gao, C.; Yuan, J.; Ji, J.; Gong, Y. and Shen, J. Surface modification of poly-L-lactide by photografting of hydrophilic polymers towards improving its hydrophilicity. *Journal of Applied Polymer Science* **2002**, 85 (10) 2163-71.
14. Patel, S.; Kurpinski, K.; Quigley, R.; Gao, H.F.; Hsiao, B.S.; Poo, M.M. and Li, S. Bioactive nanofibers: Synergistic effects of nanotopography and chemical signaling on cell guidance. *Nano Letters* **2007**, 7 (7) 2122-28.
15. Kim, T.G. and Park, T.G. Surface functionalized electrospun biodegradable nanofibers for immobilization of bioactive molecules. *Biotechnology Progress* **2006**, 22 (4) 1108-13.
16. Dobrovolskaia, M.A. and McNeil, S.E. Immunological properties of engineered nanomaterials. *Nature Nanotechnology* **2007**, 2 (8) 469-78.
17. Gasteier, P.; Reska, A.; Schulte, P.; Salber, J.; Offenhausser, A.; Moeller, M. and Groll, J. Surface grafting of PEO-Based star-shaped molecules for bioanalytical and biomedical applications. *Macromolecular Bioscience* **2007**, 7 (8) 1010-23.

18. Grafahrend, D.; Calvet, J.L.; Klinkhammer, K.; Salber, J.; Dalton, P.D.; Moller, M. and Klee, D. Control of protein adsorption on functionalized electrospun fibers. *Biotechnology and Bioengineering* **2008**, 101 (3) 609-21.

19. Dankers, P.Y.W.; Harmsen, M.C.; Brouwer, L.A.; Van Luyn, M.J.A. and Meijer, E.W. A modular and supramolecular approach to bioactive scaffolds for tissue engineering. *Nature Materials* **2005**, 4 (7) 568-74.

20. Gotz, H.; Beginn, U.; Bartelink, C.F.; Grunbauer, H.J.M. and Moller, M. Preparation of isophorone diisocyanate terminated star polyethers. *Macromolecular Materials and Engineering* **2002**, 287 (4) 223-30.

21. Groll, J.; Ameringer, T.; Spatz, J.P. and Moeller, M. Ultrathin coatings from isocyanate-terminated star PEG prepolymers: Layer formation and characterization. *Langmuir* **2005**, 21 (5) 1991-99.

22. Rech, C.; Rosencrantz, R.R.; Křenek, K.; Pelantová, H.; Bojarová, P.; Römer, C.; Hanisch, F.-G.; Křen, V. and Elling, L. Combinatorial one-pot synthesis of poly-N-acetyllactosamine oligosaccharides with leloir-glycosyltransferases. *Advanced Synthesis and Catalysis* **2011**, 353 2492-500.

23. Sauerzapfe, B.; Krenek, K.; Schmiedel, J.; Wakarchuk, W.W.; Pelantova, H.; Kren, V. and Elling, L. Chemo-enzymatic synthesis of poly-N-acetyllactosamine (poly-LacNAc) structures and their characterization for CGL2-galectin-mediated binding of ECM glycoproteins to biomaterial surfaces. *Glycoconjugate Journal* **2009**, 26 (2) 141-59.

24. Dominici, M.; Le Blanc, K.; Mueller, I.; Slaper-Cortenbach, I.; Marini, F.; Krause, D.; Deans, R.; Keating, A.; Prockop, D. and Horwitz, E. Minimal criteria for defining multipotent mesenchymal stromal cells. The International Society for Cellular Therapy position statement. *Cytotherapy* **2006**, 8 (4) 315-17.

25. Grafahrend, D.; Heffels, K.-H.; Beer, M.V.; Gasteier, P.; Möller, M.; Boehm, G.; Dalton, P.D. and Groll, J. Degradable polyester scaffolds with controlled surface chemistry combining minimal protein adsorption with specific bioactivation. *Nat Mater* **2011**, 10 (1) 67-73.

26. Khang, G.; Choee, J.H.; Rhee, J.M. and Lee, H.B. Interaction of different types of cells on physicochemically treated poly(L-lactide-co-glycolide) surfaces. *Journal of Applied Polymer Science* **2002**, 85 (6) 1253-62.

27. Groll, J.; Fiedler, J.; Engelhard, E.; Ameringer, T.; Tugulu, S.; Klok, H.A.; Brenner, R.E. and Moeller, M. A novel star PEG-derived surface coating for specific cell adhesion. *Journal of Biomedical Materials Research Part A* **2005**, 74A (4) 607-17.

28. Hersel, U.; Dahmen, C. and Kessler, H. RGD modified polymers: biomaterials for stimulated cell adhesion and beyond. *Biomaterials* **2003**, 24 (24) 4385-415.

29. Prockop, D.J. Marrow stromal cells as steam cells for nonhematopoietic tissues. *Science* **1997**, 276 (5309) 71-74.

30. Pittenger, M.F.; Mackay, A.M.; Beck, S.C.; Jaiswal, R.K.; Douglas, R.; Mosca, J.D.; Moorman, M.A.; Simonetti, D.W.; Craig, S. and Marshak, D.R. Multilineage potential of adult human mesenchymal stem cells. *Science* **1999**, 284 (5411) 143-47.

31. Li, W.J.; Tuli, R.; Huang, X.X.; Laquerriere, P. and Tuan, R.S. Multilineage differentiation of human mesenchymal stem cells in a three-dimensional nanofibrous scaffold. *Biomaterials* **2005**, 26 (25) 5158-66.

Summary

This thesis concerned the quantification of cell adhesion molecules (CAM) in and on thin hydrogel films as surface modification of biomaterials. The established and well characterized, per se inert NCO-sP(EO-*stat*-PO) hydrogel system which allows the easy and reproducible bioactivation with peptides was used as basis for this thesis. Two methods can be used to functionalize the coatings. Ligands can either be mixed into the prepolymer solution in prior to layer formation (mix-in method), or freshly prepared coatings can be incubated with ligand solution (incubation method). Divided into three major parts, the first part of the thesis dealt with the concentration of ligands in the bulk hydrogel, whereas the second part of the thesis focused on the surface sensitive quantification of CAMs at the biointerface. The results were correlated with cell adhesion kinetics. The third part of this thesis investigated the biochemical and the structural mimicry of the extracellular matrix (ECM). ECM proteins were presented via sugar-lectin mediated binding and cell behavior on these surfaces was analyzed. Cell behavior on three-dimensional fibers with identical surface chemistry as the coatings in the previous sections of the thesis was analyzed and correlated with the amount of peptide used for bioactivation. Overall, the main question of this work was '**How much**?' regarding **maximal** as well as **optimal** ligand concentrations for controlled cell-hydrogel interactions.

The focus in the first practical part of this thesis was to analyze the amount of ligands in NCO-sP(EO-*stat*-PO) hydrogels using ***classical quantification*** methods. Coatings in 96-well plates as well as on glass were functionalized with GRGDS and ^{125}I-YRGDS for radioisotopic detection (**Chapter 3**). Using the incubation method for functionalization, a maximal ligand binding using peptide concentrations of 600 µg/mL could be determined. When functionalization was introduced via the mix-in method, a clear tendency for higher ligand concentrations with increasing ligand to prepolymer ratio was observed, but no maximal ligand binding could be detected with a ligand to prepolymer ratio of 2/1 being the highest ratio investigated. This ratio of 2/1 was not exceeded to ensure that complete crosslinking of the hydrogel was not affected. In **Chapter 4**, a fluorinated amino acid and an iodinated peptide were immobilized to the hydrogels using the mix-in method and were detected by X-ray photoelectron spectroscopy (XPS) and time-of-flight secondary ion mass spectrometry (TOF-SIMS). In these measurements, maximal ligand binding was detected for a ligand to prepolymer ratio of 1/1. Higher ligand to prepolymer ratios did not result in any significant increase in ligand concentrations in the surface near regions of the crosslinked hydrogels.

To address the question of how many ligands were actually accessible for cell interaction at the interface, ***surface sensitive quantification*** methods were applied in the second part of this thesis. For the quantification with surface plasmon resonance (SPR) and surface acoustic wave technology (SAW) (**Chapter 5**), the hydrogel coating procedure needed to be transferred onto cystamine functionalized gold surfaces. Characterization with ellipsometry and atomic force microscopy (AFM) revealed inhomogeneous cystamine binding to the activated surfaces, which resulted in inhomogeneous coatings. Nevertheless, it could be shown that SPR as well as SAW were suitable methods for the surface sensitive quantification of the ligand concentration on NCO-sP(EO-*stat*-PO) hydrogels. Non-functionalized coatings resisted non-specific serum as well as streptavidin (SA) adsorption. Coatings functionalized with biocytin and GRGDSK-biotin introduced specific SA binding that was dependent on the biotin concentration at the surface. Additionally, enzyme linked immunosorbent assay (ELISA) and enzyme linked lectin assay (ELLA) (**Chapter 6**) were applied to coatings in 96-well plates and on glass. Coatings were functionalized with the model molecule biocytin, the biotinylated peptide GRGDSK-biotin, the ECM protein fibronectin (FN), as well as the carbohydrates N-acetylglucosamine (GlcNAc) and N-acetyllactosamine (LacNAc). All ligands could be successfully detected with antibodies or SA via ELISA or ELLA. Maximal GRGDSK-biotin binding to the hydrogel coatings on glass was achieved at a peptide to prepolymer ratio of 1/5, which was used as reference value in Chapter 8. Last but not least, cell adhesion (**Chapter 7**) was quantified depending on the GRGDS concentration on hydrogel coatings on glass. Maximal adhesion of primary human dermal fibroblast (HDF) was observed at GRGDS to prepolymer ratios of 1/5, when adherent cells were counted on life cell images. Quantification of adherent cells using the CASY® cell counter revealed maximal HDF adhesion at molar ligand to prepolymer ratios of 1/2. However, cell vitality detected by intracellular enzyme activities was not dependent on the GRGDS concentration. Cells which managed to adhere were vital regardless of the amount of ligands present. Additionally, adhesion of fibroblasts from the murine cell line NIH L929 was analyzed by counting on life cell images. These cells, being much smaller than the HDF cells, needed higher GRGDS to prepolymer ratios (2/1) for proper cell adhesion.

All quantification methods applied to analyze hydrogels which were functionalized by the mix-in method in Chapter 3, 4, 6 and 7, were compared in **Chapter 8**. Radiodetection gave information about the ligand concentrations throughout the whole hydrogel and no maximal amount of ligands could be detected when increasing the peptide to prepolymer ratio. In contrast, XPS and TOF-SIMS which only penetrated the surface near regions of the coating, a maximal ligand binding to the hydrogel was detected for 1/1 ratios. SPR and SAW were not included in this comparison, as the coatings on gold need to be optimized first. The two surface sensitive quantification methods (ELISA and HDF adhesion) could give information about the quantity of peptide which was sterically available for SA or cell binding. With these methods, maximal SA and cell binding was detected at ratios of 1/5. These results underline the importance of carefully compare the different methods.

Beside ligand quantification on hydrogels, the third part of this thesis was concerned with the biochemical and structural mimicry of the ECM by ***advanced ECM engineering*** to design biomimetic biomaterials that are better accepted by cells and tissue. The subject of **Chapter 9** was the biomimetic and flexible presentation of the ECM protein FN. FN was attached via sugar-lectin mediated binding to NCO-sP(EO-*stat*-PO) hydrogels. The build-up of the covalently immobilized sugar poly-N-acetyllactosamine (polyLacNAc), the subsequent non-covalent binding of the fungal galectin His_6CGL2, and FN could be elegantly proven by fluorescent staining on coatings which were functionalized with the sugar by micro contact printing (MCP). Further experiments were carried out on build-ups, where polyLacNAc was immobilized on the hydrogel by incubation. Optimal parameters for the layer build-up were determined by ELLA/ELISA. Only the complete build-up induced proper adhesion of HDFs. Compared to tissue culture polystyrene (TCPS), cells adhered and spread faster on the biomimetic surfaces. The flexible presentation of FN allowed HDFs to rearrange homogenously immobilized FN into fibrillar structures, which seemed not to be possible when FN was adsorbed on glass or covalently bound directly to the hydrogel coatings. This new approach of a flexible and biomimetic presentation of an ECM protein allows new ways to design biomaterials with best possible cell-material interactions.

The work described in **Chapter 10** focused on the structural mimicry of the fibrous ECM structures by electrospinning of synthetic, bioactive, and degradable fibers. Poly(D,L-lactide-*co*-glycolide) (PLGA) and NCO-sP(EO-*stat*-PO) were electrospun out of one solution in an easy one-step preparation resulting in fibers with an ultrathin inert hydrogel layer at the surface. By adding GRGDS to the solution prior to electrospinning, specifically interacting fibers could be obtained. In comparison to PLGA, the adsorption of bovine serum albumin (BSA) could be reduced by 99.2%. As a control, the non-active peptide GRGES was immobilized to the fiber. These fibers did not allow cell adhesion, showing that the integrity of the hydrogel coated fibers was not affected by the immobilization of peptides. HDF adhesion was obtained by functionalization with GRGDS, leading to the adhesion, spreading, and proliferation of HDFs. Also mesenchymal stem cells (MSC) could adhere to GRGDS functionalized fibers. Additionally, for ligand quantification, the ELISA technique was successfully transferred to fiber substrates. To highlight the potential of the approaches for the biochemical and structural mimicry of the ECM, the sugar polyLacNAc was immobilized on the PLGA/sP(EO-*stat*-PO) fibers followed by the subsequent layer build-up with His_6CGL2 and FN. These fibers triggered HDF adhesion.

Zusammenfassung

Diese Arbeit beschäftigte sich mit der Quantifizierung von Zelladhäsion vermittelnden Liganden in und auf dünnen Hydrogelschichten, die zur Oberflächenmodifizierung auf Biomaterialien aufgebracht wurden. Das bereits etablierte und gut charakterisierte inerte NCO-sP(EO-*stat*-PO) Hydrogelsystem, das eine einfache und reproduzierbare Bioaktivierung mit Peptiden erlaubt, wurde als Basis für diese Arbeit verwendet. Diese Hydrogele können auf zwei Weisen funktionalisiert werden. Liganden können entweder mit der Prepolymerlösung vor der Beschichtung gemischt (Einmischmethode) oder frische Hydrogelschichten mit einer Ligandenlösung inkubiert werden (Inkubationsmethode). Der erste Teil dieser in drei Hauptteile unterteilten Arbeit, beschäftigte sich mit der Konzentrationsbestimmung der Liganden in der gesamten Tiefe der Hydrogelschicht, während sich der zweite Teil auf die oberflächensensitive Quantifizierung von Zelladhäsion vermittelnden Molekülen an der biologischen Grenzfläche konzentrierte. Die Ergebnisse wurden mit Zelladhäsionskinetiken verglichen. Der dritte Teil dieser Arbeit beschäftigte sich mit der biochemischen als auch strukturellen Nachahmung der komplexen Extrazellulärmatrix (ECM). Das ECM Protein Fibronektin (FN) wurde über Zucker-Lektin Anbindung präsentiert und Zellverhalten auf diesen biomimetischen Oberflächen untersucht. Ebenfalls wurde Zellverhalten in einer dreidimensionalen Faserumgebung mit identischer Oberflächenchemie wie in den beiden ersten Teilen dieser Arbeit untersucht und mit der Peptidkonzentration korreliert. Insgesamt, war die Hauptfragestellung in dieser Arbeit '**Wie viel?**', d.h. einerseits die Ermittlung der **maximalen**, als auch der für Zelladhäsion **optimalen** Ligandendichte.

Im ersten praktischen Teil der vorliegenden Arbeit (***Klassische Quantifizierung***) wurden Liganden in der gesamten Hydrogelschicht, als auch speziell in oberen Bereichen der Schichten quantifiziert. Die Untersuchung der Hydrogelschichten in Wellplatten und auf Glas funktionalisiert mit GRGDS und ^{125}I-YRGDS erfolgte in **Kapitel 3** mittels Radioaktivmessung. Wurden Hydrogelschichten mittels Inkubationsmethode funktionalisiert, konnte eine Sättigung mit Liganden bei etwa 600 µg/mL ermittelt werden. Mittels Einmischmethode funktionalisierte Hydrogele erreichten keine maximale Ligandenkonzentration in den Schichten, mit dem Verhältnis 2/1 als maximales verwendetes Verhältnis. Höhere Liganden zu Prepolymer Verhältnisse als 2/1 wurden jedoch nicht verwendet, um eine ausreichende Vernetzung der Hydrogele nicht zu gefährden. Zur Detektion mittels Röntgenphotoelektronenspektroskopie (XPS) und Flugzeit-Sekundärionen-Massenspektrometrie (TOF-SIMS) (**Kapitel 4**) wurden eine fluorierte Aminosäure und ein iodiertes Peptid mit den Prepolymeren in molaren Verhältnissen

von 1/2, 1/1 und 2/1 gemischt. Beide Methoden ermittelten eine maximale Ligandenkonzentration bei Verhältnissen von 1/1. Zusätzliche Liganden (2/1) führten zu keiner vermehrten Anbindung.

Wesentlich im Zusammenhang mit der Ligandenquantifizierung auf Biomaterialien ist, diese an der Oberfläche, die für Zellen zugänglich ist, durchzuführen. Im zweiten Teil dieser Arbeit (***Oberflächensensitive Quantifizierung***) kamen daher Methoden zum Einsatz, die Liganden ausschließlich auf der Oberfläche quantifizierten. Zur Detektion mit Oberflächenplasmonresonanz (SPR) und akustischer Oberflächenwellentechnologie (SAW) in **Kapitel 5** musste die Standardbeschichtung der Hydrogele von Glas und Silikon auf Cystamin funktionalisierte Goldoberflächen übertragen werden. Mittels Ellipsometrie und Rasterkraftmikroskopie (AFM) konnte nur eine dünne und inhomogene Hydrogelbeschichtung nachgewiesen werden. Dennoch zeigten SPR und SAW die Unterbindung von Serum und Streptavidin (SA) Adsorption auf nicht funktionalisierten Schichten, jedoch eine spezifische und konzentrationsabhängige SA Bindung auf Hydrogelschichten, die mit Biocytin und GRGDSK-biotin funktionalisiert wurden. Die Ligandenquantifizierung mittels Enzymgekoppeltem Immunadsorptionstest (ELISA) und Enzymgekoppelten Lektinadsorptionstest (ELLA) (**Kapitel 6**) wurde auf Hydrogelschichten in Wellplatten und auf Glas angewendet, die mit verschiedenen Liganden mittels Inkubation und Einmischung funktionalisiert wurden. Das Modellmolekül Biocytin, das biotinylierte Peptid GRGDSK-biotin, das ECM Protein Fibronektin (FN), als auch die Modellzucker N-Acetylglukosamin (GlcNAc) und N-Acetyllaktosamin (LacNAc) konnten spezifisch in verschiedenen Konzentrationen nachgewiesen werden. Beispielhaft seien hier Schichten auf Glas genannt, die mittels Einmischmethode mit GRGDSK-biotin funktionalisiert wurden, da diese zum Vergleich in Kapitel 8 herangezogen wurden. Auf diesen Oberflächen wurde eine maximale Peptidkonzentration auf der Oberfläche bei einem Peptid zu Prepolymer Verhältnis von 1/5 ermittelt. Neben diesen verschiedenen Quantifzierungsmethoden ist die *in vitro* Analyse mit Zellen nicht zu vernachlässigen (**Kapitel 7**). Hierzu wurden Hydrogele auf Glas aufgebracht und mit GRGDS mittels Einmischmethode funktionalisiert. Durch Zählen adhärenter primärer humaner dermaler Fibroblasten (HDF) auf Mikroskopbildern wurde eine maximale Zelladhäsion bei dem Peptid zu Prepolymer Verhältnis von 1/5 festgestellt. Hingegen wurde ein Verhältnis von 1/2 für optimale Zelladhäsion ermittelt, wenn Zellen zur Quantifizierung von den Hydrogelen abgelöst und im CASY® Zellzähler quantifiziert wurden. Zusätzlich wurde die Zellvitalität durch Messung intrazellulärer Enzymaktivitäten gemessen, jedoch konnte kein Zusammenhang zwischen Zellvitalität und GRGDS Konzentration hergestellt werden. Adhärente HDFs waren in allen Fällen vital, unabhängig von der Ligandenkonzentration auf der Oberfläche.

Auch die Mausfibroblasten Zelllinie NIH L929 wurde auf Hydrogelen mit verschiedenen GRGDS zu Prepolymer Verhältnissen durch Zählen adhärenter Zellen auf Mikroskopbildern untersucht. Diese im Verhältnis zu HDFs wesentlich kleineren Mauszellen benötigten höhere GRGDS Konzentrationen (2/1) für maximale Zelladhäsion.

Nach der Ligandenquantifizierung in Kapitel 3 bis 7, wurden diese Ergebnisse in **Kapitel 8** miteinander verglichen. Hierzu wurden Messungen auf Hydrogelschichten verwendet, die mittels Einmischmethode funktionalisiert wurden. Während die Quantifizierung mittels Radioaktivmessung in der gesamten Tiefe der Hydrogelschichten keine maximale Ligandenkonzentration ermitteln konnte, war in den oberen Bereichen der Schicht ein Maximum an Liganden bei 1/1 festzustellen (XPS, TOF-SIMS). SPR und SAW wurden zum Vergleich nicht herangezogen, da die Beschichtung auf Gold erst optimiert werden muss. Oberflächensensitive Quantifizierung mittels ELISA und Zelladhäsion, die lediglich die sterisch zugänglichen Liganden auf einer Oberfläche nachweisen, ergaben übereinstimmend eine optimale Ligandenkonzentration für SA Bindung und Zelladhäsion bei einem Peptid zu Prepolymer Verhältnis von 1/5. Dies unterstreicht, wie wichtig der Vergleich der Methoden, als auch die Verwendung von oberflächensensitiven Methoden ist.

Der dritten Teil dieser Arbeit beschäftigte sich mit der biochemischen und strukturellen Nachahmung der komplexen extrazellulären Umgebung (***Advanced ECM engineering***), ein wichtiger Aspekt in der Biomaterialforschung, da zum größten Teil zwei-dimensionale Biomaterialien zum Einsatz kommen, die direkt mit Liganden kovalent funktionalisiert werden. Die ECM ist jedoch um ein Vielfaches komplexer und die bestmögliche Nachahmung ist Voraussetzung für eine bessere Akzeptanz durch Zellen und Gewebe. In **Kapitel 9** wurde eine Möglichkeit aufgezeigt, das ECM Protein FN nicht-kovalent über Zucker-Lektinbindungen zu immobilisieren. Ein Schichtaufbau von Hydrogel, dem darauf durch Mikrokontakt-druckverfahren (MCP) kovalent gebundenen Zucker Poly-N-Acetyllaktosamin (polyLacNAc) und den darauf nicht-kovalent gebundenen Galektin His_6CGL2 und FN, konnte mit Fluoreszenzfärbung elegant nachgewiesen werden. Optimale Konzentrationen für den Schichtaufbau wurden mittels ELLA/ELISA auf Hydrogelschichten ermittelt, die durch Inkubation mit dem Zucker funktionalisiert wurden. Nur der komplette Schichtaufbau konnte zufriedenstellende HDF Adhäsion vermitteln und im Vergleich zu Zellkulturpolystyrol (TCPS) Oberflächen konnten HDFs auf dem biomimetischen Schichtaufbau schneller adhärieren und spreiten. Zudem wurde die Umorganisierung von auf Glas adsorbiertem FN, auf NCO-sP(EO-*stat*-PO) kovalent gebundenem FN und biomimetisch über polyLAcNAc-His_6CGL2 gebundenem

FN durch HDFs verglichen. Nur auf den biomimetischen Oberflächen schien eine Umorganisation durch die Zellen möglich, wie sie auch in der ECM zu finden ist. Diese biomimetische und flexible Präsentation eines Proteins erwies sich als vielversprechende Möglichkeit eine biomimetischere Oberfläche für Zellen zu schaffen, die eine optimale Biokompatibilität ermöglichen könnte.

Auch die strukturelle Nachahmung der ECM ist eine vielversprechende Strategie zum Nachbau der ECM. In **Kapitel 10** wurde ein Einschrittverfahren zur Herstellung synthetischer, bioaktiver und degradierbarer Faserkonstrukte durch Elektrospinnen zur Nachahmung der ECM präsentiert. In diesem System wurden durch Zugabe von NCO-sP(EO-*stat*-PO) als reaktives Additiv zu Poly(D,L-laktid-*co*-Glycolid) (PLGA) Fasern hergestellt, die mit einer ultradünnen, inerten Hydrogelschicht versehen waren. Es konnte gezeigt werden, dass durch die Verwendung von NCO-sP(EO-*stat*-PO) als Additiv die Adsorption von Rinderserumalbumin (BSA) im Vergleich zu PLGA um 99,2% reduziert, die Adhäsion von HDFs verhindert und die Adhäsion von humanen mesenchymalen Stammzellen (MSC) minimiert werden konnten. Spezifische Bioaktivierung wurde durch Zugabe von Peptidsequenzen zur Spinlösung erreicht, welche kovalent in die Hydrogelschicht eingebunden werden konnten und kontrollierte Zell-Faser Interaktionen ermöglichten, Um die spezifische Zelladhäsion an solchen inerten Fasern zu erzielen, wurde GRGDS kovalent auf der Faseroberfläche gebunden. Dies erfolgte durch Zugabe des Peptids zur Polymerlösung vor dem Elektrospinnen. Als Negativkontrolle wurde die Peptidsequenz GRGES an die Faseroberfläche gebunden, welche durch Zellen nicht erkannt wird. Während die Verhinderung unspezifischer Proteinadsorption für die Peptidmodifizierten Fasern erhalten blieb, konnten HDFs lediglich auf den mit GRGDS Peptid modifizierten Fasern adhärieren, proliferieren und nach zwei Wochen eine konfluente Zellschicht aus vitalen Zellen bilden. Zusätzlich konnten MSCs auf GRGDS funktionalisierten Fasern adhärieren. Liganden konnten auf Fasern quantifiziert werden, indem die ELISA Technik aus Kapitel 6 auf Faseroberflächen transferiert wurde. Um das Potential der biochemischen und strukturellen Nachbildung der ECM aufzuzeigen, wurden beide Ansätze miteinander kombiniert. Die Immobilisierung von polyLacNAc auf die Hydrogelfasern durch Inkubation und der Schichtaufbau mit His_6CGL2 und FN resultierte in HDF Adhäsion.

Acknowledgement

„Auch ist das Suchen und Irren gut, denn durch Suchen und Irren lernt man.“ - Johann Wolfgang von Goethe –

Johann Wolfgang von Goethe once said that you learn by searching and mistaking. During my Ph.D. work I was searching a lot to find the answers I was looking for. Here, I want to thank all the people who helped me to stay focused and motivated during my search and to take the right turns to find the answers. I am truly thankful!

First of all, my gratitude goes to Prof. Jürgen Groll for giving me the opportunity to work on this interesting research study, for being an ever open door for all my concerns, for having fruitful discussions, and giving me the chance to present my work at international conferences. Thank you, I learned so much!

I want to thank Prof. Lothar Elling for the cooperation and for being my co-corrector. Prof. Martin Möller, thank you for the time I could spend at DWI in Aachen. Thank you very much Claudia Rech for discussions and good working atmosphere in our cooperation. Dr. Jochen Salber, I thank you for fascinating me working with cell cultures and biomaterials during my master thesis. I thank Dr. Alex Shard (National Physical Laboratory) for XPS and TOF-SIMS measurements and PD Marlies Fabry and Stephan Rütten for all the with radioactive experiments. I acknowledge Miguel Jimenez and Michaela Stumbaum from SAW Instruments for advice and SAW measurements. Dr. Andrea Ewald, thank you for the warm welcome and help in the cell culture laboratories in Würzburg. For providing human fibroblasts, I would like to thank PD Sabine Neuß-Stein and Prof. Jens Malte Baron (University hospital RWTH Aachen). Clemens Liedel and Marco Schürings, thank you for AFM measurements. Thanks to the group of Prof. Offenhäuser (FZ Jülich) for SPR equipment. Especially, Dr. Kristin Michael, thank you for discussions and help. May you rest in peace.

Thanks to all members of ‘AG Groll’ in Aachen and Würzburg and DWI members for cooperation, discussions, coffees, and lunch breaks. Especially Antje and Vera! All best wishes to Kalle and thanks for all the fibers and mathematic help! Thank you Sylvia and Kathrin for the interest in my research and your organized and motivated work during your thesis! Smriti, thanks for your PG synthesis! Sabrina, thanks for the detailed review of my manuscript! Sarah and Yesmin, thank you for your time joining the lab with me! Last but not least, Vera, I had a great time with you in the lab and I will always have great memories of our USA conference trips!

Danke Magdalena und Lukas für eure Design und IT Unterstützung! Sandra, danke für viele Stunden voller Reiseträume!

Vielen lieben Dank an meine lieben Eltern, meine Schwester Vivien und meinen Schwager Indra, dass ihr so eine tolle Familie seid, die mich immer unterstützt und auf die ich mich immer verlassen kann!

François, merci pour tout! Tu m’as toujours soutenu même si tu étais loin des fois!

List of publications

From this thesis the following manuscripts have been published or are submitted for publication:

Chapter 4, 6, 7, 8

Beer M.V., Hahn K., Diederichs S., Singh S., Fabry M., Salber J., Möller M., Shard A., Groll J. Comparison of quantification methods for ligand concentration and distribution in hydrogel films and correlation with cell adhesion. *In preparation.*

Chapter 6

Beer, M.V., Rech, C., Diederichs, S., Hahn, K., Bruellhoff, K., Möller, M., Elling, L., Groll, J. A hydrogel-based versatile screening platform for specific biomolecular recognition in well plate format. *In preparation.*

Chapter 9

Beer M.V., Rech, C., Gasteier P., Sauerzapfe B., Salber J., Ewald A., Möller M., Elling, L., Groll J. Sugar-lectin mediated biomimetic presentation of extracellular matrix components on inert hydrogels. *In preparation.*

Chapter 10

Grafahrend D., Heffels K.-H., Beer M.V., Gasteier P., Möller M., Boehm G., Dalton P.D., Groll J. Degradable polyester scaffolds with controlled surface chemistry combining minimal protein adsorption with specific bioactivation. *Nature Materials* **2011**, 10(1), 67-73.

Presentation

01.06.2011	*A one-step procedure to hydrogel coated electrospun fibres: ECM mimicry through specific cell adhesion* International Conference of Tissue Engineering, Chania, Greece

Posters

31.05.-05.06/2011	*A one-step procedure to hydrogel coated electrospun fibres: ECM mimicry through specific cell adhesion* International Conference of Tissue Engineering, Chania, Greece
13.-15.10/2010	*Electrospun fiber-meshes combining non-fouling properties with specific bioactivation as ECM-mimetic tissue-engineering scaffolds* BioStar Conference, Stuttgart, Germany
27.06.-03.07/2010	*Hydrogel coated electrospun fibers: ECM mimicry through specific cell adhesion* Gordon Research Conference, Signal Transduction by Engineered Extracellular Matrices, Biddeford, USA
26.-27.06/2010	*Hydrogel coated electrospun fibers: ECM mimicry through specific cell adhesion* Gordon-Kenan Seminar, Signal Transduction by Engineered Extracellular Matrices, Biddeford, USA
17.-16.03/2009	*Hydrogel coated electrospun fibers: ECM mimicry through specific cell adhesion* Biomedica Conference, Aachen, Germany
01.-06.02/2009	*Construction of a biomimetic ECM on functional hydrogel coatings* Gordon Research Conference, Fibronectin, Integrins & Related Molecules, Ventura, USA

Price

1st place in the “NMW NRW” photo competition „Nano Micro Materials“ in the category “Micro” with the picture titled “Skin cells in a micro fitness studio”